University of Alberta

Modeling spatial and temporal variability of nitrous oxide emissions from fertilized agricultural soils using the *Ecosys* mathematical model

by

Kimlin Andrea Metivier

A thesis submitted to the Faculty of Graduate Studies and Research
in partial fulfillment of the requirements for the degree of

Doctor of Philosophy
in
Soil Science

Department of Renewable Resources

Edmonton, Alberta
Fall 2008

Your file Votre référence
ISBN: 978-0-494-46382-6
Our file Notre référence
ISBN: 978-0-494-46382-6

DEDICATION

This thesis is dedicated to my Supervisor, Professor Robert Grant, for being an inspiration to me, for the opportunity to pursue this degree and for his steadfast teachings, guidance, support and patience throughout this research.

ABSTRACT

Large spatial and temporal variability of N_2O complicates calculation of emission factors (EFs) needed for N_2O inventories. To contribute towards improving these inventories, a processed-based, 3-dimensional mathematical model, *ecosys*, was used to simulate N_2O emissions for this research. *Ecosys* captured the large spatial and temporal variability of N_2O and simulated the complex feedback mechanisms involved in climate change. More accurate site-specific EFs (e.g. accounting for past and current fertilizer use, climate, soil type and topography) were modeled for agricultural soils, which are needed for adoption of an IPCC Tier III Methodology.

N_2O responded non-linearly ("threshold" response) to different water-filled pore space (60, 75 and 90%) in a laboratory experiment (< m^2 scale). Field-plot experiments (m^2 scale) showed that N_2O response to fertilizer N was non-linear due to different soil residual N. N_2O emissions were simulated simultaneously at m^2, fetch (~ 5 ha) and field (~ 42 ha) scales, using a digital elevation model to represent topography. Fertilizer application, precipitation and temperature were main factors responsible for N_2O emissions. Large coefficients of temporal variation (modeled: 25 to 51% and measured: 24 to 63%) of N_2O during emission (0 to 0.8 mg N_2O-N m^2 h^{-1}) periods was shown to cause biases in seasonal totals, when emissions were calculated from infrequent (daily or weekly) measurements. Average EFs almost quadrupled when fertilizer applications were delayed (1.67%), causing nitrification to occur in warmer soils compared to earlier applications (0.45%) when nitrification occurred in cooler soils. Large coefficients of spatial variation (CSVs) (28 to 195%) of N_2O occurred at a very small spatial scale (4

replicates in 2 x 3 m grid). Modeled field scale CSVs rose from 25% (uniform soil) to 101% with varying soil properties. Modeled EF (uniform soil) was 0.3% (lower topography) and 0.1% (higher topography) in a fairly flat field (0.2% slope). Results showed that EFs may more than double by 2050 due to climate change. Findings from this research showed the importance of using models such as *ecosys* that fully represent the complex hypotheses involved in the generation of past, current and future N_2O emissions, at high temporal and spatial resolutions.

ACKNOWLEDGEMENTS

I would first like to give Utmost Thanks To Almighty God for giving me the strength to complete this research programme. I am deeply grateful to my Supervisor, Professor Robert Grant for his steadfast guidance, advice, extensive support and encouragement from the start to the end of this project. I am very thankful for the funding he has provided through the Natural Sciences and Engineering Research Council (NSERC). I would like to thank my Co-Supervisor, Dr. Elizabeth Pattey, who provided her guidance, patience and encouragement throughout the project. I am very thankful for the funding she has provided through the Biological Greenhouse Gases Sources and Sinks (BGSS). I am also grateful to the Department of Renewable Resources for providing me with Graduate Intern Tuition Supplements (GITS) and Graduate Research Assistantships (GRA) funding, to help me pursue this degree.

Many thanks to Professor Noorallah Juma, my Committee Member, for his constant encouragement, assistance and patience throughout this research. I am very thankful to Professor Jerry Leonard, my Committee Member, for his continuous encouragement, assistance and advice throughout every step of this project. Thanks is also extended to Dr Scott Chang and Professor David Burton for their support and advice. Thanks so much to Professor John Wilson who has provided continuous advice with the Micrometeorological area of my research. I would like to thank Professor Frank Gumbs for his support and advice. My appreciation is extended to Mr Tom Goddard, Team Leader of the Canadian Agri-Food Research Council - Climate Change Funding Initiative in Agriculture (CARC-CCFIA) project, for his assistance. I would like to sincerely thank

Mr Dick Puurveen who was also involved in the CARC-CCFIA project, for his assistance with the many different areas such as meteorological instrumentation and soil measurements, providing data access and imparting his knowledge in these areas. Special thank you to Mrs Kerrianne Koelher-Munro, another member of the CARC-CCFIA project, for greenhouse gas sampling and analyses, providing data access, imparting her knowledge in these areas and also for her friendship throughout this research.

I would like to specially thank Mr Clive Figuereido for his training, assistance and patience with the use of the gas chromatograph (GC). Many thanks also to Mr Allan Harms for his assistance and support with the use of the GC. I am very grateful to Mr Dave Dow for training with the use of the tunable diode laser (TDL) and his support and assistance throughout the experiments. Thanks to Mr Christophe Forget for assistance with data analysis and other areas of the research. Thanks to Mr Rick Pelletier for training in geographical information systems (GIS) and use of Spatial Information Systems (SIS) Laboratory. Thanks to Mr Matt Hinther for his assistance and encouragement with GIS for the experiments. Thanks to Miss Lynda Blackburn her assistance as well as patience for the duration of my research endeavour. Many thanks to Mr Patrick St George for training with gas sampling protocol and GC analysis. Thanks to Mrs Monica Mollina for soil samples analyses. Special thanks is due to Dr Phillipe Rochette and Dr Ed Gregorich for use of their laboratory for GC analysis.

Many thanks to Dr Tao Li for his training and patience with GIS and other areas of my research. Thanks also to the summer students - Mr Eric Buan, Miss Shelley Hicks and

Miss Kimberley Wong, for all of their assistance. Thanks to our research group Mr Henry Zhang, Mr Johnny Montenegro, Dr Ziyu Wang, Mr Dimitre Dimitrov and Dr Muhammed Arbhar. I also wish to thank Mrs Sandy Nakashima, Mrs Darlene Saunders, Mrs Donna Thompson, Mrs Chung Nyuen and Ms. Christies Nohos and the entire staff of the Renewable Resources for all of their assistance.

I wish to thank my wonderful parents Wayne and Ann- marie, my caring brother, Ron, my caring sister, Leann and great sister-in law, Danielle, beautiful niece, Anya Ronelle Metivier and other family – Carmen, Donnie, Beverley, Agartha, Bee, Ricky, Peter, Curtis, Barry, Shawn, Sherry, Felix, Janette, Do Do Metivier and Fay, Richard, Miss George Burton, for their love and constant encouragement. Without them, my work would not have been possible. Also, thanks to Doris, Jarth, Jeremy and Hilda Ramessar and Dawn, Chris and Daniel Philpott, for being an extended family to me here in Edmonton. Thanks to my friends – Nelleen Harripaul, Kirsten and Eric Lamb, Benjamin Sey, Xiao Tan, Virginia Jacob-Cervantes, Marcos Jimenez-Casas, Miwa Mitshumashima, Kirsten Hanam, Lee Martins, Adriana Almeida-Rodriguez, Adriana Arango, Esther Kamunya, Elisa Verma, Jaime Pinzon and Irma Diaz. Many thanks to Marlun Jitta for his friendship, full support and assistance throughout my degree.

I am extremely grateful for the opportunity of being a graduate student at this great institution, University of Alberta, for all of the tremendous knowledge and friends over the years.

TABLE OF CONTENTS

LIST OF TABLES

LIST OF FIGURES

CHAPTER 1.0 – General Introduction

Nitrous oxide (N_2O) is a radiative active gas which has a 100-year global warming potential (GWP) 310 times greater than that of CO_2 (Olsen et al., 2003). It can also lead to destruction of the ozone layer in the stratosphere (Crutzen, 1981). Direct and indirect emissions from agricultural systems are now thought to contribute 6.2 Tg N_2O-N per year to a total global source of 17.7 Tg N_2O-N per year (Kroeze et al., 1999). In 2001, N_2O emissions accounted for 60% (36000 kt CO_2 eq. (kilotonne of carbon dioxide equivalent)) of the total greenhouse gases emissions from the agricultural sector in Canada (Olsen et al., 2003). Along with other countries under the Kyoto Protocol, Canada is committed to reduce its total greenhouse gases to 6% below 1990 levels (607 to 571 Mt (Megatonne)) over the period 2008 to 2012 (Olsen et al., 2003).

Currently, the Intergovernmental Panel on Climate Change (IPCC) guidelines are used to estimate N_2O emissions from agricultural practices. However, uncertainties in estimates of N_2O emissions by IPPC guidelines may be 70% to 80% in arable soil at a national scale (Lim et al., 1999). This uncertainty may be attributed to large spatial and temporal variability of N_2O emissions, in response to changes in topography (Grant and Pattey, 2003). Also, N_2O emissions are very site-specific since soil chemical, physical and biological properties, climate, and land use management practices all interact to influence N_2O production and emission from agricultural soils. An emission factor (EF) (ratio of increase in N_2O emission attributed to an increase in fertilizer application) of 1% N_2O-N for all types of synthetic fertilizers is now used in the IPCC Tier I methodology (non-country specific EF) (Eggleston, 2006). However, this factor may vary depending on site-

specific conditions. IPCC Tier II Methodology may improve current estimates because it is based on country-specific EFs, derived from country-specific activity data (land use) (Eggleston, 2006). An IPCC Tier II Methodology is now being used for Canada. It uses lower EFs (0.1 - 0.7%) in drier climates such as the Prairies and higher EFs (0.83 - 1.67%) for the more humid regions of Eastern Canada (Hegalson, 2005). IPCC Tier III Methodology involves either the use of validated mathematical models or the use of measurement data in conjunction with activity data to simulate emissions (IPCC, 2006). Unlike Tier I and Tier II, Tier III addresses more of the large spatial and temporal variability of N_2O emissions and is capable of capturing longer-term legacy effects of land use and management (Eggleston, 2006). Because of the uncertainties associated with using the current IPCC Tier I and Tier II Methodologies (Eggleston, 2006), mathematical models are required that can contribute towards the development of more accurate site - specific emission factors needed for the adoption of an IPCC Tier III Methodology.

Process – based mathematical models can represent a range of site-specific conditions. Therefore, they can take into account the effect of past and current land use, climate, soil type, topography etc. on N_2O emissions. Models can also improve estimates by contributing towards the continuity of measured data by estimating fluxes where measured data are missing or impossible to obtain because of resource constraints. Rigorous testing of mathematical models from smaller to larger spatial and temporal scales is especially important for N_2O since this trace gas is controlled by complex processes at different spatial and temporal scales. *Ecosys* (Grant, 2001a,b: website: www.ecosys.rr.ualberta.ca) is a process – based, 3-dimensional mathematical model of

natural and managed ecosystems and was used for this research because it accounts for the major hypotheses for N_2O transformations in soils, at high spatial and temporal resolutions. The model was used to simulate emissions simultaneously at site or patch (m^2), fetch (~ 5ha) and field (42 ha) spatial scales. In order to provide well-constrained tests for *ecosys*, a combination of micrometeorological techniques with tunable diode laser (TDL) technology and surface chamber measurements was used to provide measured N_2O emissions from fertilized fields at spatial scales from m^2 through ha to field, and at temporal scales from hour through days to the season and years.

1.1 N_2O formation and its temporal and spatial variability

In order to explain the high spatial and temporal variability of N_2O emissions, an understanding of the basic processes responsible for the production of N_2O is necessary. N_2O is produced via nitrification and denitrification therefore, alternating oxic and anoxic soil conditions are necessary. These processes are now considered in detail.

1.1.1 Nitrification

Nitrification in soil (Eq. [1.1]) proceeds in two steps whereby CO_2 is generally used as a C source and the energy required to reduce it is obtained by: (1) oxidation of NH_3 (NH_3 and NH_4^+ are in dynamic equilibrium) to NO_2^- by ammonia–oxidizing bacteria of the genera *nitroso*bacteria (e.g. *Nitrosomonas europaea, nitrosobolobus multiformis, nitrosospira briensis and nitrosovibrio tenuis* species) and (2) oxidation of NO_2^- to NO_3^- by nitrite-oxidizing bacteria of the genera *nitro*bacteria (e.g *Nitrobacter vulgaris, Nitrospina gracilis, nitrococcus mobilis* species*)* (Muller, 1999; Myrold, 1998). Some existing heterotrophic nitrifiers include both fungi (e.g. *Aspergillus*) and bacteria (e.g. *Alcaligenes, Arthrobacter spp.* and some actinomycetes) (Myrold, 1998). Under aerobic conditions, the enzymatic oxidation releases energy, and may be represented as follows (Myrold, 1998):-

Aerobic Reactions

[1.1a]

Step 1:

-12 e^- **(Electron loss)**

Nitrosomonas europaea **(Bacteria)**

$$2NH_4^+ + 3O_2 \rightarrow 2NO_2^- + 2H_2O + 4H^+ + 271 \text{ kJ energy mol}^{-1}\ NH_4^+$$

-3 **+3** **(N oxidation state)**

[1.1b]

Step 2:

$-4e^-$ **(Electron loss)**

Nitrobacter vulgaris **(Bacteria)**

$2NO_2^- + O_2 \rightarrow 2NO_3^- +$ 77 kJ energy mol^{-1} NO_2^-

+3 **+5** **(N oxidation state)**

(Results in acidity since 1 mole of NH_4^+ produces 2 moles of H^+).

NH_4^+ is the electron donor, and is oxidized to NO_2^- and then to NO_3^-, while O_2 is the electron acceptor, and is reduced to H_2O (Eq. [1.1a]). Nitrification is therefore at maximum when the soil is well aerated (e.g., near field capacity, ≈ 60% water-filled pore space (WFPS)). The diffusivity ($D_{g\gamma}$) of O_2 into the soil at 60% WFPS, is sufficient to meet the demands of microbes, unless this demand is very large.

When soils become anaerobic (e.g. during winter, during spring thaw or after a rainfall event in early summer) in N-fertilized agricultural fields, O_2 becomes limiting to microbes in the soil and in a process called "nitrifier denitrification", ammonium oxidizers containing nitrite reductase may use NO_2^- as an alternative electron acceptor to produce NO and N_2O (NO_2^- is reduced) (Muller, 1999; Myrold, 1998):-

Anaerobic Reaction (alternative to Eq. [1.1a]

(Eq[1.1c])

+12e$^-$ **(Electron gain)**

$2NH_4^+ + 6NO_2^- + 2H^+ \rightarrow 2NO_2^- + 3N_2O + 5H_2O$

-3 **+3** **+3** **+1** **(N oxidation state)**

(H^+ is consumed in this reaction).

This occurs because the $D_{g\gamma}$ of O_2 declines as the soil's WFPS increases or as the soil air – filled porosity (θ_g) decreases. When $D_{g\gamma}$ declines enough, O_2 can no longer diffuse into the soil fast enough to meet the demands of microbes. During spring thaw and early summer, soil moisture contents >60% WFPS leads to O_2 deficiency. High N_2O fluxes have been modeled and measured around the early spring snow-melt period (e.g. Grant et al., 1992; Grant and Pattey, 1999). In addition to high water contents after rainfall, high soil N levels due to fertilizer application in early summer may accelerate N_2O emissions (e.g. Grant and Pattey, 2003). During winter, the ice layer which develops over the soil surface may restrict O_2 diffusion into the soil thus stimulating "nitrifier denitrification". Goreau et al. (1980) also showed that *Nitrosomonas* spp. is capable of producing N_2O under low O_2 concentrations. Under aerobic conditions, the production of N_2O by this mechanism is small, less than 1% of the NH_3 oxidised (Myrold, 1998). NO and N_2O may also be produced by chemical decomposition of NO_2^- together with NH_2OH, the intermediate product between NH_4^+ and NO_2^- (Muller, 1999).

A supply of NH_4^+ e.g. from fertilizers, manure, mineralization of organic N etc. (Bouwman et al., 2002) and a population of nitrifying organisms must be present for nitrification to occur (Muller, 1999; Myrold, 1998). Nitrification follows an Arrhenius temperature response (Muller, 1999). The temperature coefficient (Q10) is 2 over the range 5 to 35°C, while optimum soil temperature for nitrification is 25 to 35°C (Linn and Doran, 1984; Paul and Clark, 1989; Prosser, 1989; Grundmann et al., 1995; Parton et al., 2001; Avrahami et al., 2003). Nitrification takes place within the pH range 4.5 to 10 but optimum pH is 8.5. Allelochemicals (e.g. tannins and polyphenols) produced by climax vegetation in natural ecosystems (Myrold, 1998) may inhibit nitrification. However, the dominant reason for low NO_3^- in these environments is the active competition for NO_3^- by plant uptake and microbial immobilization.

1.1.2 Denitrification

Under aerobic conditions, facultative heterotrophic denitrifying bacteria e.g. *Psuedomonas* and *Bacillus*, may oxidize CH_2O (reduced C) to CO_2 (Eq. [1.2a]) to obtain their energy and reduce O_2 to H_2O (Eq. [1.2a]).

Aerobic Reaction

Eq. [1.2a]

$$\underset{\textbf{0}}{CH_2O} + \underset{}{O_2} \xrightarrow[\textbf{heterotrophic}]{-4e^-} \underset{\textbf{+4}}{CO_2} + \underset{}{H_2O}$$

(Electron loss)

(Bacteria)

(C oxidation state)

However, under anaerobic conditions, similar to "nitrifier denitrification", the D_{gy} of O_2 may be insufficient to meet microbial demands, resulting in the use of alternative electron acceptors (Eq. [1.2b,c,d]):-

Anaerobic Reactions

Eq. [1.2b]

+4e$^-$ **(N Electron gain)**

facultative heterotrophic **(Bacteria)**

$$CH_2O + 2NO_3^- \rightarrow CO_2 + 2NO_2^- + H_2O$$

0 +5 +4 +3 **(C & N oxidation states)**

120 kJ energy mol^{-1} C **(Energy yield)**

Eq. [1.2c]

+4e$^-$ **(N Electron gain)**

facultative heterotrophic **(Bacteria)**

$$CH_2O + 2NO_2^- + 2H^+ \rightarrow CO_2 + N_2O + 2H_2O$$

0 +3 +4 +1 **(C & N oxidation state)**

120 kJ energy mol^{-1} C **(Energy yield)**

Eq. [1.2d]

+2e$^-$ **(N Electron gain)**

facultative heterotrophic **(Bacteria)**

$CH_2O + 2N_2O \rightarrow CO_2 + 2N_2 + H_2O$

0 +1 +4 0 **(C & N oxidation state)**

120 kJ energy mol^{-1} C **(Energy yield)**

(H^+ is consumed in denitrification so pH is increased)

Other denitrifying bacteria are autotrophs, such as *Thiobacillus denitrificans,* which obtain their energy from the oxidation of sulphide. For denitrification to occur, decomposable organic compounds (electron donor) and NO_3^- (electron acceptor) e.g. from nitrification, fertilizers, residual N, manure, mineralization of organic N etc. (Bouwman et al., 2002) must be present. Denitrification activity response to temperature changes follows an Arrhenius function (Muller, 1999), increasing rapidly from 2 to 25°C, with the optimum temperature range between 25 and 35°C (Tiedje, 1988; Paul and Clark, 1989; Merrill and Zak, 1992; Weier et al., 1993; Strong and Fillery, 2002; Simek and Cooper, 2002). Plants can increase denitrification by (a) consuming O_2 through root activity, and (b) stimulating high microbial populations through exudations of reduced C into the rhizophere. On the other hand, plants can reduce denitrification by (a) uptake of NO_3^- and NH_4^+, (b) reducing soil water with resultant increase in O_2 supply, and (c) directly increasing O_2 levels in the rhizophere of certain plants that transport O_2.

1.1.3 Ecological controls on N_2O production

Transitions from one reduction reaction to another (Eqs. [1.1b,c] and [1.2b,c]) can be caused by small changes in soil WFPS. This occurs because the $D_{g\gamma}$ of O_2 (and other gases) in the soil atmosphere varies according to a power function of θ_g (Millington and Quirk , 1960) (Eqs. [3]),which in turn depends on WFPS:-

$D_{g\gamma} = D'_{g\gamma} f_{tg} (\theta_g)^{\alpha} / \theta_p^{\beta}$ (Millington and Quirk, 1960) Eq. [1.3]

Where:

$D'_{g\gamma}$ is the gaseous diffusivity of gas γ in air at 25°C ($m^2 h^{-1}$)
α is the sensitivity of $D_{g\gamma}$ to θ_g (2) (Millington, 1960)
β is the sensitivity of $D_{g\gamma}$ to θ_p (0.67) (Millington, 1960)
θ_p is the soil total porosity ($m^3 m^{-3}$)
f_{tg} is the temperature function for gaseous diffusivity
θ_g is the air-filled porosity ($m^3 m^{-3}$)

This variation is such that small declines in θ_g (90% > WFPS > 60%) can cause large declines in $D_{g\gamma}$ that may limit O_2 gaseous transfer to microsites causing a rapid rise in demand for alternative electron acceptors. As a result, a rapid transition from the reduction of O_2 to NO_x by nitrifiers and denitrifiers occurs, increasing N_2O production.

Transitions from one reduction reaction to another can also be caused by small changes in soil temperature. A rise in temperatures can accelerate reduction of O_2 by nitrifiers/denitrifiers thereby increasing the demand for O_2 electron acceptors at the microbial sites. As a result, microbial O_2 demand may exceed O_2 supply, causing a rapid rise in the need for alternative electron acceptors (Grant and Rochette, 1994; Grant, 1995) and therefore transition to reduction of NO_2^- (nitrifiers) and NO_3^- (denitrifiers), accelerating production of N_2O. N_2O production may increase further with higher

temperature since this reduces the solubility of gases and hence, aqueous oxygen concentrations ($[O_{2s}]$) maintained by microbial microsites slowing uptake during oxidation/reduction reactions (Eqs. [1.1] and [1.2]). Another consequence of higher temperature is that the solubility of N_2O also decreases causing the degassing of previously accumulated aqueous N_2O in the soil profile to be accelerated. The WFPS threshold at which the transition among reduction reactions occurs therefore decreases with higher temperatures (Grant and Rochette, 1994; Grant, 1995). Dobbie and Smith (2001) found that apparent values of Q10 (emission rate at (T + 10)°C/emission rate at T°C) for an arable soil were about 50 when soil temperature was increased from 5 to 12°C and 8.9 for increases from 12 to 18°C.

1.1.4 Temporal variation of N_2O emissions

As described above, N_2O is produced from nitrification/denitrification when WFPS > 60%. However, N_2O usually accumulates in the soil profile because of low $D_{g\gamma}$ (Eq. [1.3]) of N_2O at high WFPS. As the soil water drains and evaporates, water is lost from soil macro-pores, subsequently increasing θ_g (Eq.[1.3]). Gaseous diffusivity increases rapidly (Eq. [1.3]), which leads to rapid N_2O emissions from the soil. N_2O has been seen to be emitted as large bursts 20-24 hours after rainfall (e.g. Wagner-Riddle et al., 1996) or during spring thaw (Grant et al., 1992; Nyborg et al., 1997). Eventually, N_2O emissions decline to ambient levels over a few days as the θ_g increases further. If rainfall occurs later in the summer (July to August), no emissions may occur because of low soil mineral

N. Lower emissions are generally observed in the fall because of drier soil conditions and lower soil temperatures.

At the diurnal time scale, temporal variability in N_2O fluxes is large, with highly skewed frequency distributions and coefficients of variation > 150% (e.g. Flessa et al., 1995; Thornton et al. 1996). Williams et al. (1999) found that diurnal variation of N_2O followed that of soil temperature at 10 cm depth, with peak emissions occurring in late afternoon. Micrometeorological studies (e.g. Phillips et al., 2007) have showed that N_2O emissions increase with increasing soil temperatures. This could be in part attributed to continuous heating of the land surface by the sun during the day, resulting in more turbulent transfer of heat and mass (Arya, 2001). Studies by Grant and Pattey (2003) suggest that the magnitude of temporal variability of N_2O emissions suggests that aggregation of flux measurements to regional scales should be based upon sub-daily measurements at representative landscape positions, rather than less frequent measurements (e.g. daily or weekly) at individual sites as currently done.

1.1.5 Spatial variability of N_2O emissions

Because of the nature of the microbiological and physical processes discussed above, N_2O emissions show very high **temporal variability** (e.g. Cates and Keeney, 1987; Flessa et al., 2002a). However, N_2O emissions also show very high **spatial variability** - Coefficients of spatial variation (CSV – the ratio (%) of standard deviation to mean of emissions over a spatial scale) in N_2O emissions can range from 120 to 230% (Flessa et

al., 1995), when measured at spatial scales of several m^2 within field plots (e.g. Frolking et al., 1998: Hanault et al., 1998). Anaerobic microsites may lead to spatial variability of N_2O at the small scale level (Christen, 1985). Sextone et al. (1985) showed that anaerobic zones can occur in the centres of saturated soil aggregates whereas the outsides of the aggregates were fully aerated. However, denitrification did not occur in all aggregates that had anaerobic zones, probably because factors other than aeration limited denitrification.

At the landscape-scale, surface topography can affect soil chemical, biological and physical properties by influencing lateral water distribution due to surface flow or emergence of shallow ground water in depressions. Studies by Grant and Pattey (2003) showed that both the temporal and spatial variability of N_2O emissions may be caused by topographically-driven flows of water and solutes (e.g. dissolved organic C (DOC), NH_3 and NO_3^-) through landscapes causing greater emissions in topographic positions in which water and solutes are gathered, than in those from which they are shed. Studies by Pennock and Corre (2001) showed that N_2O emissions were significantly higher at foot slopes than at shoulder or midslopes. Florinsky et al. (2004) found that N_2O emissions were affected by differences in accumulation of soil moisture and organic matter due to local topography. Pennock et al. (1992) have demonstrated that soil moisture is the main factor affecting N_2O emissions and that higher soil moisture is often found at lower topographic positions of a landscape.

The most common observation, when sufficient dentrification measurements are made over time and space, are that most rates are low with just a few high rates (Myrold, 1998). This results in a skewed frequency distribution that is most often described as lognormal; studies by Ball et al. (1997) showed such a pattern. This observation has been attributed to the formation of "hot spots" of activity where optimal conditions of anaerobiosis, adequate NO_3^- and available C coincide. The overall area of a site covered by flux measurements should be adequate to allow detection of "hot spots" of activity, as well as low-activity areas (Ball et al., 1997). Spatial variation in N_2O can also occur due to variation in soil temperature (Rover et al., 1999). By assessing spatial and temporal flux variability in relation to potential controlling factors, identification of the most influential factors should be possible and such information would be particularly useful in predictive emission models (Grant et al., 1993c; Li et al., 1992).

1.2 Land use practices affecting N_2O emissions

Current Intergovernmental Panel of Climate Change methodology for quantifying N_2O in greenhouse gas inventories, is based on a constant EF for all N inputs. However, emission factors may vary depending on site-specific conditions such as land use. This includes (a) past land use (e.g. quantity of residual mineral N determined by the history of N inputs versus removals), and

(b) current land use (e.g. rate at which fertilizer is applied, timing with respect to precipitation and temperature and fertilizer type).

1.2.1 Past land use

The quantity of soil residual N present may determine the response of N_2O emissions to fertilizer N addition. A review by Barnard et al. (2005) suggests that the response of N_2O flux to N addition was highly variable, and there was no clear correlation with the amount of N added. Some of the studies for this review showed that application of N fertilizer at high rates resulted in little or no N_2O emissions because fluxes may be already at near maximum rates due to N saturation of the system.

1.2.2 Current land use

1.2.2.1 Inorganic Fertilizers

At present, the global use of mineral fertilizers is 78 million tonnes N per year (FAO, 2001). Plants uptake only 50% of N applied due to losses by leaching, run-off or gaseous emissions (FAO, 2001). Generally, fertilizer application leads to enhanced N_2O emissions. However, the magnitude depends on the fertilizer type, rate, timing of application, placement etc.

1.2.2.1.1 Fertilizer type

Mulvaney et al. (1997) showed that emissions of labelled N_2 and N_2O decreased in the order: anhydrous NH_3 > urea > $(NH_4)_2HPO_4$ > $(NH_4)_2SO_4$ ~ NH_4NO_3 ~ $NH_4H_2PO_4$. This occurred because anhydrous NH_3, urea and $(NH4)_2HPO_4$ gave more alkaline reactions upon hydrolysis than did acidic salts $(NH_4)_2SO_4$, NH_4NO_3 and $NH_4H_2PO_4$. Generally, addition of N fertilizer in this study caused enhanced emissions of labelled N_2 and N_2O but the increases were usually larger for N_2O than for N_2. Thornton et al. (1996) showed

that anhydrous NH_3 lost 7.33% of the applied N while urea lost 3.77%. Liquid forms of N fertilizer will contribute to N_2O emissions by providing an anaerobic environment (Lemke et al., 1998a). Slowly available N fertilizers consists of (a) substances of low water solubility requiring decomposition e.g. urea-formaldehydes (b) water soluble materials requiring decomposition e.g. triazone and (c) nitrification and urease inhibitors e.g. nitripyrin (Havlin, 1999). These compounds are formulated to release N in accordance with crop needs and, therefore, reduce N_2O produced from nitrification/denitrification. Studies by McTaggart and Tsuruta (2003) showed that the use of controlled release N fertilizer reduced N_2O emissions. However, the magnitude of decrease was dependent on the form of fertilizer (NH_4^+ or NO_3^-) and the WFPS.

1.2.2.1.2 Fertilizer rate

Lower rate of fertilizer applications decreases N_2O emissions (Mulvaney et al. 1996). Studies by Grant et. al. (2006) showed that in a temperate, humid climate, modeled N_2O emissions rose non-linearly with fertilizer application rate. That is, when anhydrous NH_3 was applied at 3 g m^{-2}, an emission factor of 0.1% was obtained versus 1.8% when 30 g N m^{-2} was applied. This occurred because N additions at the higher fertilizer rate exceeded the crop and soil uptake capacities for added N. In other studies, Hénault et al., (1998) reported that N_2O emission rose linearly with fertilizer rate for optimally and excessively fertilized rapeseed in France. A review by Barnard et al. (2005) suggests that the response of N_2O flux to N addition was highly variable, and there was no clear correlation with the amount of N added.

1.2.2.1.3 Timing of fertilizer application

When nitrogen fertilizer is applied in the fall, N is lost over the winter and during the spring thaw. These losses do not occur when fertilizer is applied after spring thaw (Lemke et al., 1998b). The over-wintering loss of inorganic N from fall-applied fertilizer on the Canadian prairies has been largely attributed to denitrification (Mahli and Nyborg, 1983).

1.2.2.1.4 Fertilizer placement

Studies on N fertilization indicate that banding, or placing fertilizer within the vicinity of the root zone reduces N_2O emissions (McKenzie, 1998) due to more efficient plant uptake (Malhi et al., 1988).

1.2.2.2 Manure

Organic amendments supply additional quantities of C and N and increase N_2O fluxes from the soil. However, the flux of N_2O produced depends on the amount of amendment introduced and its chemical composition (Reinertsen et al., 1984; Aulakh et al., 1991). Studies done by Maag and Vinther (1999) showed that both cattle and pig manure with the same moisture contents, resulted in an increase in N_2O emissions following application, however, total emissions were higher from the pig manure. They concluded that this trend occurred because the cattle manure contained very little degradable organic matter (Maag and Vinther, 1999). Research indicates that spreading raw solid or liquid manure emits more N_2O compared to spreading composted manure because raw manure

contains more water as well as higher levels of water-soluble carbon and nitrogen (Huther et al., 1997; Van Melle et al.,1999).

1.2.3 Climate, Soil type and Tillage

Other important site-specific factors which affect N_2O are climate (e.g. precipitation), soil type, and tillage. Years with higher precipitation often result in greater N_2O emissions (e.g. Grant et. al., 2006; Lu et al., 2006). A review by Bouwman et al. (2002) showed that emissions were generally larger in mineral soils with a fine soil texture, restricted drainage, and neutral to slightly acidic conditions. Lee et al. (2006) found that N_2O emissions in standard tillage and no tillage systems were nearly equivalent at field moisture content. Emissions reached maximum after water application (75% water holding capacity) to a greater degree in no-tillage versus standard tillage, and then gradually decreased over time to emission levels at field moisture content (Lee et al. 2006). Another study by Meyer-Aurich (2006) found that conservation tillage as has been found to reduce N_2O emissions due to lower fuel use and lower crop residue inputs due to lower yields, as compared to conventional tillage. As a result, EFs for N_2O are also site specific.

1.3 Measuring N_2O emissions

In order to provide well constrained tests for *ecosys* at different spatial scales, accurate N_2O emissions measuring techniques are necessary. However, measurements of N_2O emissions are difficult because of their large spatial and temporal variability. Most measurements of N_2O emissions are currently made with surface chambers over small areas (<1 m^2) (site scale) (e.g. van den Pol-van Daaelaar et al., 1998; Ball et al., 1997; Ambus and Christensen, 1995 and Veltof et al., 1996). These measurements capture only small portions of spatial and temporal variability, and so are of limited value for long-term landscape estimates of N_2O emissions (Blackmer et al., 1982; Bouwman, 1996). Moreover, chambers tend to disturb the soil environment and require careful methodology (Hutchinson et al., 2000; Hutchinson and Livingston, 2001; Denmead, 1978; Rochette and McGinn, 2005) for minimizing inherent uncertainties. However, surface chambers are easy to use and are of low cost and recently developed automated chambers (Flessa et al., 2002) may now provide improved temporal resolution of N_2O emissions.

Nevertheless, the temporal variability of N_2O emissions may be better captured by micrometeorological techniques (field-scale) in combination with tunable diode laser (TDL) technology (Campbell Scientific Inc., Logan, Utah) (Wagner-Riddle et al., 1996; Edward et al., 1994, 2002). Reliable trace gas fluxes have been calculated using micrometeorological techniques (Pattey et al., 1993, 1996, 1999, 2002, 2006a,b, 2007) in combination with TDL (Grant and Pattey 1999; Grant and Pattey 2003, Pattey et al. 2005, a&b; Wagner-Riddle, 1996). Denmead and Raupach (1993) stated that

micrometeorological techniques are preferred for field-scale measurements if available and feasible. Micrometeorological techniques spatially integrate fluxes over large areas, do not disturb the sampled area or its microclimate and permit studies of the changes in fluxes with changing atmospheric and surface conditions (Fowler and Duyzer, 1989). Micrometeorological techniques are well adapted to provide long-term estimates of N_2O emissions at the landscape-scale, however, they have limited ability to resolve topographic and treatment effects on N_2O emissions (Grant and Pattey, 2003) and are very expensive. Currently, no measurement method can fully capture both spatial and temporal variability simultaneously.

1.4 Mathematical modelling of N_2O emissions

Because of the complex processes involved in N_2O emissions, there has been an increased use of mathematical models to account for site-specific effects on EFs for national and regional inventories (e.g. Grant et al., 2006). If complex topographic effects on N_2O emissions are to be modeled, the model must be able to simulate soil water and temperature as affected by surface and subsurface water movement within a topographically variable landscape (Grant, 2004).

Ecosys (Grant, 2001a,b) ecosystem model explicitly represents the oxidation-reduction reactions (Section 1.1) from which N_2O is generated, and gas transfer processes which control the transition between alternative reduction reactions. In this model, the key

biological processes – mineralization, immobilization, nitrification, denitrification, root and mycorrhizal uptake - controlling N_2O generation were coupled to the key physical processes – convection, diffusion, volatilization, dissolution - controlling the transport of gaseous reactants and products of these biological processes (Grant et al., 2006). Other models have been used to estimate N_2O emissions for Europe (Freibauer, 2003) and European countries (Flechard et al., 2007; Roelandt et al., 2007; Gabrielle, 2006), but, these models were empirical and, therefore, may not fully represent the complex processes involved in N_2O generation. In other cases, the energetics of microbial oxidation-reduction reactions driven by alternative electron acceptors under aerobic vs. anaerobic conditions, are not included (Li et al., 1992), as they are in *ecosys.* Gabrielle et al. (2006) models N_2O at a daily time-step which does not allow testing at an hourly time-step, which is necessary to capture the large spatial and temporal variability of N_2O (Grant and Pattey, 2003). However, *ecosys* can be tested at hourly, daily and monthly time-steps.

Simulation of nitrification and denitrification is sensitive to soil air-filled porosity (θ_g), which in turn depends on water-filled pore space (WFPS). Transitions from one reduction reaction to another can be caused by small changes in soil WFPS as well as temperature (non-linear response) (Grant and Rochette, 1994; Grant, 1995). However, in some current models (e.g. Lu et al., 2006), the response is linear. Thus, *ecosys* was used to test hypothesis (1) (Section 1.7) concerning the non-linear ("threshold") response of N_2O production to changes in WFPS, thereby capturing the effect of intra and inter-annual variations in precipitation.

Ecosys also models surface energy exchange and subsurface heat transfer, vertical (infiltration, drainage, root uptake and capillary rise) and lateral (driven by differences in topographic position) movement of water and the effect of soil temperature and water on microbiological activity and gas exchange (Grant, 2004). Differences in the movement of water and solutes due to topography (represented in *ecosys* using digital elevation models (DEM)) are as a result of lateral water redistribution due to differences in gravitational water potential. Other models (e.g. Leffelaar and Wessel 1998; McConnaughey and Bouldin 1985 a, b and c) have not yet linked the simulation of water, heat and O_2 transfer. One-dimensional models (vertical direction) (e.g. Li, 2000; Li et al., 1992; Del Grosso et al., 2005; Kelly et al., 2000; Parton et al., 1996) do not simulate the energy and mass exchanges among adjacent grid cells and, therefore, cannot represent the spatial heterogeneities of soil properties that vary according to topography. Thus, *ecosys* was used to test our hypothesis (3) (Section 1.7) concerning spatial variation in N_2O emissions.

Earlier, *ecosys* was tested using either chamber data (Grant, 1991; Grant et al., 1992; Grant et al., 1993c; Grant, 1994; Grant, 1995) or micrometeorological data (e.g. Grant and Pattey, 1999; Grant and Pattey 2003; Grant et al., 2006) in different experiments. For this research, the ability of *ecosys* to simulate N_2O emissions simultaneously at both site and fetch scales with chamber and micrometeorological measurements respectively was tested.

1.5 Emission factors for N_2O under changing climate and land use

For this research, the *ecosys* (Grant, 2001a,b) mathematical model was used to simulate the spatial and temporal variability of N_2O emissions for different land use (past and current) management practices under site-specific conditions (e.g. climate, soil type and topography) for different ecosystems. As a result, site-specific emission factors were developed for different land use systems, annual precipitations, and topographies for use in an IPCC Tier III methodology. Future research will enable *ecosys* to model emissions at larger spatial scales (regional, provincial and national scales).

1.6 Research Questions

Key research questions for this study were:-

- How sensitive is the response of N_2O emissions to changes in soil WFPS in agricultural soils?
- How sensitive is the response of N_2O emissions to changes in past (soil residual N) and current (fertilizer and manure applications) land use management practices in agricultural soils and to inter-annual variation in precipitation?
- Can we quantify temporal variability of N_2O emissions?
- Can we quantify the spatial variability of N_2O emissions over a landscape?
- How will N_2O emissions change under climate change and different management practices?

1.7 Research Hypotheses

In order to answer the research questions above, quantitative, testable hypotheses were derived, based on the literature review, for a comprehensive range of processes believed to control N_2O fluxes. These hypotheses were already incorporated into a detailed mathematical model of terrestrial ecosystems, *ecosys* (Grant, 2001a,b). The model hypotheses were then tested against measured data from laboratory and field experiments. The model hypotheses tested were as follows:-

CHAPTER 2.0: Modeling temporal variability of N_2O emissions from a fertilized agricultural soil using the *Ecosys* mathematical model (site scale: $1 < m^{-2}$)

This chapter tested the **model hypothesis in *ecosys* (Grant, 2001a,b) that N_2O production increases sharply (threshold, non-linear response) at 90% > WFPS > 60%. It was proposed that the non-linear response of D_g (Millington and Quirk, 1960) of O_2 to changes in WFPS can be used to explain the sudden rise/threshold/ non-linear response of N_2O emissions commonly observed in the field, whereby N_2O emissions rises with WFPS > 60%. This occurs because at WFPS < 60% in the model, the D_g (Eq. [2.28]) of O_2 is large enough to meet microbial demands. However, as WFPS increases above 60%, the D_g (Eq. [2.28]) of O_2 declines sharply and the unmet O_2 demand forces the need for alternative electron acceptors (Eqs. [2.10] – [2.18]) thus, higher N_2O production via nitrification (Eq. [2.10]) and denitrification (Eq. [2.18]) in the model.**

CHAPTER 3.0 – Modeling the sensitivity of N_2O emissions from agricultural soils to changes in past and current land use management practices and inter-annual variation in precipitation using the *Ecosys* mathematical model (site scale: m^{-2})

Because N_2O production is driven by soil residual N (controls availability of alternative electron acceptors e.g. NH_4^+, NO_3^-), then rises in N_2O emissions will depend on rises in soil residual N. **It is hypothesized in *ecosys* (Grant, 2001a,b) that these rises occur in stages (non – linear response) (Figure 2-1) upon fertilizer N addition and can be explained by the immobilization capacity of the ecosystem (Grant et al., 2006):-**

Stage 1: Low initial soil residual N, then low rise in N_2O emissions upon fertilizer application. The model explanation for this trend is that when soil residual N is low due to low rates of past fertilizer application, current fertilizer N added (Figure 2-1; AB) will largely be immobilized (crop and soil uptake capacity) (N limited) (Grant et al., 2006) (Figure 2-1; B'). Consequently, low soil residual N remains, thus low N_2O production via nitrification (Eq. [2.10]) and denitrification (Eq. [2.18]) in the model (Figure 2-1; AB').

Stage 2: Higher initial soil residual N, then higher rise in N_2O emissions upon fertilizer application. The model explanation for this trend is that when soil residual N is higher due to larger rates of past fertilizer application, less of the current fertilizer N added (Figure 2-1; BC) will be immobilized compared to that of the Stage 1 response, due to the addition of N greater than the immobilization capacity

of the ecosystem (Grant et al., 2006) (Figure 2-1; C'). Consequently, higher soil residual N remains, thus higher rises in N_2O production via nitrification (Eq. [2.10]) and denitrification (Eq. [2.18]) in the model (Figure 2-1; BC').

Stage 3: Very high initial soil residual N, then low rise in N_2O emissions upon fertilizer application. The model explanation for this trend is that when soil residual N is very high due to very large rates of past fertilizer application, N_2O emissions are already high and even less of the current fertilizer N added (Figure 2-1; DE) will be immobilized (Figure 2-1; E'). Consequently, very high soil residual N remains but little further increase in N_2O production occurs because of an N excess in the ecosystem, which lead to the maximum rate for N_2O production via nitrification (Eq. [2.10]) and denitrification (Eq. [2.18]) in the model (Figure 2-1; DE'). Little N_2O production in this stage could be attributed to another source of limitation e.g. C limitation. (Testing of the Stage 3 response hypothesis was described in chapter 2).

A consequence of the Stage 2 response hypothesis above is that: An organic source (hog manure) will give higher N_2O emissions than those of inorganic source (urea). The model explanation for this trend is that readily available N and organic C in hog manure (less C limitation) increases the demand for alternative electron acceptors (Eqs. [2.10] – [2.18]) compared to that of urea fertilizer (C limited), leading to higher N_2O emissions since N and organic C promote microbiological activity of nitrification (Eq. [2.10]) and denitrification (Eq. [2.18]) in the model.

Organic C from hog manure may increase heterotrophic respiration (Eq. [8] and [9] of Grant, 2004) in the model, thereby leading to O_2 limitations and, thus, increased demand for alternative electron acceptors (Eqs. [2.10] – [2.18]) compared to that of urea fertilizer.

Rainfall in *ecosys* determines modeled surface flow (Eq. [2.21]) and subsurface flow (Eqs. [21] and [24] and [A94 - A96] of Grant et al., 2004) thus, WFPS. The effect of precipitation on N_2O emissions is also based on **the hypothesis in *ecosys* (Grant, 2001a,b) that N_2O production increases sharply (threshold, non-linear response) at 90% > WFPS > 60%.** This hypothesis in *ecosys* was tested in chapters 2 and 4.

CHAPTER 4.0 Using the *Ecosys* mathematical model to simulate temporal variability of nitrous oxide emissions from a fertilized agricultural soil (field scale: ~ 5ha)

Same as Chapter 2, but at larger spatial scales. The study investigated the implication of rainfall distribution and intensity on this hypothesis to derive recommendations for improving national N_2O inventories.

CHAPTER 5.0: Using the *Ecosys* mathematical model to simulate topographic effects on spatial variability of nitrous oxide emissions from a fertilized agricultural soil (site: 1 < m^{-2}, fetch: ~ 5ha & field: ~ 42ha scales)

This study tested **the hypotheses in *ecosys* that spatial variation in N_2O emissions can be explained in the model by (1) spatial and temporal variation in soil water-filled pore space (WFPS). The three-dimensional capability of the model allows the simulation of spatial and temporal variation of WFPS among topographic positions that shed or collect water according to topographically-driven water movement (surface Eq. [2.21]) and subsurface flow (Eqs. [21] and [24] and [A94 - A96] of Grant et al., 2004), even at a site with low topographic differences. Spatial variation in N_2O emissions can also be explained by (2) spatial variation in soil properties which may themselves be caused by topographically driven water movement.**

CHAPTER 6.0: Using *Ecosys* to project the impact of climate change (increasing CO_2 and temperature) on future spatial and temporal variability of N_2O emissions from an agricultural soil

***Ecosys* (Grant, 2001a.b) mathematical model was used to predict the impact of climate change (increasing CO_2 and temperature) on future spatial and temporal variability of N_2O emissions from an agricultural soil.**

1.7 REFERENCES

Ambus, P., Christsensen, S., 1995. Spatial and seasonal nitrous oxide and methane fluxes in Danish Forest Grassland and agroecosytems. Journal of Environmental Quality 24, 99-1001.

Ambus, P., Christsensen, S., 1994. Measurement of N_2O emission from fertilized grassland. An analysis of spatial variability. Journal of Geophysical Research 99, 16549-16555.

Arya, S. P., 2001. Introduction to micrometeorology, second edition. Academic press: A Harcourt science and technology company – San Diego, San Francisco, New York, Boston, London, Sidney, Tokyo.

Aulakh, M.S., Doran, J.W., Walters, D.T., Mosier, A.R., Francis, D.D., 1991. Crop residue type and placement effects on denitrification and mineralization. Soil Science Society of America Journal 55, 1020-1025.

Avrahami, S., Liesack, W., Conrad R., 2003. Effects of temperature and fertilizer on activity and community structure of soil ammonia oxidizers. Environmental Microbiology 5, 691– 705.

Ball, B.C., Horgan, G.W., Clayton, H., Parker, J.P., 1997. Spatial variability of nitrous oxide fluxes and controlling soil topographic properties. Journal of Environmental Quality 26, 1399-1409.

Barnard, R., Leadley, P.W., Hungate, B.A., 2005. Global change, nitrification, and denitrification: A review. Global Biogeochemical cycles 19, GB1007, doi:10.1029/2004GB002282.

Blackmer, A.M., Robbins, S.G., Bremner, J.M., 1982. Diurnal variability in rate of emission of nitrous oxide from soils. Soil Science Society of America Journal 46, 937-942.

Bouwman, A.F., Boumans, L.J.M., Batjes, N.H., 2002. Emissions of N_2O and NO from fertilized fields: Summary of available measurement data. Global Biogeochemical cycles 16(4), 1058, doi:10.1029/2001GB001811.

Bouwman, A.F., 1996. Direct emission of nitrous oxide from agricultural soils. Nutrient Cycling in Agroecosystems 46, 53-70.

Cates, R.L., Keeney, D.R., 1987. Nitrous oxide production throughout the year from fertilized and manured maize fields. Journal of Environmental Quality 16, 443-447.

Crutzen, P.J., 1981. Atmospheric chemical processes of the oxides of nitrogen, including nitrous oxide. In: Denitrification, nitrification and atmospheric nitrous oxide (ed. C.C. Delwiche), Wiley & Sons, New York, pp. 17-44.

Del Grosso, S.J., Mosier, A.R., Parton, W.J., Ojima, D.S., 2005. DAYCENT model analysis of past and contemporary soil N_2O and net greenhouse gas flux for major crops in the USA Soil & Tillage Research 83, 9–24.

Denmead, O.T., 1978. Chamber systems for measuring Nitrous oxide emission from soils in the field. Soil Science Society of America Journal 43, 89-95.

Denmead, O.T., M.R. Raupach., 1993. Methods for measuring gas transport in agricultural and forest systems. P. 19-44. In: L.A. Harper et al. (ed) Agricultural ecosystem effects on trace gas and global climate change. ASA Spec. Publ. 55 ASA. CSSA, and SSSA, Madison, WI.

Eggleston 2006. Intergovernmental Panel on Climate Change (IPCC), IPCC Guidelines for National Greenhouse Gas Inventories Volume 4; Agriculture, Forestry and other land use. Institute for Global Environmental Strategies, kanagawan Hayama, Japan.

Flechard, C.R., Ambus, P., Skiba, U., Rees, R.M., Hensen, A., van Amstel, A., van den Pol-van Dasselaar, A., Soussana, J.-F., Jones, M., Clifton-Brown, J., Raschi, A., Horvath, L., Neftel, A., Jocher, M., Ammann, C., Leifeld, J., Fuhrer, J., Calanca, P., Thalman, E., Pilegaard, K., Di Marco, C., Campbell, C., Nemitz, E., Hargreaves, K.J., Levy, P.E., Ball, B.C., Jones, S.K., van de Bulk, W.C.M., Groot, T., Blom, M., Domingues, R., Kasper, G., Allard, V., Ceschia, E., Cellier, P., Laville, P., Henault, C., Bizouard, F., Abdalla, M., Williams, M., Baronti, S., Berretti, F., Grosz, B., 2007. Effects of climate and management intensity on nitrous oxide emissions in grassland systems across Europe. Agriculture, Ecosystems and Environment 121, 135-152.

Flessa, H., Dörsch, P., Beese, F., 1995. Seasonal variation of N_2O and CH_4 fluxes in differently managed arable soils in southern Germany. Journal of Geophysical Research 100, 23115-23124.

Flessa, H., Ruser, R., Schilling, R., Loftfield, N., Munch, J.C., Kaiser, E.A. and Beese, F. 2002. N_2O and CH_4 fluxes in potato fields: automated measurement, management effects and temporal variation. Geoderma 105, 307-325.

Florinsky, I.V., McMahon, S., Burton, D.L., 2004. Topographic control of soil microbial activity: a case study of denitrifiers. Geoderma 119, 33–53.

Food and Agriculture Organization (FAO), 2001. Global estimated of gaseous emissions of NH_3, NO and N_2O from agricultural land, Rome.

Fowler, D.M Duyzer, J.H., 1989. Microbiological basis of NO and N_2O production and consumption in soil. In: Exchange of trace gases between terrestrial ecosystems and the atmosphere. Dahlem Workshop Proceedings. John Wiley and Sons, Berlin, pp. 189-208.

Frolking, S.E., et al., 1998. Comparison of N_2O emissions from soils at three temperate agricultural sites: simulations of year-round measurements by four models. Nutrient Cycling in Agroecosystems 52, 77–105.

Gabrielle, B., Laville, P., Duval, O., Nicoullaud, B., Germon, J.C., Henault, C., 2006. Process-based modeling of nitrous oxide emissions from wheat cropped soils at the subregional level. Global Biochemical Cycles 20, 1-11.

Goreau, T.J., Kaplan, W.A., Wofsy, S.C., McElroy, M.B., Valois, F.W. and Watson, S.W., 1980. Production of NO_2^- and N_2O by nitrifying bacteria at reduced concentrations of oxygen. Applied and Environmental Microbiology 40, 526-532.

Grant, R.F., 1991. A technique for estimating denitrification rates at different soil temperatures, water contents, and nitrate concentrations. Soil Science 152, 41-52.

Grant, R.F., 1994. Simulation of ecological controls on nitrification. Soil Biology & Biochemistry 26, 305–315.

Grant, R.F., 1995. Mathematical modelling of nitrous oxide evolution during nitrification. Soil Biology & Biochemistry 27, 1117–1125.

Grant, R.F., 1997. Changes in soil organic matter under different tillage and rotation: mathematical modeling in *ECOSYS*. Soil Science Society of America Journal 61, 1159-1175.

Grant, R.F., 2001a. A Review of the Canadian Ecosystem Model - *ecosys*. In: Shaffer M. J., Ma, L., Hansen, S. (Ed), Modeling Carbon and Nitrogen Dynamics for Soil Management. CRC Press. Boca Raton, FL, pp. 173-263.

Grant, R.F., 2001b. Modeling Transformations of Soil Organic Carbon and Nitrogen at Differing Scales of Complexity. In: Shaffer M. J., Ma, L., Hansen, S. (Ed), Modeling Carbon and Nitrogen Dynamics for Soil Management. CRC Press. Boca Raton, FL, pp. 597-614.

Grant, R.F., 2004. Modeling topographic effects on net ecosystem productivity of boreal black spruce forests. Tree Physiology 24, 1-18.

Grant, R.F., Rochette, P., 1994. Soil Microbial respiration at Different Water Potentials and Temperatures: Theory and Mathematical Modeling. Soil Science Society of America Journal 58, 1681-1690.

Grant, R.F. and Pattey, E., 1999. Mathematical modeling of nitrous oxide emissions from an agricultural field during spring thaw. Global Biogeochemical Cycles 13, 679-694.

Grant, R.F., Pattey, E., 2003. Modelling variability in N_2O emissions from fertilized agricultural fields. Soil Biology & Biochemistry 35, 225-243.

Grant, R.F., and Pattey, E., Submitted 2007. Temperature sensitivity of N_2O emissions from fertilized agricultural soils: mathematical modelling in *ecosys*.

Grant, R.F., Nyborg, M., Laidlaw, J.W., 1992. Evolution of nitrous oxide from soil: II. Experimental results and model testing. Soil Science 156, 266-277.

Grant, R.F., Juma, N.J., McGill, W.B., 1993a. Simulation of carbon and nitrogen transformations in soils. I: mineralization. Soil Biology & Biochemistry 25, 1317-1329.

Grant, R.F., Juma, N.J., McGill, W.B., 1993b. Simulation of carbon and nitrogen transformation in soil: Microbial biomass and metabolic products. Soil Biology & Biochemistry 25, 1331-1338.

Grant, R.F., Nyborg, M., Laidlaw, J.W., 1993c. Evolution of nitrous oxide from soil: I. Model development. Soil Science 156, 259-265.

Grant, R.F., Izaurralde, R.C., Nyborg, M., Malhi, S.S., Solberg, E.D., Jans-Hammermeister, D., Stewart, B.A., 1998. Modeling tillage and surface residue effects on soil C storage under ambient versus elevated CO_2 and temperature in *ECOSYS*. In: Lal, R., Kimble, J.M., Follet, R.F. (Eds), Soil processes and carbon cycle. CRC Press Inc. Boca Raton, USA, pp. 527-547.

Grant, R.F., Amrani, M., Heaney, D.J., Wright, R., Zhang, M., 2004. Mathematical Modeling of Phosphorus Losses from Land Application of Hog and Cattle Manure. Journal of Environmental Quality 33, 210-231.

Grant, R.F., Pattey, E., Goddard, T.W., Kryzanowski, L.M., Puurveen, H., 2006. Modeling the effects of fertilizer application rate on nitrous oxide emissions. Soil Science Society of America Journal 70, 235-248.

Grundmann, G. L., Renault, P., Rosso, L., Bardin R., 1995. Differential effects of soil water content and temperature on nitrification and aeration. Soil Science Society of America Journal 59, 1342– 1349.

Havlin, J.L., Beaton, J.D., Tisdale, S.L., and Nelson, W.L., 1999. Soil fertility and fertilizers. An introduction to nutrient management. Sixth Edition. Prentice Hall: New Jersey.

Helgason, B.L., Janzen, H.H., Angers, D.A., Boehm, M., Bolinder, M., Desjardins, R.L., Dyer, J., Ellert, B.H., Gibb, D.J., Gregorich, E.G., Lemke, R., Massé, D., McGinn, S.M.,

McAllister, T.A., Newlands, N., Pattey, E., Rochette, P., Smith, W., VandenBygaart, A.J., Wang, H., 2005. GHGFarm: An assessment tool for estimating net greenhouse gas emissions fromCanadian farms. Agriculture & Agri-Food Canada, pp. 5-6.

Hénault, C., Devis, X., Page, S., Justes, E., Reau, R., Germon, J.C., 1998. Nitrous oxide emissions under different soil and land management conditions. Biology and Fertility of Soils 26, 199-207.

Hutchinson, G.L., Livingston, G.P., Healy, R.W., Striegl, R.G., 2000. Chamber measurement of surface-atmosphere traces gas exchange: Numerical evaluation of dependence on soil, interfacial layer, and source/sink properties. Journal of Geophysical Research 105, 8865-8875.

Hutchinson, G.L., Livingston, G.P., 2001. Vents and seals in non-steady-chambers used for measuring gas exchange between soil and the atmosphere. European Journal of Soil Science 52, 675-682.

Huther, L, Schuchardt F, Willke, T, Ahlgrimm, H.J., and Vorlop, K.D. 1997. Methane and nitrous oxide emissions during storage and composting of cattle manure- a study using gas chromatography. Traslation Silsoe Research Institute. 62, 219-2222.

Lee, J, Six, J., King, A.P., van Kessel, C., Rolston, D.E., 2006. Tillage and Field Scale Controls on Greenhouse Gas Emissions. Journal of Environmental Quality 35, 714-725.

Leffelaar, P.A., Wessel., 1998. Denitrification in a homogeneous, closed system: Experiment and simulation. Soil Science 146, 335-349.

Lemke, R.L., Izaurralde, R.C., Malhi, S.S., Arsad, M.A., Nyborg, M., 1998a. Nitrous oxide emissions from agricultural soils of the Boreal and Parkland regions of Alberta. Soil Science Society of America Journal 62, 1096-1102.

Lemke, R.L., Izaurralde, R.C., Nyborg, M., 1998b. Seasonal distributions of Nitrous oxide emissions from soils in the Parkland regions. Soil Science Society of America Journal 62, 1320-1326.

Linn, D. M., Doran, J.W., 1984. Effect of water-filled pore space on carbon dioxide and nitrous oxide production in tilled and nontilled soils. Soil Science Society of America Journal 48, 1267–1272.

Li, C., Frolking, S., Frolking, T.A., 1992. A model of nitrous oxide evolution from soil driven by rainfall events: 1. Model structure and sensitivity. Journal of Geophysical Research 97, 9759-9776.

Li, C., 2000. Modeling trace gas emissions from agricultural ecosystems.. Nutrient Cycling in Agroecosystems 58, 259– 276.

Lu, Y., Huang, Y., Zou, J., Zheng, X., 2006. An inventory of N_2O emissions from agriculture in China using precipitation-rectified emission factor and background emission. Chemosphere 65, 1915-1924.

Lim, B., Boileau, P., Bonduki, Y., van Amstel, A.R., Janssen, L.H.J.M., Olivier, J.G.J., Kroeze, C., 1999. Improving the quality of national greenhouse gas inventories. Environmental Science and Policy 2, 335-346.

Maag, M. and Vinther, F.P. 1999. Effect of Temperature and Water on Gaseous Emissions from Soils Treated with Animal Slurry. Soil Science Society of America Journal 63, 858–865.

Mahli, S.S., and Nyborg, M., 1983. Field study of the fate of fall-applied ^{15}N fertilizers in three Alberta soils. Agronomy Journal 75:71-74.

Mahli, S.S., Nyborg, M., 1988. Control of nitrification of fertilizer nitrogen: effect of inhibitors, banding and nesting. Plant and soil 107, 245-250.

McKenzie, R. 1998. crop nutrition and fertilizer requirements. Alberta Agriculture, Food and Rural Development, Edmonton, Alberta. 10pp. URL: http://www.agric.gov.ab.ca/crops/cer-fertnutrit.html.

McConnaughey, P.K., Bouldin, D.R., 1985a. Transient microsite models of denitrification. I. Model development. Soil Science Society of America Journal 49, 886-891.

McConnaughey, P.K., Bouldin, D.R., 1985b. Transient microsite models of denitrification. II. Model results. Soil Science Society of America Journal 49, 891-895.

McConnaughey, P.K., Bouldin, D.R., 1985c. Transient microsite models of denitrification. III. Comparison of experimental and model results. Soil Science Society of America Journal 49, 896-901.

McTaggart, I.P., Tsuruta, H., 2003. The influence of controlled release fertilisers and the form of applied fertiliser nitrogen on nitrous oxide emissions from an andosol. Nutrient Cycling in Agroecosystems 67, 47–54.

Merrill, A. G., Zak, D.K., 1992, Factors controlling denitrification rates in upland and swamp forests. Canadian Journal of Forest Research 22, 1597– 1604.

Meyer-Aurich, A., Weersink, A., Janovicek, K. Deen, B., 2006. Cost efficient rotation and tillage options to sequester carbon and mitigate GHG emissions from agriculture in Eastern Canada. Agriculture, Ecosystems and Environment 117, 119–127.

Millington, R.J., Quirk, J.M., 1960. Transport in porous media. In: Van Beren, F.A. et al. (Eds.), 7th Trans. Int. Congr. Soil Sci. Vol. 1. Madison, WI. 14-24 Aug. Elsevier, Amsterdam, Science, pp. 97-06.

Muller, C., 1999. Modelling soil-biosphere interactions. CABI Publishing, Wallingford, UK, pp. 52-53.

Myrold, D.D., 1998. Transformation of nitrogen. In: Sylvia, D.M., Fuhrmann, J.J., Hartel, P.G., Zuberer (Eds.). Principles and Applications of soil microbiology. Prentice Hall: Upper Saddle River, New Jersey, pp. 259-294.

Nyborg, M., Laidlaw, J.W., Solberg, E.D., Malhi, S.S., 1997. Denitrification and nitrous oxide emissions from a black Chernozemic soil during spring thaw in Alberta. Canadian Journal of Soil Science 77,153-160.

Olsen, K., Wellisch, M., Boileau, P., Blain, D., Ha, C., Henderson, L., Liang, C., McCarthy, J., McKibbon, S., 2003. Canada's Greenhouse Gas Inventory 1990-2001, pp. 1-4.

Parton, W.J., Mosier, A.R. ojima, D.S. Valentine, D.W. Schimel, D.S. Weier K. Kulmala, A.E., 1996. General model for N_2 and N_2O production from nitrification and denitrification. Global Biogeochemical Cycles 10, 401-412.

Parton, W. J., Holland, E. A., Del Grosso, S. J., Hartman, M. D., Martin, R. E., Mosier, A. R., Ojima, D. S., Schimel, D.S., 2001. Generalized model for NO_x and N_2O emissions from soils, Journal of Geophysical Research 106, 17,403– 17,419.

Pattey E., Desjardins R. L. and Rochette, P., 1993. Accuracy of the relaxed eddy-accumulation technique evaluated using CO_2 flux measurement. Boundary-layer meteorology 66, 341-355.

Pattey, E., Royds, W.G., Desjardins, R.L., Buckley, D.J., Rochette, P., 1996. Software description of a data acquisition and control system for measuring trace gas and energy fluxes by eddy-accumulation and correlation techniques. Computers and Electronics in Agriculture 15, 303-321.

Pattey E., Desjardins, R.L. Wesberg, H., Lamb, B., Zhu, T., 1999. Measurement of isoprene emissions over a black spruce stand using tower-based eddy-accumulation system. Journal of Applied Meteorology 38, 870-877.

Pattey, E., Strachan, I.B., Desjardins, R.L. Massheder, J., 2002. Measuring nighttime CO_2 flux over terrestrial ecosystems using eddy covariance and nocturnal boundary layer methods. Agriculture & Forest Meteorology 113, 145-153.

Pattey, E., Edwards, G.C., Strachan, I.B., Desjardins, R.L., Kaharabata, S., Wagner-Riddle, C., 2006a. Towards standards for measuring greenhouse gas flux from agricultural fields using instrumented towers. Canadian Journal of Soil from agricultural fields using instrumented towers. Canadian Journal of Soil Science 86, 373-400.

Pattey, E., Strachan, I.B., Desjardins, R.L., Edwards, G.C., Dow, D., MacPherson, J.I., 2006b Application of a tunable diode laser to the measurement of CH_4 and N_2O fluxes from field to landscape scale using several micrometeorological techniques. Agriculture & Forest Meteorology 13, 222-236.

Pattey E., Edwards, G.C., Desjardins, R.L., Pennock, D., Smith W., Grant, B., MacPherson, J.I., 2007. Tools for quantifying N_2O emissions from Agroecosystems. Agriculture & Forest Meteorology 142(2-4), 103-119.

Paul, E. A., Clark, F.E., 1989. Soil Microbiology and Biochemistry, Academic, San Diego, Califonia.

Pennock, D.J., van Kessel, C., Farrell, R.E., Sutherland, R.A., 1992. Landscape-scale variations in denitrification. Soil Science Society of America Journal 56, 770-776.

Pennock, D.J., Corre, M.D., 2001. Development and application of landform segmentation procedures. Soil & Tillage Research 58, 151-162.

Phillips, F.A, Leuning, R., Baigent, R., Kelly, K.B., Denmead, O.T. 2007. Nitrous oxide flux measurements from an intensively managed irrigated pasture using micrometeorological techniques. Agricultural & Forest Meteorology 143, 92–105.

Prosser, J. I., 1989. Autotrophic nitrification in bacteria, Adv. Microb. Physiol., 30, 125–181.

Reinertsen, S.A., Elliott, L.F., Cochran, V.L., Campbell, G.S., 1984. Role of available carbon and nitrogen in determining the rate of wheat straw decomposition. Soil Biology & Biochemistry 16, 459-464.

Rochette, P., McGinn, S.M., 2005. Methods for measuring soil-surface gas fluxes. In: Handbook of Applied Techniques for Characterizing Processes in the Soil Environment. Alvarez-Benedí, J. and MuZoz-Carpena, R. (Eds.) CRC Press, in press.

Roelandt, C., Dendoncker, N., Rounsevell, M., Perrin, D. and Van Wesemael, B. 2007. Projecting future N_2O emissions from agricultural soils in Belgium. Global Change Biology 13, 18-27.

Röver, M., Heinemeyer, O., Munch, J.C., Kaiser, E.-A., 1999. Spatial heterogeneity within the plough layer: high variability of N_2O emissions rates. Soil Biology & Biochemistry 31, 167-173.

Sextone, A.J., Revsech, N.P., Parkin, T.B. Tiedje, J.M., 1985. Direct measurement of oxygen profiles and denitrification rates in soil aggregates. Soil Science Society of American Journal 49, 645-651.

Simek, M., Cooper, J.E., 2002. The influence of soil pH on denitrification: Progress towards the understanding of this interaction over the last 50 years. European Journal of Soil Science 53, 345– 354.

Strong, D. T., Fillery, I.R.P., 2002. Denitrification response to nitrate concentrations in sandy soils. Soil Biology & Biochemistry 34, 945– 954.

Thornton, F.C., Bock, B.R., Tyler, D.D., 1996. Soil emissions of nitric oxide and nitrous oxide from injected anhydrous ammonium and urea. Journal of Environmental Quality 25, 1378-1384.

Tiedje, J. M., 1988. Ecology of denitrification and dissimilatory nitrate reduction to ammonium, in Biology of Anaerobic Microorganisms, edited by A. J. B. Zehnder, pp. 179–244, John Wiley, Hoboken, N. J.

van den Pol-van Dasselaar, A., Corre, W.J., Prieme, A., Klemedtsson, A.K., Weslien, P., Stein, A., Klemedtsson, L., Oenema, O., 1998. Spatial variability of methane, nitrous oxide and carbon dioxide emissions from drained grasslands. Soil Science Society of America Journal 62, 810-817.

Van Melle, B.M., Knight, J.D., Schoenau, J.J. and Farrell, R.E. 1999. Nitrous oxide emissions from fall- applied manure. Proceedings from the soil and sir quality connection: 36th Annual Alberta Soil Science Workshop, February 1999. Alberta Soil Science Workshop, Edmonton AB, pp. 253-256.

Velthof, G.L., Jarvis, S.C., Stein, A., Allen, A.G., Oemems, O., 1996. Spatial variability of nitrous oxide fluxes in mown a grazed grasslands on a poorly drained clay soil. Soil Biology & Biochemistry 28, 1215-1225.

Wagner-Riddle, C., Thurtell, G.W., Kidd, G.E., Edwards, G.C., Simpson, I.J., 1996. Micrometeorological measurements of trace gas fluxes and natural ecosystems. Infrared Physics and Technology 37, 51-158.

Weier, K. L., Doran, J. W., Power, J. F., Walters, D.T., 1993. Denitrification and the dinitrogen/nitrous oxide ratio as affected by soil water, available carbon, and nitrate. Soil Science Society of America Journal 57, 66– 72.

CHAPTER 2.0: Modeling temporal variability of N_2O emissions from a fertilized agricultural soil using the *Ecosys* mathematical model (site scale: 1 < m^{-2})

2.1 INTRODUCTION

In 2001, N_2O emissions were estimated to account for 60% of the total CO_2-equivalent greenhouse gas emissions from the agricultural sector in Canada (Olsen et al., 2003). Canada is committed to reduce its total greenhouse gas emissions to 6% below 1990 levels over the period 2008 to 2012, under the Kyoto Protocol (Olsen et al., 2003). Current Intergovernmental Panel of Climate Change (IPCC) Tier I methodology for quantifying N_2O in greenhouse gas inventories, is based on a constant emission factor (EF) of 1% for all N inputs (Eggleston, 2006). However, uncertainties in estimates of N_2O emissions by IPCC guidelines may be 70% to 80% in arable soil at a national scale (Lim et al., 1999). This uncertainty may be attributed to large spatial and temporal variability of N_2O emissions (e.g. Pennock et al., 1992; Pennock and Corre, 2001; Grant and Pattey, 2003). An IPCC Tier II Methodology is now being used for Canada. It uses lower EFs (0.1 - 0.7%) in drier climates such as the Prairies and higher EFs (0.83 - 1.67%) for the more humid regions of Eastern Canada (Hegalson, 2005).

Mathematical models can improve N_2O emission estimates by contributing towards the continuity of measured data by estimating fluxes where measured data are missing. However, before these estimates can be made, we first need a process-based understanding of the complex biological, physical and chemical processes involved in the production of N_2O in agricultural soils at site scale (< 1 m^2), and then at larger spatial scales such as field scale (> ha). To achieve this, we need to derive quantitative, testable hypotheses from basic scientific theory for a comprehensive range of processes believed

to control N_2O fluxes at different spatial scales. This chapter discusses the testing of the *ecosys* (Grant, 2001a,b) mathematical model to simulate N_2O emissions at the **site scale.** Chapters 4 and 5 describe testing of the model at larger spatial scales. Because of the uncertainties associated with using the current IPCC Tier I and Tier II Methodologies (Eggleston, 2006), mathematical models such as *ecosys* (Grant, 2001a,b: website: www.ecosys.rr.ualberta.ca), can contribute towards the development of more site - specific emission factors needed for an IPCC Tier III methodology.

Temporal variability in N_2O fluxes is large, with highly skewed frequency distributions and coefficients of variation > 150% at diurnal time scales (e.g. Flessa et al., 1995; Thornton et al. 1996). N_2O emissions from soils are produced from the microbiological processes of nitrification and denitrification (e.g. Henault et al., 1998; Myrold, 1998). Nitrification is most rapid when O_2 is sufficient (water contents near or below field capacity, $\approx$ 60% WFPS), whereby NH_3 is oxidized to NO_2^- then to NO_3^- and O_2 is reduced to H_2O by nitrifying bacteria. However, under O_2-limiting conditions (e.g. after rainfall when 90% > WFPS > 60%), in a process called "nitrifier denitrification", ammonium oxidizers containing nitrite reductase may reduce NO_2^- as an alternative electron acceptor to produce NO and N_2O (Muller, 1999; Myrold, 1998). Denitrifiers can oxidize reduced C to CO_2 and reduce O_2 to H_2O under non-limiting O_2 conditions. When O_2 is insufficient (> 60% WFPS) to meet the demands of microbes, NO_3^- (e.g. from nitrification, fertilizer, residual N) becomes the alternative electron acceptor to O_2 and is reduced in a series of steps ($NO_3^- \rightarrow NO_2^- \rightarrow N_2O \rightarrow N_2$) via denitrification. Davidson (1991) showed that greatest N_2O production occurs within the range of 60 –

80% WFPS.

Transitions from one reduction reaction to another can be caused by small changes in soil WFPS ("threshold response"). This occurs because the diffusivity (D_g) of O_2 (and other gases) in the soil atmosphere varies according to a power function of the soil air-filled porosity (θ_g) (Millington, 1960), which in turn depends on WFPS. This variation is such that, at certain WFPS values small declines in θ_g can cause large declines in D_g that may limit O_2 gaseous transfer to microsites causing a greater demand for alternative election acceptors. As a result, these small declines may cause a transition from the reduction of O_2 to that of NO_x by nitrifiers and denitrifiers, increasing N_2O production. Temporal variation in WFPS, therefore, strongly influences variation in N_2O emissions. A review by Bouwman et al. (2002) showed that N_2O emissions from poorly drained soils exceeded those from well-drained soils in all cases.

At very high WFPS following rainfall, N_2O produced from denitrification usually accumulates in the aqueous phase of the soil profile so that N_2O emissions are delayed. Because of low D_g, N_2O can be emitted as large bursts 20-24 hours after rainfall (e.g. Wagner-Riddle et al., 1996) or during spring thaw (Grant et al., 1992; Nyborg et al., 1997; Grant and Pattey, 1999; Pattey et al., 2007). This occurs because, as soil water drains and evaporates, water is lost from soil macro-pores, increasing θ_g. Gaseous diffusivity increases rapidly, which leads to rapid N_2O volatilization and emission from the soil. Eventually, as the θ_g increases further and O_2 replaces NO_x as the terminal electron acceptor, N_2O emissions return to ambient levels several days after an emission

event (Grant and Pattey, 2003). Since N_2O is produced via nitrification and denitrification, alternating oxic and anoxic soil conditions are necessary for N_2O emissions.

Ecosys (Grant, 2001a,b), the most detailed ecosystem model available, was used for this study because it accounts for the major hypotheses for N_2O transformations and it captures the large temporal variability of N_2O at high temporal and spatial resolution, under site-specific conditions such as climate, soil type, land use etc. *Ecosys* explicitly represents the oxidation-reduction reactions from which N_2O is generated and the gas transfer processes which control the transition between alternative reduction reactions. In *ecosys*, the key biological processes – mineralization, immobilization, nitrification, denitrification, root and mycorrhizal uptake controlling N_2O generation are coupled to the key physical processes – convection, diffusion, volatilization, dissolution - controlling the transport of gaseous reactants and products of these biological processes (Grant et al., 2006). Other models have been used to estimate N_2O emissions for Europe (Freibauer, 2003) and European countries (Flechard et al., 2007; Roelandt et al., 2007; Gabrielle, 2006) but, these models are empirical and, therefore, may not fully represent the complex processes involved in N_2O generation. In other cases, the energetics of microbial oxidation-reduction reactions driven by alternative electron acceptors under aerobic vs. anaerobic conditions, are not included (Li et al., 1992), as they are in *ecosys*. Other models (e.g. Gabrielle et al., 2006) simulate N_2O at a daily time-step which does not allow testing at an hourly time-step, which is necessary to capture the large spatial and temporal variability of N_2O (Grant and Pattey, 2003). However, *ecosys* can be tested at

hourly, daily and monthly time-steps.

Simulation of nitrificiation and denitrification in *ecosys* is sensitive to soil air-filled porosity (θ_g), which in turn depends on WFPS. Transitions from one reduction reaction to another can be caused by small changes in soil WFPS as well as temperature (Grant and Rochette, 1994; Grant, 1995). However, in some current models (e.g. Lu et al., 2006), the response is linear. *Ecosys* can therefore capture the non-linear (threshold) response of N_2O production to changes in WFPS.

Simulation of nitrificiation and denitrification in *ecosys* is also based on Michaelis-Menten kinetics whereas other models (e.g. Molina et al., 1983 and Clay et al., 1985) simulate denitrification based on first order kinetics with respect to soluble C or NO_3^- (e.g. Rolston et al., 1984 and Rao et al., 1984) as modified by dimensionless factors of temperature and WFPS. The Michaelis-Menten kinetics used in *ecosys* is an advantage because it enables the model to simulate the sensitivity of nitrificiation and denitrification thus of, N_2O emissions to different past (soil residual N/ initial N concentration) and current fertilizer N application (non-linear response). Some models impose constraints either on the magnitude of N_2O produced from nitrification (Li et al., 2005) or on the magnitude of N_2O emitted during snow cover (Li et al., 1992), even if environmental conditions favour higher emissions. However, in *ecosys*, there are no set constraints placed on N_2O production.

Ecosys also models surface energy exchange and subsurface heat transfer, vertical

(infiltration, drainage, root uptake and capillary rise) and lateral (driven by differences in topographic position) movement of water and solutes within complex landscapes, and the effect of soil temperature and water on microbiological activity and gas exchange (Grant and Pattey, 2003; Grant, 2004). The model can integrate temporal scales from seconds to centuries, allowing validation against data from experiments that range from short-term laboratory incubations to long-term field studies. *Ecosys* can also integrate spatial scales ranging from mm to km in 1, 2 or 3 dimensions by representing state and rate variables according to their west to east (x), north to south (y) and vertical (z) positions in a complex landscape, allowing the scaling up of microscale phenomena to the landscape scale. *Ecosys* has the potential, therefore, to give better N_2O EFs to contribute towards the development of an IPCC Tier III methodology.

The objective of this research was to test the **hypothesis in *ecosys* (Grant, 2001a,b) that N_2O production increases sharply (threshold, non-linear response) at 90% > WFPS > 60%. It was proposed that the non-linear response of D_g (Millington and Quirk, 1960) of O_2 to changes in WFPS can be used to explain the sudden rise/threshold/ non-linear response of N_2O emissions commonly observed in the field, whereby N_2O emissions rises with WFPS > 60%. This occurs because at WFPS < 60% in the model, the D_g (Eq. [2.28]) of O_2 is large enough to meet microbial demands. However, as WFPS increases above 60%, the D_g (Eq. [2.28]) of O_2 declines sharply and the unmet O_2 demand forces the need for alternative electron acceptors (Eqs. [2.10] – [2.18]) thus, higher N_2O production via nitrification (Eq. [2.10]) and denitrification (Eq. [2.18]) in the model.** The D_g of O_2 therefore controls the demand

and supply of O_2 (electron acceptor) in the soil. Studies by Grant (1991) have shown that transitions from one reduction reaction to another can be caused by very small changes in soil H_2O content. Many current N_2O estimates are based on discrete chamber measurements, but, there may be a bias when these measurements are aggregated for inventories compared to those of continuous measurements. This bias is directly related to the episodic nature of N_2O emissions (large temporal variation) as described above, as a result of sensitivity to weather (precipitation and temperature). Consequently, temporal aggregations of N_2O emissions over 24 hours calculated solely from a few measured fluxes may be overestimated, if the measurements were taken only during peaks of emission events. A study by Pattey et al. (2007) showed that estimates were lower when continuous 30-min flux data from a micrometeorological tower were used compared to estimates calculated from data collection frequencies of once day^{-1} and twice and once $week^{-1}$. Bouwman et al. (2002) showed that high frequency measurements ($> 1\ d^{-1}$) gave lower estimates of N_2O emissions than did time-integrated emissions of low frequency measurements ($< 1\ d^{-1}$). It is therefore important for mathematical models to capture the large temporal variability of N_2O at an appropriate time-step (e.g., hourly).

Application of nitrogenous fertilizers is another important factor which affects EF for N_2O inventories. In conventional agriculture, enhanced N_2O emissions are often associated with large applications of mineral fertilizers (e.g. Smith et al., 1998) because they provide a source of NH_4^+ and NO_3^- for nitrification/denitrification. N_2O emissions due to chemical fertilizer use have been estimated to range from 0.03 to 2.0 Tg N yr^{-1} (Matthews 1994). It is suggested that agriculture's contribution to global N_2O loading

from 1986 to 2026 will increase by 90%, mainly due to N fertilizers (Isermann, 1994). The nature of N_2O emission response to fertilizer N application is variable. Grant et al. (2006) showed that N_2O emission factors rose non-linearly with fertilizer application rate once this rate exceeded the crop and soil uptake capacities for added N. However, a review by Barnard et al. (2005), suggests that the response of N_2O flux to N addition was highly variable, and there was no clear correlation with the amount of N added. Some of the studies for this review showed that application of N fertilizer at high rates resulted in little increase in N_2O emissions because fluxes may be already at near maximum rates due to N saturation of the system. Grant et al. (2006) also found that the relationship between N_2O emissions and current fertilizer inputs, depended on residual N left from earlier N inputs.

Soil residual N depends on the agricultural history of a plot e.g., past fertilizer management and cropping system. Because N_2O production is driven by soil residual N (controls availability of alternative electron acceptors e.g. NH_4^+, NO_3^-), then rises in N_2O emissions will depend on rises in soil residual N. **It is hypothesized in *ecosys* (Grant, 2001a,b) that these rises occur in stages (non – linear response) (Figure 2-1) upon fertilizer N addition and can be explained by the immobilization capacity of the ecosystem (Grant et al., 2006):-**

Stage 1: Low initial soil residual N, then low rise in N_2O emissions upon fertilizer application. The model explanation for this trend is that when soil residual N is low due to low rates of past fertilizer application, current fertilizer N added (Figure 2-1;

AB) will largely be immobilized (crop and soil uptake capacity) (N limited) (Grant et al., 2006) (Figure 2-1; B'). Consequently, low soil residual N remains, thus low N_2O production via nitrification (Eq. [2.10]) and denitrification (Eq. [2.18]) in the model (Figure 2-1; AB').

Stage 2: Higher initial soil residual N, then higher rise in N_2O emissions upon fertilizer application. The model explanation for this trend is that when soil residual N is higher due to larger rates of past fertilizer application, less of the current fertilizer N added (Figure 2-1; BC) will be immobilized compared to that of the Stage 1 response, due to the addition of N greater than the immobilization capacity of the ecosystem (Grant et al., 2006) (Figure 2-1; C'). Consequently, higher soil residual N remains, thus higher rises in N_2O production via nitrification (Eq. [2.10]) and denitrification (Eq. [2.18]) in the model (Figure 2-1; BC').

Stage 3: Very high initial soil residual N, then low rise in N_2O emissions upon fertilizer application. The model explanation for this trend is that when soil residual N is very high due to very large rates of past fertilizer application, N_2O emissions are already high and even less of the current fertilizer N added (Figure 2-1; DE) will be immobilized (Figure 2-1; E'). Consequently, very high soil residual N remains but little further increase in N_2O production occurs because of an N excess in the ecosystem, which lead to the maximum rate for N_2O production via nitrification (Eq. [2.10]) and denitrification (Eq. [2.18]) in the model (Figure 2-1; DE'). Little N_2O production in this stage could be attributed to another source of

limitation e.g. C limitation.

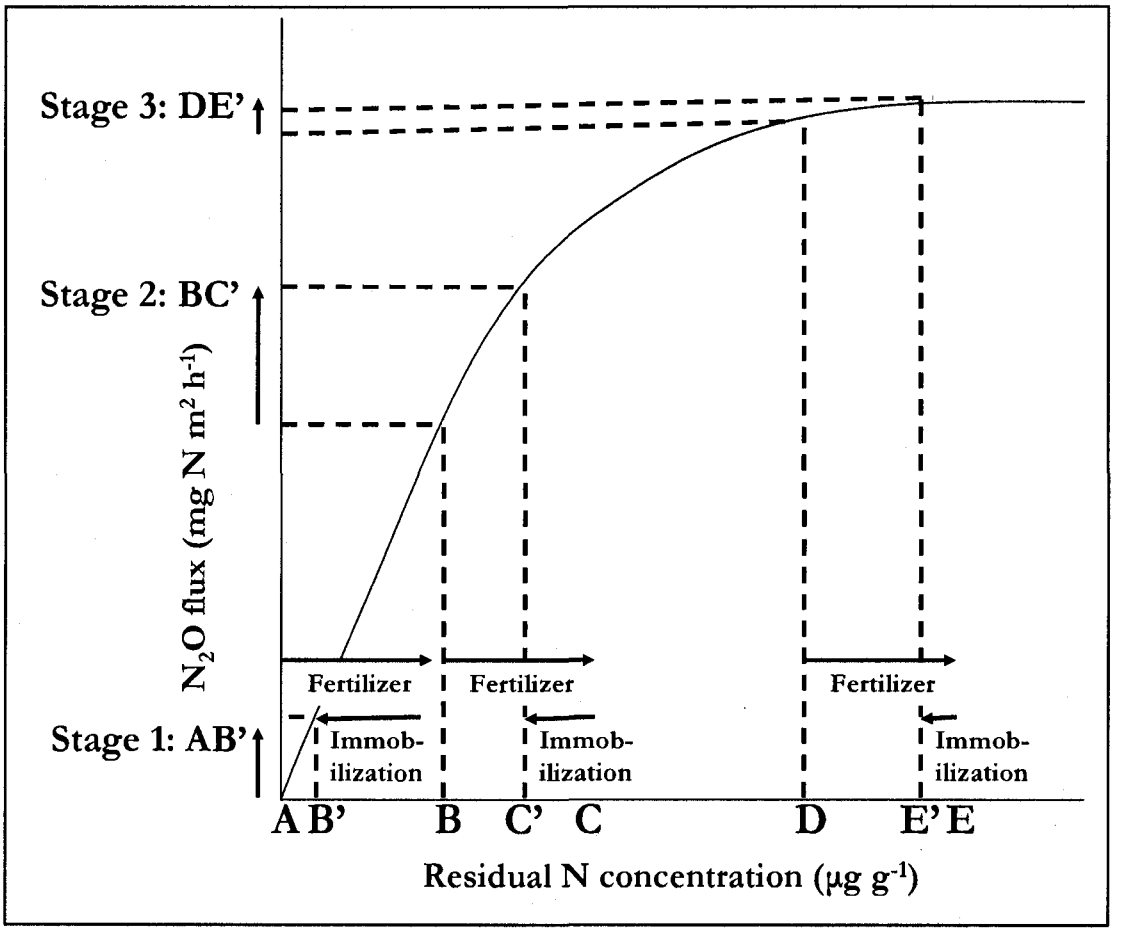

Figure 2-1: Hypothesis in *Ecosys* (Grant, 2001a,b) - Rises in N_2O emissions occurs in stages (non – linear response) upon fertilizer N addition and can be explained by the immobilization capacity of the ecosystem (Grant et al., 2006).

These stages follow a Michaelis-Menten response whereby emissions increase non-linearly with increasing amounts of mineral N up to a maximum reaction rate.

Consequently, an EF for a given fertilizer rate can vary depending on initial soil residual N and C (immobilization capacity). As a result, an addition of a given unit of fertilizer does not necessarily result in a proportional increase in N_2O emissions (Figure 2-1). EFs in N_2O inventories therefore need to account for the initial soil residual, to capture this non-linear rise of N_2O emissions with fertilizer N addition. This chapter describes the testing of *ecosys* to simulate a Stage 3 response of N_2O emissions to fertilizer N addition. *Ecosys* was also tested to simulate Stage 1 and 2 responses of N_2O to fertilizer N addition (Chapter 3).

Ecosys has been used to model N_2O emissions at various scales from laboratory experiments (Grant, 1991; Grant et al., 1992; Grant et al., 1993c; Grant, 1994; Grant; 1995) to agricultural field experiments using micrometeorological towers (Grant and Pattey, 1999; Grant and Pattey, 2003; Grant et al., 2006). For this research, *ecosys* was further tested under controlled laboratory conditions at site scale in order to better understand this "threshold" response of N_2O under transient aerobic and anaerobic conditions caused by temporal changes in WFPS. Also in the laboratory, the sensitivity of N_2O emissions to fertilizer application to a soil with high residual N was investigated. Testing *ecosys* to model N_2O at the smaller spatial scales first, will later improve confidence at larger spatial scales (e.g. regional and national) for inventories.

2.2 MODEL DESCRIPTION

2.2.1 Introduction

The *ecosys* (Grant, 2001a,b) model can simulate the transport and transformation of heat, water, C, O_2, N, phosphorus (P) and ionic solutes through soil-plant-atmosphere systems with the atmosphere as the upper boundary and soil parent material as the lower boundary. All rate and state variables are defined by their x, y, z position but this is omitted in the following description of these variables for the sake of clarity. The inputs required for this model are:-

(1) Site (geographic, atmospheric and site characteristics).

(2) Topography (slope, aspect, surface roughness).

(3) Soil (depth, bulk density, water content at field capacity and wilting point, vertical and horizontal saturated hydraulic conductivity, texture, organic C, N and P, pH).

(4) Weather (half-hourly, hourly or daily radiation, temperature, wind-speed, humidity and precipitation).

(5) Soil Management (tillage, fertilizer and irrigation) and

(6) Plant Management (planting and harvest dates; crop species – plant functional type, CO_2 kinetics, phenology/morphology, root and organ characteristics and water relations).

Output data are state and rate variables for C, N, P, H_2O and heat in soils and vegetation at hourly and daily time steps.

2.2 Hypotheses for N_2O transformations in *ecosys*

For full details of hypotheses for N_2O transformations in *ecosys*, refer to Grant and Pattey (2003) and Grant et al. (2006).

2.2.1 Microbial functional types & stages of N_2O response to fertilizer N addition in ecosys

There are five (5) organic states in the model among which C, N and P may move: solid substrate, soluble substrate (Dissolved organic carbon (DOC) from hydrolysis and fermentation products), sorbed substrate, microbial biomass and microbial residues. These exist within each of 5 substrate-microbe complexes: coarse woody residue, fine non-woody residue, manure, particulate organic C and humus. Each state within each complex is resolved into functional types (e.g. microbial biomass is resolved into functional types - obligate aerobic bacterial heterotrophs, facultative anaerobic denitrifier heterotrophs, fungi, anaerobic fermenters plus H_2-producing acetogens, methanogens, and methanotrophs, autotrophic nitrifiers and non-symbiotic diazotrophs) and kinetic components (e.g., plant residue is resolved into protein, soluble carbohydrate, cellulose, and lignin), each of which is further resolved into elemental fractions (C,N,P) (Grant and Pattey, 2003).

The C and N litterfall (e.g. Grant, 2004) in *ecosys* (Grant, 2001a,b) affect the C:N ratio in the DOC and dissolved organic nitrogen (DON) state variables (Figure 2-2 shows a summary of the major hypotheses for N_2O transformations in *ecosys*, with reference to equations). Each microbe functional type in each substrate-microbe complex in *ecosys*

(Grant, 2001a,b) seeks to conserve its C/N ratio during growth by mineralizing NH_4^+ or by immobilizing NH_4^+ or NO_3^- (Eqs. [A1a] – [A1c]) of Grant et al., 2006). These reactions control soil mineral N concentrations which in turn drive nitrification (Eqs. [2.1] – [2.11]) and denitrification (Eqs. [2.12] – [2.20]) reactions in the model. If modeled soil residual N (determined by the agricultural history of the site) is low, then fertilizer N application may lead to microbial immobilization of NH_4^+ or NO_3^- (Eqs. [A1a] – [A1c]) of Grant et al., 2006), thus little N will be available for nitrification (Eqs. [2.1] – [2.11]) and denitrification (Eqs. [2.12] – [2.20]) reactions (**Stage 1** response). The immobilization or ecosystem (crop and soil uptake) N capacity (Grant et al., 2006) therefore may be sufficient to immobilize most of the added N (N limitation) in a **Stage 1** response. Ecosystem N capacity in *ecosys* (Grant et al., 2006) includes (1) soil N uptake capacities - immobilization (Eq. [A1] in Grant et al., 2006), volatilization (Eq. [A29] in Grant et al., 2006), emission (Eqs. [A33], [A36] in Grant et al., 2006) and (2) plant N uptake capacities - (Eq. [A1] in Grant et al., 2006).

When fertilizer is applied to a soil with higher residual N levels, and if this fertilizer rate exceeds the immobilization capacity of the ecosystem, then microbes may mineralize NH_4^+ or NO_3^- (Eqs. [A1a] – [A1c]) of Grant et al., 2006). Consequently, there will be greater oxidation of NH_3 and reduction of O_2 by nitrifiers to produce NO_2^- (Eqs. [2.1] – [2.4]) and this will drive the larger oxidation of NO_2^- and reduction of O_2 by nitrifiers (Eqs. [2.5] – [2.8]) to produce NO_3^-. Under O_2-limiting conditions, NH_3 may then be oxidized and NO_2^- reduced by nitrifiers (Eqs. [2.9] – [2.11]) to produce N_2O (**Stage 2** response - transition from N to C limitation (Grant et al., 2006)). Also, under O_2 limiting

conditions, NO_3^- (Eqs. [2.8]) produced from nitrification or from other sources (e.g., fertilizers) may then be denitrified (Eqs. [2.12] – [2.20]) to produced N_2O.

Ecosys (Grant, 2001a,b) also includes a **Stage 3** response, since the presence of very high residual N levels can lead to high N_2O emissions. However, upon fertilizer application there may be little further increase in N_2O emissions because N saturation of the ecosystem may lead to near maximum reaction rates for nitrification/denitrification (Eqs. [2.1] – [2.20]) according to the Michaelis-Menten kinetics (Eqs. [2.1], [2.3b], [2.5], [2.7b], [2.10], [2.12], [2.14b], and [2.17] - [2.19] (C limitation). Other models (e.g. Molina et al., 1983 and Clay et al., 1985) simulate denitrification based on first order kinetics with respect to soluble C or NO_3^- (e.g. Rolston et al., 1984 and Rao et al., 1984) as modified by dimensionless factors of temperature and WFPS. Thus, *ecosys* would test the integrated hypothesis above, that is, the immobilization capacity of an ecosystem.

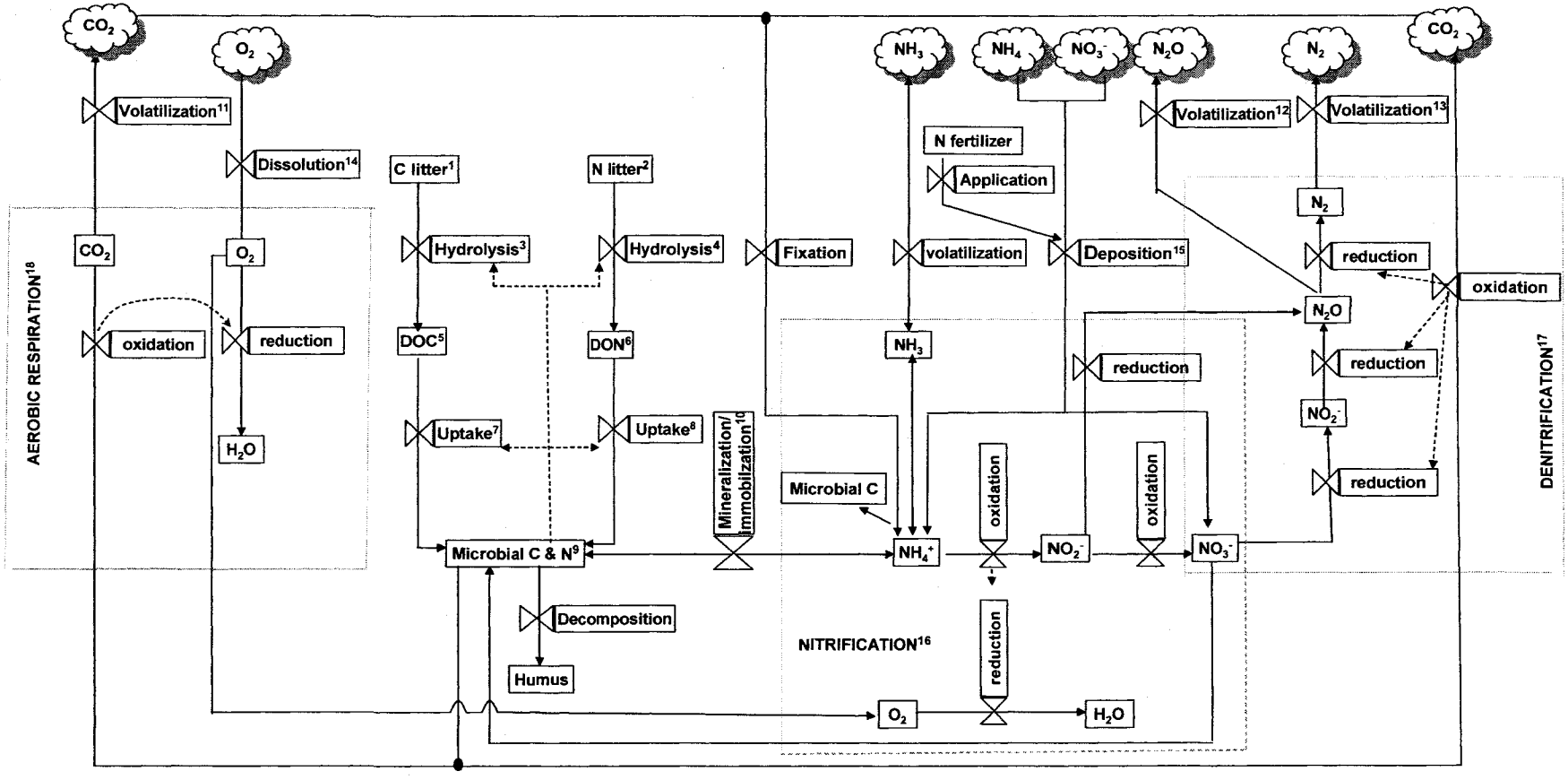

Figure 2-2: Major hypotheses for N_2O transformations in *ecosys*.
References: Example [1-9]Eqs. [8] –[9] of Grant, 2004, [10]Eqs. ([A1a-A1c] of Grant et al. 2006, [11-15] Eq. [A30] in Grant et al., 2006, [16]Eqs. [1] – [11], [17]Eqs. [12] – [15], [18]Eqs. [16] – [20] of Model Decription.

2.2.2.2 Nitrification

2.2.2.2.1 Oxidation of Ammonia and Reduction of Oxygen by Nitrifiers

NB – Key model inputs are given in bold face

NH_3 oxidation under non-limiting O_2 is calculated from active nitrifier biomass and from NH_3 and CO_2 concentrations:

$$X'_{NH3i,n} = \boldsymbol{X'_{NH3}}\, M_{i,n,a}\, \{[NH_{3s}]/([NH_{3s}] + \boldsymbol{K_{NH3n}})\}\, \{[CO_{2s}]/([CO_{2s}] + \boldsymbol{K_{CO2}})\}\, f_t \qquad [2.1a]$$

Where:

$X'_{NH3i,n}$ is the rate of NH_3 oxidation by $M_{i,n,a}$ under non-limiting $[O_{2s}]$ (g N m^{-2} h^{-1})
$\boldsymbol{X'_{NH3}}$ is the specific rate of NH_3 oxidation by $M_{i,n,a}$ at 25°C under non-limiting $[O_{2s}]$ (0.625 g N g^{-1} $M_{i,n,a}$ h^{-1}, Belser and Schmidt, 1980)
$M_{i,n,a}$ is the active biomass (component *a*) of NH_3 oxidizer (functional type *n*) (g C m^{-2}) in substrate-microbe complex *i* (Grant et al., 1993a, 1993b)
$[NH_{3s}]$ is the aqueous concentration of NH_3 (g m^{-3})
$\boldsymbol{K_{NH3n}}$ is the Michaelis-Menten constant for oxidation of NH_{3s} by $M_{i,n,a}$ (0.01 g N m^{-3}, Suzuki et al., 1974)
$[CO_{2s}]$ is the aqueous CO_2 concentration (g C m^{-3})
$\boldsymbol{K_{CO2}}$ is the Michaelis-Menten constant for reduction of CO_{2s} by $M_{i,n,a}$ and $M_{i,o,a}$ (0.15 g C m^{-3})
f_t is the (Arrhenius) temperature function for microbial processes (e.g. Grant et al., 1990; Grant, 1991; Grant, 1992; Grant et al., 1993a; Grant, 1994; Grant and Rochette, 1994; Grant, et al.1995; Grant, 2001a)

$$f_t = T_l\, \{e^{[A\text{-}H_a/(RT_l]}\} / \{1+e^{[(H_{dl}\text{-}ST_l)/(RT_l)]} + e^{[(ST_l\text{-}H_{dh})/(RT_l)]}\} \text{ (Grant, 2001a)} \qquad [2.2b]$$

Where:

T_l is the soil temperature layer *l* (K)
A is the parameter such that $f_t = 1.0$ at $T_l = 303.15$K
H_a is the energy of activation (J mol^{-1})
R is the gas constant (J $mol^{-1}K^{-1}$)
H_{dl} is the energy of low-temperature deactivation (J mol^{-1})
S is the change in entropy (J $mol^{-1}K^{-1}$)
H_{dh} is the energy of high-temperature deactivation (J mol^{-1})

O_2 reduction under non-limiting O_2 is then calculated from Eq. [2.1] using set respiratory quotients:

$$R'_{O2i,n} = \boldsymbol{RQ}_{NH3} X'_{NH3i,n} + \boldsymbol{RQ}_{C} X'_{Ci,n} \quad [2.2]$$

Where:

$R'_{O2i,n}$ is the rate of O_{2s} reduction by $M_{i,n,a}$ under non-limiting $[O_{2s}]$ (g O_2 m^{-2} h^{-1})
$\boldsymbol{RQ}_{NH3}$ is the respiratory quotient for reduction of O_2 coupled to oxidation of NH_{3s} (3.43g O_2 g N^{-1}, Brock and Madigan, 1991)
$\boldsymbol{RQ}_{C}$ is the respiratory quotient for reduction of O_2 coupled to oxidation of fixed C for microbial respiration (2.67 g O_2 g C^{-1}, Brock and Madigan, 1991)
$X'_{Ci,n}$ is the rate of C oxidation by $M_{i,n,a}$ under non-limiting $[O_{2s}]$ (g C m^{-2} h^{-1})

O_2 reduction under ambient O_2 is then calculated from $[O_{2mi,n}]$ at which radial O_2 diffusion through water films of thickness determined by soil water potential ([2.3a]) equals active uptake at nitrifier surfaces driven by Eq. [2.2] ([2.3b]);

$$R_{O2i,n} = 4\pi \, n \, M_{i,n,a} \, D_{sO2} \, [r_m \, r_w/(r_w - r_m)] \, ([O_{2s}] - [O_{2mi,n}]) \quad [2.3a]$$

$$= R'_{O2i,n} \, [O_{2mi,n}]/([O_{2mi,n}] + \boldsymbol{K}_{O2n}) \quad [2.3b]$$

Where:

$R_{O2i,n}$ is the rate of O_{2s} reduction by $M_{i,n,a}$ under ambient $[O_{2s}]$ (g O_2 m^{-2} h^{-1})
n is the concentration of microbial microsites (m^{-3})
D_{sO2} is the aqueous dispersivity-diffusivity of O_2 (m^2 h^{-1})
$\mathbf{r_m}$ is the radius of microbial sphere (10^{-6} m)
r_w is thickness of r_m + water film at current soil water potential (m)
$[O_{2s}]$ is the O_2 concentration in soil solution (g O_2 m^{-3})
$[O_{2mi,n}]$ is the O_2 concentration at $M_{i,n,a}$ surfaces (g O_2 m^{-3})
$\boldsymbol{K}_{O2n}$ is the Michaelis–Menten constant for reduction of O_{2s} by $M_{i,n,.a}$ (0.16 g O_2 m^{-3}, Focht and Verstraete, 1977)

O_2 uptake by nitrifiers $R_{O2i,n}$ is also constrained in Eq. [2.3a] by competition for O_2 uptake with heterotrophic DOC oxidizers, roots and mycorrhizae.

NH_3 oxidation under ambient O_2 is calculated using the results of Eqs. [2.2] and [2.3];

$$X_{NH3i,n} = X'_{NH3i,n}\ R_{O2i,n}/R'_{O2i,n} \qquad [2.4]$$

Where:

> $X_{NH3i,n}$ is the rate of NH_3 oxidation by $M_{i,n,a}$ coupled with reduction of O_2 under ambient $[O_{2s}]$ (g N m^{-2} h^{-1})

The energy yield of NH_3 oxidation drives the fixation of CO_2 for construction and maintenance of microbial biomass $M_{i,n}$ according to construction energy costs of each nitrifier population (Eq. [32] to [34] in Grant and Pattey, 2003).

Aqueous CO_2 and NH_3 concentrations are controlled by heterotrophic oxidation and mineralization of organic substrates and by a pH-dependent equilibrium among $[CO_{2s}]$, bicarbonate concentration $[HCO_3^-]$ and between $[NH_{3s}]$ and $[NH_4^+]$ in soil solution. Equilibrium between $[NH_{3s}]$ and $[NH_{3g}]$, the concentration of NH_3 in the gaseous state (g m^{-3}), is also maintained through volatilization-dissolution and between $[NH_4^+]$ and exchangeable NH_4^+ as part of a solute chemistry sub-model (Grant and Pattey, 2003).

2.2.2.2.2 Oxidation of Nitrite and Reduction of Oxygen by Nitrifiers

Constraints on nitrifier oxidation of NO_2^- imposed by O_2 uptake ([2.5] to [2.8]) are solved in the same way as are those of NH_3 ([2.1] to [2.4]):

$$X'_{NO2i,o} = \boldsymbol{X'_{NO2}}\ M_{i,o,a}\ \{[NO_2^-]/([NO_2^-] + \boldsymbol{K_{NO2o}})\}\ \{[CO_{2s}]/([CO_{2s}] + K_{CO2})\}\ f_t \qquad [2.5]$$

Where:

> $X'_{NO2i,o}$ is the rate of NO_2^- oxidation under non-limiting $[O_{2s}]$ (g O_2 m^{-2} h^{-1})

$\boldsymbol{X'_{NO2}}$ is the specific rate of NO_2^- oxidation by $M_{i,o,a}$ at 25°C under non-limiting $[O_{2s}]$ (2.50 g N g^{-1}, Belser, 1977)
$M_{i,o,a}$ is the active biomass of NO_2^-oxidizers (g C m^{-2})
$[NO_2^-]$ is the concentration of NO_2^- in soil solution (g N m^{-3})
$\boldsymbol{K_{NO2o}}$ is the Michaelis-Menten constant for oxidation of NO_2^- by $M_{i,o,a}$ (10.0 g N m^{-3} , Yoshinari et al., 1977)

$$R'_{O2i,o} = \boldsymbol{RQ_{NO2}}\, X'_{NO2i,o} + \boldsymbol{RQ_C}\, X'_{Ci,o} \qquad [2.6]$$

Where:

$R'_{O2i,o}$ is the rate of O_{2s} reduction by $M_{i,o,a}$ under non-limiting $[O_{2s}]$
$\boldsymbol{RQ_{NO2}}$ is the respiratory quotient for reduction of O_2 coupled to oxidation of NO_2^- (1.14 g O_2 g N^{-1})
$X'_{Ci,o}$ is the rate of C oxidation by $M_{i,o,a}$ under non-limiting $[O_{2s}]$ (g O_2 m^{-2} h^{-1})

O_2 reduction under ambient O_2 is then calculated from $[O_{2mi,n}]$ at which radial O_2 diffusion through water films of thickness determined by soil water potential ([2.7a]) equals active uptake at nitrifier surfaces driven by Eq. [2.6] ([2.7b]);

$$R_{O2i,o} = 4\pi\, n\, M_{i,o,a}\, D_{sO2}\, [r_m\, r_w/(r_w - r_m)]\, ([O_{2s}] - [O_{2mi,o}]) \qquad [2.7a]$$

$$= R'_{O2i,o}\, [O_{2mi,o}]/([O_{2mi,o}] + K_{O2o}) \qquad [2.7b]$$

Where:

$R_{O2i,o}$ is the rate of O_{2s} reduction by $M_{i,o,a}$ under ambient $[O_{2s}]$ (g O_2 m^{-2} h^{-1})
$[O_{2mi,o}]$) is the O_2 concentration at $M_{i,o,a}$ surfaces (g O_2 m^{-3})

NO_2^- oxidation under ambient O_2 is calculated from Eqs. [2.6] and [2.7] ([2.8]);

$$X_{NO2i,o} = X'_{NO2i,o}\, R_{O2i,o}/R'_{O2i,o} \qquad [2.8]$$

Where:

$X_{NO2i,o}$ is the rate of NO_2^- oxidation by $M_{i,o,a}$ coupled with reduction of O_2 under ambient $[O_{2s}]$ (g O_2 m^{-2} h^{-1})

2.2.2.2.3 Oxidation of Ammonia and Reduction of Nitrite by Nitrifiers

The stochiometry, kinetics and energetics of NO_2^- reduction during nitrification (Eq. [30] and Table 1 of Grant and Pattey, 2003) is assumed to be the same as that during denitrification (Eq. [3] and [5] of Grant and Pattey, 2003). The following are the steps for this process:

(1) NO_2^- reduction under non-limiting NO_2^- is calculated from the rate at which electrons demanded by NH_3 oxidation are not accepted by O_2 because of diffusion limitations, forcing a transition to NO_2^- as an alternative electron acceptor ([2.9]):

$$R'_{NO2i,n} = \boldsymbol{E_{NOx}}\, \boldsymbol{f_e}\, (R'_{O2i,n} \text{ (From Eq. [2.3])} - R_{O2i,n}) \qquad [2.9]$$

Where:

> $R'_{NO2i,n}$ is the rate of NO_2^- reduction by $M_{i,n,a}$ under non-limiting $[NO_2^-]$ and $[CO_{2s}]$ (g O_2 m^{-2} h^{-1})
> $\boldsymbol{E_{NOx}}$ is electrons accepted by NO_x vs. O_2 when oxidizing DOC (0.438 g N g O_2^{-1})
> $\boldsymbol{f_e}$ is the fraction of electrons not accepted by O_2 which are transferred to N oxides (0.25, Koike and Hattori, 1975)

(2) NO_2^- reduction under ambient NO_2^- and CO_2 is calculated from Eq. [2.10], competing with oxidation of NO_2^- from [2.8]:

$$R_{NO2i,n} = R'_{NO2i,n}\, \{[NO_2^-]/([NO_2^-] + \boldsymbol{K_{NO2n}})\}\, \{[CO_{2s}]/([CO_{2s}] + \boldsymbol{K_{CO2}})\} \qquad [2.10]$$

Where:

> $R_{NO2i,n}$ is the rate of NO_2^- reduction by $M_{i,n,a}$ under ambient $[NO_2^-]$ and $[CO_{2s}]$ (g O_2 m^{-2} h^{-1})
> $\boldsymbol{K_{NO2n}}$ is the Michaelis-Menten constant for reduction of NO_2^- by $M_{i,n,a}$ (2.5 g N m^{-3}, Yoshinari et al., 1977)

(3) Additional NH_3 oxidation enabled by NO_2^- reduction in Eq. [2.10] is added to that enabled by O_2 reduction from Eq. [2.4]. The energy yield from this oxidation drives the

fixation of additional CO_2 for construction of $M_{i,n}$. The total rate of NH_3 oxidation represented in Eq. [2.11]:

$$X_{NH3i,n} = X_{NH3i,n} \text{ (from Eq.[4])} + E_{NO2}\, R_{NO2i,n} \qquad [2.11]$$

Where:

> $X_{NH3i,n}$ is the rate of NH_3 oxidation by $M_{i,n,a}$ coupled with reduction of $O_2 + NO_2^-$ under ambient $[O_{2s}]$ (g O_2 m^{-2} h^{-1})
> E_{NO2} = ratio of electrons accepted by NO_2^- vs. donated by NH_3 (0.33) (Grant and Pattey, 1999)

2.2.2.2.4 Growth of Nitrifiers

The energy yield of NH_3 and NO_2^- oxidation (Eqs. [2.1] and [2.8] respectively) drives the fixation of CO_2 for maintenance and construction of autotrophic microbial biomass $M_{i,n}$ and $M_{i,o}$ according to construction energy costs of each nitrifier population. This biomass drives further NH_3 and NO_2^- oxidation (Eqs. [2.1] and [2.5]).

2.2.2.3 Denitrification

2.2.2.3.1 Oxidation of DOC and reduction of oxygen by heterotrophs.

Hydrolysis of substrate in the model is driven by the heterotrophic biomass, temperature using Arrhenius function, water content and substrate concentration (Grant, 2001a,b). Oxidation of hydrolyzed products (DOC) under non-limiting O_2 is first calculated in the model from active biomass and DOC concentration:

$$X'_{DOC_{i,h}} = \{\boldsymbol{X'_{DOC}}\, M_{i,h,,a}\, [DOC_i]/([DOC_i]) + \boldsymbol{K_{Xh}}\}\, f_t \qquad [2.12]$$

Where:

$X'_{DOC_{i,h}}$ is the rate of DOC oxidation by $M_{i,h,a}$ under non-limiting $[O_2]$ (g N m^{-2} h^{-1})
$\boldsymbol{X'_{DOC}}$ is the specific rate of DOC oxidation by $M_{i,h,a}$ at 25°C under non-limiting [DOC] and $[O_2]$ (0.125 g C g^{-1} $M_{i,h,a}$ h^{-1}, Shields et al., 1974)
$M_{i,h,a}$ is the active biomass of heterotroph (g C m^{-2}) (functional type h (heterotrophic community) in complex i (substrate-microbe complex) and active component a of substrate-microbe complex (Grant et al., 1993a, 1993b)
$[DOC_i]$ is the concentration of dissolved decomposition products (g C m^{-3})
$\boldsymbol{K_{Xh}}$ is the Michaelis-Menten constant for oxidation of DOC by heterotrophs (36.0 g C m^{-3}, McGill et al., 1981)

O_2 reduction under non-limiting O_2 is then calculated from Eq. [2.12] using a set respiratory quotient:

$$R'_{O2_{i,h}} = \boldsymbol{RQ_C}\, X'_{DOC_{i,h}} \qquad [2.13]$$

Where:

$R'_{O2_{i,h}}$ is the rate of O_{2s} reduction by $M_{i,h,a}$ under non-limiting $[O_{2s}]$ (g O_2 m^{-2})

O_2 reduction under ambient O_2 is calculated from the value of $[O_{2mi,h}]$ at which radial O_2 diffusion through water films of thickness determined by soil water potential ([14a]) equals active uptake at heterotroph surfaces driven by Eq. [2.13] ([2.14b]);

$$R_{O2_{i,h}} = 4\pi\, n\, M_{i,h,a}\, D_{sO2}\, ([O_{2s}] - [O_{2mi,h}])[\mathbf{r_m} r_w/(r_w - \mathbf{r_m})] \qquad [2.14a]$$

$$= R'_{O2_{i,h}}[O_{2mi,h}]/([O_{2mi,h}] + \boldsymbol{K_{O2h}}) \qquad [2.14b]$$

Where:

$R_{O2_{i,h}}$ is the rate of O_{2s} reduction by $M_{i,ha}$ under ambient $[O_2]$ (g O_2 m^{-2} h^{-1})
$[O_{2mi,h}]$ is the O_2 concentration at heterotrophic microsites (g O_2 m^{-3})
$\boldsymbol{K_{O2h}}$ is the Michaelis–Menten constant for reduction of O_{2s} by $M_{i,h,a}$ (0.032g O_2 m^{-3} (Griffin, 1972))

DOC oxidation under ambient O_2 is calculated from Eq. [2.13] and constrained by Eqs. [2.14a] and [2.14b] ([2.15]).

$$X_{DOCi,h} = X'_{DOCi,h}\, R_{O2i,h}/R'_{O2i,h} \qquad [2.15]$$

Where:

$X_{DOCi,h}$ is the rate of DOC oxidation by $M_{i,h,a}$ under ambient [O_{2s}] (g N m^{-2} h^{-1})

2.2.2.3.2 Oxidation of Dissolved Organic Carbon and Reduction of Nitrate, Nitrite, and Nitrous Oxide by Denitrifiers

Under aerobic conditions, with large air-filled porosity θ_g, the gaseous diffusivity (D_{gy}) (Eqs [2.27] and [2.28] below) of O_2 is rapid and, therefore, [$O_{2mi,h}$] remains high with respect to K_{O2h} (Eq. [2.14]). Under these conditions X_{DOC} approaches X'_{DOC} and $R_{O2i,h}$ approaches $R'_{O2i,h}$ (Eq. [2.5]). However, under lower θ_g, caused by high WFPS, O_2 diffusivity is slow so that [O_{2s}] declines. Under these conditions [$O_{2mi,h}$] declines with respect to K_{O2h} (Eq. [2.3]) and hence $R_{O2i,h}$ declines with respect to $R'_{O2i,h}$ creating a demand for alternative electron acceptors (Eq. [2.14a,b]). The demand can be met by NO_3^-, NO_2^- and N_2O reduction sequentially producing NO_2^-, N_2O and N_2 (Grant, 1993a, b; Grant, 1995; Grant, 2001a,b; Grant and Pattey, 2003; Grant et al., 2006). NO_3^- reduction under non-limiting NO_3^- is first calculated from a fraction of electrons demanded by DOC oxidation but not accepted by O_2 because of diffusion limitations (Eq. [2.16]):

$$R'_{NO3i,d} = E_{NOx} f_e (R'_{O2i,d} - R_{O2i,d}) \quad [2.16]$$

Where:

$R'_{NO3i,d}$ is NO_3^- reduction by heterotrophic denitrifiers (functional type d) under non-limiting $[NO_3^-]$ (g N m^{-2} h^{-1}) in substrate-microbe complex i (Grant et al., 1993a, 1993b)
$R'_{O2i,d}$ is the rate of O_{2s} reduction by $M_{i,d,a}$ under non-limiting $[O_{2s}]$ (Eq. [13]) (g O_2 m^{-2} h^{-1}) (Grant et al., 1993a, 1993b)
$M_{i,d,a}$ is the active biomass of (component a) heterotrophic denitrifiers (functional type d) (g C m^{-2}) in complex i (substrate-microbe complex) (Grant et al., 1993a, 1993b)
$R_{O2i,d}$ is the rate of O_{2s} reduction by $M_{i,d,a}$ under ambient $[O_{2s}]$ (g O_2 m^{-2} h^{-1}) (Eq. [14])

NO_3^- reduction under ambient NO_3^- is then calculated from Eq. [2.16] ([2.17]):

$$R_{NO3i,d} = R'_{NO3i,d} [NO_3^-]/([NO_3^-] + \boldsymbol{K_{NO3d}}) \quad [2.17]$$

Where:

$R_{NO3i,d}$ is NO_3^- reduction by heterotrophic denitrifiers under ambient $[NO_3^-]$ (g N m^{-2} h^{-1})
$[NO_3^-]$ is the concentration of NO_3^- in soil solution (g N m^{-3})
$\boldsymbol{K_{NO3d}}$ is the Michaelis-Menten constant for reduction of NO_3^- by heterotrophic denitrifiers (2.5 g N m^{-3}, Yoshinari et al., 1977)

NO_2^- reduction under ambient NO_2^- is calculated from demand for electrons not met by NO_3^- in Eq. [2.17] (Eq. [2.18]):

$$R_{NO2i,d} = (R'_{NO3i,d} - R_{NO3i,d})[NO_2^-]/([NO_2^-] + \boldsymbol{K_{NO2d}}) \quad [2.18]$$

Where:

$R_{NO2i,d}$ is NO_2^- reduction by heterotrophic denitrifiers (g N m^{-2} h^{-1})
$\boldsymbol{K_{NO2d}}$ is the Michaelis-Menten constant for reduction of NO_2^- by heterotrophic denitrifiers (2.5 g N m^{-3}, Yoshinari et al., 1977)

N_2O reduction under ambient NO_2^- is calculated from demand for electrons not met by NO_2^- in Eq [2.18] (Eq. ([2.19]);

$$R_{N2Oi,d} = 2\,(R'_{NO3i,d} - R_{NO3i,d} - R_{NO2i,d})[N_2O]/([N_2O] + \boldsymbol{K_{N2Od}}) \qquad [2.19]$$

Where:

$R_{N2Oi,d}$ is the N_2O reduction by heterotrophic denitrifiers (g N m^{-2} h^{-1})
$[N_2O_s]$ concentration of N_2O in soil solution (g N m^{-3})
$\boldsymbol{K_{N2Od}}$ is the Michaelis-Menten constant for reduction of N_2O by heterotrophic denitrifiers (2.5 g N m^{-3}, Yoshinari et al., 1977)

NO_x reduction permits additional oxidation of DOC by denitrifiers. Total DOC oxidation by denitrifiers is then calculated as:

$$X_{DOCi,d} = X_{DOCi,d} \text{ (from [Eq. 2.12])} + F_{NOx}\,(R_{NO3i,d} + R_{NO2i,d}) + F_{N2O}\,R_{N2Oi,d} \qquad [2.20]$$

Where:

$X_{DOCi,d}$ is the total rate of DOC oxidation by $M_{i,d,a}$ under ambient $[O_{2s}]$ and $[NO_x]$
F_{NOx} is the e^- donated by C vs. e^- accepted by NO_x when oxidizing DOC (0.86 g C g N^{-1})
F_{N2O} is the e^- donated by C vs. e^- accepted by N_2O when oxidizing DOC (0.43 g C g N^{-1})

2.2.2.3.3 Growth of denitrifiers

Carbon oxidation by obligate aerobes and facultative anaerobes (Eq. [2.20]) is used for maintenance respiration (Eqs. [18] and [19] of Grant et al., 1993a) and growth respiration, calculated as the difference between C oxidation and maintenance respiration. Growth respiration drives biomass growth and hence $M_{i,h,a}$ according to energy yields of O_2 and NO_x reduction.

2.2.2.4 Transport of water

Surface and sub-surface flows of water determine WFPS in soils. This is important in N_2O production as well as emissions from the soil profile since WFPS controls gaseous diffusivity of O_2 (D_{sO2} in Eqs. [2.3a], [2.7a] and [2.14a]) and N_2O, and hence $[O_{2s}]$ (Eqs. [2.3a,b], [2.7a,b] and [2.14a,b]) and demand for NO_x (Eqs. [2.9] and [2.16]).

2.2.2.4.1 Surface flow

Surface flow is calculated as the product of runoff velocity (v), depth of mobile surface water (d), and width of flow paths (L) in west to east (x) and north to south (y) directions for each landscape position x,y (Eq. [2.21]). Changes in the depth of surface water d_w arise from differences in surface flows among adjacent landscape positions. Runoff velocity (Eq. [2.22]) is calculated in x and y directions for each x,y from the hydraulic radius R (Eq. [2.23]), slope s, and Manning's roughness coefficient z_r calculated from microtopographic roughness and particle size according to Morgan et al. (1998).

$$Q_{x(x,y)} = v_{(x,y)} dL_{(x,y)} \qquad [2.21]$$

Where:

$Q_{x(x,y)}$ is the surface flow ($m^3\ m^{-2}\ h^{-1}$) in x or y directions
$v_{(x,y)}$ is the velocity of surface flow in x or y directions ($m\ h^{-1}$)

$$v_{(x,y)} = \frac{R^{0.67} s_{(x,y)}^{0.5}}{z_{r(x,y)}} \qquad [2.22]$$

R is ratio of cross-sectional area to perimeter of surface flow (m) ([2.23]; Figure 2-3).

$$R = \frac{s_r d}{(2(s_r^2 + 1)^{0.5})} \qquad [2.23]$$

s_r is the slope of channel sides during surface flow (m m^{-1})
$z_{r(x,y)}$ is the Manning's roughness coefficient (m$^{1/3}$ h)
$S_{(x,y)}$ is the slope of the sureface (m m^{-1})
d is the depth of mobile surface water (m)
$L_{(x,y)}$ is the length of the landscape element in x or y direction (m)

The depth of mobile surface water d in Eq. [2.23] is the positive difference between the surface water d_w + ice d_i and the maximum depth of surface water storage (d_s).

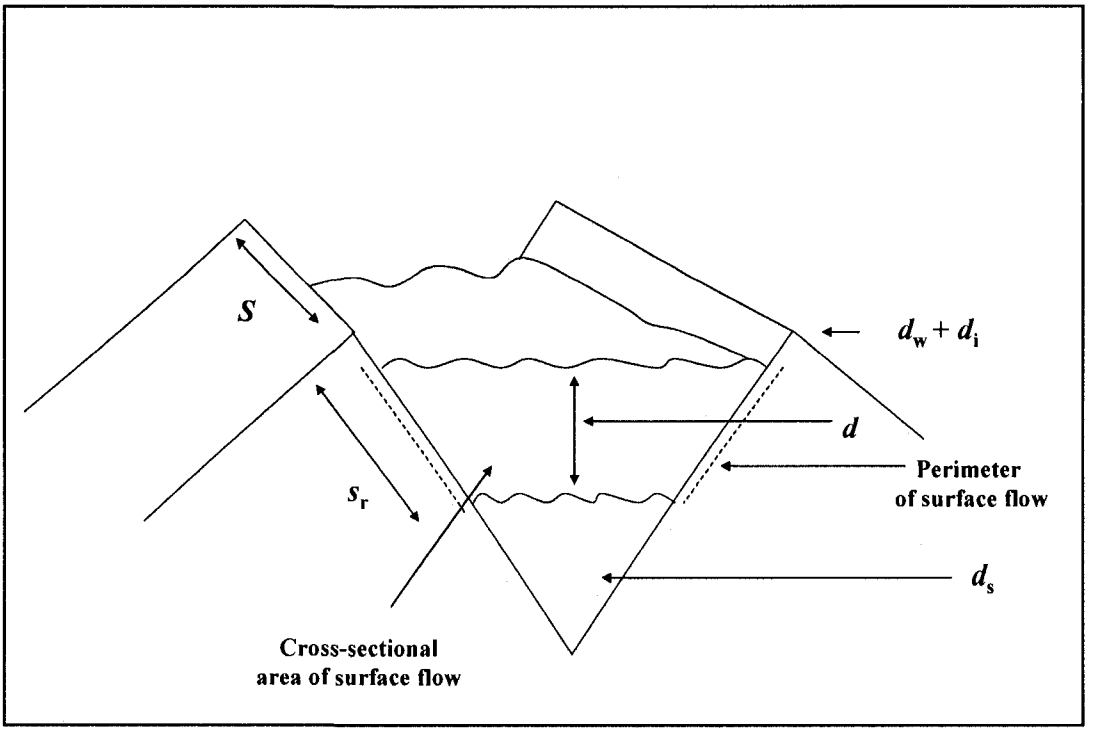

Figure 2-3: Surface flow in *Ecosys* (Eqs. [2.21 – [2.23]).

2.2.2.4.2 Subsurface flow

Surface water accumulates when precipitation is greater than infiltration, determined from water fluxes through soil profiles. These fluxes are calculated as the product of hydraulic conductance (K') and water potential (ψ) differences in west to east (x), north to south (y) and vertical (z) directions for each landscape position x, y, z.

$$Q_{w,(x,y,z)} = K'_{(x,y,z)} (\delta\psi_{(x,y,z)}/\delta Z_{(x,y,z)}) \quad [2.24]$$

Where:

$Q_{w,(x,y,z)}$ is the subsurface water flow in x,y or z directions ($m^3\ m^{-2}\ h^{-1}$)
$K'_{(x,y,z)}$ is the hydraulic conductance in x, y or z directions (m $MPa^{-1}\ h^{-1}$)
$\delta\psi_{(x,y,z)}$ is the soil water potential difference in x, y or z directions (MPa)
$\delta Z_{(x,y,z)}$ is the distance in x, y or z directions (m)

Water potentials are the sum of matric, osmotic and gravitational components. $K'_{(x,y,z)}$ is calculated from hydraulic conductivities of adjacent landscape positions (Eq. [41a], [42a] and [43a] of Grant and Pattey, 2003). However, if ψ of one position exceeds the air entry potential (ψ_e), $K'_{(x,y,z)}$ is calculated from saturated hydraulic conductivities while $\delta\psi_{(x,y,z)}$ is calculated across the wetting front caused by saturated flow. Water movement between adjacent landscape positions thus alternates between Richards and Green-Ampt flow depending upon ψ vs. ψ_e in each position.

2.2.2.5 Transport of gaseous and aqueous substrates and products

2.2.2.5.1 Surface transport

Solute transport ($Q_{r\gamma}$) in x and y directions across the soil surface Eq. [2.25] is calculated for each gas, solute (γ_s) and mineral (Eq. [A1] to [A55] in Grant et al., 2004) in each landscape position (x, y) from surface water flow Q_r (Eq. [2.21]) and surface

concentration [γ_s] in g m^{-3}.

$$Q_{r\gamma(x,y)} = Q_{r(x,y)}[\gamma_s] \quad \text{Eq. [2.25]}$$

Where :

$Q_{r\gamma(x,y)}$ is the surface flow of γ in x or y direction (g m^{-2} h^{-1})

2.2.2.5.2 Subsurface transport

All gases generated or consumed by microbial oxidation-reduction reactions undergo convective-dispersive transport through and volatilization-dissolution transfer between, aqueous and gaseous phases of the soil and root. Transfer of each gas γ (γ = CH_4, O_2, CO_2, N_2, N_2O, NH_3 and H_2) between its soil gaseous (γ_g) and aqueous phases (γ_s) in each landscape position x, y, z (Eq. [44] of Grant and Pattey, 2003) is driven by concentration differences between its aqueous concentration [γ_s] and the aqueous equivalent of its gaseous concentration [γ_g] in g m^{-3} calculated from its temperature dependent solubility. Transfer is determined by a diffusive transfer coefficient acting across an air-water interfacial area.

Aqueous transport $Q_{s\gamma}$ in x, y, and z directions through the soil (Eq. [2.26]) is calculated for each solute γ_s as the sum of convective (from subsurface water flow Q_w in Eq. [2.24]) and dispersive–diffusive components.

$$Q_{s\gamma(x,y,z)} = Q_{w(x,y,z)}\,[\gamma_{s(x,y,z)}] + 2D_{s\gamma(x,y,z)}\,\delta[\gamma_{s(x,y,z)}]/\delta Z_{(x,y,z)} \quad \text{Eq. [2.26]}$$

Where :

$Q_{s\gamma(x,y,z)}$ is the aqueous transport of solute γ in x, y or z direction (g m^{-2} h^{-1})
$Q_{w(x,y,z)}$ is the subsurface water flow in y direction (m^3 m^{-2} h^{-1})
$D_{s\gamma(x,y,z)}$ is the aqueous dispersivity–diffusivity of solute γ during transport in x, y or z directions (m^2 h^{-1})

$D_{s\gamma}$ is controlled by WFPS and soil temperature (θ_s in Eq. [46] of Grant and Pattey, 2003).

Gaseous transport $Q_{g\gamma}$ in x, y, and z directions through the soil is also calculated for each solute γ_g as the sum of convective and dispersive–diffusive components.

$$Q_{g\gamma(x,y,z)} = -Q_{w(x,y,z)}\,[\gamma_g] + 2D_{g\gamma(x,y,z)}\,\delta[\gamma_{g(x,y,z)}]/\delta Z_{(x,y,z)} \qquad \text{Eq. [2.27]}$$

Where:

$Q_{g\gamma(x,y,z)}$ is the gaseous transport of solute γ in x, y or z direction (g m^{-2} h^{-1})
$Q_{w(x,y,z)}$ is the subsurface water flow in y direction (m^3 m^{-2} h-^{1})
$D_{g\gamma(x,y,z)}$ is the gaseous diffusivity of gas γ (m^2 h^{-1})
Z is the soil depth (m)

$D_{g\gamma}$ is controlled by air-filled porosity θ_g according to:

$$D_{g\gamma} = \boldsymbol{D'}_{g\gamma}\, f_{tg}\, 0.5(\theta_{g(x,y,z)} + \theta_{g(x,y,z)+1})^{\alpha} / \theta_p^{\beta} \qquad \text{(Millington and Quirk, 1960) Eq. [2.28]}$$

Where:

$\boldsymbol{D'}_{g\gamma}$ is the gaseous diffusivity of gas γ in air at 25°C (m^2 h^{-1})
$\boldsymbol{\alpha}$ is the sensitivity of $D_{g\gamma}$ to θ_g (2) (Millington, 1959)
$\boldsymbol{\beta}$ is the sensitivity of $D_{g\gamma}$ to θ_p (0.67) (Millington, 1959)
θ_p is the soil total porosity (m^3 m^{-3})
f_{tg} is the temperature function for gaseous diffusivity

2.2.2.5.3 Atmosphere-Surface Transport

Exchange of all gases between the atmosphere and both aqueous and gaseous states at the soil surface are driven by concentration differences. This exchange is controlled by boundary layer conductance calculated from wind-speed, surface roughness and overlying plant canopy and surface residue (Grant et al., 2006).

2.2.2.6 Heat Transport

In *ecosys* soil temperature is modeled by coupling surface energy exchange to subsurface conductive, convective and latent heat transfers using a forward differencing scheme with heat capacities and thermal conductivities calculated from de Vries (1963) (Eqs.[A.24])-[A.27] of Grant, 2001a).

2.3 MATERIALS & METHODS

2.3.1 Laboratory Experiments

2.3.1.1 Objectives

The temporal variability of N_2O emissions was first investigated under laboratory conditions in which spatial variability was removed by uniform mixing of soil. A preliminary experiment was conducted (1) To determine the incubation period after rewetting previously air-dried soil, before N_2O emissions can be measured, and (2) To determine a suitable sampling time strategy for N_2O emissions using non flow-through non steady state chambers (Hutchinson and Mosier, 1981) during which N_2O concentration in the chamber headspace increases with time and (3) To develop a better understanding of the sensitivity of N_2O emissions to changes in WFPS over time as well as the effects of fertilizer applications on the magnitude of N_2O emissions.

The information gathered from the preliminary experiment was then used to design a fully replicated experiment. The objectives of the replicated experiment were (1) To test the ability of *ecosys* (Grant, 2001a,b) to simulate the sensitivity ("threshold response") of N_2O emissions to changes in WFPS and (2) To test the ability of *ecosys* (Grant, 2001a,b) to simulate the effects of fertilizer applications on the magnitude of N_2O emissions, at the site scale (< 1 m^2). These objectives were designed to test hypotheses (1) and (2) (Section 2.1).

2.3.1.2 Experimental design & treatments

The soil type used was the A horizon of an Orthic Black Chernozem from the University Research Station, Edmonton, Alberta, Canada (53°19'N, 113°34'W). However, soil samples for the preliminary experiment were taken at a different location at the station from that of the fully replicated experiment. The soil was first air-dried and sieved through a 7mm sieve. Table 2-1 shows some major properties of the soil samples used in both preliminary and replicated experiments.

Table 2-1: Soil chemical properties for Orthic Black Chernozem in preliminary experiment and replicated experiment

.

	Preliminary Experiment	**Replicated Experiment**
*D_b, (Mg m^{-3})		0.94
*θ_{FC}, (m^3 m^{-3})		0.31
*θ_{WP}, (m^3 m^{-3})		0.15
*Ks_{at}, (mm h^{-1})		5.3
Sand, (g kg^{-1})		280
Silt, (g kg^{-1})		450
pH		6.3
CEC, (cmol kg^{-1})		20
Org. C, (g kg^{-1})	48.4	60.5
Org. N, (g Mg^{-1})	3900	5042
NH_4^+, (μg g^{-1})	11	21
NO_3^-, (μg g^{-1})	53	154

***Abbreviations: D_b, bulk density, θ_{FC}, water content at -0.033 MPa; θ_{WP}, water content at -1.5 MPa; K_{sat}, saturated hydraulic conductivity.**

Field capacity, wilting point and hydraulic conductivity were estimated using the Saxton (2006) pedo-transfer function calculator.

A completely randomized design with different WFPS (calculated from the bulk density of air-dried soil and using deionized water to avoid contamination with solutes such as NO_3) and fertilizer treatments, were used for both experiments. Treatments for the preliminary experiment were:

(1) WFPS: 80 and 90% (equivalent water volume - 1493.3 and 1706.3 mL respectively).

(2) Fertilizer: no-fertilizer and 100 kg N ha^{-1} (urea).

Treatments for the replicated experiment (three replicates) were:

(1) WFPS: 60, 75 and 90% (equivalent water volume - 1067.3, 1386.8 and 1706.3 mL respectively).

(2) Fertilizer: 0, 75 and 150 kg N ha^{-1} (urea).

Four litre pots (15cm height, 19cm diameter) were filled to a depth of 11cm with 3.4 kg of air-dried. All pots were brought to 60% WFPS (refer to treatments above for volume of water applied) and allowed to incubate for a 10 day period for the preliminary experiment and 2 weeks for the replicated experiment, to allow activation of microbial populations. After the incubation period, both irrigation (using a garden sprinkler can to apply water until pot weights were equal to irrigation treatments above plus the air-dried soil) and fertilizer (surface applied) treatments were applied on day 1 and another irrigation treatment was applied on day 28, for the preliminary experiment. For the replicated experiment, irrigation treatments were applied on days 1, 26, 41 and 53 and fertilizer treatments were applied once on day 41.

2.3.1.3 N_2O and WFPS measurements

Non flow-through, non steady-state chambers (Hutchinson and Mosier, 1981) of 13-cm height and 12-cm diameter were used to monitor N_2O emissions. For the replicated experiment, chambers were fitted into installed collars of 3-cm depth and 11.5-cm diameter in each pot, in order to minimize soil disturbance. Headspace gas samples (20mL) were taken using a syringe via a rubber septum within each chamber and then samples were stored at room temperature (~ 21°C) in evacuated containers (Exetainers (12mL); Labco Limited, Buckinghamshire, United Kingdom). Before the start of the preliminary experiment, gas samples were initially taken 0, 10, 20, 30, 40, 50 and 60 min after chamber placement, on a few samples representative of the treatment combinations used for this experiment. Linearity was found to be maintained up to 30 min sampling time, therefore samples were then taken at 0 and 30 min for the results presented for this experiment. However, further N_2O measurements in another preliminary experiment revealed that linearity for N_2O was achieved at 20 min (Figure 2-1, Section 2.4.1, shows an example) and, therefore, the sampling time for the replicated experiment was revised to 0, 10 and 20 min. Samples from both preliminary and replicated experiments were then analysed for N_2O using a Varian 3400 gas chromatograph (GC) equipped with a ^{63}Ni-electron capture detector operated at 300°C, Poropak QC column at 60°C, injector at 60°C and Argon-Methane (30ml min^{-1}) carrier gas. Fluxes were calculated using the linear model of N_2O accumulation over time.

N_2O emissions and gravimetric soil moisture contents were measured daily to closely monitor the temporal variability of N_2O and WFPS

2.3.1.4 Analysis of results

Analysis of variance (ANOVA) was performed on log-transformed N_2O data from the replicated experiment, to determine which treatments led to significant emissions as well as root mean square error for replication (RMSE) for comparison with model results, using the Statistical Analysis System (SAS).

2.3.2 Model Laboratory Experiment

2.3.2.1 Model Inputs

The *ecosys* model was used to conduct a simulated experiment using input data from the replicated experiment (Section 2.3.1). The objective of this experiment was to test the sensitivity of N_2O emissions to changes in WFPS from Eqs. [2.1] – [2.28], as represented in *ecosys*. The model was initialized using soil characteristics of the Black Chernozem (Table 2-1) soil and run for five years under Ellerslie, Alberta, weather (obtained from a meteorological station located near soil sampling site) with a fertilized spring wheat crop to simulate the site history prior to sampling.

After this period, the upper 10 cm of the modelled soil profile was mixed by tillage and the model run was continued for the periods of soil storage and experimentation using weather data (radiation, irrigation, humidity, temperature and wind-speed) and soil amendments measured for the replicated laboratory experiment. The model was run under hourly boundary conditions whereby water fluxes (Eqs. [2.21-2.26]) were

calculated 25 times per hour and gas fluxes (Eqs. [2.27-2.28]) were calculated 500 times per hour, thus enabling the model to capture the high temporal variability of these emissions.

2.3.2.2 Model Testing

Modeled N_2O emissions were compared to Hutchinson chamber measurements (Section 2.3.1.3) using regression analysis in which root mean square for difference (RMSD) between modeled and measured results was compared with root mean square error for replication (RMSE) from the measured data.

2.4 RESULTS

2.4.1 Preliminary experimental results

Results showed that above ambient gaseous-N emissions from the fertilized pots were first observed on the 10th day after incubation. The reason for this delay of N_2O emissions was probably because the nitrifier and denitrifier populations needed some time to re-activate and multiply after drying and storage, before any nitrification and denitrification processes can occur.

There was a linear accumulation of N_2O up to time 20 min because after this time, net increase in emissions for every 10 min interval, started to decline (Figure 2-4 shows an example of this).

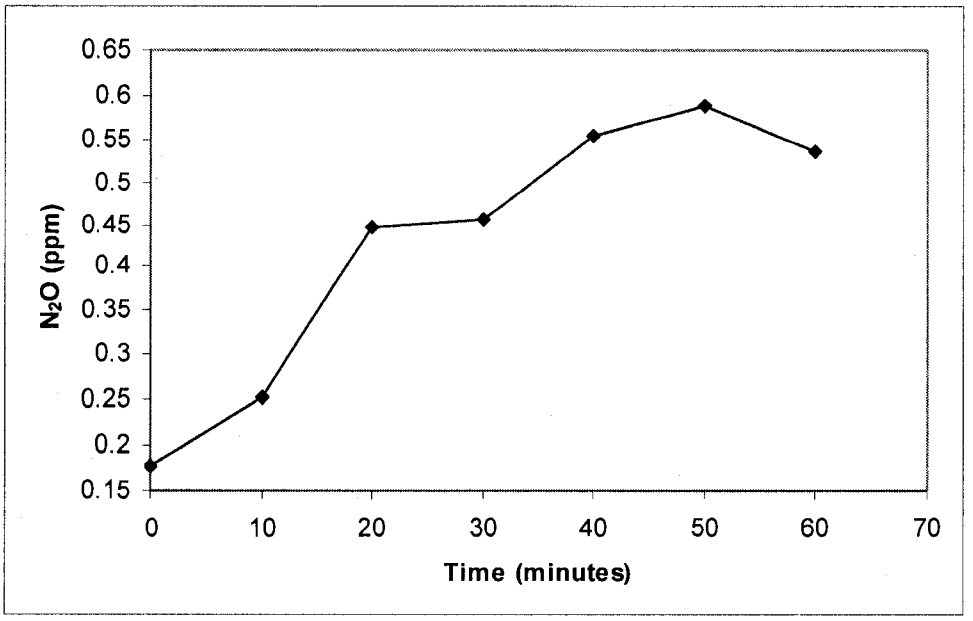

Figure 2-4: An example of N_2O accumulation in Hutchinson chambers

This aspect of N_2O sampling is important because if a very long sampling time is used, a build-up of gas concentrations within the chamber headspace can lead to feedback mechanisms influencing the processes involved in producing or consuming the gas (Glatzel, 1999). An example is if the N_2O concentration within the chamber headspace is higher than that of the soil atmosphere, then N_2O within the soil atmosphere and chamber may eventually equilibrate over a long time period. Measurements made at this time will not be a true representation of the microbial production of N_2O.

Figure 2-5 shows that on day 1 of the experiment (DOE 1), no N_2O emissions were measured irrespective of the treatments. The addition of water may have filled the soil macro and micro pores with water, thus reducing the diffusivity of O_2 into the soil. Limited O_2 in the soil would have led to the demand for alternative electron acceptors. N_2O production from nitrification (reduction of NO_2^- to N_2O) and denitrification (reduction of NO_3^- to N_2O) may have occurred, but, the diffusion of N_2O out of the soil profile to soil surface at high WFPS, could have been limited. Since the diffusion of gases is slower in water than air, this explains why no noticeable gaseous N-fluxes were observed during this time. Another explanation is that N_2O produced can be further reduced to N_2 under high WFPS, hence decreasing the amounts of N_2O produced in the soil. Before urea ($CO(NH_2)_2$) can be utilized by microorganisms, it must be hydrolyzed first. Therefore if urea is used after fertilization, N_2O emissions as a result of this may not be detected within the first day of the experiment.

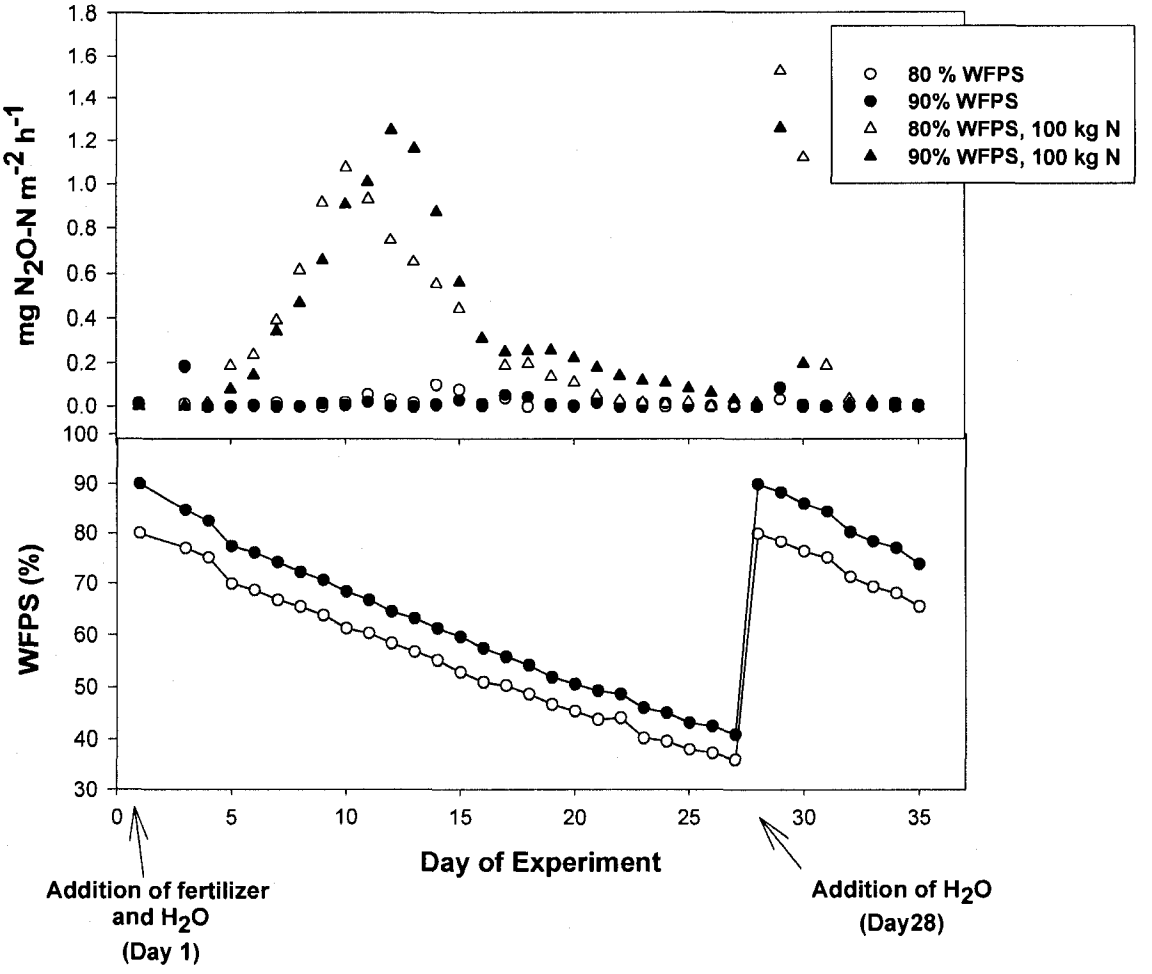

Figure 2-5: (a) Measured N_2O emissions (symbols) and (b) water-filled pore space (WFPS) (symbols and lines) for preliminary experiment.

For the No-fertilizer treatment (90% WFPS) on DOE 2, there was a small gaseous N-flux. This probably occurred because of denitrification of the residual soil N (NH_4^+ = 11 $\mu g\ g^{-1}$ and NO_3^- = 53.1 $\mu g\ g^{-1}$). On DOE 4 and 29, both fertilizer treatments showed rapid gaseous N-fluxes. This occurred because the macropores began to drain (increased air-filled θ_g) and this increased the D_g of N_2O. As a result, previously dissolved N_2O volatilized into the soil atmosphere and then diffused rapidly to the soil surface. The lag between irrigation and emissions for the fertilized treatments was shorter for the second

cycle. This trend occurred probably because the urea fertilizer applied was fully hydrolyzed at this time of the incubation therefore, more NH_4^+ was available for N_2O production via nitrification/denitrification prior to the second cycle. Consequently, peak N_2O emissions occurred earlier and the magnitude of these emissions was greater upon soil drying for the second cycle, compared to those of the first cycle.

For the first water cycle, peak gaseous N-fluxes for fertilized treatments occurred earlier for the 80 % WFPS than the 90% WFPS because of delayed soil drying in the higher moisture level. Emissions eventually were higher for the 90% WFPS compared to the 80% WFPS fertilized treatments probably because of higher nitrification/denitrifcation under more anaerobic conditions.

For the second watering cycle, the 90% treatment gave lower N_2O emissions compared to the 80% treatment. This may have occurred because at the lower moisture contents, nitrification may have been more rapid prior to the addition of the second moisture treatment, thus higher NO_3^- accumulated compared to the 90% WFPS. For this reason, gaseous N-fluxes are more pronounced under alternating aerobic and anaerobic conditions.

There was a decline in gaseous N-fluxes after days 17 and 32 of the first and second water cycles for the fertilizer treatments because of declining soil moisture. There was a sharp decrease in gaseous N-fluxes on day 29 of N_2O measurements for the fertilizer

treatments probably because of depletion of NO_3^- supply thus less denitrification took place.

2.4.2 Replicated Laboratory Experiment

2.4.2.1 Effect of WFPS on temporal variability of N_2O emissions

In *ecosys*, changes in WFPS (Figure 2-6b) following irrigation caused N_2O emissions (Figure 2-6a) to rise non-linearly (Figure 2-7; R^2 of cumulative N_2O emissions versus WFPS = 0.99) with WFPS from values of 60% through 75% to 90%, in a way that was consistent with the measured data (Figure 2-6: close to 0 mg N_2O-N m^{-2} h^{-1} at 60% to ~ 4.6 N_2O-N m^{-2} h^{-1} at 90%; Table 2-2: R^2: 0.26 (75%) and 0.67 (90%) WFPS ($P < 0.001$) and similar RMSD and RMSE). These changes in WFPS were caused by evaporation, determined from a surface energy balance (Eqs. [A.1], [A3], [A4], [18], [24], [25] and [A27] of Grant, 2001a) and from subsurface flow, determined using both Richards (Eq. [2.24]) and Green-Ampt equations (Eqs. [A94 - A96] of Grant et al., 2004).

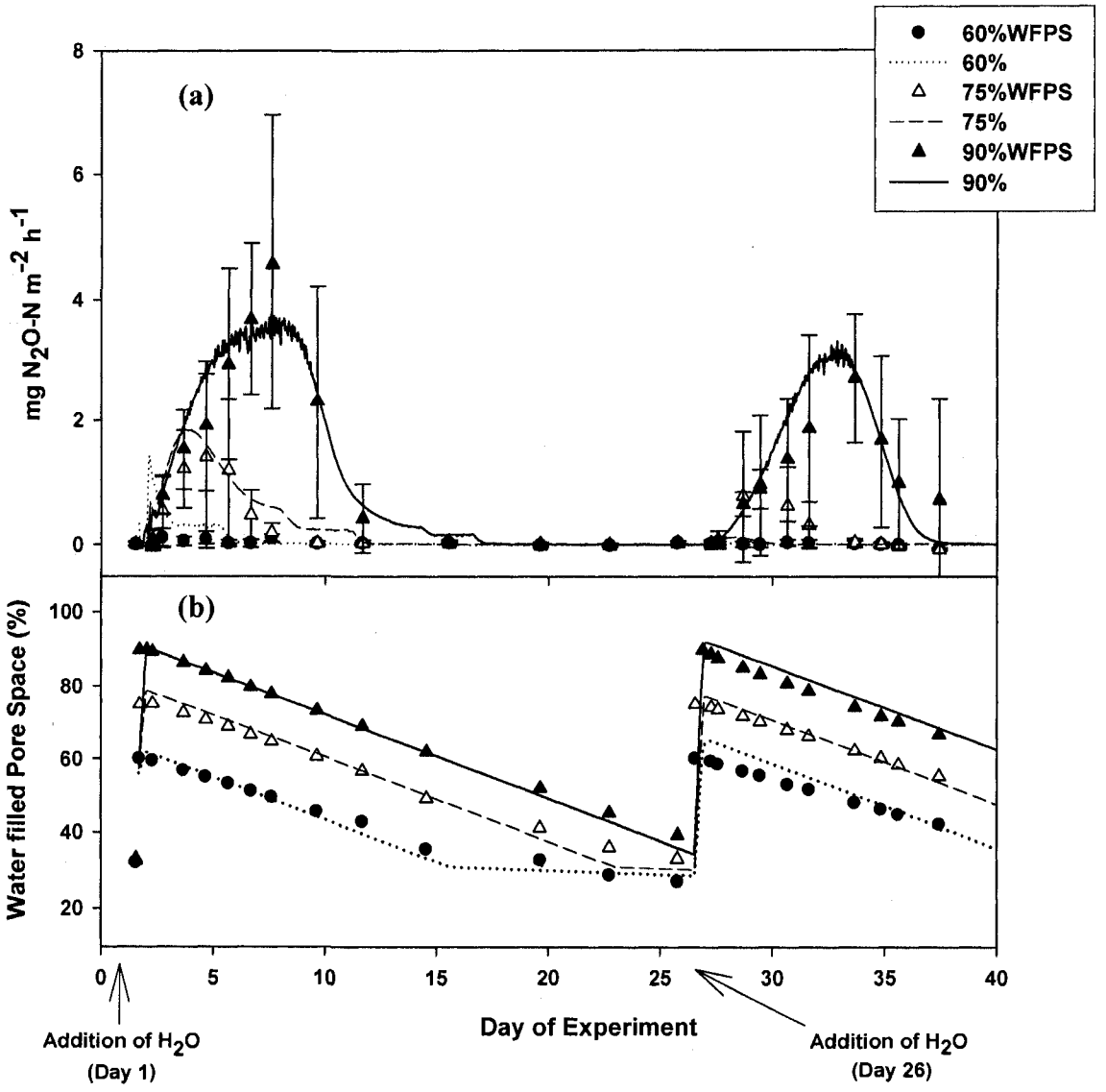

Figure 2-6: Modeled (lines) and measured (symbols: mean (± standard deviation (n = 3)) of (a) N_2O emissions (0 kg N ha^{-1}) (b) water filled pore space (WFPS) for day of experiment 0 - 40.

Table 2-2: Statistics for regression of log-transformed measured vs. modeled N_2O fluxes and analysis of variance (ANOVA) of log-transformed measured fluxes

	R^2	P	Modeled versus measured variation: Root mean square for difference (RMSD)	Root mean square for error (RMSE)
75% WFPS	0.26	< 0.001	0.73	0.48
90%WFPS	0.67	< 0.001	0.45	0.37

For the 60% WFPS irrigation treatment, air filled porosity (θ_g) (Eq. [2.28]) and thus gas diffusivity D_g (D_{gy} in Eq. [2.28]) were large, so that surface O_2 exchange and soil O_2 transport in the model were rapid. This resulted in more rapid dissolution of gaseous O_2 (O_{2g}) to O_{2s} (Eq. [A30] in Grant et al., 2006), so that $[O_{2s}]$ (Eqs. [2.3a] and [2.7a]) remained well above K_{O2} (Eqs. [2.3b] and [2.7b]). Aqueous O_2 supply for the 60% WFPS was therefore sufficient to meet the demands of nitrifiers during nitrification of residual N (Table 2-2) whereby NH_3 was oxidized to NO_2^- (Eqs. [2.1] - [2.4]) and NO_2^- was oxidized to NO_3^- (Eqs. [2.5] - [2.8]). Consequently, little or no N_2O emissions were modeled and measured for the 60% WFPS (Figure 2-6a).

Larger soil WFPS for the (75 and 90%) led to lower θ_g, which caused declines in gas diffusivity D_g (D_{gy} in Eq. [2.28]). These declines in turn reduced surface O_2 exchange and soil O_2 transport lowering gaseous O_2 ($[O_{2g}]$) in the soil profile and slowing dissolution of O_{2g} to O_{2s} (Eq. [A30] in Grant et al., 2006). Therefore $[O_{2s}]$ declined with respect to K_{O2}, becoming insufficient to meet the demands of nitrifiers during nitrification (Eqs. [2.3a,b] and [2.7a,b]). Nitrifier demand for electron acceptors unmet by O_2 was transferred to NO_2^- ($R'_{NO2i,n}$ in Eq. [2.9]), which was then reduced to N_2O ($R_{NO2i,d}$ in Eq. [2.10]) leading to rises in $[N_2O_s]$. Aqueous O_2 also became insufficient to meet demands of

denitrifiers (Eqs. [2.14a,b]), causing a demand for alternative electron acceptors (Eq. [2.13]) that was first transferred to NO_3^- ($R_{NO3i,d}$ in Eq. [2.17]), which was reduced to NO_2^- (Eq. [2.17]). Any remaining demand was transferred to NO_2^-, which was then reduced to N_2O ($R_{NO2i,d}$ in Eq. [2.18]), and any remaining demand thereafter was transferred to N_2O, which was reduced to N_2 ($R_{N2Oi,d}$ in Eq. [2.19]). Cumulative emission measured from the 75% and 90% WFPS treatments were 20 and 97-fold larger, respectively, than that of the 60% WFPS treatment (Figure 2-7) which illustrates the non-linear response of N_2O emissions to changes in WFPS.

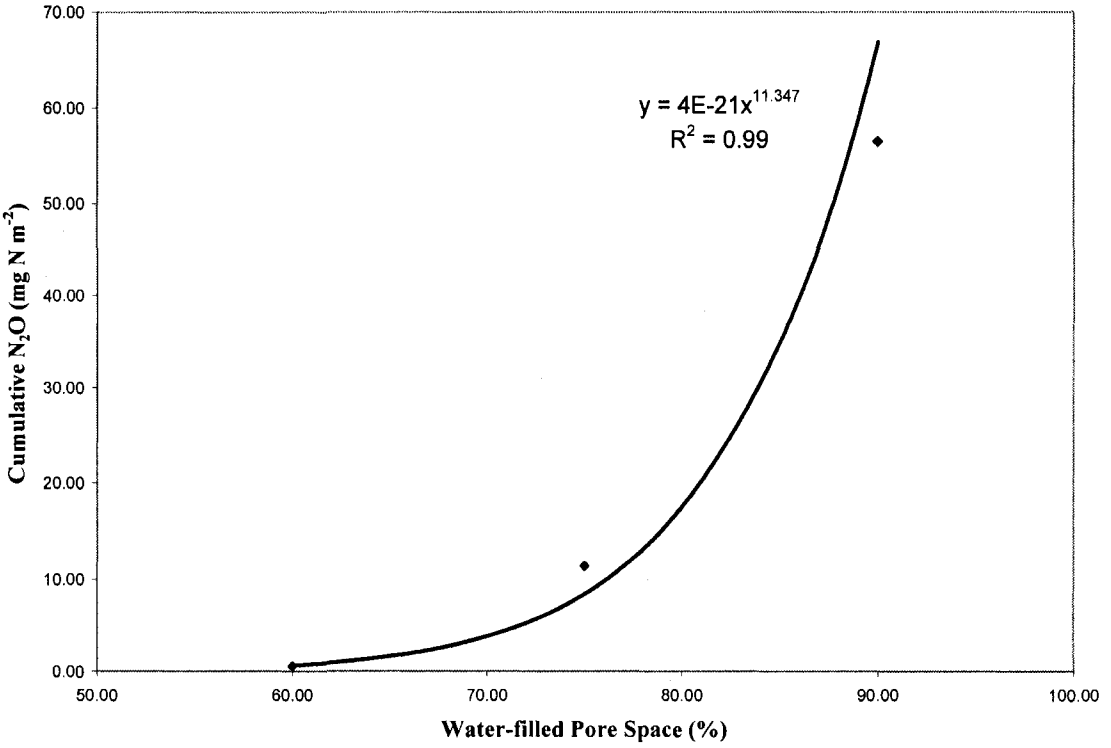

Figure 2-7: Effect of water-filled pore space (WFPS) on cumulative N_2O emissions (measured) for day of experiment 0 – 70.

Low emissions were observed on the first day of each irrigation cycle for the modeled 75 and 90% WFPS treatments (Figure 2-6a). This delay in emissions in the model occurred because the high WFPS led to low θ_g which lowered [O_{2s}]. This caused an increase in N_2O production. However, emissions into the atmosphere were delayed because of a reduction in the gaseous diffusivity of N_2O ($D_{g\gamma}$ in Eq. [2.28]). Also, under high WFPS conditions, denitrification in the model may proceed to the terminal electron acceptor (N_2) ($R_{N2Oi,d}$ in Eq. [2.19]), resulting in a higher proportion of N_2 versus N_2O being produced. Re-establishment of gaseous pathways during evaporation of soil water (Figure 2-6b) later led to volatilization of [N_2O_s] (Eq. [A30] in Grant et al., 2006) allowing N_2O emissions to rise. Peak N_2O emissions for the 75% WFPS occurred on the 3rd (modeled) and 4th (measured) day after the application of water while this occurred at the 7th (modeled and measured) day for the 90% WFPS (first irrigation cycle: DOE 1 - 25). This is because of faster restoration of θ_g due to soil drying, for the 75% treatment, giving higher D_g of N_2O, compared to the 90% WFPS.

The 90% WFPS treatment sustained the longest emissions events compared to the other treatments, showing that WFPS is an important driver of N_2O emissions. High WFPS led to a longer duration of low gas diffusivity D_g in *ecosys* ($D_{g\gamma}$ in Eq. [28]). Thus, surface O_2 exchange and soil O_2 transport were also low for a longer period. Consequently, gaseous O_2 ([O_{2g}]) in the soil profile and dissolution of O_{2g} to O_{2s} (Eq. [A30] in Grant et al., 2006), were small for a longer period, leading to more sustained N_2O production via nitrification (Eq. [10]) and NO_3^- (Figure 2-4) for N_2O production via denitrification (Eq. [18]). For each rewetting event in the laboratory experiment, there were repeated

emissions from the 90% treatment indicating background emissions are given off by a soil without fertilizer treatments. However, even though each re-wetting cycle was similar, there was a general trend for peak N_2O emissions to decrease over time (Figure 2-6). This may be attributed to the oxidation of labile C or DOC and reduction of oxygen by heterotrophs (Eq. [12 - 15]), which led to a decline in readily available C for N_2O production via denitrification (Eq. [16 - 18]). This indicated a C-limitation since the soil residual N was high (Table 2-1).

2.4.2.2 Effect of fertilizer addition on N_2O emissions

Addition of the fertilizer treatment (Figure 2-8b,c) did not result in any further increase in modeled and measured emissions (third irrigation cycle: DOE 41-52) since presence of high residual N (Table 2-1) led to near maximum reaction rates for nitrification/denitrification (Eq. [2.1] – [2.20]) according to the Michaelis-Menten kinetics (Eqs. [2.1], [2.3b], [2.5], [2.7b], [2.10], [2.12], [2.14b], and [2.17] - [2.19]. However, after addition of water on day 53 (fourth irrigation cycle: DOE 53-66), modeled emissions for the fertilized treatments (90%WFPS, 75 kg N and 90%WFPS, 150 kg N) gave higher emissions than for the 90% WFPS treatment without fertilization, but measured emissions did not show this trend. Agreement between modeled and measured emissions were larger for the 90% WPFS fertilized treatments (Figure 2-8; R^2 of modeled versus measured data: 0.57 (90% + 75 kg N) and 0.33 (90% + 150 kg N) WFPS, $P <$ 0.001). than that of the 75 % WPFS fertilized treatments (R^2: < 0.1 (75% + 75 kg N) and (75% + 150 kg N) WFPS).

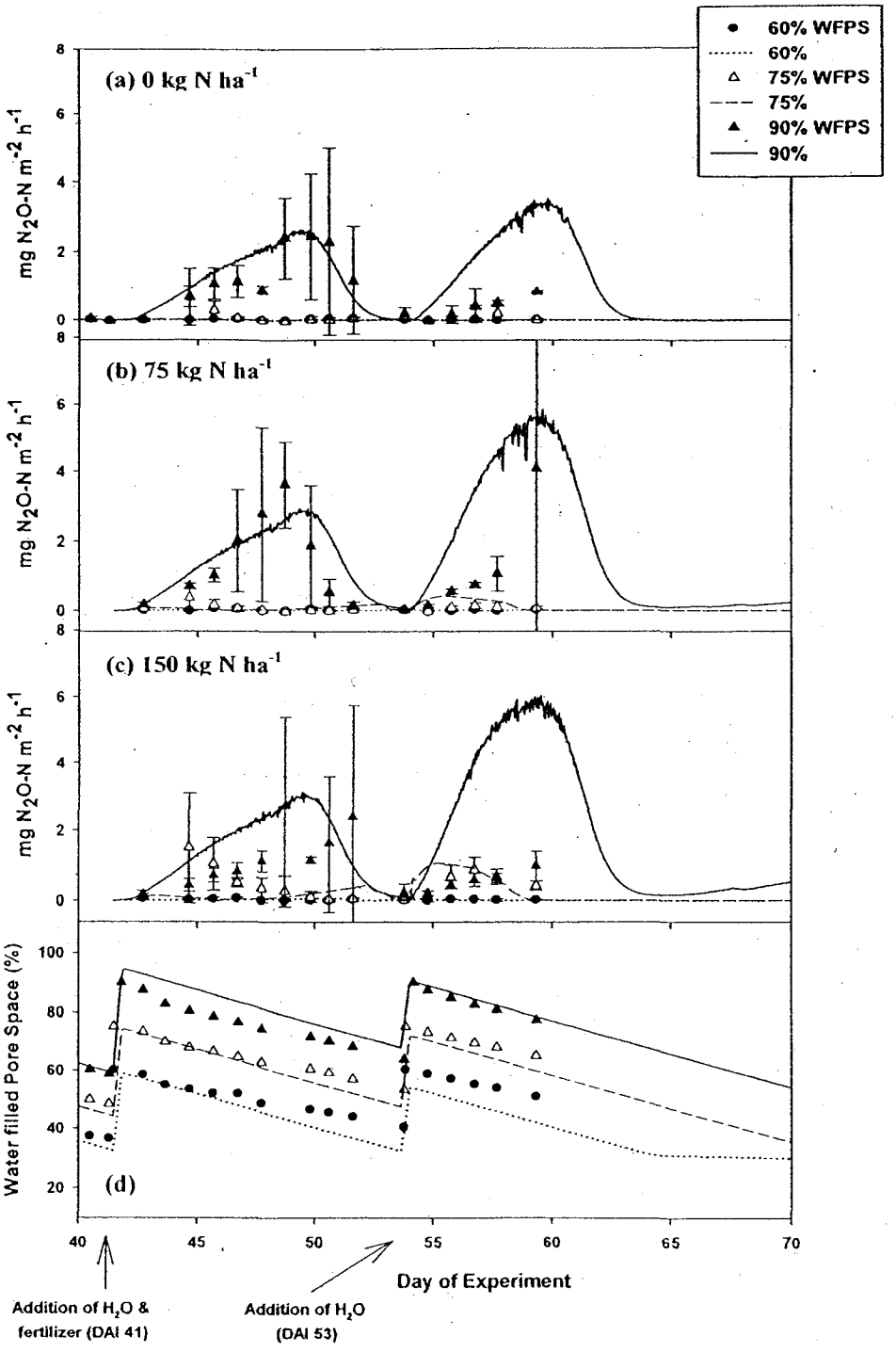

Figure 2-8: Modeled (lines) and measured (symbols) N_2O emissions for (a) 0 kg N ha^{-1} (b) 75 kg N ha^{-1} (c) 150 kg N ha^{-1} and (d) water-filled pore space (WFPS) for day of experiment 40 – 70.

2.5 DISCUSSION

The results described showed that *ecosys* (Grant, 2001a,b) captured the temporal variation of N_2O emissions and the sensitivity of these emissions to fertilizer application, at a very small site (< $1m^{-2}$) scale in the laboratory.

Ecosys represented the sensitivity of N_2O emissions in response to changes in WFPS (threshold response) thereby providing a better understanding of the episodic nature of these emissions. The threshold response in *ecosys* (Grant, 2001a,b) occurs because the D_g (Eq. [2.28]) of gases in the soil atmosphere is highly sensitive to changes in the soil's WFPS or θ_g (Millington and Quirk, 1960). The findings reported have indicated that modeled emissions rose non-linearly (Figure 2-7; R^2 of cumulative N_2O emissions versus WFPS = 0.99) with WFPS from values of 60% through 75% to 90% in a way that was consistent with the measured data (Figure 2-6: close to 0 mg N_2O-N m^{-2} h^{-1} at 60% to ~ 4.6 N_2O-N m^{-2} h^{-1} at 90%; Table 2-2: R^2: 0.26 (75%) and 0.67 (90%) WFPS, $P < 0.001$ and similar RMSD and RMSE). The consistency of modeled and measured results **supports the hypothesis in *ecosys* (Grant, 2001a,b) outlined in the Introduction (section 2.1), that N_2O production increases sharply (threshold, non-linear response) at 90% > WFPS > 60%. This non-linear rise of N_2O emissions in the model can be explained by the D_g (Eq. [2.28]) of O_2 whereby at WFPS < 60%, the D_g (Eq. [2.28]) of O_2 is large enough to meet microbial demands. However, as WFPS increases above 60%, the D_g (Eq. [2.28]) of O_2 declines sharply and the unmet O_2 demand forces the need for alternative electron acceptors (Eqs. [2.10] – [2.18]) thus, higher N_2O production via nitrification (Eq. [2.10]) and denitrification (Eq. [2.18]) in the**

model. In an incubation experiment, Dobbie and Smith (2001) found similar results whereby N_2O emissions from an arable soil increased about 30-fold as the WFPS increased from 60 to 80%. For WFPS > 60% in both preliminary and replicated experiments, our results showed that N_2O emissions increased upon water addition but then declined with soil drying; such temporal variability was also found by Dobbie and Smith, 2001. Studies by Rusier et al. (2006) showed that N_2O emission rates were generally small at soil water contents $\leq$ 60% WFPS while significantly higher N_2O emissions rates were measured at soil water contents $\geq$70% WFPS, with the highest N_2O fluxes occurring at the highest soil moisture level of 90% WFPS. Another study by Bateman and Baggs (2005) showed that emissions were 6 times higher at 70% WPFS compared to 60%WFPS. This threshold response of N_2O simulated in *ecosys* shows the importance of linking biological controls of N_2O to physical controls in mathematical models as well as of simulating N_2O emissions at an hourly time-step versus daily or monthly time-steps, in order to better capture the timing and magnitude of the entire emission events. This will improve estimates for greenhouse gas inventories since calculation of emission factors based on few data may tend to overestimate emissions.

Results from the laboratory experiment showed that WFPS was an important driver of the duration of N_2O emissions since the 90% WFPS sustained the longest emission event for each water cycle, compared to the other treatments (Figures 2-6a, 2-8a). Akiyama et al. (2004) showed that after application of water at 80 % WFPS, N_2O emissions took about 21 days to decrease to initial low values. For each rewetting event, there were repeated emissions (Figures 2-6a, 2-8a) from the 90% treatment indicating background emissions are given off by a soil without fertilizer treatments. These results show that for the same

soil residual N, variations in WFPS can affect the magnitude of emissions. These findings show the importance of using mathematical models such as *ecosys*, which represent site conditions e.g. soil residual N (based on fertilizer history), precipitation, in order to contribute towards the development of more site-specific emission factors for an IPCC Tier III Methodology.

Emissions from the laboratory experiment generally decreased over time (except for the 4th cycle) for the 90 % WFPS treatment, even though each successive re-wetting was similar. This may be attributed to a C limitation (decline in readily available C) since the soil used had high residual N (Table 4). A review by Bouwman et al. (2002) showed that N_2O emissions generally increased in soils with high organic C. These results further support the highly temporally variable nature of N_2O emissions. Dobbie and Smith (2001) also showed that emissions decreased over time for a grassland soil at 80 and 95% WPFS, for each re-wetting cycle.

For the preliminary experiment (Figure 2-5a), little or no emissions were measured for treatments without fertilizer in contrast to those of the replicated experiment (Figure 2-7a). This was attributed to the lower residual N in the soil used for the preliminary experiment compared to that of the replicated experiment (Table 2-1). Emissions were high in *ecosys* (Grant, 2001a,b) for the replicated experiment even without fertilizer N addition in a way that was consistent with the measured data (Figure 2-6; Table 2-2: R^2 of modeled versus measured data: 0.26 (75%) and 0.67 (90%) WFPS, $P < 0.001$), due to the presence of very high soil residual N (Table 2-1). After the addition of the fertilizer

treatment in the model, little N_2O emissions were simulated and this was also consistent with the measured data especially for the 90% WFPS and first cycle (Figure 2-8; R^2 of modeled versus measured data: 0.57 (90% + 75 kg N) and 0.33 (90% + 150 kg N) WFPS, $P < 0.001$). The consistency of modeled and measured results **supports the Stage 3 (non – linear) response hypothesis in *ecosys* (Grant, 2001a,b) outlined in the Introduction (section 2.1), whereby very high soil residual N due to very large rates of past fertilizer application, leads to high N_2O emissions and little of the current fertilizer N added (Figure 2-1; DE) is immobilized (Figure 2-1; E'). Consequently, very high soil residual N remains but little further increase in N_2O production occurs because of an N excess in the ecosystem, which lead to the maximum rate for N_2O production via nitrification (Eq. [2.10]) and denitrification (Eq. [2.18]) in the model (Figure 2-1; DE').** These conditions are represented in the model as v-max (maximum reaction rate) for nitrification/denitrification (Eqs. [2.1] - [2.0]) according to the Michaelis-Menten kinetics (Eqs. [2.1], [2.3b], [2.5], [2.7b], [2.10], [2.12], [2.14b] and [2.17] - [2.19]. Thus calculation of emission factors for an IPCC Tier III Methodology can vary depending on initial soil residual N. Studies by Grant et al. (2006) also show that N_2O emissions were higher with an increase in soil residual N as well as with precipitation. Studies by Dobbie and Smith (2001) showed that, when fertilizer was applied to an arable and grassland soil, there was a huge increase in N_2O emissions due to initially low available N. However, a review by Barnard (2005) suggests that the response of N_2O flux to N addition was highly variable, and there was no clear correlation with the amount of N added. A greater understanding of the stages of N excess (stages leading to maximum reaction rate for nitrification/denitrification) should

resolve the reason(s) for these variable responses. Our findings showed the importance of the use of a process-based mathematical model *ecosys* (Grant, 2001a,b), which take into account fertilizer history (soil residual N) in addition to other site conditions (e.g. soil type, climate, land use), for site-specific EF for N_2O, since an increase in fertilizer rate does not necessarily cause a proportional increase in emissions.

Future modeling work will enable *ecosys* to scale N_2O emissions from landscape to regional and national scales. The *ecosys* ecosystem model can simulate microbial oxidation/reduction reactions under different soil amendments such as crop residue (Grant et al., 1993a), fertilizer (Grant et al., 1992; Grant, 1995; Grant et al., 2006) or manure application, and under different soil management practices such as rotation and tillage (Grant, 1997; Grant et al., 1998; Grant et al., 1995; Grant and Rochette, 1994) or irrigation. Future modeling work will also enable *ecosys* to make predictions under different land use and climate change scenarios and, thus, make recommendations for sustainable land use management in order to enhance crop productivity and maintain environmental quality.

2.6 CONCLUSIONS

The results described showed that *ecosys* (Grant, 2001a,b) captured the temporal variation of N_2O emissions and the sensitivity of these emissions to fertilizer application, at a very small site (< $1m^{-2}$) scale in the laboratory. The findings reported have indicated that modeled emissions rose non-linearly (Figure 2-7; R^2 of cumulative N_2O emissions versus WFPS = 0.99) with WFPS from values of 60% through 75% to 90% in a way that was consistent with the measured data (Figure 2-6: close to 0 mg N_2O-N m^{-2} h^{-1} at 60% to ~ 4.6 N_2O-N m^{-2} h^{-1} at 90%; Table 2-2: R^2: 0.26 (75%) and 0.67 (90%) WFPS, $P <$ 0.001 and similar RMSD and RMSE). The consistency of modeled and measured results **supports the hypothesis in *ecosys* (Grant, 2001a,b) outlined in the Introduction (section 2.1), that N_2O production increases sharply (threshold, non-linear response) at 90% > WFPS > 60%.** These findings showed the importance of using mathematical models such as *ecosys* (Grant, 2001a,b) that linked biological controls of N_2O to physical controls, thereby enabling the threshold response to be simulated.

Inaccurate EFs may limit our ability to track our progress in meeting the reduction targets for the Kyoto protocol (Olsen et al., 2003). Results from the laboratory experiment showed that frequent sampling may be necessary in order to fully capture the episodic nature of N_2O emissions and thus, help improve the accuracy of EFs for inventories. However, continuous measurements of N_2O fluxes may be difficult sometimes. Mathematical models such as *ecosys* (Grant, 2001a,b) can provide continuous data sets for calculations of more accurate EFs needed for the development of an IPCC Tier III Methodology. In addition, results from this experiment demonstrated the importance of

short model time steps required to represent rapid changes in N_2O emissions. In addition to simulating N_2O emissions at smaller temporal resolutions (e.g. daily, monthly, annually etc.), *ecosys* (Grant, 2001a,b) simulated N_2O emissions at an hourly time-step which was necessary to better capture the timing and magnitude of the entire emission events versus daily (e.g. Gabrielle et al., 2006) or monthly time-step models.

Emissions were high in *ecosys* (Grant, 2001a,b) for the replicated experiment even without fertilizer N addition in a way that was consistent with the measured data, due to the presence of very high soil residual N (Table 2-1). After the addition of the fertilizer treatment in the model, little N_2O emissions were simulated and this was also consistent with the measured data especially for the 90% WFPS and first cycle after fertilizer addition (Figure 2-8; R^2 of modeled versus measured data: 0.57 (90% + 75 kg N) and 0.33 (90% + 150 kg N) WFPS, $P < 0.001$). The consistency of modeled and measured results **supports the Stage 3 (non – linear) response hypothesis in *ecosys* (Grant, 2001a,b) (Figure 2-1; DE') outlined in the Introduction (section 2.1), whereby very high soil residual N due to very large rates of past fertilizer application, leads to high N_2O emissions and little of the current fertilizer N added (Figure 2-1; DE) is immobilized (Figure 2-1; E').** Thus calculation of emission factors for an IPCC Tier III Methodology can vary depending on initial soil residual N. A review by Barnard et al. (2005) suggests that the response of N_2O flux to N addition was highly variable, and there was no clear correlation with the amount of N added. A greater understanding of the stages of N excess (stages leading to maximum reaction rate for nitrification/denitrification) should resolve the reason(s) for these variable responses. Our

findings showed the importance of the use of a process-based mathematical model *ecosys* (Grant, 2001a,b), which take into account fertilizer history (soil residual N) in addition to other site conditions (e.g. soil type, climate, land use), for site-specific EF for N_2O, since an increase in fertilizer rate does not necessarily cause a proportional increase in emissions.

There was also large replicate variation even though the soil was well mixed. These findings suggest that microspatial variation in the soil leads to variation in N_2O emissions and that there may be even larger spatial variation of N_2O emissions in the field. Consequently, there is a need for greater understanding of this spatial variation and its effects on N_2O EFs in the field. Future modeling work will enable *ecosys* to scale N_2O emissions from field to regional and national scales.

2.7 REFERENCES

Akiyama, H., Mctaggart, I.P., Ball, B.C., Scott, A., 2004. N_2O, NO, and NH_3 emissions from soil after the application of organic fertilizers, urea and water. Water, Air, and Soil Pollution 156,113–129.

Barnard, R., Leadley, P.W., Hungate, B.A., 2005. Global change, nitrification, and denitrification: A review. Global Biogeochemical cycles 19, GB1007, doi:10.1029/2004GB002282.

Bateman, E.J., Baggs, E.M., 2005. Contributions of nitrification and denitrification to N_2O emissions from soils at different water-filled pore space. Biology & Fertility of Soils 41, 379-388.

Belser, L.W., 1977. Nitrate reduction to nitrite, a possible source of nitrite for growth of nitrite-oxidizing bacteria. Applied and Environmental Microbiology 34, 403–410.

Belser, L.W., Schmidt, E.L., 1980. Growth and oxidation kinetics of the three genera of ammonia oxidizers. FEMS Microbiology Letters 7, 213-216.

Blackmer, A.M., Robbins, S.G., Bremner, J.M., 1982. Diurnal variability in rate of emission of nitrous oxide from soils. Soil Science Society of America Journal 46, 937-942.

Bouwman, A.F., Boumans, L.J.M., Batjes, N.H., 2002. Emissions of N_2O and NO from fertilized fields: Summary of available measurement data. Global Biogeochemical cycles 16(4), 1058, doi:10.1029/2001GB001811.

Bouwman, A.F., 1996. Direct emission of nitrous oxide from agricultural soils. Nutrient Cycling in Agroecosystems 46, 53-70.

Brock, T.D., Madigan, M.T., 1991. Biology of Microorganisms, 6th ed., Prentice Hall, Englewood Cliffs, NJ.

Clay, D.E., Molina, J.A.E., Clapp, C.E., Linden, D.R., 1985. Nitrogen-tillage-residue management: II. Calibration of potential rate of nitrification by model simulation. Soil Science Society of America Journal 49, 322-325.

Davidson, E.A., 1991. Fluxes of nitrous oxide and nitric oxide from terrestrial ecosystems. In: Rogers, J.E., Whitman, W.B. (Eds.), Microbial Production and Consumption of Greenhouse Gases: Methane, Nitrogen Oxides and Halomethanes. American Society of Microbiology, Washington, D.C., pp. 219-235.

de Vries, D.A. 1963. Thermal properties of soils. In R. van wijk (Ed.). Physics of Plant Environment. North Holland Publishing, Amsterdam, The Netherlands, 210-235.

Dobbie, K.E., Smith, K.A., 2001. The effects of temperature, water-filled pore space and land use on N_2O emissions from an imperfectly drained gleysol. European Journal of Soil Science 52, 667-673.

Dobbie, K.E., Smith, K.A., 2003. Nitrous oxide emission factors for agricultural soils in Great Britain: the impact of soil water-filled pore space and other controlling variables. Global Change Biology 9, 204–218.

Eggleston, 2006. Intergovernmental Panel on Climate Change (IPCC), IPCC Guidelines for National Greenhouse Gas Inventories Volume 4; Agriculture, Forestry and other land use. Institute for Global Environmental Strategies, kanagawan Hayama, Japan.

Flessa, H., Dörsch, P., Beese, F., 1995. Seasonal variation of N_2O and CH_4 fluxes in differently managed arable soils in southern Germany. Journal of Geophysical Research 100, 23115-23124.

Flechard, C.R., Ambus, P., Skiba, U., Rees, R.M., Hensen, A., van Amstel, A., van den Pol-van Dasselaar, A., Soussana, J.-F., Jones, M., Clifton-Brown, J., Raschi, A., Horvath, L., Neftel, A., Jocher, M., Ammann, C., Leifeld, J., Fuhrer, J., Calanca, P., Thalman, E., Pilegaard, K., Di Marco, C., Campbell, C., Nemitz, E., Hargreaves, K.J., Levy, P.E., Ball, B.C., Jones, S.K., van de Bulk, W.C.M., Groot, T., Blom, M., Domingues, R., Kasper, G., Allard, V., Ceschia, E., Cellier, P., Laville, P., Henault, C., Bizouard, F., Abdalla, M., Williams, M., Baronti, S., Berretti, F., Grosz, B., 2007. Effects of climate and management intensity on nitrous oxide emissions in grassland systems across Europe. Agriculture, Ecosystems and Environment 121, 135-152.

Focht, D.D., Verstraete, W., 1977. Biochemical ecology of nitrification and denitrification. Advances in Microbial Ecology 1, 135-214.

Gabrielle, B., Laville, P., Duval, O., Nicoullaud, B., Germon, J.C., Henault, C., 2006. Process-based modeling of nitrous oxide emissions from wheat cropped soils at the subregional level. Global Biochemical Cycles 20, 1-11.

Glatzel, S. N., 1999. The greenhouse gas exchange of grassland agroecosystmes. University of Hohenheim, D-70593 Stuttgart.

Grant, R.F., 1991. A technique for estimating denitrification rates at different soil temperatures, water contents, and nitrate concentrations. Soil Science 152, 41-52.

Grant, R.F., 1994. Simulation of ecological controls on nitrification. Soil Biology & Biochemistry 26, 305–315.

Grant, R.F., 1995. Mathematical modelling of nitrous oxide evolution during nitrification. Soil Biology & Biochemistry 27, 1117–1125.

Grant, R.F., 1997. Changes in soil organic matter under different tillage and rotation: mathematical modeling in *ECOSYS*. Soil Science Society of America Journal 61, 1159-1175.

Grant, R.F., 2001a. A Review of the Canadian Ecosystem Model - *ecosys*. In: Shaffer M. J., Ma, L., Hansen, S. (Ed), Modeling Carbon and Nitrogen Dynamics for Soil Management. CRC Press. Boca Raton, FL, pp. 173-263.

Grant, R.F., 2001b. Modeling Transformations of Soil Organic Carbon and Nitrogen at Differing Scales of Complexity. In: Shaffer M. J., Ma, L., Hansen, S. (Ed), Modeling Carbon and Nitrogen Dynamics for Soil Management. CRC Press. Boca Raton, FL, pp. 597-614.

Grant, R.F., 2004. Modeling topographic effects on net ecosystem productivity of boreal black spruce forests. Tree Physiology 24, 1-18.

Grant, R.F., Rochette, P., 1994. Soil Microbial respiration at Different Water Potentials and Temperatures: Theory and Mathematical Modeling. Soil Science Society of America Journal 58, 1681-1690.

Grant, R.F. and Pattey, E., 1999. Mathematical modeling of nitrous oxide emissions from an agricultural field during spring thaw. Global Biogeochemical Cycles 13, 679-694.

Grant, R.F., Pattey, E., 2003. Modelling variability in N_2O emissions from fertilized agricultural fields. Soil Biology & Biochemistry 35, 225-243.

Grant, R.F., and Pattey, E., 2007 (Submitted). Temperature sensitivity of N_2O emissions from fertilized agricultural soils: mathematical modelling in *ecosys*.

Grant, R.F., Izaurralde, R.C., Chanasyk, D.S., 1990. Soil temperature under conventional and minimum tillage: Simulation and experimental verification. Canadian Journal of Soil Science 70, 289-304.

Grant, R.F., Nyborg, M., Laidlaw, J.W., 1992. Evolution of nitrous oxide from soil: II. Experimental results and model testing. Soil Science 156, 266-277.

Grant, R.F., Juma, N.J., McGill, W.B., 1993a. Simulation of carbon and nitrogen transformations in soils. I: mineralization. Soil Biology & Biochemistry 25, 1317-1329.

Grant, R.F., Juma, N.J., McGill, W.B., 1993b. Simulation of carbon and nitrogen transformation in soil: Microbial biomass and metabolic products. Soil Biology & Biochemistry 25, 1331-1338.

Grant, R.F., Nyborg, M., Laidlaw, J.W., 1993c. Evolution of nitrous oxide from soil: I. Model development. Soil Science 156, 259-265.

Grant, R.F., Izaurralde, R.C., Chanasyk, D.S., 1995. Soil temperature under different soil managements: testing a simulation model. Agriculture & Forest Meteorology 73, 89-113.

Grant, R.F., Izaurralde, R.C., Nyborg, M., Malhi, S.S., Solberg, E.D., Jans-Hammermeister, D., Stewart, B.A., 1998. Modeling tillage and surface residue effects on soil C storage under ambient versus elevated CO_2 and temperature in *ECOSYS*. In: Lal, R., Kimble, J.M., Follet, R.F. (Eds), Soil processes and carbon cycle. CRC Press Inc. Boca Raton, USA, pp. 527-547.

Grant, R.F., Amrani, M., Heaney, D.J., Wright, R., Zhang, M., 2004. Mathematical Modeling of Phosphorus Losses from Land Application of Hog and Cattle Manure. Journal of Environmental Quality 33, 210-231.

Grant, R.F., Pattey, E., Goddard, T.W., Kryzanowski, L.M., Puurveen, H., 2006. Modeling the effects of fertilizer application rate on nitrous oxide emissions. Soil Science Society of America Journal 70, 235-248.

Griffin, D.M., 1972. Ecology of soil fungi. Syracuse Univ. Press, Syracuse, NY.

Helgason, B.L., Janzen, H.H., Angers, D.A., Boehm, M., Bolinder, M., Desjardins, R.L., Dyer, J., Ellert, B.H., Gibb, D.J., Gregorich, E.G., Lemke, R., Massé, D., McGinn, S.M., McAllister, T.A., Newlands, N., Pattey, E., Rochette, P., Smith, W., VandenBygaart, A.J., Wang, H., 2005. GHGFarm: An assessment tool for estimating net greenhouse gas emissions fromCanadian farms. Agriculture & Agri-Food Canada, pp. 5-6.

Hénault, C., Devis, X., Page, S., Justes, E., Reau, R., Germon, J.C., 1998. Nitrous oxide emissions under different soil and land management conditions. Biology and Fertility of Soils 26, 199-207.

Hutchinson, G.L., Mosier, A.R., 1981. Improved soil cover method for field measurement of nitrous oxide fluxes. Soil Science Society of America Journal 45, 311-316.

IPCC (Intergovernmental Panel on Climate Change), 2006. 2006 IPCC Guidelines for National Greenhouse Gas Inventories, Prepared by the National Greenhouse Gas Inventories Programme, Eggleston H.S., Buendia L., Miwa K., Ngara T. and Tanabe K. (Eds). Published: IGES, Japan.

Isermann, K., 1994. Agriculture's share in the emission of trace gases affecting the climate and some cause-oriented proposals for sufficiently reducing this share. Environ. Pollut, 83, 95-111.

Koike, I., Hattori, A., 1975. Growth yield of a denitrifying bacterium, *Pseudomonas denitrificans*, under aerobic and denitrifying conditions. Journal of General Microbiology 88, 1-10.

Laville, P., Jambert, C., Cellier, P., Delmas, R. 1999. Nitrous oxide fluxes from a fertilised maize crop using micrometeorological and chamber methods Agricultural & Forest Meteorology 96 (1999) 19 – 38.

Li, C., Frolking, S., Frolking, T.A., 1992. A model of nitrous oxide evolution from soil driven by rainfall events: 1. Model structure and sensitivity. Journal of Geophysical Research 97, 9759-9776.

Li., Y., Chen, D., Zhang, Y., Edis, R., Ding, H., 2005. Comparison of three modeling approaches for simulating denitrification and nitrous oxide emissions from loam-textured arable soils. Global Biogeochemical Cycles, 19, GB3002, doi:10.1029/2004GB002392.

Lim, B., Boileau, P., Bonduki, Y., van Amstel, A.R., Janssen, L.H.J.M., Olivier, J.G.J., Kroeze, C., 1999. Improving the quality of national greenhouse gas inventories. Environmental Science and Policy 2, 335-346.

Lu, Y., Huang, Y., Zou, J., Zheng, X., 2006. An inventory of N_2O emissions from agriculture in China using precipitation-rectified emission factor and background emission. Chemosphere 65, 1915-1924.

McGill, W.B., Hunt, H.W., Woodmansee, R.G., Reuss, J.O., 1981. Phoenix, a model of the dynamics of carbon and nitrogen in grassland soils. In F.E. Clark and T. Rosswall (Ed.) Terrestrial nitrogen cycles. Ecological Bulletin 33, 49-115.

Metivier, K.A, Grant, R.F. and Pattey, In. Prep. Modeling topographic effects on spatial variability of nitrous oxide emissions from fertilized agricultural fields.

Millington, R.J., 1959. Gas diffusion in porous media. Science. 130, 100-102.

Millington, R.J., Quirk, J.M., 1960. Transport in porous media. In: Van Beren, F.A. et al. (Eds.), 7th Trans. Int. Congr. Soil Sci. Vol. 1. Madison, WI. 14-24 Aug. Elsevier, Amsterdam, Science, pp. 97-06.

Molina, J.A.E., Clapp, C.E., Shaffer, M.J., Chichester, F.W., Larson, W.E., 1983. NCSOIL, a model of nitrogen and carbon transformations in soil: Description, calibration and behavior. Soil Science Society of America Journal 47, 85-91.

Morgan, R.P.C., Quinton, J.N., Smith, R.E., Govers, G., Poesen, J.W.A., Auerswald, K., Chisci, G., Torri, D., Styczen, M.E., Folly, A.J.V., 1998. The European Soil Erosion Model (EUROSEM): Documentation and user guide. Version 3.6. Silsoe College, Cranfield University, Silsoe, Bedford, UK.

Muller, C., 1999. Modelling soil-biosphere interactions. CABI Publishing, Wallingford, UK, pp. 52-53.

Myrold, D.D., 1998. Transformation of nitrogen. In: Sylvia, D.M., Fuhrmann, J.J., Hartel, P.G., Zuberer (Eds.). Principles and Applications of soil microbiology. Prentice Hall: Upper Saddle River, New Jersey, pp. 259-294.

Nyborg, M., Laidlaw, J.W., Solberg, E.D., Malhi, S.S., 1997. Denitrification and nitrous oxide emissions from a black Chernozemic soil during spring thaw in Alberta. Canadian Journal of Soil Science 77,153-160.

Olsen, K., Wellisch, M., Boileau, P., Blain, D., Ha, C., Henderson, L., Liang, C., McCarthy, J., McKibbon, S., 2003. Canada's Greenhouse Gas Inventory 1990-2001, pp. 1-4.

Pattey, E., Royds, W.G., Desjardins, R.L., Buckley, D.J., Rochette, P., 1996. Software description of a data acquisition and control system for measuring trace gas and energy fluxes by eddy-accumulation and correlation techniques. Computers and Electronics in Agriculture 15, 303-321.

Pattey, E., Edwards, G.C., Strachan, I.B., Desjardins, R.L., Kaharabata, S., Wagner-Riddle, C., 2006a. Towards standards for measuring greenhouse gas flux from agricultural fields using instrumented towers. Canadian Journal of Soil from agricultural fields using instrumented towers. Canadian Journal of Soil Science 86, 373-400.

Pattey, E., Strachan, I.B., Desjardins, R.L., Edwards, G.C., Dow, D., MacPherson, J.I., 2006b. Application of a tunable diode laser to the measurement of CH_4 and N_2O fluxes from field to landscape scale using several micrometeorological techniques. Agriculture & Forest Meteorology 13, 222-236.

Pattey E., Edwards, G.C., Desjardins, R.L., Pennock, D., Smith W., Grant, B., MacPherson, J.I., 2007. Tools for quantifying N_2O emissions from Agroecosystems. Agriculture & Forest Meteorology 142(2-4), 103-119.

Pennock, D.J., van Kessel, C., Farrell, R.E., Sutherland, R.A., 1992. Landscape-scale variations in denitrification. Soil Science Society of America Journal 56, 770-776.

Pennock, D.J., Corre, M.D., 2001. Development and application of landform segmentation procedures. Soil & Tillage Research 58, 151-162.

Phillips, F.A, Leuning, R., Baigent, R., Kelly, K.B., Denmead, O.T. 2007. Nitrous oxide flux measurements from an intensively managed irrigated pasture using micrometeorological techniques. Agricultural & Forest Meteorology 143, 92–105.

Rao, P.S.C., Jessup, R.E., Reddy, K.R., 1984. Simulation of nitrogen dynamics in flooded soils. Soil Science 138, 54-62.

Rochette, P., Desjardins, R.L, Gregorich, E.G., Pattey, E., Lessard, R., 1992.

Soil respiration in barley (Hordeum vulgare L.) and fallow fields. Canadian Journal of Soil Science 72, 591-603.

Roelandt, C., Dendoncker, N., Rounsevell, M., Perrin, D., Van Wesemael, B., 2007. Projecting future N_2O emissions from agricultural soils in Belgium. Global Change Biology 13, 18-27.

Rolston, D.E., Rao, P.S.C., Davidson, J.M., Jessup, R.E., 1984. Simulation of denitrification losses of nitrate fertilizer applied to uncropped, cropped and manure-amended field plots. Soil Science, 137, 270-279.

Ruser, R., Flessa, H., Russow, R., Schmidt, G., Buegger, F., Munch, J.C., 2006. Emission of N_2O, N_2 and CO_2 from soil fertilized with nitrate: effect of compaction, soil moisture and rewetting. Soil Biology & Biochemistry 38, 263–274.

Saxton, K.E. Rawls, W.J., 2006. Soil water characteristic estimates by texture and organic matter for hydrologic solutions. Soil Science Society of American Journal 70, 1569-1578.

Schmid, H.P., 2002. Footprint modeling for vegetation atmosphere exchange studies: a review and perspective. Agricultural and Forest Meteorology 113, 159-183.

Shields, J.A., Paul, E.A., Lowe, W.E., 1974. Factors influencing the stability of labelled microbial materials in soils. Soil Biology & Biochemistry 6, 31-37.

Smith, K.A., Thomson, P.E., Clayton, H., McTaggart, I.P., Conen, F., 1998. Effects of temperature, water content and nitrogen fertilisation on emissions of nitrous oxideby soils. Atmospheric Environment 32, 3301-3309.

Suzuki, I., Dular, U., Kwok, S.C., 1974. Ammonia or ammonium ion as substrate for oxidation by *Nitrosomonas europeae* cells and extracts. Journal of Bacteriology 120, 556-558.

Thornton, F.C., Bock, B.R., Tyler, D.D., 1996. Soil emissions of nitric oxide and nitrous oxide from injected anhydrous ammonium and urea. Journal of Environmental Quality 25, 1378-1384.

Wagner-Riddle, C., Thurtell, G.W., Kidd, G.E., Edwards, G.C., Simpson, I.J., 1996. Micrometeorological measurements of trace gas fluxes and natural ecosystems. Infrared Physics and Technology 37, 51-158.

Xu-Ri, Wang, M., Wang, Y., 2003. Using a modified DNDC model to estimate N_2O fluxes from semi-arid grassland in China. Soil Biology & Biochemistry 35, 615-620.

Yoshinari, T., Hynes, R., Knowles, R., 1977. Acetylene inhibition of nitrous oxide reduction and measurement of denitrification and nitrogen fixation in soil. Soil Biology & Biochemistry 9, 177–183.

CHAPTER 3.0 – Modeling the sensitivity of N_2O emissions from agricultural soils to changes in past and current land use management practices and inter-annual variation in precipitation using the *Ecosys* mathematical model (site scale: m^{-2})

3.1 INTRODUCTION

Canada's Greenhouse Gas Inventories (CGHGI), produced annually by Environment Canada (EC), are necessary to allow Canada to track its progress in meeting its emission reduction goals under the Kyoto Protocol (Olsen et al., 2003). Current Intergovernmental Panel of Climate Change (IPCC) methodology for quantifying N_2O in greenhouse gas inventories, is based on a constant emission factor (EF) of 1% for all N inputs (Eggleston, 2006) and does not take into account site-specific conditions. However, N_2O emissions are highly variable spatially and temporally, which complicates the calculation of emission factors and creates difficulties in measurement (e.g. Grant and Pattey, 2003).

Emission factors may vary depending on site-specific past (e.g. agricultural history of N inputs) and current land use (e.g. fertilizer rate and source, tillage, crop rotations) climate (e.g. precipitation and temperature), soil type and topography. Past land use can lead to high soil residual N levels, which subsequently result in high emission factors (Chang and Janzen, 1998). For current land use, studies have shown that model N_2O estimates using the *ecosys* (Grant 2001a,b) mathematical model resulted in an emission factor of 0.1 % at a rate of 3 g NH_4-N m^{-2} versus 1.83% at a higher fertilizer rate of 30 g NH_4-N m^{-2} (non-linear response) (Grant et. al., 2006). Other studies (e.g. Akiyama et al., 2004) showed that higher emissions were obtained from organic versus inorganic fertilizer sources. Lee et al. (2006) found that N_2O emissions in standard tillage and no tillage systems were nearly equivalent at field moisture content. Emissions reached maximum

after water application (75% water holding capacity) to a greater degree in no-tillage versus standard tillage, and then gradually decreased over time to emission levels at field moisture content (Lee et al. 2006). Another study by Meyer-Aurich (2006) found that conservation tillage as has been found to reduce N_2O emissions due to lower fuel use and lower crop residue inputs due to lower yields, as compared to conventional tillage. Emissions were found to be highest for leguminous crops, followed by other upland crops, grass, wetland rice and grass/clover mixtures (Bouwman et al., 2002). However, other studies (Meyer-Aurich, 2006) showed that even though legumes contribute considerably to the emissions of greenhouse gases by fixing nitrogen in the soil, these emissions are more than offset by reduced emissions from less fertilizer use, the reduced induced emissions from manufacturing the fertilizer and increased carbon sequestration in the soil. Higher N_2O emissions were found in cropped than in fallow fields (Verma et al., 2006). The NGAS model (Parton et al., 1996) estimates suggest that the conversion of 10.5 million hectares of cropland to grassland in the US would have a N_2O mitigation potential of 31 Gg N_2O-N $year^{-1}$, since the grassland sites generally have lower N_2O emissions than those of croplands (Mummey et al., 1998).

Inter-annual variation of precipitation can also affect emission factors. For instance, EFs obtained using the *ecosys* (Grant 2001a,b) mathematical model were 0.17% (rainfall - 223mm, 2001) compared to 2.52% (rainfall - 457mm, 2003) for a fertilizer rate of 18 g N-urea m^{-2} in Edmonton, Alberta (cool, dry climate) (Grant et. al., 2006). Several studies (e.g. Grant, 1995; Dobbie and Smith, 2001 and Smith et al. 1998) have showed that N_2O emissions are lower at lower soil temperatures. N_2O emissions can vary depending on

soil type with organic soils giving higher N_2O emissions compared to mineral soils (Bouwman et al., 2002). Emissions were generally larger in mineral soils with a fine soil texture, restricted drainage, and neutral to slightly acidic conditions compared to those from medium soil texture, good drainage, and alkaline soils (Bouwman et al., 2002). Studies by Grant and Pattey (2003) showed that modeled emissions were highest at depressional topographic positions compared to the upper and mid positions, in a fairly flat field (0.5m maximum elevational differences). Based on landform segmentation procedures to classify landform elements into landform element complexes (LEC) from digital elevation models (DEM) (Penock et al., 1987; Penock et al., 1994), Pennock and Corre (2001) found that measured N_2O emissions were significantly higher at level depressions than at foot slopes, shoulder or midslopes LECs. Pennock et al. (1992) have demonstrated that soil moisture is the main factor affecting measured N_2O emissions and that higher soil moisture is often found at lower topographic positions of a landscape. Other studies (e.g. Ball et. al., 1997; Flessa et. al., 1995) have also shown that measured N_2O emissions can vary even in seemingly uniform landscapes.

More site-specific emission factors are therefore needed to give better estimates of N_2O, for an IPCC Tier III Methodology. To achieve this, a full processed-based, three-dimensional ecosystem model should be used to represent detailed site-specific conditions as well as the spatial and temporal variability of ecological controls in N_2O emissions. One such model is *ecosys* (Grant 2001a,b), which can simulate the transport and transformation of heat, water, C, O_2, N, P and ionic solutes through soil-plant-atmosphere systems with the atmosphere as the upper boundary and soil parent material

as the lower boundary. Simulation of N_2O emissions can also improve estimates by contributing towards the continuity of measured data by estimating fluxes where measured data are missing or impossible because of resource constraints (labour, time etc.).

N_2O emissions are highly sensitive to environmental conditions because of interacting physical (soil water content, oxygen, temperature), biological (soil organic matter, nitrifying and denitrifying bacteria populations) and chemical (ammonia (NH_3) and nitrate (NO_3^-) concentrations) controls on N_2O production. N_2O emissions from soils are produced from the microbiological processes of nitrification (conversion of $NH_4^+ \rightarrow NO_2^- \rightarrow NO_3^-$) and denitrification ($NO_3^- \rightarrow NO_2^- \rightarrow N_2O \rightarrow N_2$) (e.g. Henault et al., 1998; Myrold, 1998). Nitrification generally occurs under aerobic soil conditions and NH_4^+ substrate must be present. Under O_2-limiting conditions (e.g. after rainfall), in a process called "nitrifier denitrification" ammonium oxidizers containing nitrite reductase, may reduce NO_2^- as an alternative electron acceptor to produce NO and N_2O (Muller, 1999; Myrold, 1998). Denitrification generally occurs under anaerobic soil conditions and a source of labile C as well as NO_3^- substrate must be present.

Current land use management practices can control the magnitude of N_2O emissions and, thus N_2O emission factors. In conventional agriculture, enhanced N_2O emissions are often associated with large applications of mineral fertilizers (e.g. Smith et al., 1998) because they provide a source of NH_4^+ and NO_3^- for nitrification/denitrification to occur. However, the magnitude of N_2O emissions produced by fertilizer addition is affected by

the amount of soil residual NH_4^+ and NO_3^- (Grant et al., 2006). Soil residual NO_3^- will vary depending on the agricultural history or past agricultural land use of a plot e.g., *past* fertilizer management and cropping system. Studies have shown that emissions rise linearly (Henault et. al., 1998) or exponentially (Kachonoski et. al., 2003; Izaurralde et. al., 2004) with fertilizer additions. A review by Barnard et al. (2005) suggests that the response of N_2O flux to N addition is highly variable, and there is no clear correlation with the amount of N added. Some of the studies for this review showed that application of N fertilizer at high rates resulted in little or no increase in N_2O emissions because fluxes may be already at near maximum rates due to N saturation of the system. Because N_2O production is driven by soil residual N (controls availability of alternative electron acceptors e.g. NH_4^+, NO_3^-), then rises in N_2O emissions will depend on rises in soil residual N. **It is hypothesized in *ecosys* (Grant, 2001a,b) that these rises occur in stages (non – linear response) (Figure 2-1) upon fertilizer N addition and can be explained by the immobilization capacity of the ecosystem (Grant et al., 2006):-**

Stage 1: Low initial soil residual N, then low rise in N_2O emissions upon fertilizer application. The model explanation for this trend is that when soil residual N is low due to low rates of past fertilizer application, current fertilizer N added (Figure 2-1; AB) will largely be immobilized (crop and soil uptake capacity) (N limited) (Grant et al., 2006) (Figure 2-1; B'). Consequently, low soil residual N remains, thus low N_2O production via nitrification (Eq. [2.10]) and denitrification (Eq. [2.18]) in the model (Figure 2-1; AB').

Stage 2: Higher initial soil residual N, then higher rise in N_2O emissions upon fertilizer application. The model explanation for this trend is that when soil residual N is higher due to larger rates of past fertilizer application, less of the current fertilizer N added (Figure 2-1; BC) will be immobilized compared to that of the Stage 1 response, due to the addition of N greater than the immobilization capacity of the ecosystem (Grant et al., 2006) (Figure 2-1; C'). Consequently, higher soil residual N remains, thus higher rises in N_2O production via nitrification (Eq. [2.10]) and denitrification (Eq. [2.18]) in the model (Figure 2-1; BC').

Stage 3 response - Testing of the Stage 3 response hypothesis was described in chapter 2.

N_2O emissions may also vary depending on the type of fertilizer. Kaiser and Ruser (2000) found that organic fertilizers resulted in higher annual emissions than mineral N fertilizers. Manure applications can enhance N_2O emissions (e.g. Tiedje et al., 1984) However, the flux depends on the amount of manure applied and its chemical composition (Reinertsen et al., 1984; Aulakak et al., 1991). **A consequence of the Stage 2 response hypothesis above is that: An organic source (hog manure) will give higher N_2O emissions than those of inorganic source (urea). The model explanation for this trend is that readily available N and organic C in hog manure (less C limitation) increases the demand for alternative electron acceptors (Eqs. [2.10] – [2.18]) compared to that of urea fertilizer (C limited), leading to higher N_2O emissions since N and organic C promote microbiological activity of nitrification (Eq. [2.10]) and denitrification (Eq. [2.18]) in the model. Organic C from hog**

manure may increase heterotrophic respiration (Eq. [8] and [9] of Grant, 2004) in the model, thereby leading to O_2 limitations and, thus, increased demand for alternative electron acceptors (Eqs. [2.10] – [2.18]) compared to that of urea fertilizer.

These complex hypotheses based on the site-specific effects of current and past land use and other environmental controls (e.g. climate, soil type, topography from which N_2O is generated) have been incorporated into *ecosys* (Grant, 2001a,b) the most detailed ecosystem model currently available. *Ecosys* (Grant, 2001a,b) is particularly suited for testing these hypotheses because it explicitly represents oxidation-reduction reactions from which N_2O is generated, and gas transfer processes which control the transition between alternative reduction reactions. In this model, the key biological processes – mineralization, immobilization, nitrification, denitrification, root and mycorrhizal uptake-controlling N_2O generation were coupled to the key physical processes – convection, diffusion, volatilization, dissolution - controlling the transport of gaseous reactants and products of these biological processes (Grant et al., 2006).

Ecosys can also capture the effect of precipitation on N_2O emissions. Rainfall in *ecosys* determines modeled surface flow (Eq. [2.21]) and subsurface flow (Eqs. [21] and [24] and [A94 - A96] of Grant et al., 2004) thus, WFPS. The effect of precipitation on N_2O emissions is also based on **the hypothesis in *ecosys* (Grant, 2001a,b) that N_2O production increases sharply (threshold, non-linear response) at 90% > WFPS > 60%. It was proposed that the non-linear response of D_g (Millington and Quirk,**

1960) of O_2 to changes in WFPS can be used to explain the sudden rise/threshold/ non-linear response of N_2O emissions commonly observed in the field, whereby N_2O emissions rises with WFPS > 60%. This occurs because at WFPS < 60% in the model, the D_g (Eq. [2.28]) of O_2 is large enough to meet microbial demands. However, as WFPS increases above 60%, the D_g (Eq. [2.28]) of O_2 declines sharply and the unmet O_2 demand forces the need for alternative electron acceptors (Eqs. [2.10] – [2.18]) thus, higher N_2O production via nitrification (Eq. [2.10]) and denitrification (Eq. [2.18]) in the model. The D_g of O_2 therefore controls the demand and supply of O_2 (electron acceptor) in the soil. This hypothesis in *ecosys* was tested in chapter 2 and WFPS was found to have a large impact on N_2O emissions. Transitions from one reduction reaction to another can be caused by small changes in soil WFPS as well as temperature (Grant and Rochette, 1994; Grant, 1995). *Ecosys* has been used to simulate the temporal variability (Grant, 1991; Grant et al., 1992; Grant et al., 1993c; Grant, 1994; Grant; 1995) and temporal and spatial variability (Grant et al., 1992; Grant and Pattey, 1999; Grant and Pattey, 2003; Grant et al., 2006) of N_2O emissions. For this research, we proposed to further test *ecosys* in order to better understand the sensitivity of N_2O emissions to past and current land use as well as inter-annual variation in precipitation. The research would thus contribute towards the development of more site-specific emission factors for an IPCC Tier III methodology.

3.2 MODEL DESCRIPTION

3.2.1 Introduction

Hypotheses for N_2O transformations embodied in the *ecosys* mathematical model (Grant 2001a,b) involve the microbial driven processes of nitrification (Eqs. [2.1] – [2.12]) and denitrification (Eqs. [1][2.12] – [2.20]). Physical processes in *ecosys* involved in N_2O emissions include surface (Eqs. [2.21] – [2.23]) and subsurface (Eqs. [2.24]) transport of water, and surface (Eqs. [2.25]) and sub-surface (Eqs. [2.26] – [2.28]) transport of gaseous and aqueous substrates and products.

3.2.2 Stages of N_2O response to fertilizer N addition in *ecosys*

CO_2 fixation (Eqs. [20] – [29]) of Grant, 2004), thus plant litterfall (Eqs. [29] – [37]) of Grant, 2004), and microbial residues, plant N uptake (Eqs. [A22] of Grant et al., 2006), soil type and external C and N input in *ecosys* (Grant, 2001a,b) affect the total C:N ratio in the soil (Figure 2-1 (chapter 2) shows a summary of the major hypotheses for N_2O transformations in *ecosys*, with reference to equations in this section). Each microbe functional type in each substrate-microbe complex in *ecosys* (Grant, 2001a,b) seeks to conserve its C/N ratio during growth by mineralizing NH_4^+ or by immobilizing NH_4^+ or NO_3^- (Eqs. [A1a] – [A1c]) of Grant et al., 2006). These reactions control soil mineral N concentrations which, in turn, drive nitrification (Eqs. [2.1] – [2.11]) and denitrification

[1]Refer to Chapter 2, Section 2.2 for equations beginning with "2."

(Eqs. [2.12] – [2.20]) reactions in the model (Refer to chapter 2, section 2.2.1 for a description of Stages 1, 2 and 3 responses to of N_2O fertilizer N addition in *ecosys*).

In addition to providing a source of N, manure may also provide a C source. In *ecosys*, this C source accelerates oxidation of dissolved organic carbon (DOC) and reduction of oxygen by heterotrophs (Eqs. [2.12] – [2.15]) under non-limiting O_2 conditions. This may lead to a decline in O_2 supply resulting in the need for alternative electron acceptors. Consequently, in the Stage 2 response outlined previously N_2O may be produced via nitrification (Eq. [2.10]) and denitrification (Eq. [2.18]). Also, under O_2 limiting conditions, high DOC will provide more electron donors for denitrification (Eqs. [2.16] – [2.20]).

3.3 METHODOLOGY

3.3.1 Field experiment

3.3.1.1 Experimental site, design & treatments

Three field plot experiments were conducted at Ellerslie (Long-term fertilized and Short-term fertilized sites) and Devon (Manured site, a few kilometres away from the Ellerslie site), near Edmonton, Alberta, Canada ($53^0$19'N $113^0$34'W, mean annual temperature 2.4°C, mean annual precipitation 483 mm), for the period 2001 to 2003. The soil type present at Ellerslie and Devon was an Orthic Black Chernozem (Table 3-1, 3-2). At each site, barley was planted and a randomized block design was used with three replicates.

Table 3-1: Soil chemical properties for Orthic Black Chernozem at Ellerslie

Depth (m)	Surface – 0.10	0.10 - 0.15	0.20 - 0.30	0.30- 0.60	0.60 - 0.90
D_b, (Mg m^{-3})*	1.1	1.35	1.4	1.5	1.5
θ_{FC}, m^3 m^{-3}*	0.31	0.31	0.31	0.32	0.32
θ_{WP}, m^3 m^{-3} *	0.15	0.15	0.15	0.17	0.17
Ks_{at}, mm h^{-1}*	5.3	5.3	5.6	3.9	3.9
Sand, g kg^{-1}	280	280	250	270	270
Silt, g kg^{-1}	450	450	470	420	420
pH	6.3	6.3	6.5	6.6	6.6
CEC, cmol kg^{-1}	20	15	18	21	21
Org. C, g kg^{-1}	60.5	40.7	40.7	3	3
Org. N, g Mg^{-1}	5042	3400	3400	300	300

***Abbreviations: D_b, bulk density, θ_{FC}, water content at -0.033 MPa; θ_{WP}, water content at -1.5 MPa; K_{sat}, saturated hydraulic conductivity.**

Table 3-2: Soil chemical properties for Orthic Black Chernozem at Devon

Depth (m)	Surface – 0.10	0.10 - 0.15	0.15 - 0.30	0.30- 0.50	0.50 - 0.90
D_b, (Mg m^{-3})*	1.15	1.35	1.4	1.5	1.5
θ_{FC}, m^3 m^{-3}*	0.3	0.3	0.32	0.33	0.33
θ_{WP}, m^3 m^{-3} *	0.15	0.15	0.17	0.17	0.17
Ks_{at}, mm h^{-1}*	8.2	3.7	4.1	3.1	4.5
Sand, g kg^{-1}	450	450	210	320	311
Silt, g kg^{-1}	350	350	360	350	327
pH	6.1	6.1	6.7	6.9	6.97
CEC, cmol kg^{-1}	20	15	18	21	17.5
Org. C, g kg^{-1}	33	12	6	3	3.5
Org. N, g Mg^{-1}	2750	1040	500	300	291.7

***Abbreviations: D_b, bulk density, θ_{FC}, water content at -0.033 MPa; θ_{WP}, water content at -1.5 MPa; K_{sat}, saturated hydraulic conductivity.**

Bulk density, field capacity, wilting point and hydraulic conductivity were estimated from the Saxton (2006) pedo-transfer function calculator.

Different fertilizer rates were used to test the hypothesis (Section 3.1), that N_2O response to fertilizer application (current land use) depends on the soil residual N. The treatments were designed to test for non-linearity of N_2O emissions with fertilizer rate under (a) long history of fertilization applications: high residual N and transition from N to C – limitation (**Stage 2** response, section 3.1) and (b) short history of fertilizer application: low residual N and N – limitation (**Stage 1** response, section 3.1). The treatments were:

(1) Long-term fertilized site – Fall and spring-banded urea at:

(a) 90 kg N ha^{-1}(Designed to test a **Stage 1** response)

(b) 180 kg N ha^{-1} (Designed to test a **Stage 2** response) and

(c) 0 kg N ha^{-1} (control).

(2) Short-term fertilized site – Fall-banded urea at:

(a) 50 kg N ha^{-1}

(b) 100 kg N ha^{-1} (Designed to test a **Stage 1** response) and

(c) 0 kg N ha^{-1} (control).

The Long-term fertilized site was fertilized for 18 years prior to the start of the experiment (high soil residual N) while the Short-term fertilized site was only fertilized for 3 years prior to the start of the experiment (low soil residual N). Therefore, similar fertilizer rates (90 kg N ha^{-1} for Long-term fertilized site and 100 kg N ha^{-1} for Short-term fertilized site) were compared to determine the effect of different soil residual N due to past land use, on N_2O emissions. An organic N source in the form of hog manure (Table 3 – 3) was used to compare with the Long-term fertilized (current land use), to test the **Stage 2** response hypothesis (Section 3.1) that readily available NH_4^+, and organic C in manure and high moisture content leads to higher N_2O emissions compared to that of urea fertilizer. Hog manure was applied in the spring and was surface-incoporated for 6 years prior to the start of the experiment at rates of - Spring applied hog manure at (a) 87 kg N ha^{-1} y^{-1}(15 Mg ha^{-1} y^{-1}) and (b) 271 kg N ha^{-1} $3y^{-1}$ (45 Mg ha^{-1} $3y^{-1}$ - applied only once in 2001).

Table 3-3: Chemical composition of hog manure (15 Mg ha^{-1})

Total N	Total inorganic N	Total organic N	Total organic C	P	K	S	Moisture (%)	Organic C/N ratio
(kg N ha^{-1})								
87	75	12	173	5.14	37	3.07	98	14

3.3.1.2 N_2O and soil moisture measurements

N_2O emissions were measured using non-steady-state, non-flow-through surface flux chambers from April to November of each year, 2 - 3 three times per week. These measurements were obtained from Mrs Kerrianne Koelher-Munro and Mr Tom Goddard as part of research funded by a previous Canadian Agri-Food Research Council - Climate Change Funding Initiative in Agriculture (CARC-CCFIA) grant. Chambers were located on collars (0.65 x 0.17m) which were installed after seeding by inserting 5cm into the soil. Sampling was done by placing a chamber on each collar and then later withdrawing samples from the headspace using a syringe at intervals of 0 and 30 minutes after chamber placement. Samples were then stored in previously evacuated, sealed containers (Exetainers (12mL); Labco Limited, Buckinghamshire, United Kingdom) prior to gas chromatograph (GC) (Varian Canada Inc., Mississauga, ON) analyses. Fluxes were calculated using a linear model.

3.3.1.3 Available N measurements

Soil samples were taken in April and September of each year at depths 0-15, 15-30 and 30-45 cm, to measure exchangeable NH_4^+ and NO_3^- concentrations. Mineral N extracts

were obtained by adding 2M KCl (ratio 1:5 soil to KCl by weight) to soil samples and shaking for 30 min. Extracts were analyzed for exchangeable NH_4^+ and NO_3^- concentrations using an auto analyzer (Auto analyzer II, Selkirk Scientific).

3.3.1.4 Soil moisture content and temperature

A datalogger (CR500, Campbell Scientific Logan, Utah) was placed at each experimental site to continuously record soil volumetric water content using TDR probe sensors (CS615; Campbell Scientific Logan, Utah) at depths of 0-5, 5-15 and 15-30cm, and soil temperature using thermistors at depths of 5 and 15 cm. These data were used to explain dynamics of N_2O under different soil moisture and temperature conditions. These measurements were obtained from Mr Dick Puurveen as part of previous research funded by the Canadian Agri-Food Research Council - Climate Change Funding Initiative in Agriculture (CARC-CCFIA) Program.

3.3.1.5 Meteorological data

Hourly rainfall, air temperature, humidity, wind speed and solar radiation data were collected from a weather station installed at the edge of each experimental site for the period 1999 - 2003. These measurements were taken by Dick Puurveen as part of previous research funded by the Canadian Agri-Food Research Council - Climate Change Funding Initiative in Agriculture (CARC-CCFIA). The effect of inter-annual variation of precipitation (Table 3-4) on N_2O emissions was examined.

Table 3-4: Precipitation for 2001 – 2003 at experimental sites

Year	Total Precipitation (mm)
2001	362
2002	260
2003	484

3.3.2 Model Experiment

The *ecosys* model (Grant 2001a,b) was used to conduct a simulated experiment using input data from the field plot experiments. Soil properties of the Orthic Black Chernozem at Ellerslie (Table 3-1) and Devon (Table 3-2) were used for the model experiment.

In order to represent the agricultural history for each site (Section 3.3.1.1) and establish model equilibrium for soil organic C and N, the model runs commenced in 1979. Long-term fertilized plots were modeled as unfertilized grain crop from 1979 to 1983, then with fertilizer treatments from 1984 to 2003, since this site was fertilized for 18 years prior to the start of the experiment (High soil residual N site). Short-term fertilized plots were modeled as unfertilized grain crop from 1979 to 1998, then with fertilizer treatments from 1999 to 2003, since this site was fertilized for 3 years prior to the start of the experiment (Low soil residual N site). Manured plots were modeled as fertilized grain crop from 1979 to 1994, then with manure treatments (Table 3-3) from 1995 to 2003, since manure treatments were applied for 6 years prior to the start of the experiment. Weather data (from Section from 3.3.1.5) for the model were obtained from a weather station at the experimental site and from Environment Canada, repeating sequences of

hourly 1999 – 2003 weather data.

Modeled N_2O emissions, soil temperature and moisture were compared to measured data during 2001 - 2003.

3.4 RESULTS

3.4.1 Effect of fertilizer rate on modeled and measured N_2O emissions

3.4.1.1 Long-term fertilized site

Urea fertilizer was hydrolyzed in the *ecosys* model to produce [NH_{3s}]. The presence of an abundance of NH_{3s} in *ecosys* provided substrates for N_2O production via nitrification (Eq. [2.10]) and denitrification (Eq. [2.18]). Rainfall events, e.g., during DOY 167, 2001 (Figure 3-1a) led to increases in WFPS > 60% (Figure 3-1b) which caused declines in surface and subsurface gaseous diffusivity ($D_{gγ}$ in Eq. [2.28]), lowering gaseous O_2 ([O_{2g}]) in the soil profile and slowing dissolution of O_{2g} to O_{2s} (Eq. [A30] in Grant et al., 2006). Dissolution slowed further when higher soil temperatures in the field during soil warming for the spring/summer period (e.g. Figure 3-1c), reduced the aqueous solubility of O_2 (Eq. [A30] in Grant et al., 2006), lowering [O_{2s}] that sustained O_2 uptake by microbial populations (Eqs. [2.3], [2.7] and [2.14]). Higher soil temperatures also led to an increase in microbial activity and therefore a higher demand for O_2 (Eqs. [2.2], [2.3a,b], [2.13] and [2.14a,b], through the Arrhenius function in Eqs. [2.1] & [2.12]. Aqueous O_2 concentrations at nitrifier microsites ([$O_{2mi,n}$] in Eqs. [2.3a,b] and [2.7a,b]) declined with respect to the Michaelis-Menten K_{O2n} in Eqs. [2.3b] and [2.7b], therefore O_2 uptake by nitrifiers ($R_{O2i,n}$ in Eqs. [2.3a] and [2.7a]) failed to meet O_2 demand (Eqs. [2.2] and [2.6]).

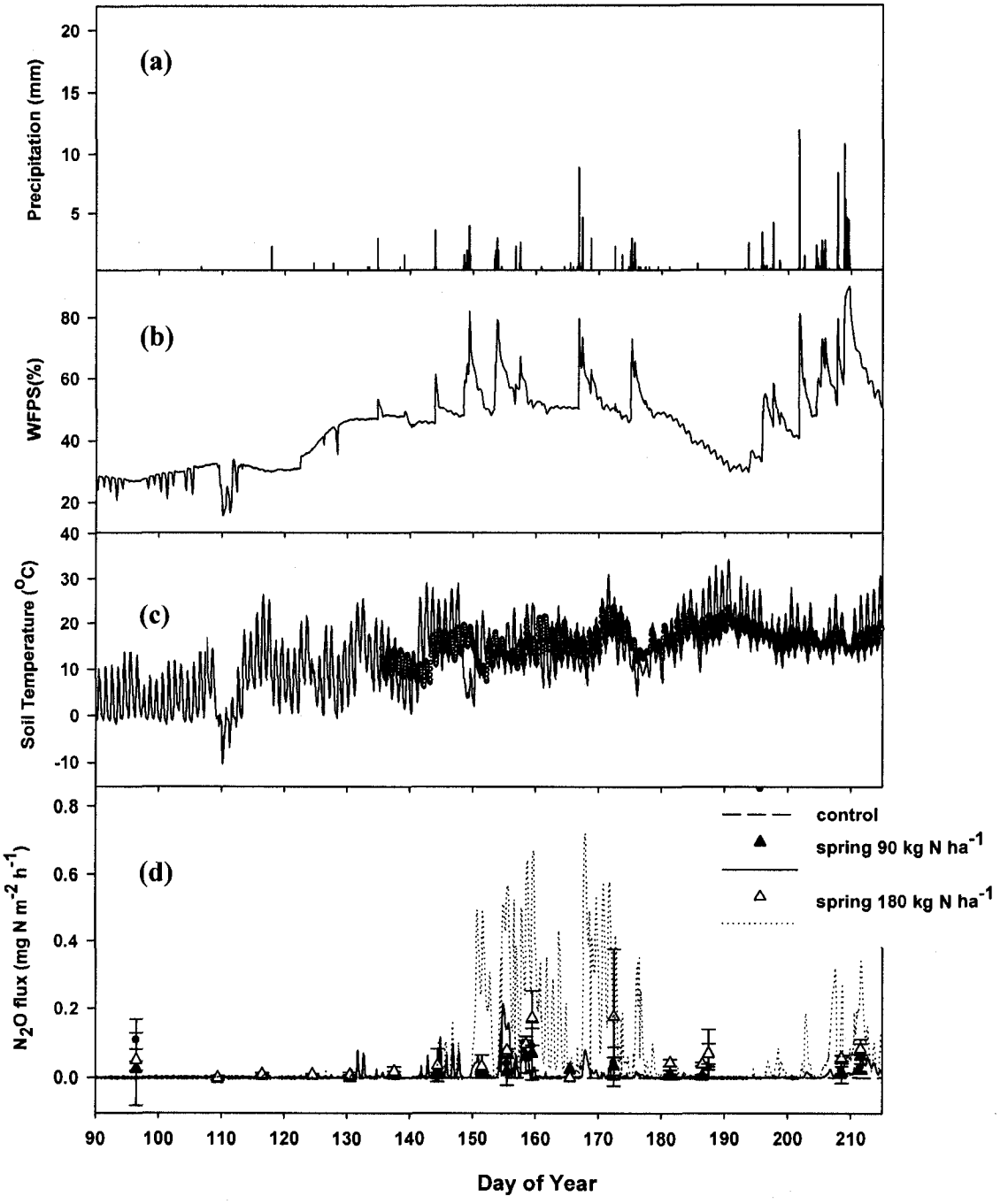

Figure 3-1: (a) Precipitation (b) modeled (lines) water-filled pore space (WFPS) (5cm) (c) modeled (lines) and measured (symbols) soil temperature (5cm) and (d) modeled (lines) and measured (symbols) N_2O emissions at Ellerslie during 2001, for spring – applied fertilizer at Long-term fertilized site. (Measured data obtained from Kerrianne Koehler-Munro and Tom Goddard from CARC-CCFIA grant).

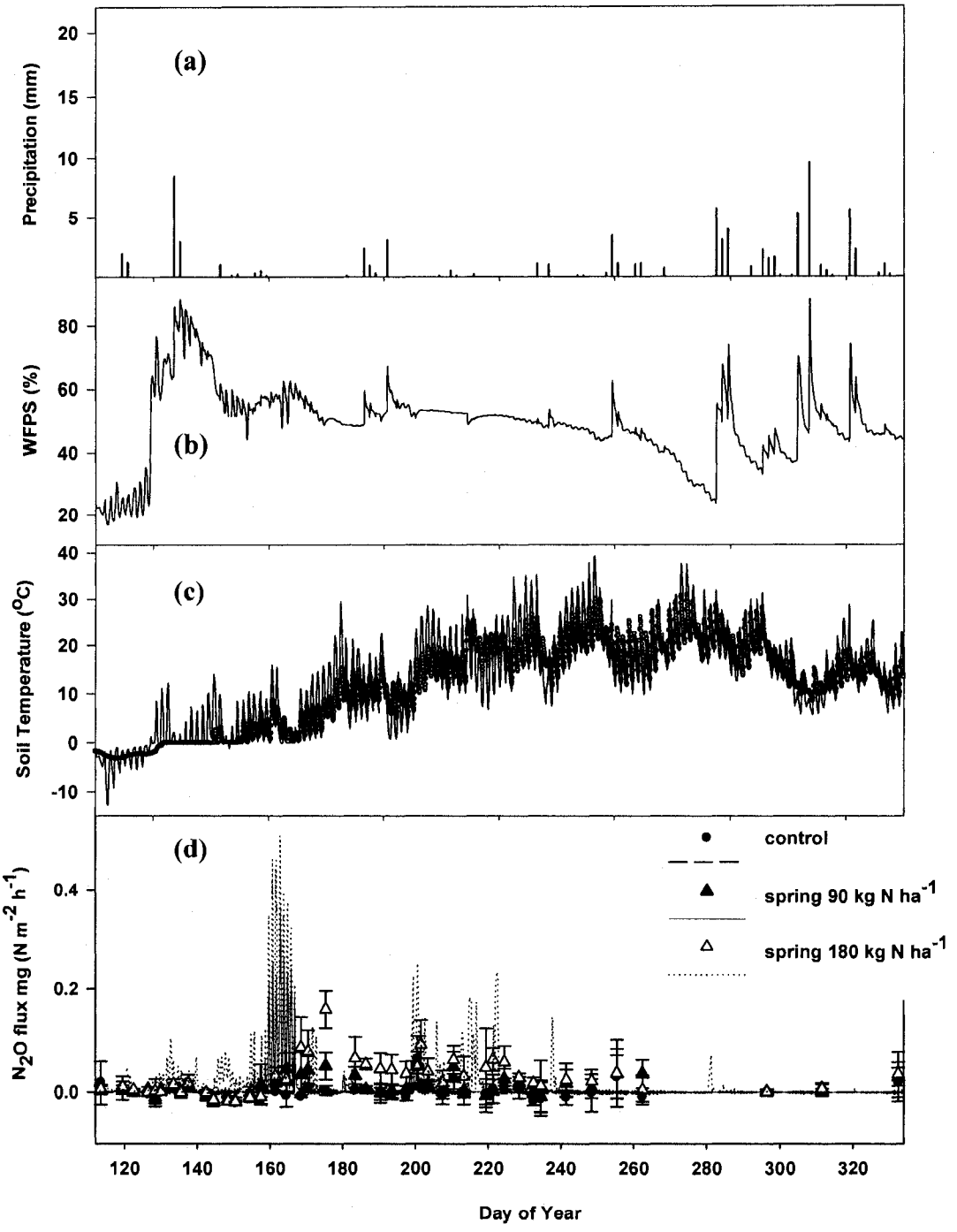

Figure 3-2: (a) Precipitation (b) modeled (lines) water-filled pore space (WFPS) (5cm) (c) modeled (lines) and measured (symbols) soil temperature (5cm) and (d) modeled (lines) and measured (symbols) N_2O emissions at Ellerslie during 2002, for spring – applied fertilizer at Long-term fertilized site. (Measured data obtained from Kerrianne Koehler-Munro and Tom Goddard from CARC-CCFIA grant).

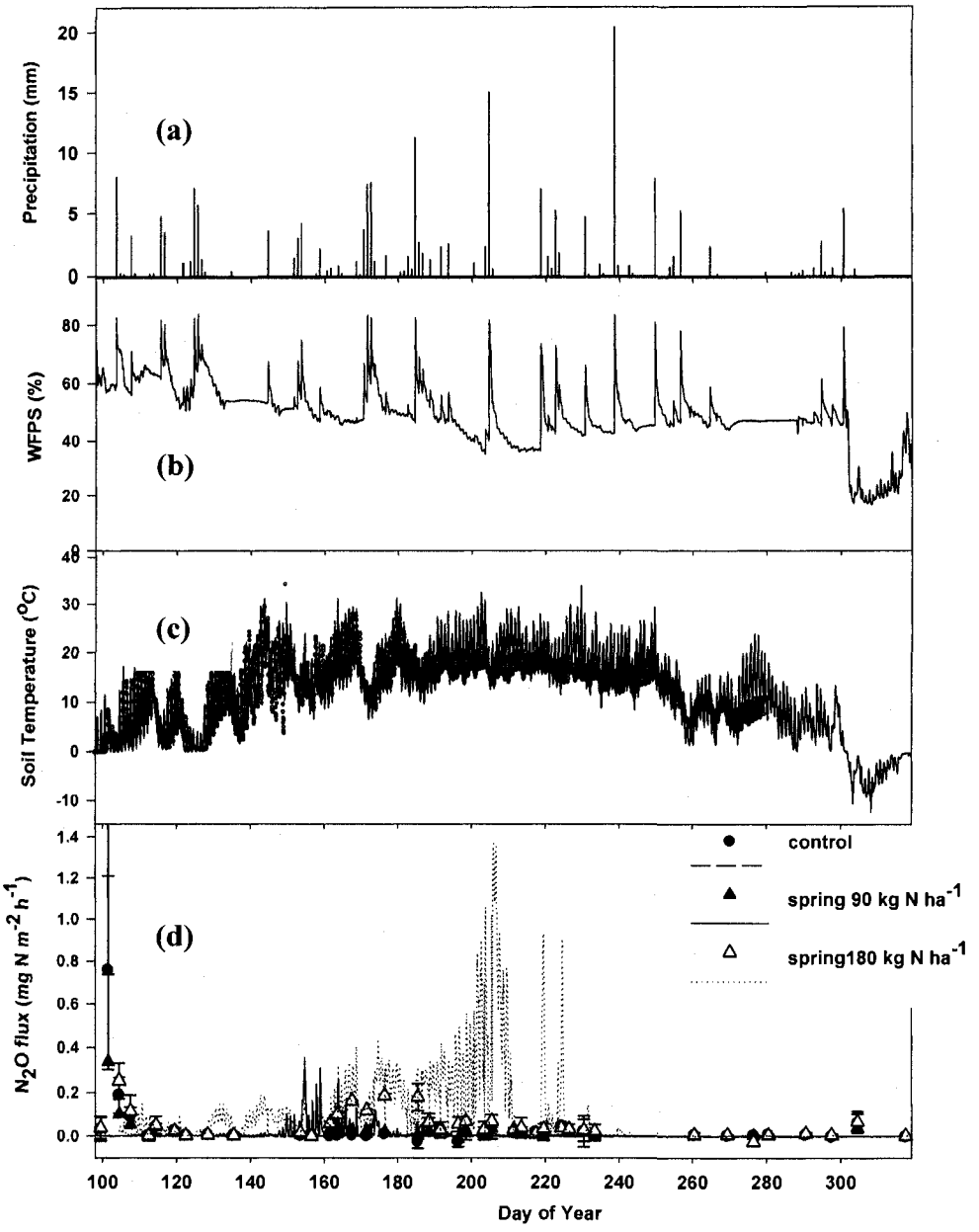

Figure 3-3: (a) Precipitation (b) modeled (lines) water-filled pore space (WFPS) (5cm) (c) modeled (lines) and measured (symbols) soil temperature (5cm) and (d) modeled (lines) and measured (symbols) N_2O emissions at Ellerslie during 2003, for spring – applied fertilizer at Long-term fertilized site. (Measured data obtained from Kerrianne Koehler-Munro and Tom Goddard from CARC-CCFIA grant).

Subsequently, in the *ecosys* model alternative electron acceptors were used to produce N_2O via nitrification (Eq. [2.10]) and denitrification (Eq. [2.18]), due to a combination of fertilizer application, rainfall and soil warming. However, the N_2O produced followed a non-linear response for the different fertilizer rates i.e. little emissions were modeled or measured at 0 or 90 kg N ha^{-1} but high emissions were predicted by the model at 180 kg N ha^{-1}. However, inter – annual variation of precipitation (Table 3-4) dictated the magnitude of N_2O emission response to fertilizer.

Modeled and measured emissions from the lower fertilizer rate (Figures 3-1d, 3-2d, and 3-3d) was similar to a Stage 1 response (Section 3.1) whereby there was lower soil residual N and higher residue C:N ratio compared to the higher fertilizer rate (Table 3-5) therefore, little emissions was observed because most of the added N was immobilized by the ecosystem (Grant et al., 2006) and thus little was available for nitrification (Eq. [2.10]) and denitrification (Eq. [2.18]).

Table 3-5: Modeled and measured fall (October) residual N for long-term fertilized site

Year	Treatment (kg N ha^{-1})	§Mineral N (g m^{-2})	
		Modeled	Measured
2001	Spring-control	3	17 ± 3
	Fall-90	28	26 ± 8
	Fall -180	74	76 ± 12
	Spring-90	6	27 ± 10
	Spring-180	55	71 ± 44
2002	Spring-control	2	11 ± 2
	Fall-90	32	19 ± 4
	Fall -180	147	63 ± 22
	Spring-90	36	39 ± 6
	Spring-180	169	109 ± 31
2003	Spring-control	3	19 ± 2
	Fall-90	24	20.8 ± 4
	Fall -180	136	41.5 ± 10
	Spring-90	29	20 ± 3
	Spring-180	171	47.4 ± 15

§Exchangeable + soluble NH_4^+ + NO_3^- (0-15cm)

±Standard deviation of 3 replicates

In contrast to the Stage 1 response , modeled results from *ecosys* (Grant, 2001a,b) showed that N_2O emissions and EFs for the higher fertilizer rate (180 kg N m^{-2} y^{-1}) for the Long-term fertilized site (Figure 3-1 – 3-3; Table 3-6, 3-7) were higher (Stage 2 response) and this was generally consistent with the measured data (Table 3-10) with a few significant correlations in some cases (e.g., R^2 of modeled versus measured data: 0.77

(2001, spring 180 kg N ha^{-1}), $P < 0.001$), due to the presence of higher soil residual N and comparatively low C:N ratios (Tables 3-5; 3-8). These conditions led to N in excess of the ecosystem's uptake capacity thus more N was available for nitrification (Eq. [2.10]) and denitrification (Eq. [2.18]), leading to greater N_2O emissions (Figures 3-1d, 3-2d, and 3-3d). Consequently, modeled annual cumulative emissions (Table 3-6) and EFs (calculated as N_2O emissions with fertilizer application minus those of the control, divided by the total N fertilizer applied) (Table 3-7) for both fall and spring applications rose with fertilizer rate, especially in the wettest year (2003).

Table 3-6 - Annual site-specific cumulative N_2O emissions (mg N m^{-2} y^{-1}) derived from *Ecosys*.

Treatments (kg N ha^{-1} $year^{-1}$)	**Year (January –December) & Annual Precipitation**		
	2001 (362mm)	**2002 (260mm)**	**2003 (484mm)**
Short-term fertilized site			
Control	0.2	0	0.2
50	0.8	4.4	1
100	8.8	9.7	8.2
Long-term fertilized site			
Control	0.4	0.9	2.0
Fall 90	27	5.1	16
Fall 180	155	121	501
Spring 90	27	28	43
Spring 180	206	102	453
Manured site			
Control	6.6	7.9	10
87	110	105	251
261 ($3y^{-1}$) (applied in 2001)	270	37	64

Table 3-7: Annual site-specific emission factors (%) derived from *Ecosys*

Treatments ($kg\ N\ ha^{-1}\ year^{-1}$)	Year (Jan.–Dec.) & Annual Precipitation		
	2001 (362mm)	2002 (260mm)	2003 (484mm)
Short-term fertilized site			
50	0	0.1	0
100	0.1	0.1	0.1
Long-term fertilized site			
Fall 90	0.3	0	0.2
Fall 180	0.9	0.7	2.8
Spring 90	0.3	0.3	0.5
Spring 180	1.1	0.6	2.5
Manured site			
87	1.3	1.2	3
261 ($3y^{-1}$) (applied in 2001)	1.1	0.1	0.2

The use of these alternative electron acceptors in the model caused emissions e.g. on DOY 207 (Figures 3-1d) in the model to be delayed for several hours following rainfall on DOY 206 (Figure 3-1a), due to high WFPS (Figure 3-1b). High WFPS led to low θ_g which lowered $[O_{2s}]$ causing an increase in N_2O production. However, emissions into the atmosphere were delayed because of a reduction in the gaseous diffusivity of N_2O (D_{gy} in Eq. [2.28]). Also, during high WFPS, denitrification in the model may proceed to the terminal electron acceptor (N_2) ($R_{N2Oi,d}$ in Eq. [2.19]), therefore a higher proportion of N_2 versus N_2O may be produced. Emissions immediately followed volatilization of N_2O_s (Eq. [A30] in Grant et al., 2006) following re-establishment of gaseous pathways during drainage.

Even though there was rainfall later in the crop season (e.g. on DOY 301 in 2003 (Figure 3-3a)) and, thus an increase in WFPS (Figure 3-3b), modeled and measured emissions were low (Figure 3-3d). This was due to a decline in available NH_4^+ and NO_3^-, because of crop uptake. As a result, NH_3 oxidation ([2.1]-[2.4]) was slowed by declining $[NH_{3s}]$. Thus, the rate of NO_2^- reduction ([2.5]-[2.8]) also declined, leading to a reduction in N_2O generation (Eqs. [2.19] and [2.10]). The reduction in N_2O emissions later in the season was also attributed to the decline in WFPS (Figure 3-3b) caused by more rapid evapotranspiration

3.4.1.2 Short-term fertilized site

Modeled results from *ecosys* (Grant 2001a,b) showed that N_2O emissions and EFs for all rates for the Short-term fertilized site (Figure 3-4; Table 3-6, 3-7) were low and this was generally consistent with the measured data (Table 3-10). These results indicate a Stage 1 response to both fertilizer rates (50 and 100 kg N ha^{-1}) due to low soil residual N and high residual C:N ratio (Table 3-5; 3-8).

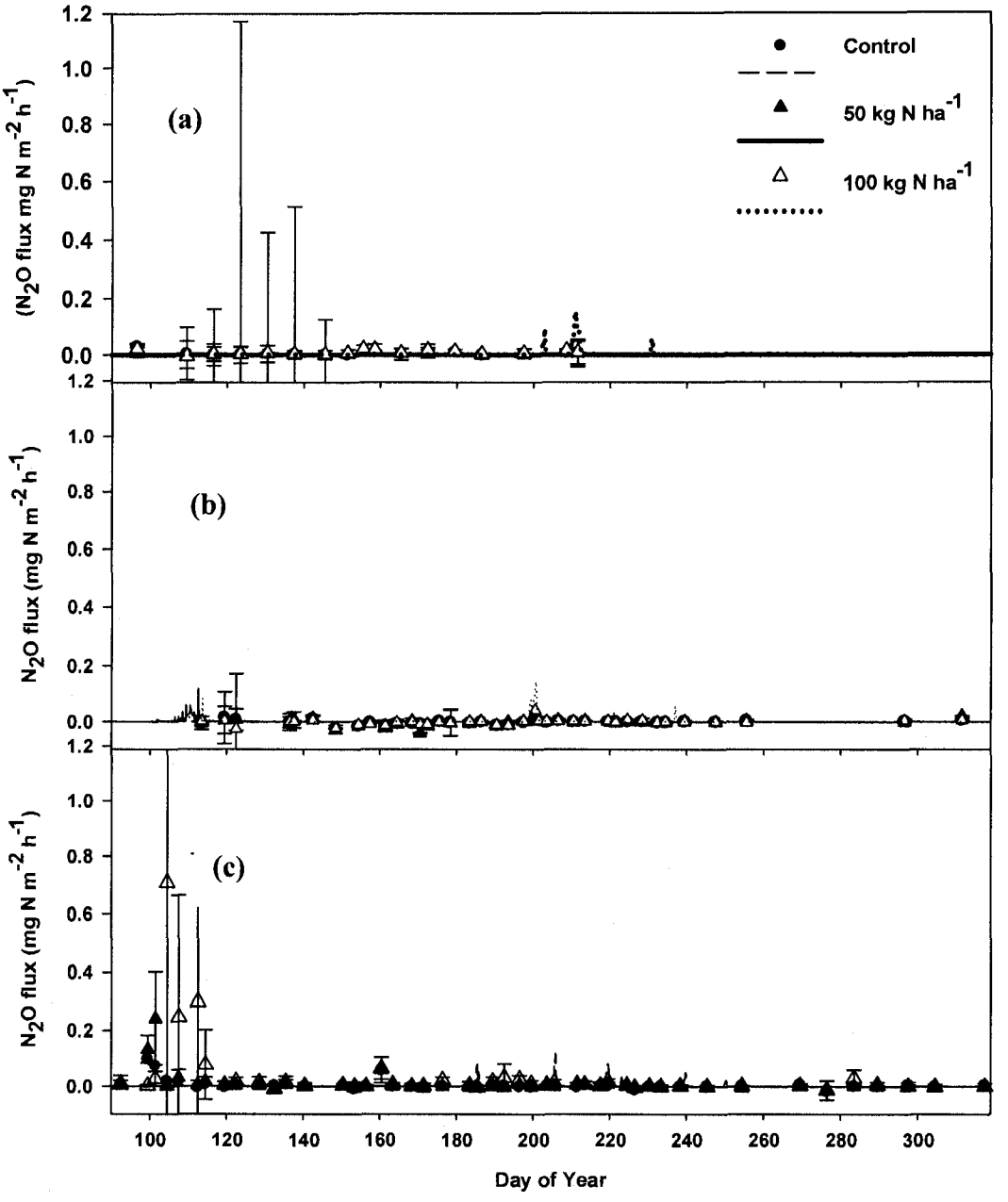

Figure 3-4: Modeled (lines) and measured (symbols) N_2O emissions for (a) 2001 (b) 2002 (c) 2003 at Ellerslie during 2003, for fall – applied fertilizer at Short-term fertilized site. (Measured data obtained from Kerrianne Koehler-Munro and Tom Goddard from CARC-CCFIA grant).

Emissions (Table 3-6; Figure 3-5a) and emission factor (Table 3-7) for fertilizer rate (fall - 90 kg N ha^{-1} (correlations were between modeled and measured emissions were $R^2 < 0$ (90 kg N ha^{-1}); $R^2 = 0.53$, $P < 0.05$ (180 kg N ha^{-1})) at long-term fertilized plots were higher than that of the short- term fertilized site (100 kg N ha^{-1}) (Figure 3-4a), in 2001. This was due to the higher soil residual N at the long-term fertilized plots lower (Tables 3-5) compared to that of the Short- term fertilized site (Tables 3-8). Even though both fertilizer rates gave responses similar to a Stage 1 response, the differences in emissions shows the importance of past land use effect on soil residual N and, thus, N_2O emissions. However, this trend was not consistent in 2002 and not strong in 2003 (2002 ($R^2 = 0.61$, $P = 0.06$ (90 kg N ha^{-1}); $R^2 = 0.18$, $P > 0.05$ (180 kg N ha^{-1}) and 2003 ($R^2 < 0$)).

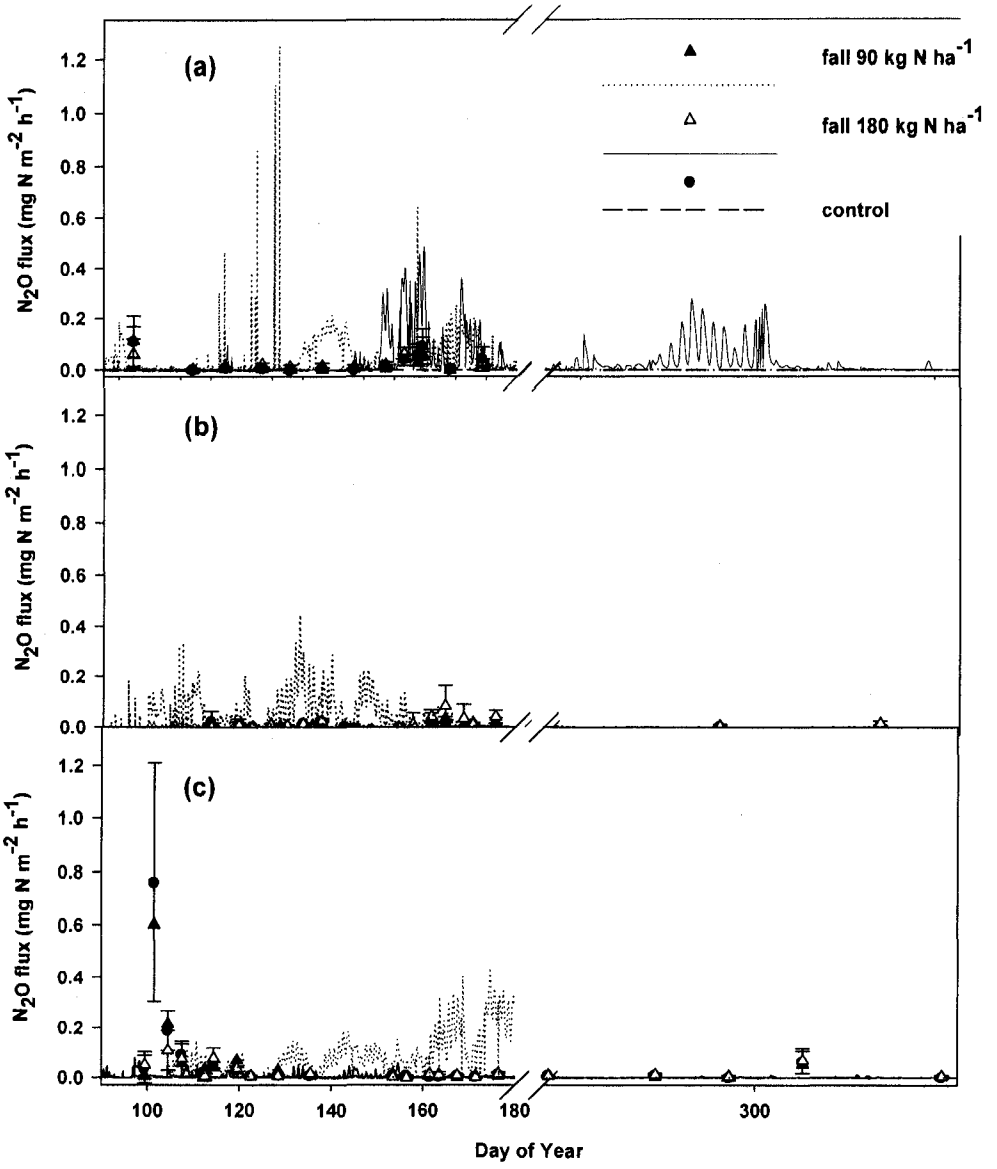

Figure 3-5: Modeled (lines) and measured (symbols) N_2O emissions for (a) 2001 (b) 2002 (c) 2003 at Ellerslie during 2003, for fall – applied fertilizer at Long-term fertilized site. (Measured data obtained from Kerrianne Koehler-Munro and Tom Goddard from CARC-CCFIA grant).

Table 3-8 – Modeled and measured fall (October) residual N and C:N for Short-term fertilized site

Year	Treatment (kg N ha^{-1})	§Mineral N (g m^{-2})	
		Modeled	Measured
2001	Control	2.3	8.2 ± 1.1
	Fall-50	2.4	10.4 ± 5.3
	Fall-100	7.3	6.6 ± 1.2
2002	Control	2.6	9.5 ± 1.2
	Fall-50	15.9	18.8 ± 12.8
	Fall-100	41.5	10.4 ± 1.5
2003	Control	3.3	10.5 ± 1.9
	Fall-50	15.2	11.3 ± 1.9
	Fall-100	30.6	12.4 ± 1.4

§Exchangeable + soluble NH_4^+ + NO_3^- (0-15cm)

±Standard deviation of 3 replicates

3.4.1.3 Effect of inter-annual variation of precipitation on N_2O emissions

Modeled results from *ecosys* (Grant 2001a,b) showed that N_2O emissions and EFs were highest in 2003 (Figures 3-1-3-3; Tables 3-6, 3-7) compared to the other years, with general consistency (Table 3-10; e.g. Higher modeled and measured EFs for spring urea applications in 2003 versus 2002 (drought year in Alberta, Canada)), due to highest precipitation in 2003. Higher rainfall (Figure 3-3a vs. Figures 3-1a, 3-2a) in *ecosys* can be used to explain larger surface flow (Eq. [2.21]) and subsurface flow (Eqs. [21] and [24] and [A94 - A96] of Grant et al., 2004) which resulted in further increases in WFPS > 60% (Figure 3-3b vs. Figures 3-1b, 3-2b). Higher WFPS caused greater declines in surface and subsurface gaseous diffusivity ($D_{g\gamma}$ in Eq. [2.28]), lowering gaseous O_2

([O_{2g}]) in the soil profile and slowing dissolution of O_{2g} to O_{2s} (Eq. [A30] in Grant et al., 2006). This resulted in a greater need for alternative electron acceptors (Eqs. [2.10] – [2.18]) thus, in *ecosys*, more N_2O was produced via nitrification (Eq. [2.10]) and denitrification (Eq. [2.18]) (Figure 3-3d vs. Figures 3-1d, 3-2d).

3.4.2 Effect of source of fertilizer on modeled and measured N_2O emissions

Modeled results from *ecosys* (Grant 2001a,b) showed that N_2O emissions (Figure 3-6) were higher for the hog manure (87 kg N ha^{-1}) compared to urea fertilizer (spring – 90 kg N ha^{-1}) even though N additions were similar, with a few significant correlations in some cases (e.g., R^2 of modeled versus measured data:0.48 (2003, 87 kg N ha^{-1}), $P < 0.001$). In addition to inorganic N (Table 3-9), the organic C (Table 3-3) in the hog manure provided an additional source of electron donors for denitrification (Eqs. [2.12] – [2.19]) in *ecosys*. Readily available N and organic C in hog manure (less C limitation) increases the demand for alternative electron acceptors (Eqs. [2.10] – [2.18]) compared to that of urea fertilizer (C limited), leading to higher N_2O emissions since N and organic C promote microbiological activity of nitrification (Eq. [2.10]) and denitrification (Eq. [2.18]) in the model. Organic C from hog manure may increase heterotrophic respiration (Eq. [8] and [9] of Grant, 2004) in the model, thereby leading to O_2 limitations and, thus, increased demand for alternative electron acceptors (Eqs. [2.10] – [2.18]) compared to that of urea fertilizer. Also, the low C/N ratio (carbon was added in comparatively small amounts with respect to N) contributed towards the mineralization of NH_4^+ (Eqs. [A1a] – [A1c]) of Grant et al., 2006) for N_2O production via nitrification (Eq. [2.10]) and denitrification (Eq. [2.18]) in *ecosys*. Consequently, modeled annual cumulative

emissions (Table 3-6) and annual emission factors (Table 3-7) for the hog 87 kg N ha^{-1} hog manure treatment was higher than for spring-urea (90 kg N ha^{-1}). These results are consistent with a Stage 2 response as described in Section 3.1. Agreement between modeled and measured N_2O emissions (Figure 3-6) was generally small in other years ((a) 2001: R^2 = 0.20, $P > 0.05$ (87 kg N ha^{-1}); R^2: 0.25, $P > 0.05$ (261 kg N ha^{-1}), (b) 2002: $R^2 < 0$ (87 kg N ha^{-1}); R^2: 0.25, $P > 0.05$ (261 kg N ha^{-1})).

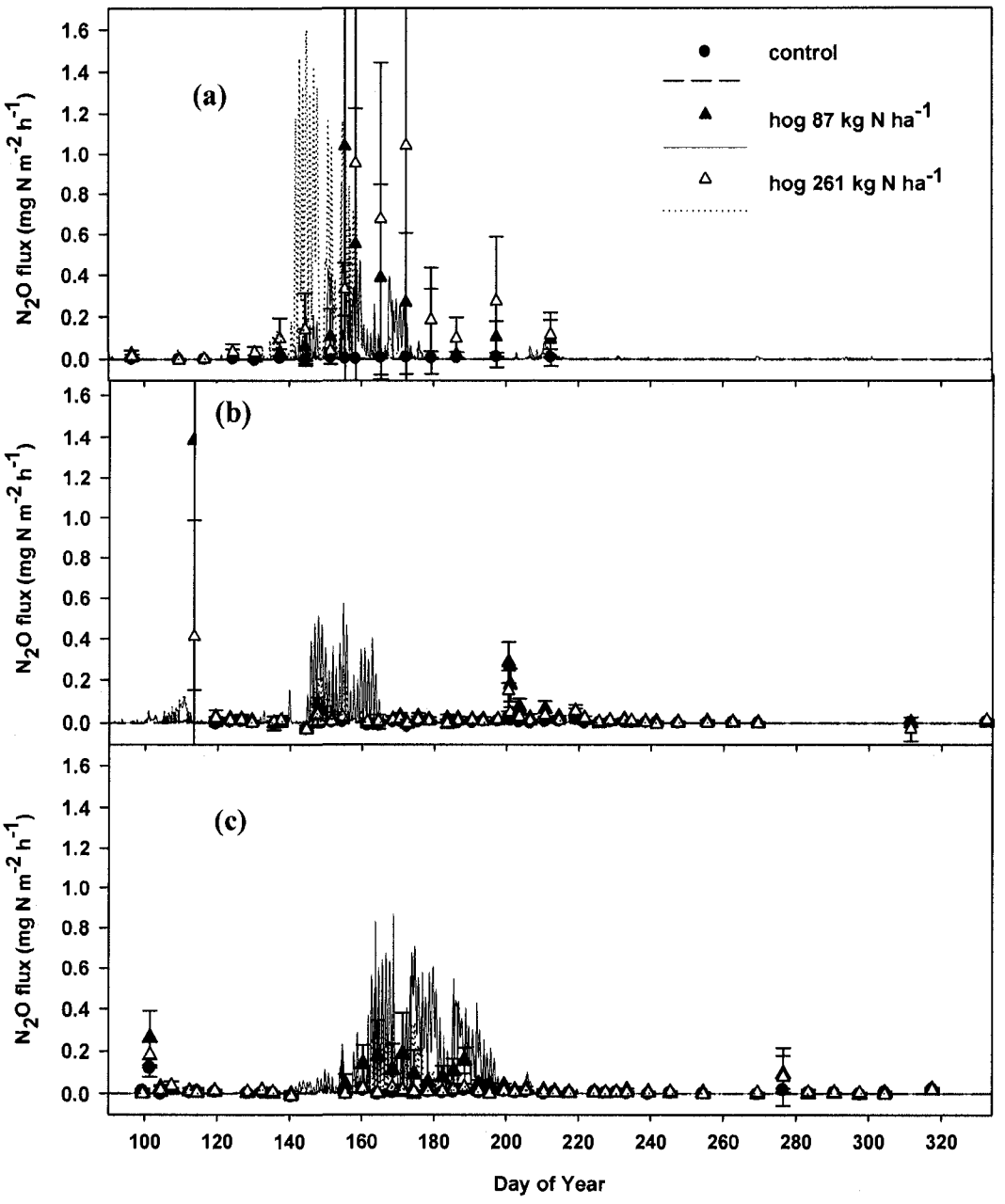

Figure 3-6: Modeled (lines) and measured (symbols) N_2O emissions for (a) 2001 (b) 2002 and (c) 2003 at Ellerslie during 2001, for spring – applied hog manure at Manured site. (Measured data obtained from Kerrianne Koehler-Munro and Tom Goddard from CARC-CCFIA grant).

Table 3-9 – Modeled and measured fall (October) residual N for Manured site

Date	Treatment (kg N ha^{-1})	§Mineral N ($\mu g\ g^{-1}$)	
		Modeled	Measured
2001	Control	3.8	4.7 ± 1.8
	87	9.5	12.5 ± 4.5
	261 ($year^{-3}$)	5.8	15.0 ± 1.5
2002	Control	18.5	6.1 ± 0.5
	87	53.3	10.5 ± 1.2
	261 ($year^{-3}$)	30.6	7.0 ± 0.5
2003	Control	8.2	10.3 ± 1.1
	87	34.0	20.0 ± 8.5
	261 ($year^{-3}$)	18.8	12.9 ± 2.5

§Exchangeable + soluble NH_4^+ + NO_3^- (0-15cm)

±Standard deviation of 3 replicates

3.4.3 Problems associated with chamber measurements.

Generally Figures 3-1 - 3-6 show that there were large spatial variations in the chamber readings. This were probably due to the heterogeneous nature of the soil due to factors such as differences in soil water content as a result of small topographic variations. Figure 3-5a also shows large diurnal variations in modeled emissions which limited comparability with chamber measurements. Modeled diurnal variations in N_2O were attributed to diurnal variations in soil temperature. Higher soil temperatures can reduce the aqueous solubility of O_2 (Eq. [A30] in Grant et al., 2006), lowering [O_{2s}] that sustains O_2 uptake by microbial populations (Eqs. [2.3], [2.7] and [2.14]). Higher soil temperatures also cause an increase in microbial activity and therefore a higher demand for O_2 (Eqs. [2.2], [2.3a,b], [2.13] and [2.14a,b]). In *ecosys* the combined effects of

solubility and demand can lead to higher production of N_2O via nitrification (Eq. [2.10]) and denitrification during soil warming (Eq. [2.18]). To better capture this temporal variability of N_2O for model testing, more frequent chamber measurements, use of automated chambers, or micrometeorological techniques are needed.

As a result of the large spatial variation in the chamber readings as well as the infrequent chamber readings which did not fully measure the temporal variability of N_2O emissions, modeled and measured emission factors (Table 3-10) were very different in some cases. Emission factors derived from the aggregation of N_2O emission measurements based on infrequent chamber readings can be over or under-estimated, depending on the time of day samples were taken.

Table 3-10: Annual site-specific emission factors (%) derived from *Ecosys* & Measured data

Treatments (kg N ha^{-1} $year^{-1}$)	Fertilizer year & Annual Precipitation					
	May, 2001 – April, 2002		May, 2002 – April, 2003		May, 2003 – May, 2004	
Short-term fertilized site	**Modeled**	**Measured**	**Modeled**	**Measured**	**Modeled**	**Measured**
50	0.1	0.4	0	0.7	0	1.3
100	0	0.5	0	0.5	0	0.5
Long-term fertilized site						
Fall 90	0.3	0	0.1	0.1	0.2	0
Fall 180	1.1	0.3	0.8	1.2	2.7	2.2
Spring 90	0.3	0.2	0.3	0.4	0.5	0.3
Spring 180	1.2	1.1	0.6	1.0	2.5	1.8
Manured site						
87	1.4	14	1.1	1	3.0	1
261 ($3y^{-1}$) (applied in 2001)	1.1	11	0.1	0	0.2	0

3.5 DISCUSSION

N_2O emissions in *ecosys* (Grant, 2001a,b) varied with land use and inter-annual variation of precipitation. The use of a processed-based, three-dimensional mathematical model, such as *ecosys* is important for simulating N_2O since it takes into account these complex site-specific effects of past and current land use and other environmental controls N_2O emissions. Site-specific EFs from this study were derived, which can contribute towards the development of an IPCC Tier III Methodology. Although there were a few significant correlations between modeled and measured N_2O emissions for this study, there were also many small and insignificant correlations. These low correlations may be attributed to the large spatial variation in the chamber readings as well as the infrequent chamber readings which limited the model testing experiment thus, reduced the certainty of the findings. As result, further testing of *ecosys* was done using data with higher temporal and spatial resolutions (chapters 4 and 5). The use of automated chambers in the future may also improve the temporal resolution of the N_2O emissions measurements.

N_2O emission response to fertilizer N addition in *ecosys* varied depending on soil residual N levels. Modeled results from *ecosys* (Grant, 2001a,b) showed that N_2O emissions and EFs for the lower fertilizer rate (90 kg N m^{-2} y^{-1}) for the Long-term fertilized site (Figure 3-1 – 3-3; Table 3-6, 3-7) and all rates for the Short-term fertilized site (Figure 3-4; Table 3-6, 3-7) were low and this was generally consistent with the measured data (Table 3-10), due to the presence of low soil residual N and comparatively high C:N ratios (Tables 3-5; 3-8). The general consistency of modeled and measured results **supports the Stage 1 (non – linear) response hypothesis in *ecosys* (Grant, 2001a,b) outlined in the**

Introduction (section 3.1), whereby low soil residual N due to low rates of past fertilizer application, leads largely to immobilization (crop and soil uptake capacity) (N limited) (Grant et al., 2006) (Figure 2-1; B') of all or most of current fertilizer N added (Figure 2-1; AB). Consequently, low soil residual N remains thus low N_2O production via nitrification (Eq. [2.10]) and denitrification (Eq. [2.18]) in the model (Figure 2-1; AB').

In contrast to the Stage 1 response, modeled results from *ecosys* (Grant, 2001a,b) showed that N_2O emissions and EFs for the higher fertilizer rate (180 kg N m^{-2} y^{-1}) for the Long-term fertilized site (Figure 3-1 – 3-3; Table 3-6, 3-7) were higher and this was generally consistent with the measured data (Table 3-10) with a few significant correlations in some cases (e.g., R^2 of modeled versus measured data: 0.77 (2001, spring 180 kg N ha^{-1}), $P < 0.001$), due to the presence of higher soil residual N and comparatively low C:N ratios (Tables 3-5; 3-8). The general consistency of modeled and measured results in these cases **supports the Stage 2 (non – linear) response hypothesis in *ecosys* (Grant, 2001a,b) outlined in the Introduction (section 3.1), whereby higher soil residual N due to larger rates of past fertilizer application, leads to less immobilization (Figure 2-1; C') of the current fertilizer N added (Figure 2-1; BC') compared to that of the Stage 1 response, due to the addition of N greater than the immobilization capacity of the ecosystem (Grant et al., 2006). Consequently, higher soil residual N remains thus higher N_2O production via nitrification (Eq. [2.10]) and denitrification (Eq. [2.18]) in the model (Figure 2-1; BC').** The higher fertilizer rate for the Long-term fertilized site therefore gave intermediate emissions in response to fertilizer N addition.

Thus calculation of EFs for an IPCC Tier III Methodology can vary depending on initial soil residual N. Studies by Grant et al. (2006) also show that N_2O emissions were higher with an increase in soil residual N as well as with precipitation. However, a review by Barnard (2005) suggests that the response of N_2O flux to N addition was highly variable, and there was no clear correlation with the amount of N added. A greater understanding of the stages of N excess (stages leading to maximum reaction rate for nitrification/denitrification) should resolve the reason(s) for these variable responses. Our findings show the importance of the use of process-based mathematical models such as *ecosys* (Grant, 2001a,b) which take into account fertilizer history (soil residual N), other past and current land use, climate, soil type, topography etc. for site-specific EF for N_2O, since an increase in fertilizer rate does not necessarily cause a proportional increase in emissions. Emissions can therefore be under or over estimated if inventories are based on a single emission factor irrespective of fertilizer land use history.

N_2O emission response to fertilizer N addition in *ecosys* also varied with fertilizer source. Modeled results from *ecosys* (Grant, 2001a,b) showed that N_2O emissions and EFs were higher for the hog manure (Figure 3-6; Tables 3-6, 3-7) compared to urea fertilizer (Figure 3-1; Tables 3-6, 3-7) for similar N application rates (e.g. Modeled EFs (2003): 0.5% (90 kg N ha^{-1} (urea)) versus 3% (87 kg N ha^{-1} (hog manure)), with a few significant correlations in some cases (e.g., R^2 of modeled versus measured data:0.48 (2003, 87 kg N ha^{-1}), $P < 0.001$), due to the presence of both mineral N and organic C sources in hog manure (Table 3-3). The consistency of modeled and measured results in these cases **supports the Stage 2 (non – linear) response hypothesis in *ecosys* (Grant, 2001a,b)**

outlined in the Introduction (section 3.1). A consequence of this hypothesis is that: An organic source (hog manure) will give higher N_2O emissions than those of inorganic source (urea). The model explanation for this trend is that readily available N and organic C in hog manure (less C limitation) increases the demand for alternative electron acceptors (Eqs. [2.10] – [2.18]) compared to that of urea fertilizer (C limited), leading to higher N_2O emissions since N and organic C promote microbiological activity of nitrification (Eq. [2.10]) and denitrification (Eq. [2.18]) in the model. Organic C from hog manure may increase heterotrophic respiration (Eq. [8] and [9] of Grant, 2004) in the model, thereby leading to O_2 limitations and, thus, increased demand for alternative electron acceptors (Eqs. [2.10] – [2.18]) compared to that of urea fertilizer. Bergstom et al. (1994) found that simultaneous additions of C and NH_4^+ additions enhanced N_2O emissions more than additions of NH_4^+ alone. These finding again show the importance of the use of site-specific EFs as is done in *ecosys* since a similar fertilizer rate can give different emissions depending on whether the source is organic or inorganic.

N_2O emissions in *ecosys* also varied with inter-annual variation in precipitation. Modeled results from *ecosys* (Grant, 2001a,b) showed that N_2O emissions and EFs were highest in 2003 (Figures 3-1-3-3; Tables 3-6, 3-7) compared to the other years, with general consistency (Table 3-10; e.g. Higher modeled and measured EFs for spring urea applications in 2003 versus 2002 (drought year in Alberta, Canada)), due to highest precipitation in 2003. Higher rainfall (e.g. Figure 3-3a versus 3-2a) in *ecosys* can be used to explain larger surface flow (Eq. [2.21]) and subsurface flow (Eqs. [21] and [24] and

[A94 - A96] of Grant et al., 2004) which resulted in further increases in WFPS > 60% (e.g. Figure 3-3b versus Figure 3-2b). The general consistency of modeled and measured results **supports the hypothesis in *ecosys* (Grant, 2001a,b) outlined in the Introduction (section 3.1), that N_2O production increases sharply (threshold, non-linear response) at 90% > WFPS > 60%. This non-linear rise of N_2O emissions in the model can be explained by the D_g (Eq. [2.28]) of O_2 whereby at WFPS < 60%, the D_g (Eq. [2.28]) of O_2 is large enough to meet microbial demands. However, as WFPS increases above 60%, the D_g (Eq. [2.28]) of O_2 declines sharply and the unmet O_2 demand forces the need for alternative electron acceptors (Eqs. [2.10] – [2.18]) thus, higher N_2O production via nitrification (Eq. [2.10]) and denitrification (Eq. [2.18]) in the model.** Other studies (e.g. Lu et al., 2006) also found a similar trend. Flechard et al. (2007) showed that the 2003 heat wave in Europe resulted in lower emission factors at different grassland sites, compared to 2002 and 2004. Consequently, in order to have better quantification of N_2O, the inter-annual variation of precipitation should be taken into account. Flechard et al (2007) also proposed an empirical model which showed that EF were higher with higher soil WFPS and temperature. However, at some sites the total precipitation was lower than others but emissions were higher due to the soil WFPS remaining high throughout the year than most sites. These results show the importance using mathematical models such as *ecosys* to simulate WFPS distribution based on intra-annual variation of precipitation, and its effects on N_2O emissions.

As mentioned earlier, high spatial variability of chamber measurements as well as infrequent measurements, limited the model testing experiment. Studies by Grant and

Pattey (2003) showed that both the temporal and spatial variability of N_2O emissions may be caused by topographically-driven flows of water and solutes (e.g. DOC, NH_3 and NO_3^-) through landscapes causing greater emissions in topographic positions in which water and solutes are gathered, than at positions from which they are shed. Emission factors based on infrequent chamber readings (Table 3-10) can be over or under-estimated, depending on the time of day samples were taken. A review by Bouwman et al. (2002) show that intensive measurements ($\geq$1 per day) yield lower emissions than less intensive measurements (2–3 per week). In order to obtain better measurements of the spatial and temporal variability N_2O for testing *ecosys*, both chamber and micrometeorological techniques were used in work described in chapter 4. Also, a digital elevation model (DEM) of the field was used in order to understand topographic effects on N_2O emissions.

3.6 CONCLUSIONS

Ecosys (Grant, 2001a,b) was further tested at the site scale (m^2), but now to simulate the sensitivity of N_2O emissions to changes in past and current fertilizer use and also to simulate the effect of inter-annual variation of precipitation. Although there were a few significant correlations between modeled and measured N_2O emissions for this chapter, there were also many small and insignificant correlations (chapter 3, section 3.4). These low correlations may be attributed the large spatial variation in the chamber readings as well as the infrequent chamber readings which limited the model testing experiment thus, reduced the certainty of the findings. Consequently, *ecosys* was further tested using measured data from both micrometeorological (high temporal resolution) and chamber techniques (chapters 4 and 5), to investigate the effect of topography and also soil properties on N_2O emissions. The use automated chambers in the future may also improve the temporal resolution of the N_2O emissions measurements.

N_2O emission response to fertilizer N addition in *ecosys* varied depending on soil residual N levels. Results **supported the hypothesis in *ecosys* (Grant, 2001a,b) outlined in the Introduction (section 3.1), that these rises in soil residual N, thus N_2O emissions, occurs in stages (non – linear response) upon fertilizer N addition and can be explained by the immobilization capacity of the ecosystem (Grant et al., 2006). Modeled results from *ecosys* (Grant 2001a,b) showed that N_2O emissions and EFs for the lower fertilizer rate (90 kg N m^{-2} y^{-1}) for the Long-term fertilized site (Figure 3-1 – 3-3; Table 3-6, 3-7) and all rates for the Short-term fertilized site (Figure 3-4; Table 3-6, 3-7) were low and this was generally consistent with the measured data**

(Table 3-10), due to the presence of low soil residual N and comparatively high C:N ratios (Tables 3-5; 3-8) (Stage 1 response).

In contrast to the Stage 1 response, **modeled results from *ecosys* (Grant, 2001a,b) showed that N_2O emissions and EFs for the higher fertilizer rate (180 kg N m^{-2} y^{-1}) for the Long-term fertilized site (Figure 3-1 – 3-3; Table 3-6, 3-7) were higher and this was generally consistent with the measured data (Table 3-10) with a few significant correlations in some cases (e.g., R^2 of modeled versus measured data: 0.77 (2001, spring 180 kg N ha^{-1}), $P < 0.001$), due to the presence of higher soil residual N and comparatively low C:N ratios (Tables 3-5; 3-8) (Stage 2 response).** Findings from this chapter showed that an increase in fertilizer rate does not necessarily cause a proportional increase in N_2O emissions, due to complex site-specific conditions such as soil residual mineral N levels. Emissions can therefore be under or over estimated if inventories are based on a single EF irrespective of fertilizer land use history, as done in the IPCC Tier 1 Methodology. A greater understanding of the stages of N excess (stages leading to maximum reaction rate for nitrification/denitrification) should resolve the reason(s) for these variable responses. Future studies involving the response of N_2O to N addition should therefore be accompanied by frequent soil residual N measurements. Findings from our study emphasizes the importance of incorporating the non-linear rise of N_2O emissions due to different soil residual N levels in inventories – This can be achieved by using a process-based three-dimensional mathematical model *ecosys*, in an IPCC Tier III Methodology.

N_2O emission response to fertilizer N addition in *ecosys* also varied with fertilizer source. Modeled results from *ecosys* (Grant, 2001a,b) showed that N_2O emissions and EFs were higher for the hog manure (Figure 3-6; Tables 3-6, 3-7) compared to urea fertilizer (Figure 3-1; Tables 3-6, 3-7) for similar N application rates (e.g. Modeled EFs (2003): 0.5% (90 kg N ha^{-1} (urea)) versus 3% (87 kg N ha^{-1} (hog manure)), with a few significant correlations in some cases (e.g., R^2 of modeled versus measured data:0.48 (2003, 87 kg N ha^{-1}), $P < 0.001$), due to the presence of both mineral N and organic C sources in hog manure (Table 3-3). The consistency of modeled and measured results in these cases **supports the Stage 2 (non – linear) response hypothesis in *ecosys* (Grant, 2001a,b) outlined in the Introduction (section 3.1).** These finding again show the importance of the use of site-specific EFs as is done in *ecosys* since a similar fertilizer rate can give different emissions depending on whether the source is organic or inorganic.

N_2O emissions in *ecosys* also varied with inter-annual variation in precipitation. Modeled results from *ecosys* (Grant, 2001a,b) showed that N_2O emissions and EFs were highest in 2003 (Figures 3-1-3-3; Tables 3-6, 3-7) compared to the other years, with general consistency (Table 3-10; e.g. Higher modeled and measured EFs for spring urea applications in 2003 versus 2002 (drought year in Alberta, Canada)), due to highest precipitation 2003. Higher rainfall (e.g. Figure 3-3a versus 3-2a) in *ecosys* can be used to explain larger surface flow (Eq. [2.21]) and subsurface flow (Eqs. [21] and [24] and [A94 - A96] of Grant et al., 2004) which resulted in further increases in WFPS > 60% (e.g. Figure 3-3b versus Figure 3-2b). The general consistency of modeled and measured results **supports the hypothesis in *ecosys* (Grant, 2001a,b) outlined in the**

Introduction (section 3.1), that N_2O production increases sharply (threshold, non-linear response) at 90% > WFPS > 60%. Consequently, in order to have better quantification of N_2O emissions, the inter-annual variation of precipitation should be taken into account in inventories. Such complex relationships again highlights the importance of using process-based mathematical model *ecosys* (Grant, 2001a,b), that accounts for inter and intra-annual variations of precipitation and its effects on N_2O emissions, in addition to many other site-specific factors. Using an IPCC Tier III Methodology thus may help us improve the accuracy of N_2O inventories thereby allowing us to better track our reduction targets.

3.7 REFERENCES

Akiyama, H., Mctaggart, I.P., Ball, B.C., Scott, A., 2004. N_2O, NO, and NH_3 emissions from soil after the application of organic fertilizers, urea and water. Water, Air, and Soil Pollution 156,113–129.

Aulakh, M.S., Doran, J.W., Walters, D.T., Mosier, A.R., Francis, D.D., 1991. Crop residue type and placement effects on denitrification and mineralization. Soil Science Society of America Journal 55, 1020-1025.

Ball, B.C., Horgan, G.W., Clayton, H., Parker, J.P., 1997. Spatial variability of nitrous oxide fluxes and controlling soil topographic properties. Journal of Environmental Quality 26, 1399-1409.

Barnard, R., Leadley, P.W., Hungate, B.A., 2005. Global change, nitrification, and denitrification: A review. Global Biogeochemical cycles 19, GB1007, doi:10.1029/2004GB002282.

Bouwman, A.F., Boumans, L.J.M., Batjes, N.H., 2002. Emissions of N_2O and NO from fertilized fields: Summary of available measurement data. Global Biogeochemical cycles 16(4), 1058, doi:10.1029/2001GB001811.

Bouwman, A.F., 1996. Direct emission of nitrous oxide from agricultural soils. Nutrient Cycling in Agroecosystems 46, 53-70.

Chang, C., C.M. Cho, Janzen, H.H., 1998. Nitrous oxide emission from long-term manured soils. Soil Science Society of America Journal 62, 677–682.

Dobbie, K.E., Smith, K.A., 2001. The effects of temperature, water-filled pore space and land use on N_2O emissions from an imperfectly drained gleysol. European Journal of Soil Science 52, 667-673.

Eggleston, 2006. Intergovernmental Panel on Climate Change (IPCC), IPCC Guidelines for National Greenhouse Gas Inventories Volume 4; Agriculture, Forestry and other land use. Institute for Global Environmental Strategies, kanagawan Hayama, Japan.

Flessa, H., Dörsch, P., Beese, F., 1995. Seasonal variation of N_2O and CH_4 fluxes in differently managed arable soils in southern Germany. Journal of Geophysical Research 100, 23115-23124.

Flechard, C.R., Ambus, P., Skiba, U., Rees, R.M., Hensen, A., van Amstel, A., van den Pol-van Dasselaar, A., Soussana, J.-F., Jones, M., Clifton-Brown, J., Raschi, A., Horvath, L., Neftel, A., Jocher, M., Ammann, C., Leifeld, J., Fuhrer, J., Calanca, P., Thalman, E., Pilegaard, K., Di Marco, C., Campbell, C., Nemitz, E., Hargreaves, K.J., Levy, P.E., Ball, B.C., Jones, S.K., van de Bulk, W.C.M., Groot, T., Blom, M., Domingues, R., Kasper, G., Allard, V., Ceschia, E., Cellier, P., Laville, P., Henault, C., Bizouard, F., Abdalla, M.,

Williams, M., Baronti, S., Berretti, F., Grosz, B., 2007. Effects of climate and management intensity on nitrous oxide emissions in grassland systems across Europe. Agriculture, Ecosystems and Environment 121, 135-152.

Grant, R.F., 1991. A technique for estimating denitrification rates at different soil temperatures, water contents, and nitrate concentrations. Soil Science 152, 41-52.

Grant, R.F., 1994. Simulation of ecological controls on nitrification. Soil Biology & Biochemistry 26, 305–315.

Grant, R.F., 1995. Mathematical modelling of nitrous oxide evolution during nitrification. Soil Biology & Biochemistry 27, 1117–1125.

Grant, R.F., 1997. Changes in soil organic matter under different tillage and rotation: mathematical modeling in *ECOSYS*. Soil Science Society of America Journal 61, 1159-1175.

Grant, R.F., 2001a. A Review of the Canadian Ecosystem Model - *ecosys*. In: Shaffer M. J., Ma, L., Hansen, S. (Ed), Modeling Carbon and Nitrogen Dynamics for Soil Management. CRC Press. Boca Raton, FL, pp. 173-263.

Grant, R.F., 2001b. Modeling Transformations of Soil Organic Carbon and Nitrogen at Differing Scales of Complexity. In: Shaffer M. J., Ma, L., Hansen, S. (Ed), Modeling Carbon and Nitrogen Dynamics for Soil Management. CRC Press. Boca Raton, FL, pp. 597-614.

Grant, R.F., 2004. Modeling topographic effects on net ecosystem productivity of boreal black spruce forests. Tree Physiology 24, 1-18.

Grant, R.F., Rochette, P., 1994. Soil Microbial respiration at Different Water Potentials and Temperatures: Theory and Mathematical Modeling. Soil Science Society of America Journal 58, 1681-1690.

Grant, R.F. and Pattey, E., 1999. Mathematical modeling of nitrous oxide emissions from an agricultural field during spring thaw. Global Biogeochemical Cycles 13, 679-694.

Grant, R.F., Pattey, E., 2003. Modelling variability in N_2O emissions from fertilized agricultural fields. Soil Biology & Biochemistry 35, 225-243.

Grant, R.F., and Pattey, E., Submitted 2007. Temperature sensitivity of N_2O emissions from fertilized agricultural soils: mathematical modelling in *ecosys*.

Grant, R.F., Nyborg, M., Laidlaw, J.W., 1992. Evolution of nitrous oxide from soil: II. Experimental results and model testing. Soil Science 156, 266-277.

Grant, R.F., Juma, N.J., McGill, W.B., 1993a. Simulation of carbon and nitrogen transformations in soils. I: mineralization. Soil Biology & Biochemistry 25, 1317-1329.

Grant, R.F., Juma, N.J., McGill, W.B., 1993b. Simulation of carbon and nitrogen transformation in soil: Microbial biomass and metabolic products. Soil Biology & Biochemistry 25, 1331-1338.

Grant, R.F., Nyborg, M., Laidlaw, J.W., 1993c. Evolution of nitrous oxide from soil: I. Model development. Soil Science 156, 259-265.

Grant, R.F., Izaurralde, R.C., Nyborg, M., Malhi, S.S., Solberg, E.D., Jans-Hammermeister, D., Stewart, B.A., 1998. Modeling tillage and surface residue effects on soil C storage under ambient versus elevated CO_2 and temperature in *ECOSYS*. In: Lal, R., Kimble, J.M., Follet, R.F. (Eds), Soil processes and carbon cycle. CRC Press Inc. Boca Raton, USA, pp. 527-547.

Grant, R.F., Amrani, M., Heaney, D.J., Wright, R., Zhang, M., 2004. Mathematical Modeling of Phosphorus Losses from Land Application of Hog and Cattle Manure. Journal of Environmental Quality 33, 210-231.

Grant, R.F., Pattey, E., Goddard, T.W., Kryzanowski, L.M., Puurveen, H., 2006. Modeling the effects of fertilizer application rate on nitrous oxide emissions. Soil Science Society of America Journal 70, 235-248.

Hénault, C., Devis, X., Page, S., Justes, E., Reau, R., Germon, J.C., 1998. Nitrous oxide emissions under different soil and land management conditions. Biology and Fertility of Soils 26, 199-207.

Izaurralde, R.C., Lemke, R.L., Goddard, T.W., McConkey, B., Zhang, Z., 2004. Nitrous oxide emissions from agricultural toposequences in Alberta and Saskatchewan. Soil Science Society of America Journal 68, 1285–1294.

Kachanoski, R.G., O'Halloran, I., Rochette, P., 2003. Site-specific application of fertilizer N for reducing greenhouse gas emissions. Climate change funding initiative in Agriculture, Canadian Agri- Food Research Council, Ottawa ON.

Kaiser, E.A., Ruser, R., 2000. Nitrous oxide emissions from arable soils in Germany—an evaluation of six long-term field experiments. Journal of Plant Nutrition and Soil Science 163, 249–260.

Lee, J, Six, J., King, A.P., van Kessel, C., Rolston, D.E., 2006. Tillage and Field Scale Controls on Greenhouse Gas Emissions. Journal of Environmental Quality 35, 714-725.

Lu, Y., Huang, Y., Zou, J., Zheng, X., 2006. An inventory of N_2O emissions from agriculture in China using precipitation-rectified emission factor and background emission. Chemosphere 65, 1915-1924.

Meyer-Aurich, A., Weersink, A., Janovicek, K. and Deen, B., 2006. Cost efficient rotation and tillage options to sequester carbon and mitigate GHG emissions from agriculture in Eastern Canada. Agriculture, Ecosystems and Environment 117, 119–127.

Muller, C., 1999. Modelling soil-biosphere interactions. CABI Publishing, Wallingford, UK, pp. 52-53.

Mummey, D.L., Smith, J.L. Bluhm, G., 1998. Assessment of alternative soil management practices on N2Ovemissions from US agriculture. Agriculture, Ecosystems and Environment 70, 79-87.

Myrold, D.D., 1998. Transformation of nitrogen. In: Sylvia, D.M., Fuhrmann, J.J., Hartel, P.G., Zuberer (Eds.). Principles and Applications of soil microbiology. Prentice Hall: Upper Saddle River, New Jersey, pp. 259-294.

Olsen, K., Wellisch, M., Boileau, P., Blain, D., Ha, C., Henderson, L., Liang, C., McCarthy, J., McKibbon, S., 2003. Canada's Greenhouse Gas Inventory 1990-2001, pp. 1-4.

Parton, W.J., Mosier, A.R. ojima, D.S. Valentine, D.W. Schimel, D.S. Weier K. Kulmala, A.E., 1996. General model for N_2 and N_2O production from nitrification and denitrification. Global Biogeochemical Cycles 10, 401-412.

Pennock, D.J., Zebarth, B.J., de Jong, E., 1987. Landform classification and soil distribution in hummocky terrain, Saskatchewan, Canada. Geoderma 40, 297-315.

Pennock, D.J., van Kessel, C., Farrell, R.E., Sutherland, R.A., 1992. Landscape-scale variations in denitrification. Soil Science Society of America Journal 56, 770-776.

Pennock, D.J., Anderson, D.W., de Jong, E., 1994. Landscape-scale changes in indicators of soil quality due to cultivation in Saskatchewan, Canada. Geoderma 64, 1-19.

Pennock, D.J. Corre, M.D., 2001. Development and application of landform segmentation procedures. Soil and Tillage Research 58, 151-162.

Reinertsen, S.A., Elliott, L.F., Cochran, V.L., Campbell, G.S., 1984. Role of available carbon and nitrogen in determining the rate of wheat straw decomposition. Soil Biology & Biochemistry 16, 459-464.

Smith, K.A., Thomson, P.E., Clayton, H., McTaggart, I.P., Conen, F., 1998. Effects of temperature, water content and nitrogen fertilisation on emissions of nitrous oxideby soils. Atmospheric Environment 32, 3301-3309.

Tiedje, J. M., Sexstone, A.J., Parklin, T. B., Revsbech, N.P., Shelton, D.R., 1984. Anaerobic processes in soil. Plant and Soil 76, 197-212.

CHAPTER 4.0 Using the *Ecosys* mathematical model to simulate temporal variability of nitrous oxide emissions from a fertilized agricultural soil (field scale: ~ 5ha)

4.1 INTRODUCTION

In 2001, N_2O emissions accounted for 60% of the total CO_2-equivalent emissions from the agricultural sector in Canada (Olsen et al., 2003). Under the Kyoto Protocol, Canada is required to reduce its total greenhouse gases to 6% below 1990 levels over the period 2008 to 2012. Current Intergovernmental Panel of Climate Change (IPCC) Tier I Methodology for quantifying N_2O emissions in greenhouse gas inventories, is based on a constant emission factor (EF) of 1% for all N inputs (IPCC, 2006). However, uncertainties in estimates of N_2O emissions by IPCC guidelines may be 70% to 80% in arable soil at a national scale (Lim et al., 1999). This uncertainty may be attributed to large spatial and temporal variability of N_2O emissions (e.g., Pennock et al., 1992; Pennock and Corre, 2001; Grant & Pattey, 2003). IPCC Tier II Methodology may improve estimates because it is based on country-specific EFs, derived from country-specific activity data (land use). An IPCC Tier II Methodology is now being used for Canada. It uses lower EFs (0.1 - 0.7%) in drier climates such as the Prairies and higher EFs (0.83 - 1.67%) for the more humid regions of Eastern Canada (Hegalson, 2005).

IPCC Tier III Methodology involves either the use of validated mathematical models or the use of measurement data in conjunction with activity data to simulate emissions (IPCC, 2006). Unlike Tier I and II, Tier III addresses more of the large spatial and temporal variability of N_2O emissions and is capable of capturing longer-term legacy effects of land use and management (IPCC, 2006). Mathematical models can also

improve N_2O inventories by contributing towards the continuity of measured data by modeling fluxes where measured data are missing. However, before these simulations can be made, a processed-based understanding of the complex biological, physical and chemical processes involved in the production of N_2O emissions in agricultural soils, is necessary. To achieve this, quantitative, testable hypotheses from basic scientific theory for a comprehensive range of processes believed to control N_2O emissions, should be derived. Because of the uncertainties associated with using the current IPCC Tier I and Tier II Methodologies, mathematical models such as *ecosys* (Grant, 2001a, b: website: www.ecosys.rr.ualberta.ca), can contribute towards the development of more site-specific EFs needed for the adoption an IPCC Tier III methodology.

Temporal variability in N_2O fluxes is large, with highly skewed frequency distributions and coefficients of variation > 150% at diurnal time scales (e.g., Flessa et al., 1995; Thornton et al., 1996). Temporal variation in N_2O emissions creates difficulties when estimating aggregated fluxes for N_2O emissions inventories. Many current N_2O emissions estimates are based on discrete chamber measurements; however, there may be a bias when these measurements are aggregated to annual values for use in inventories compared to aggregates of continuous measurements. This bias is directly related to the episodic nature of N_2O emissions (large temporal variation) as described above, as a result of their sensitivity to weather (precipitation and temperature). Consequently, temporal aggregations of N_2O emissions calculated solely from a few measured fluxes may be overestimated, if the measurements were taken only during emission peaks. A study by Pattey et al. (2007) showed that estimates were lower when continuous 30-min

flux data from a micrometeorological tower were compared to estimates calculated from data frequencies of once d^{-1} and twice and once wk^{-1}. It is therefore important for mathematical models to simulate key processes known to control N_2O generation in soils in order to capture the large temporal variability of N_2O emissions at an appropriate time-step (i.e., hourly).

The processes involved in N_2O generation are very sensitive to changes in water and temperature. N_2O emissions from soils are produced from the microbiological processes nitrification and denitrification (e.g., Henault et al., 1998; Myrold, 1998). Nitrification is most rapid when O_2 is sufficient (water contents near or below field capacity, $\approx$ 60% WFPS), whereby NH_3 is oxidized to NO_2^- then to NO_3^- and O_2 is reduced to H_2O by nitrifying bacteria. However, under O_2-limiting conditions (e.g., after rainfall when 90% > WFPS > 60%), in a process called "nitrifier denitrification", ammonium oxidizers containing nitrite reductase may reduce NO_2^- as an alternative electron acceptor to produce NO and N_2O (Myrold, 1998; Muller, 1999). Denitrifiers can oxidize reduced C to CO_2 and reduce O_2 to H_2O under non-limiting O_2. When O_2 is insufficient (> 60% WFPS) to meet the demands of microbes, NO_3^- (e.g., from nitrification, fertilizer, residual N) becomes the alternative electron acceptor to O_2 and is reduced in a series of steps ($NO_3^- \rightarrow NO_2^- \rightarrow N_2O \rightarrow N_2$) via denitrification. Davidson (1991) showed that greatest N_2O production occurs within the range of 60 – 80% WFPS.

Transitions from one reduction reaction to another can be caused by small changes in soil WFPS and follows a threshold response. This occurs because the diffusivity (D_g) of O_2

(and other gases) in the soil atmosphere varies according to a power function of the soil air-filled porosity (θ_g) (Millington, 1960), which in turn depends on WFPS. This variation is such that at certain WFPS, small declines in θ_g can cause large declines in D_g that may limit O_2 gaseous transfer to microsites causing a greater demand for alternative electron acceptors. As a result, these small declines may cause a transition from the reduction of O_2 to that of NO_x by nitrifiers and denitrifiers, increasing N_2O production. Temporal variation in WFPS therefore strongly influences that in N_2O emissions. Studies by Grant (1991) have shown that transitions from one reduction reaction to another can be caused by very small changes in soil H_2O content. A review by Bouwman et al. (2002) showed that soil N_2O emissions from poorly drained soils with fluctuating θ_g exceeded those from well-drained soils in all cases.

Transitions from one reduction reaction to another can also be caused by small changes in soil temperature. Higher temperatures can accelerate reduction of O_2 by nitrifiers/denitrifiers thereby increasing the demand for O_2 electron acceptors at the microbial sites. As a result, microbial O_2 demand may exceed O_2 supply, resulting in the need for alternative electron acceptors (Grant and Rochette, 1994; Grant, 1995) and therefore transition to reduction of NO_2^- (nitrifiers) and NO_3^- (denitrifiers), accelerating production of N_2O. N_2O production may increase further with higher temperature because gaseous solubility is reduced and hence aqueous O_2 concentrations ($[O_{2s}]$) maintained at microbial microsites decline. The solubility of N_2O also decreases, therefore accelerating the release of previously accumulated aqueous N_2O in the soil

profile. The temperature effect on gaseous solubility and O_2 demand will cause this transition to be sharper and the WFPS threshold value to be lower at higher temperatures.

Studies by Rusier et al. (2006) showed that N_2O emission rates were generally small at soil water contents $\leq$ 60% WFPS while significantly higher N_2O emissions rates were measured at soil water contents $\geq$70% WFPS, with the highest N_2O fluxes occurring at the highest soil moisture level of 90% WFPS. Dobbie and Smith (2001) found that N_2O emissions in a laboratory experiment from an arable soil increased about 30-fold as the WFPS increased from 60 to 80% and emissions were highest at 95% WFPS treatment and lowest at 60% WPFS. At grassland sites (Dobbie and Smith, 2003), large N_2O fluxes occurred at WFPS > 60% when soil NO_3^--N was not limiting. Another study by Bateman and Baggs (2005) showed that emissions were 6 times higher at 70% WPFS compared to 60%WFPS.

At very high WFPS following rainfall, N_2O produced from denitrification usually accumulates in the aqueous phase of the soil profile so that N_2O emissions are delayed because of low D_g. N_2O has been emitted as large bursts 20-24 hours after rainfall (e.g., Wagner-Riddle et al., 1996) or during spring thaw (Grant et al., 1992; Nyborg et al., 1997, Grant and Pattey, 1999; Pattey et al., 2007). This occurs because as soil water drains and evaporates, water is lost from soil macro-pores, increasing θ_g. Gaseous diffusivity increases rapidly, which leads to rapid N_2O volatilization and emission from the soil. Eventually, N_2O emissions return to ambient levels several days after an emission event (Grant and Pattey, 2003), as the θ_g increases further and O_2 replaces NO_x

as the terminal electron acceptor. Since N_2O is produced via nitrification and denitrification, alternating oxic and anoxic soil conditions are necessary for N_2O emissions.

The *ecosys* (Grant, 2001a, b) model of natural and managed ecosystems was used for this study because it has the major hypotheses for N_2O transformations and captures the large temporal variability of N_2O at high temporal and spatial resolution, under site-specific conditions such as climate, soil type, land use, topography etc. The model can integrate temporal scales from seconds to century, allowing validation against data from experiments that range from short-term laboratory incubations to long-term field studies. *Ecosys* can also integrate spatial scales ranging from mm to km in 1, 2 or 3 dimensions by representing state and rate variables according to their west to east (x), north to south (y) and vertical (z) positions in a complex landscape, allowing the scaling up of microscale phenomena to the landscape level.

Ecosys explicitly represents oxidation-reduction reactions from which N_2O is generated and gas transfer processes which control the transition between alternative reduction reactions. In *ecosys*, the key biological processes – mineralization, immobilization, nitrification, denitrification, root and mycorrhizal uptake controlling N_2O generation were coupled to the key physical processes – convection, diffusion, volatilization, dissolution controlling the transport of gaseous reactants and products of these biological processes (Grant et al., 2006). Simulation of nitrification and denitrification in *ecosys* is sensitive to soil air-filled porosity (θ_g), which in turn depends on WFPS. Transitions from

one reduction reaction to another can be caused by small changes in soil WFPS as well as temperature (non-linear response) (Grant and Rochette, 1994; Grant, 1995). However, in some current models (e.g., Lu et al., 2006), the response of N_2O to WFPS is linear. *Ecosys* will therefore test the hypothesis on the non-linear threshold response of N_2O production to changes in WFPS, thereby it will capture the effect of intra and inter-annual variations in precipitation.

Simulation of nitrification and denitrification in *ecosys* is also based on Michaelis-Menten kinetics whereas other models (e.g., Molina et al., 1983 and Clay et al., 1985) simulate denitrification based on first order kinetics with respect to soluble C or NO_3^- (e.g., Rolston et al., 1984 and Rao et al., 1984) as modified by dimensionless factors of temperature and WFPS. Some models impose constraints either on the magnitude of N_2O produced from nitrification (Li et al., 2005) or on the magnitude of N_2O emitted during snow cover (Li et al., 1992; Xu-Ri et al., 2003), even if environmental conditions favour higher emissions. However, in *ecosys*, there are no set constraints placed on N_2O production. *Ecosys* also models surface energy exchange and subsurface heat transfer, vertical (infiltration, drainage, root uptake and capillary rise) and lateral (driven by differences in topographic position) movement of water and solutes within complex landscapes and the effect of soil temperature and water on microbiological activity and gas exchange (Grant and Pattey, 2003; Grant, 2004). *Ecosys* can therefore improve N_2O inventories to contribute towards the development of an IPCC Tier III methodology.

Ecosys, a detailed processed-based ecosystem mathematical model, can represent a range of site-specific conditions and therefore can take into account the effect of site-specific past and current land use, climate, soil type and topography on N_2O emissions. *Ecosys* can simulate microbial oxidation/reduction reactions under different soil amendments such as crop residue (Grant et al., 1993a), fertilizer (Grant et al., 1992; Grant, 1995; Grant and Pattey, 1999; Grant and Pattey, 2003; Grant et al., 2006) or manure (Grant et al., 2004), and under different soil management practices such as rotation and tillage (Grant and Rochette, 1994; Grant, 1995; Grant, 1997; Grant et al., 1998;) or irrigation. *Ecosys* has been used to model N_2O emissions at site scale from laboratory experiments (Grant, 1991; Grant et al., 1992; Grant et al., 1993c; Grant, 1994; Grant; 1995) and agricultural field experiments using micrometeorological towers (Grant et al., 1992; Grant and Pattey, 1999; Grant and Pattey, 2003; Grant et al., 2006). For this research, *ecosys* will be further tested *in situ* at the field scale, in order to better understand this "threshold" response of N_2O emissions under transient aerobic and anaerobic conditions caused by temporal changes in WFPS and soil temperature.

This research will test the model hypothesis in *ecosys* (Grant, 2001a,b) that N_2O production increases sharply (threshold, non-linear response) at 90% > WFPS > 60%. It was proposed that the non-linear response of D_g (Millington and Quirk, 1960) of O_2 to changes in WFPS can be used to explain the sudden rise/threshold/ non-linear response of N_2O emissions commonly observed in the field, whereby N_2O emissions rises with WFPS > 60%. This occurs because at WFPS < 60% in the model, the D_g (Eq. [2.28]) of O_2 is large enough to meet microbial demands.

However, as WFPS increases above 60%, the D_g (Eq. [2.28]) of O_2 declines sharply and the unmet O_2 demand forces the need for alternative electron acceptors (Eqs. [2.10] – [2.18]) thus, higher N_2O production via nitrification (Eq. [2.10]) and denitrification (Eq. [2.18]) in the model (same as chapter 2, except the hypothesis is now tested under field conditions). N_2O produced may accumulate in the aqueous phase ($[N_2O_s]$) within the soil profile because its D_g is also low. At WFPS > 90%, nitrification and denitrification in the model may proceed to the terminal electron acceptor (N_2), therefore a higher proportion of N_2 versus N_2O may be produced. The implication of changes in precipitation and temperature on this hypothesis will be investigated in order to improve accuracy of N_2O national inventories.

In order to provide well constrained tests of N_2O emissions in *ecosys* at different spatial scales, accurate measuring techniques of N_2O emissions are necessary. Most measurements of N_2O emissions are currently made with manually operated surface chambers over small areas, referred to as site scale. These measurements capture only small portions of spatial and temporal variability, and so are of limited value for long-term landscape estimates of N_2O emissions (Blackmer et al., 1982; Bouwman, 1996). In order to improve the temporal resolution of chambers, thus providing better data set for model testing, more frequent chamber readings should be taken. The temporal variability of N_2O emissions may also be better captured by micrometeorological techniques at field and landscape scales in combination with the tunable diode laser technology. Data obtained from these techniques also provide better testing of model hypotheses (Grant and Pattey, 1999; Grant and Pattey, 2003; Grant et al., 2006), however these techniques

have low spatial resolution within the field and measure aggregated emissions from diverse topographic positions (Grant and Pattey, 2003).

The implication of this "threshold" response of N_2O emissions on temporal aggregation of emissions for inventories from infrequent measurements will be examined. The effect of changes in timing of fertilizer application on EFs by changing WFPS and temperature during nitrification of fertilizer N following application, will then examined. Testing *ecosys* to model N_2O emissions at the field scale, will later improve confidence in using it to derive N_2O emissions at larger spatial scales (i.e., regional and national) for inventories.

4.2 MODEL DESCRIPTION

4.2.1 Introduction

Ecosys (Grant, 2001a,b) mathematical model can simulate the transport and transformation of heat, water, C, O_2, N, phosphorus (P) and ionic solutes through soil-plant-atmosphere systems with the atmosphere as the upper boundary and soil parent material as the lower boundary, for different ecosystems under a wide range of site-specific conditions (e.g. climate, land use, soil type, topography etc.). For full details of hypotheses of the model, refer to Grant, 2001a,b. For hypotheses specific to N_2O transformations in *ecosys*, refer to Grant and Pattey, 2003 and Grant et al., 2006. Refer to Chapter 2, Section 2.2 for equations beginning with "2."

4.3 MATERIALS & METHODS

4.3.1. Field Experiment

4.3.1.1. Management practices

The temporal variability of N_2O emissions was investigated during a field experiment from 29 April to 31 July 2004, on an Orthic Humic Gleysol soil located at the Canadian Food Inspection Agency Farm (0.2% slope) in Ottawa, Canada (45°17' N, 75°46'W). Results from this experiment were used to test the sensitivity of N_2O emissions to changes in WFPS in *ecosys* under field conditions, at a scale of about 5 ha. The annual precipitation for this area is 944 mm and annual average temperature is 6°C. Urea fertilizer was applied on 4 May at 112 kg N ha^{-1} to different fetch areas (low topography (east) and high topography (west)) of the field (Figure 4-1). On the same day following fertilizer application, the soil was tilled using a disc plough thereby incorporating of fertilizer and plant residues from the previous crop (spring wheat in 2003). Canola (*B. napus*) was planted at 7.2 kg ha^{-1} on 7 May, and harvested on 1 September and 2 September 2004.

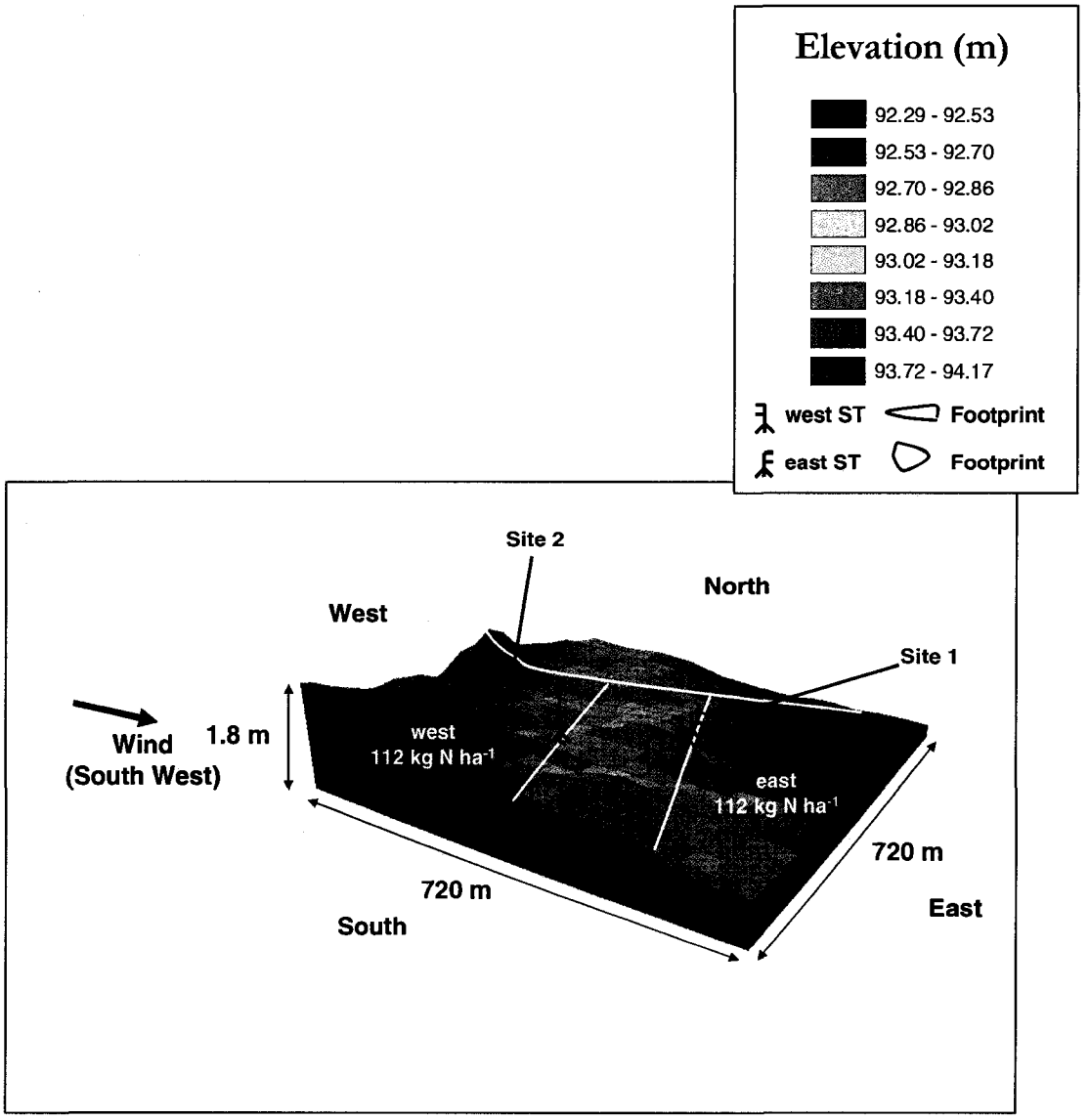

Figure 4-1: Field site showing fertilizer treatment, stationary flux (ST) towers and datalogger sites (Sites 1 and 2), at the Greenbelt Research Farm, Ottawa, 2004.

4.3.1.2. N_2O flux measurements

A closed-path tunable diode laser (TGA-100, Campbell Scientific, Logan, Utah) was used to measure N_2O concentration at 10 Hz at two sampling heights separated by 1 m (Pattey et al., 2006b), in both the lower (east stationary tower (ST) and upper topography (west ST) sections of the field (Figure 4-1).

4.3.1.3 N_2O Flux calculations

N_2O concentration differences measured by ST towers were used to calculate half-hourly N_2O fluxes using the flux gradient technique (Pattey et al., 2006a). This required an eddy diffusivity coefficient which was calculated with sensible heat flux and friction velocity (Pattey et al., 1996), measured using a 3-dimensional ultrasonic anemometer (Solent R3-HS, Gill Instruments Ltd, Lymington, Hampshire, UK).

The following describes the equations used in the flux gradient technique (For full description, refer to Pattey et al., 2005a):

$$F_{N2O} = K\rho_{N2O}\frac{c_L - c_U}{z_2 - z_1} \qquad \text{Eq. [4.1]}$$

Where:

F_{N2O} is the N_2O flux (ng N_2O m^{-2} s^{-1})
K is the eddy diffusivity (m^2 s^{-1})
ρ_{N2O} is the density of N_2O in air (g m^{-3})
c_L is the N_2O concentration (ηmol mol^{-1}) at lower inlet height z_1 (m)

c_U is the N_2O concentration (ηmol mol^{-1}) at upper inlet height z_2 (m)

K was calculated using the following equations:

$$K = \frac{(u * \Delta z\ k)}{\ln\left(\frac{(z_2 - d - z_0)}{(z_1 - d - z_0)}\right) - \psi(z_2) + \psi(z_1)} \qquad \text{Eq. [4.2]}$$

Where:

$$u* = \left(\frac{\tau_0}{\rho_f}\right)^{1/2} \qquad \text{Eq. [4.3]}$$

is the friction velocity (m s^{-1}) calculated from momentum flux $\frac{\tau_0}{\rho_f}$

$\tau_0\ (\rho_f u_*^2) = \rho_f C_D U_r^2$ is the surface drag

ρ_f is the fluid (air) density

C_D is a dimensionless drag coefficient which depends on the surface roughness

U_r^2 is the wind speed at reference height z_r.

$\Delta z = (z_2 - z_1)$ is the inlet height difference (m)

k is the von Karman's constant (0.4)

d is the zero-plane displacement height (m) (calculated as 66% of the crop height representing the effective height at which energy is exchanged between the complex surface (canopy) and atmosphere)

z_0 is the roughness length (m) (the height above d where the mean wind-speed is zero or where U = 0 from the plot of ln z (measurement heights) versus U (wind speed)

ψ accounts for the stability of atmosphere at z_1 and z_2 under the conditions below:

(a) Unstable atmospheric conditions (turbulence as a result of both buoyancy and shear effects dominate):

$$\text{If } -0.0001 > \frac{z-d-z0}{L} > -5, \quad \psi = 2\ln\frac{\left(1+\left(\left(1-15\frac{z-d-zo}{L}\right)^{0.25}\right)^2\right)}{2} \qquad \text{Eq. [4.4]}$$

(b) Stable atmospheric conditions (turbulence as a result of shear effects):

$$\text{If } 5 > \frac{z-d-z0}{L} > 0.0001,\ \psi = -4.7\frac{z-d-z0}{L} \qquad \text{Eq. [4.5]}$$

(c) Neutral atmospheric conditions (no buoyancy effects):

$$\text{If } 0.0001 \geq \frac{z-d-z0}{L} \geq -0.0001,\ \psi = 0 \qquad \text{Eq. [4.6]}$$

Where:

z represents inlet heights z_1 and z_2

L is the Monin-Obukhov length (m)

$$L = \frac{-u^{*3}}{\left(\frac{kgH}{T\rho_a C_p}\right)} \qquad \text{Eq. [4.7]}$$

g is the gravitational coefficient (9.81 m s^{-2})

H is the sensible heat flux (W m^{-2})

T is the air temperature (K)

ρ_a is the density of dry air (g m^{-3})

C_p is the specific heat of moist air (J g^{-1} K^{-1})

Fluxes were only calculated when u^*>0.08 ms^{-1}. Data was gap-filled using linear interpolation for gaps less than 3.5 h, in order to provide seasonal estimates of total emissions.

4.3.1.4 Aggregation of seasonal totals

A lot of linear interpolation of infrequent measurements will be biased if the measurements are less than the diurnal variation in N_2O emissions. Season totals of N_2O emissions was done to test whether differences can arise in seasonal estimates of N_2O emissions aggregated from daily and weekly compared to half-hourly measurements. Season totals of N_2O emissions for the period 8 May – 12 July 2004 were calculated using continuous data sets, from one measurement per day for different times of the day (10:00 am to 4:00pm) and from two and one measurement per week using linear interpolation.

4.3.1.5 Soil moisture, temperature, available N and supporting meteorological data

Dataloggers (CR500, Campbell Scientific Logan, Utah) were placed at different sites within the 112 kg N ha^{-1} footprint area (Figure 4-1), to continuously record soil volumetric water content (TDR CS615 water content reflectometer) and soil temperature (thermistors). The TDR probes were placed diagonally at depths of 0 to 10, 10 to 20 and 20 to 30 cm and thermistors at depths of 5, 15 and 25 cm. Soil samples were taken near each CR500 at different depths for calibrating the TDR probes in 20-L buckets. Available NH_4^+ and NO_3^- measurements were also taken once (16 June 2004) during the season at depths 0-7.5, 7.5-15 and 15-30cm. Hourly rainfall (Tipping bucket rain gauge TE525, Campbell Scientific, Canada Corp. Edmonton, Alberta), air temperature, humidity (Temperature and relative humidity probe HMP35C, Campbell Scientific, Canada Corp. Edmonton, Alberta), pressure, wind speed (Wind monitor R.M. Young Company

Meteorological Instruments, Traverse City, Michigan) and solar radiation were collected from a weather station installed at the edge of the field.

4.3.2. Model Field Experiment

4.3.2.1. Model Inputs

The experimental field was represented in *ecosys* as a 20 x 20 matrix of 36m x 36m grid cells rendered in ArcGIS from a DEM of the field. Boundary conditions included surface run-off through the north, east, south and west boundaries and subsurface drainage through the lower boundary of the landscape. Field topography was simulated from the slope and aspect of each grid cell, obtained in ArcGIS from the DEM. Soil chemical and physical properties (texture and soil organic C and N and inorganic N) for each grid cell were measured through grid soil sampling (70 x 70m) of the field. Bulk density, field capacity, wilting point and hydraulic conductivity of each grid cell were estimated using the Saxton (2006) pedo transfer function calculator. Soil properties were averaged into one soil type for this model run (Table 4-1).

Table 4-1: Properties of Orthic Humic Gleysol used in the modeling experiment.

Depth (m)	Surface – 0.10	0.10-0.20	0.20-0.30	0.30- 0.60	0.60-0.90
D_b, (Mg m^{-3})*	1.24	1.31	1.5	1.5	1.5
θ_{FC}, m^3 m^{-3}*	0.31	0.32	0.32	0.32	0.32
θ_{WP}, m^3 m^{-3} *	0.16	0.17	0.17	0.17	0.17
Ks_{at}, mm h^{-1}*	20	20	15	5	5
Sand, g kg^{-1}	364	364	364	491	491
Silt, g kg^{-1}	431	431	431	331	331
Clay, g kg^{-1}	205	205	205	178	178
pH	7	7	7	7	7
CEC, cmol kg^{-1}	16.8	16.8	16.8	17.5	17.5
Org. C, g kg^{-1}	26	26	26	18	18
Org. N, g Mg^{-1}	2210	2210	2210	1430	1430

***Abbreviations: D_b-bulk density, θ_{FC}-water content at -0.033 MPa; θ_{WP}-water content at -1.5 MPa; K_{sat}-saturated hydraulic conductivity.**

A 4-yr model run was used to represent the agricultural history of the site in 2001 and 2002 (corn fertilized at 155 kg N ha^{-1}) and in 2003 (spring wheat fertilized at 78 kg N ha^{-1}) prior to the experiment in 2004. Management practices for 2004 were applied in the model as in the field experiments (Section 4.3.1.1). All biological transformations were solved on an hourly time step (Eqs. [2.1-2.20]); water fluxes (Eqs. [2.21-2.26]) were calculated 25 times per time step and gas fluxes (Eqs. [2.27-2.28]) were calculated 500 times per time step, assuming constant surface boundary conditions during each hour. No adjustments of parameters were made to fit the model to the field site. All model parameters remained unchanged from earlier studies (e.g. Grant and Pattey, 2003; Grant et al., 2006).

4.3.2.2. Model Testing

N_2O emissions from grid cells within the tower fetch were aggregated according to a footprint model (Schmid, 2002) for comparison to tower measurements. Statistical analyses performed were regression analyses and model use efficiency (MUE):

$$\text{MUE} = 1 - \left\{ \frac{\sum \left(y - \hat{y} \right)^2}{\sum \left(y - \bar{y} \right)^2} \right\} \qquad \text{Eq. [4.8]}$$

Where:

y is the log-transformed measured N_2O emissions

$\hat{y}$ is the log-transformed modeled N_2O emissions

$\bar{y}$ is the mean of the log-transformed measured N_2O emissions

4.3.2.3. Effect of different precipitation and temperature patterns on N_2O emissions

Model simulations (same as Section 5.3.2.1.) for a single grid were performed using original planting and fertilizer dates and then using dates one, two and three weeks earlier, and one, two and three weeks later than the original dates. A control run (no fertilizer) was also conducted for each of the seven planting and fertilizer dates to calculate annual EFs. These simulations were done to show the influence of different WFPS and temperature on N_2O emissions, following fertilizer application with the same crop and fertilizer application rate. The implications of these findings for N_2O inventories were examined by comparing the different EFs derived from the seven timing scenarios.

4.4 RESULTS

4.4.1 Soil water content and temperature

A series of rainfalls in May 2004 such as those of DOY 144-147 (Figure 4-2a) led to increases in measured and modeled WFPS (Figure 4-2b). This was due to surface flow (Eq. [2.21]) and subsurface flow (Eqs. [2.21] and [2.24]) and [A94-A96] of Grant et al., 2004) among interconnected grid cells in *ecosys*, each having defined slopes and aspects from which relative elevations were computed. Topographically-driven flows of water and solutes in *ecosys* are, as a result of lateral water redistribution, due to differences in gravitational water potential. Spatial variation in N_2O emissions resulting from water redistribution are described in a chapter 5. The overall temporal variability of modeled and measured WFPS was similar. However, rainfalls in June 2004 caused small increases in WFPS in the model that were not recorded by probes e.g., DOY 178, indicating that the TDR probes were probably not sensitive enough to small changes in soil water content.

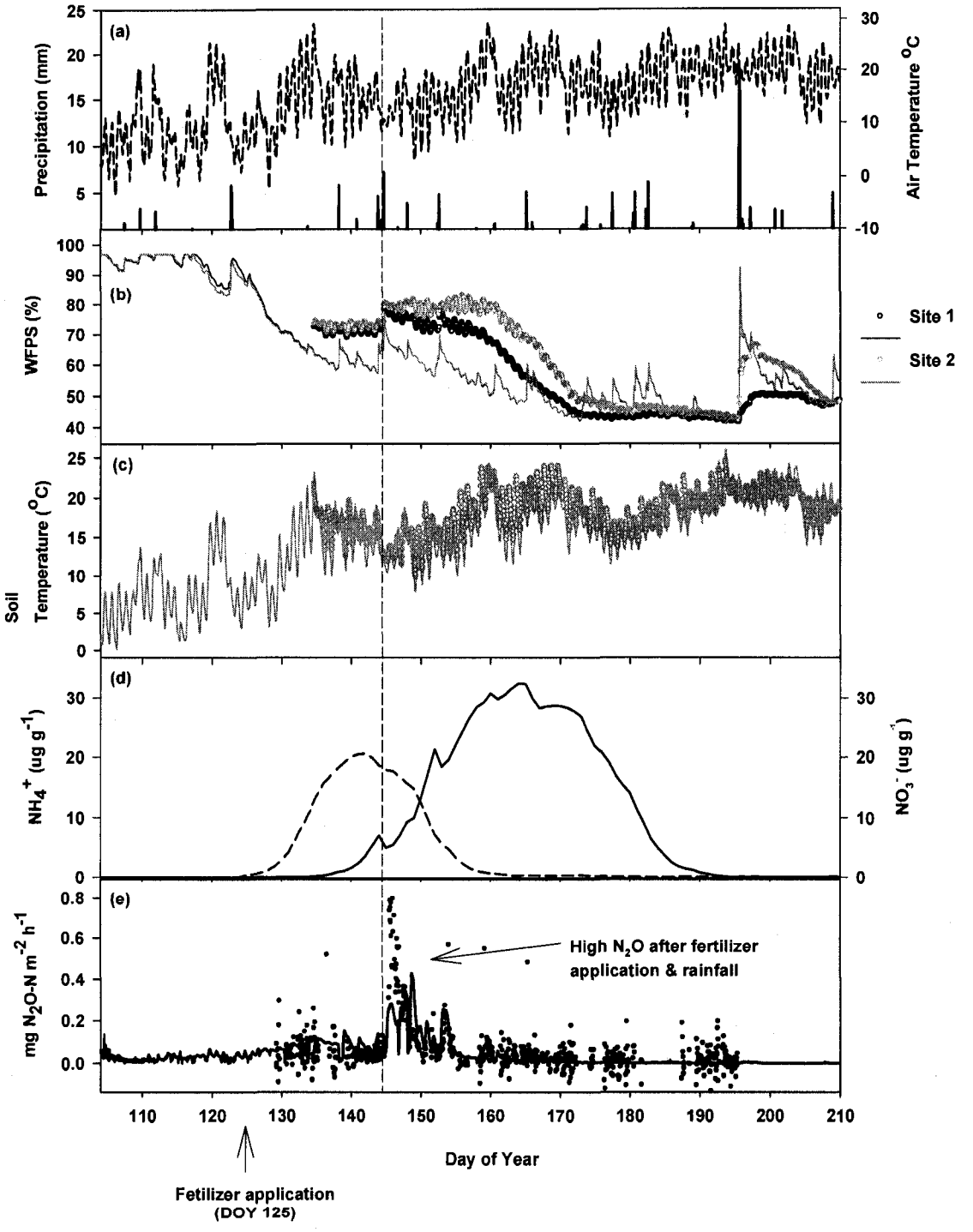

Figure 4-2: (a) Rainfall and air temperature (b) Measured (symbols) modeled (lines) soil water-filled space (WFPS) and (c) Soil temperature (5cm) (d) Modeled soil NH_4^+ (dashed line) and NO_3^- concentrations (solid line) (0 – 10cm) and (e) Measured (symbols) and modeled (lines) N_2O emissions at Ottawa during 2004.

Declining air temperatures (T_a) (Figure 4-3a) caused decreases in soil temperatures during DOY 144-147 (Figure 4-3c) (Site 1 temperature data was not shown since it was similar to that of Site 2). Low soil temperatures for this period coincided with increases in WFPS due to rainfall (Figure 4-3a, b). Rising T_a after DOY 147 led to increases in soil temperatures. Measured and modeled soil temperatures showed similar temporal variability during the experimental period.

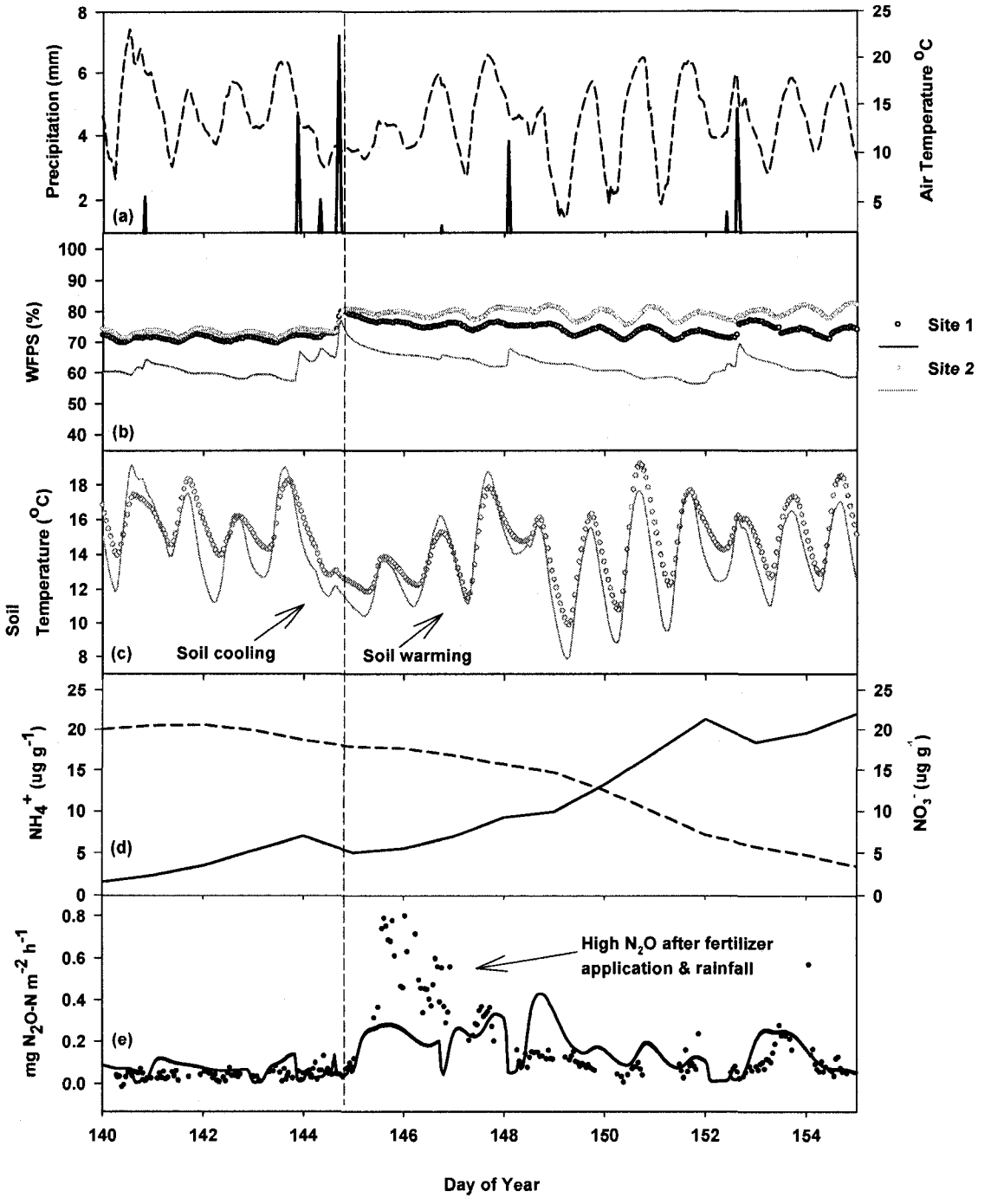

Figure 4-3 (same as Figure 4-2 but x-axis shortened to DOY 140-155): (a) Rainfall and air temperature (b) Measured (symbols) modeled (lines) soil water-filled space (WFPS) and (c) Soil temperature (5cm) (d) Modeled soil NH_4^+ (dashed line) and NO_3^- concentrations (solid line) (0 – 10cm) and (e) Measured (symbols) and modeled (lines) N_2O emissions at Ottawa during 2004.

4.4.2. Temporal variability of N_2O emissions during the season

In *ecosys*, urea was hydrolyzed to produce [NH_{3s}] during DOY 125 – 140 following application on 4 May (DOY 125). Nitrification during DOY 140 – 155 (Figure 4-2d) caused a rapid decline in NH_4^+ and increase in NO_3^-, which coincided with the largest N_2O emission events (Figure 4-2e) for the season. These changes were attributed in the model to rapid oxidation of NH_{3s} (NH_{3s} and NH_4^+ are in dynamic equilibrium) (Figure 4-2d) and reduction of O_2 by nitrifiers to produce NO_2^- (Eqs. [2.1] – [2.4]). This drove the oxidation of NO_2^- and reduction of O_2 by nitrifiers to produce NO_3^- (Eqs. [2.5] – [2.8]). This oxidation occurred because of overall declining WFPS (Figure 4-2b) whereby the diffusivity ($D_{g\gamma}$ in Eq. [2.28]) of O_2 into the soil at ≈ 60% WFPS, was sufficient to meet the demands of nitrifiers. This provided NO_2^- for N_2O production in *ecosys* via nitrification (Eq. [2.10]) and NO_3^- for N_2O production via denitrification (Eq. [2.18]). Low NH_4^+ (NH_4^+ = 0.31 μg g^{-1} (modeled) and NH_4^+ = 1.71 ± 1.4 μg g^{-1} (measured)) and high NO_3^- (NO_3^- = 29 μg g^{-1} (modeled) and NO_3^- = 41 ± 16 μg g^{-1} (measured)) on DOY 168 indicated that nitrification of fertilizer had been largely completed by this date.

N_2O emissions generally followed rainfall and increase in WFPS during nitrification (Eqs. [2.1] – [2.8]). Rainfalls e.g. during DOY 144-147 (Figure 4-3a) led to increases in WFPS (Figure 4-2b), which caused declines in surface and subsurface gaseous diffusivity ($D_{g\gamma}$ in Eq. [2.28]), lowering gaseous O_2 ([O_{2g}]) in the soil profile and slowing dissolution of O_{2g} to O_{2s} (Eq. [A30] in Grant et al., 2006). Dissolution slowed further when higher soil temperatures in the field during soil warming on DOY 148-157 (Figure 4-2c), reduced the aqueous solubility of O_2 (Eq. [A30] in Grant et al., 2006), lowering [O_{2s}] that

sustained O_2 uptake by microbial populations (Eqs. [2.3], [2.7] and [2.14]). Higher soil temperatures also led to an increase in microbial activity and therefore a higher demand for O_2 (Eqs. [2.2], [2.3a,b], [2.13] and [2.14a,b], through the Arrhenius function in Eqs. [2.1] and [2.12]. Aqueous O_2 concentrations at nitrifier microsites ($[O_{2mi,n}]$ in Eqs. [2.3a,b] and [2.7a,b]) declined with respect to the Michaelis-Menten constant for O_2 uptake (K_{O2n} in Eqs. [2.3b] and [2.7b]), therefore O_2 uptake by nitrifiers ($R_{O2i,n}$ in Eqs. [2.3a] and [2.7a]) failed to meet O_2 demand (Eqs. [2.2] and [2.6]). Subsequently, alternative electron acceptors were used to produce N_2O in *ecosys* (Eqs. [2.10] and [2.18]) due to a combination of fertilizer application, rainfall and soil warming. Most modeled and measured N_2O emissions from towers (0.1-0.8 mg N_2O-N m^{-2} h^{-1}) occurred late May to early June (DOY 146-154) (Figure 4-3e). Most of the N_2O emissions (99%) in *ecosys* were attributed to nitrification while a small fraction (1%) was due to denitrification for the main emission period (DOY 146-154). During this main emission period, the largest rainfalls (e.g. DOY 143 – 146 = 25 mm of rainfall; Figure 4-2a) resulted in the largest peak and longest emissions compared with emissions following smaller rainfalls (e.g. DOY 148-151 = 4.9 mm of rainfall). Modeled emissions during DOY 146-147 (Figure 4-3e) were suppressed by low soil temperatures (Figure 4-3c) although measured emissions were large. Subsequent warming on DOY 148-153 led to increased N_2O emissions in the model. The modeled emissions were able to capture the main measured emission events for this period. Coefficients of diurnal temporal variation (CTV) of N_2O emissions was high ranging from 25 to 51% (modeled) and 24 to 63% (measured) at a daily time scale, during emission events for the season.

Emissions modeled in the field on DOY 146 (Figure 4-3e) were delayed for several hours following rainfall on DOY 145 (Figure 4-3a), because of a reduction in the D_g [Eq. [2.28] of N_2O. Consequently, N_2O produced ([Eqs. [10] and [18]) accumulated in the aqueous phase ($[N_2O_s]$) within the soil profile. Re-establishment of gaseous pathways during drainage (Eqs. [21] and [24] and [A94 - A96] of Grant et al., 2004) and evapotranspiration (Eqs.[A.1], [A3], [A4], [18], [24], [25] and [A27] of Grant, 2001a) led to subsequent emissions into the atmosphere through volatilization of $[N_2O_s]$ (Eq. [A30] in Grant et al., 2006). Even though there was rainfall later in the crop season on DOY 196 (Figure 4-2a), and thus increase in WFPS (Figure 4-2b), little or no emissions were modeled or measured after DOY 160. This was due to the disappearance of available NO_3^- (Figure 4-2d) following that of NH_4^+, and consequent constraints to denitrification. The reduction in N_2O emissions later in the season was also attributed to the decline in WFPS (Figure 4-2b) caused by rising evapotranspiration in response to canola growth (Eqs. [A.1], [A3], [A4], [18], [24], [25] and [A27] of Grant, 2001a). Overall, the findings have indicated that modeled emissions in *ecosys* (Grant 2001a,b) rose sharply with WFPS > 60% in a way that was consistent with the measured data (Figures 4-2, 4-3 and 4-4; R^2 of modeled versus measured data: 0.46; $P < 0.001$; regression slope = 0.77; MUE = 0.4) since such correlations are often low in the literature.

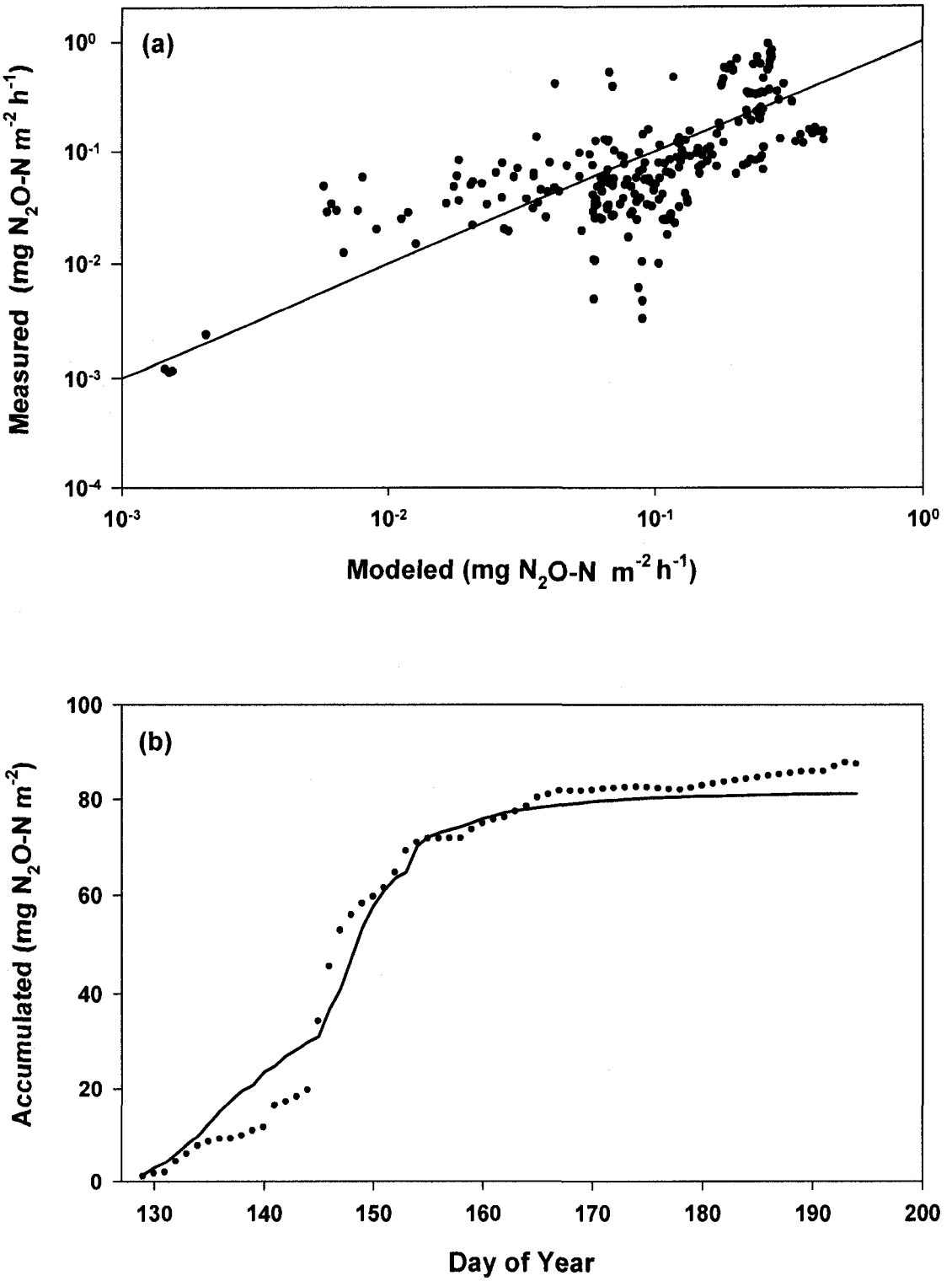

Figure 4-4 (a) Predicted versus observed N_2O emissions (b) Modeled (line) and measured (symbols) accumulated predicted and observed N_2O emissions at Ottawa during 2004.

Results showed that seasonal (8 May – 12 July) N_2O emissions in the model (81 mg N m^{-2}) were similar to those estimated from tower results using a continuous data set (87 mg N m^{-2}) (Figure 4-4b; Table 4-2). However, seasonal N_2O emissions in many studies are frequently estimated by interpolating discrete measurements taken every day to several days. Such estimates may suffer from bias caused by short term changes (e.g., diurnal) in these N_2O fluxes. Seasonal emissions estimated from one value per day, were mostly overestimated (Table 4-2) compared to seasonal emissions estimated from the continuous values, depending on the time of day that daily values were taken (CV = 24% for estimates 10:00 – 4:00pm). This trend seems to happen because the high emission peaks last less than a day, so integrating over 24 h lead to an overestimation. Consequently, if temporal aggregation of N_2O emissions to derive EF is based on one sample per day e.g., at 3.00 pm (Table 4-2), then estimates for inventories may be almost twice as large compared to estimates based on continuous data set (per half-hour) (Table 4-2). Estimates based on measurements taken once or twice per week (Table 4-2) taken following rainfalls and during emission peaks as sometimes done in the field, were even more inaccurate (twice wk^{-1} = 309 mg N m^{-2} and once wk^{-1} = 468 mg N m^{-2}) compared to that of continuous measurements (once half-$hour^{-1}$ = 87 mg N m^{-2}). This implication is based on the assumption that temporal variation of N_2O from flux towers may be similar to that of chambers.

Table 4-2: Seasonal N_2O emissions calculated using one tower-based flux value per day, and two and one tower-based flux per week for the period between 8 May and 12 July 2004.

Measurement frequency	Seasonal Totals (mg N m^{-2})
Calculated from continuous measurement:	87
Calculated from one measurement day^{-1} taken at:	
8:00 am	67
9:00 am	77
10:00 am	68
11:00 am	106
12:00 noon	87
1:00 pm	132
2:00 pm	106
3:00 pm	143
4:00 pm	101
5:00 pm	108
Calculated from two measurements wk^{-1} taken at:	
8:00 am	111
9:00 am	162
10:00 am	123
11:00 am	180
12:00 noon	155
1:00 pm	169
2:00 pm	106
3:00 pm	309
4:00 pm	190
5:00 pm	193
Calculated from one measurement wk^{-1} taken at:	
8:00 am	98
9:00 am	184
10:00 am	128
11:00 am	198
12:00 noon	198
1:00 pm	189
2:00 pm	232
3:00 pm	468
4:00 pm	211
5:00 pm	233

4.4.3 Effect of different precipitation and temperature patterns on temporal variability of N_2O emissions during the season

Some of the variation in fertilizer EF frequently found in field experiments may be caused by differences in temperature and O_2 during nitrification following fertilizer application. Figures 4-5 and 4-6 show that for the same fertilizer rate, the magnitude of N_2O emissions was very different due the influence of changing precipitation and temperature patterns on substrates NH_4^+ and NO_3^- caused by different planting dates. A rapid decline in NH_4^+ and increase in NO_3^- from nitrification (Figure 4-5b, c; similar to Figure 4-2) coincided with the largest emission events (Figure 4-5a) for the season, when planting and fertilizer dates were shifted 1, 2 and 3 weeks earlier in *ecosys*.

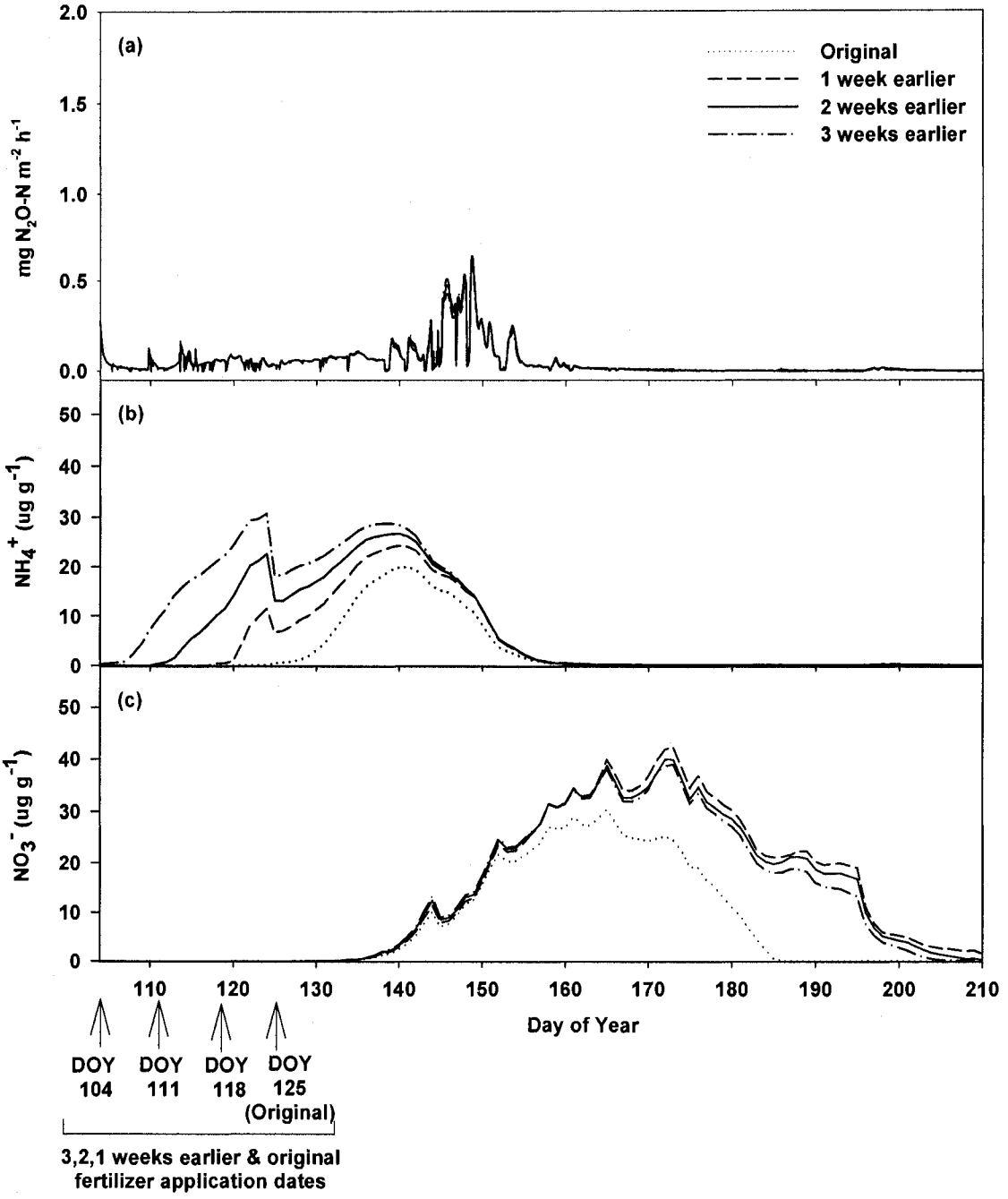

Figure 4-5: Modeled influence of precipitation pattern on (a) N_2O emissions and (b) soil NH_4^+ and (c) NO_3^- concentrations (0 – 10cm). Dotted lines - original planting and fertilizer application dates, short-dashed line – one week earlier, solid line – two weeks earlier and dot and line – three weeks earlier from original planting and fertilizer application dates.

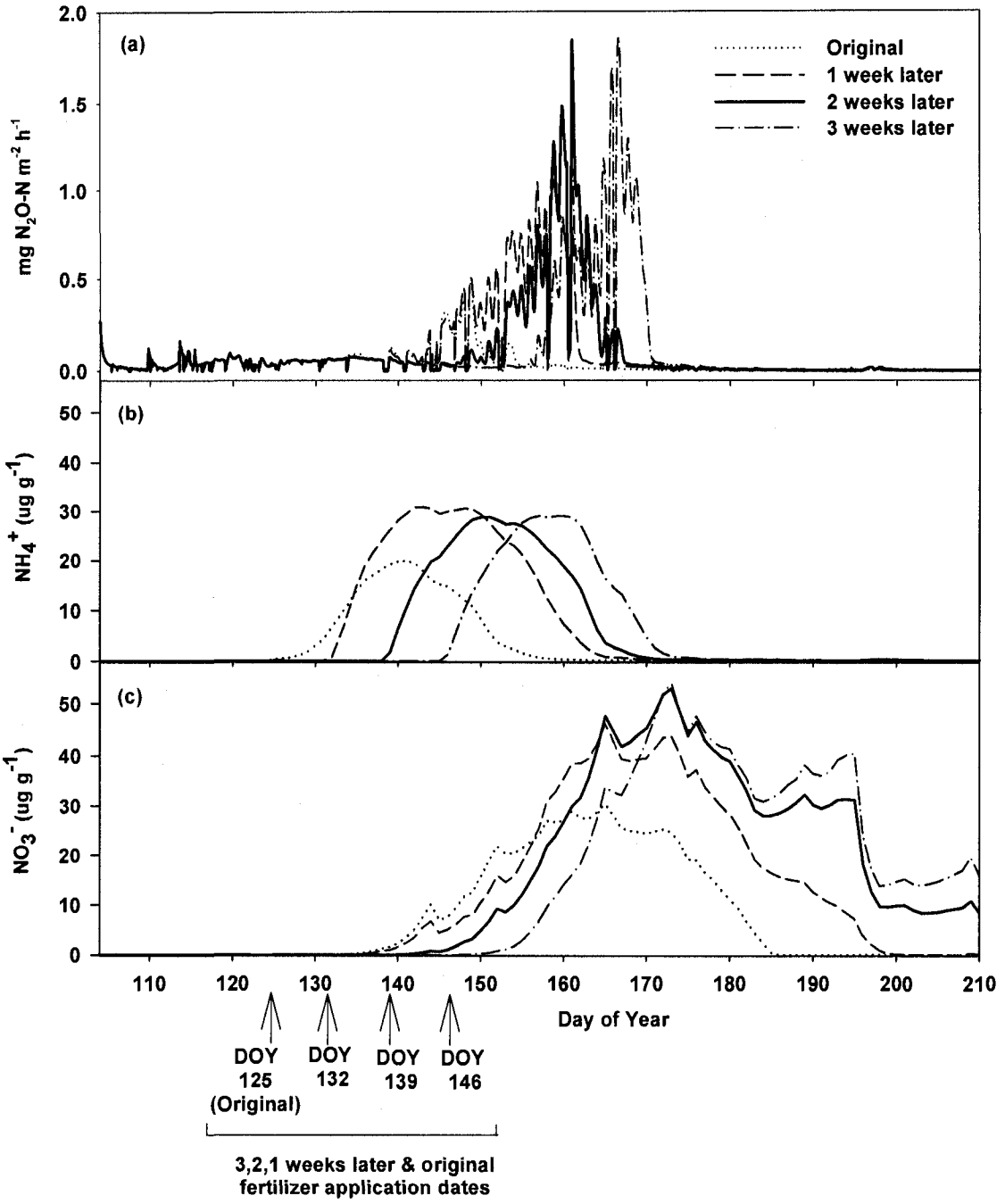

Figure 4-6: Modeled influence of precipitation pattern on (a) N_2O emissions and (b) soil NH_4^+ and (c) NO_3^- concentrations (0-10 cm). Short-dashed line – one week later, solid line – two weeks later and dot and line – three weeks later from original planting and fertilizer application dates.

Earlier planting and fertilizer dates in the model did not affect timing of nitrification because nitrification of fertilizer N (Eqs. [2.1] – [2.8]) began with soil warming and drying after DOY 140, so that emissions (Figure 4-5a; plots overlap) and EFs (Table 4-3) were similar to those of the original date. This occurred due a combination of wet (high modeled WPFS: > 80%, Figure 4-2b) and cold soil (Figure 4-2c). Low soil temperatures led to an overall decrease in microbial activity and therefore a lower demand for O_2 (Eqs. [2.2], [2.3a,b], [2.13] and [2.14a,b], through the Arrhenius function in Eqs. [2.1] and [2.12]. Consequently, less N_2O was produced (Eqs. [10] and [18]). High precipitation (rainfall and snowmelt (Eq. [A.27] of Grant, 2001a)) from around DOY 104 – 125 led to increases in WFPS > 60% (Figure 2b), which caused declines in surface and subsurface gaseous diffusivity (D_{gy} in Eq. [2.28]), thus lowering O_{2s} (Eq. [A30] in Grant et al., 2006). Low O_{2s} led to limited nitrification (Eqs. [2.1] – [2.8]; Figure 5c) therefore, less substrates (NO_2^- and NO_3^-) were available for N_2O production (Eqs. [2.10] and [2.18]). Also, during prolonged high WFPS, nitrification (Eq. [2.10]) and denitrification (Eq. [2.18]) in the model may proceed to the terminal electron acceptor (N_2) (Eq. [2.19]), therefore a higher proportion of N_2 versus N_2O may be produced.

Table 4-3: Annual fertilizer emission factors (EFs) (including snowmelt) derived from *ecosys* simulations for scenarios on which the date of N application varied.

Model scenario (single grid)	Fertilizer dates (DOY)	N_2O emissions (112 kg N ha^{-1}) (mg N m^{-2} yr^{-1})	N_2O emissions (Control) (mg N m^{-2} yr^{-1})	*EFs (%)
3 weeks earlier	104	165	110	0.49
2 weeks earlier	111	163	107	0.50
1 week earlier	118	159	120	0.35
Original (Section 4.3.2.1.)	125	123	89	0.31
1 week later	132	286	101	1.65
2 weeks later	139	279	104	1.57
3 weeks later	146	305	105	1.79

***EFs - Annual emission factors calculated as N_2O emissions attributed to fertilizer application minus those of the control, divided by the total N fertilizer applied.**

When planting and fertilizer dates were shifted 1, 2 and 3 weeks later in *ecosys*, emissions (Figure 4-6a) thus EFs (Table 4-3) were higher than those of the original and earlier dates (Figure 4-5a). Later fertilizer applications caused nitrification (Eqs. [2.1] – [2.8]) (decline in NH_3 and increase NO_3^-) to be delayed until after DOY 149 so that it occurred in warmer soil than that of earlier applications. Rising soil temperatures had a stronger effect on N_2O production than did rainfall since there was a general decrease in modeled WFPS (Figure 4-2b) after DOY 132. Higher soil temperatures led to an increase in microbial activity (Eqs. [2.1], [2.2], [2.3a,b], [2.13], [2.14a,b], and [2.12]) thus nitrification (Eqs. [2.1] – [2.8]; Figure 6c) (more substrates for N_2O production (Eqs. [2.10] and [2.18] after rainfall events) was more rapid than when fertilizer was applied earlier (Figure 4-5c). Also, with more rapid microbial activity, O_2 uptake by nitrifiers ($R_{O2i,n}$ in Eqs. [2.3a] and [2.7a]) failed to meet O_2 demand (Eqs. [2.2] and [2.6]). Higher soil temperatures resulted in the overall reduction of the aqueous solubility of O_2 (Eq.

[A30] in Grant et al., 2006). Subsequently, alternative electron acceptors were used to produce N_2O in *ecosys* (Eqs. [2.10]) and [2.18]). Example, our results showed that delaying fertilization by 3 days caused peak modeled emissions to be higher (~ 1.85 mg N m^{-2} h^{-1}; Figure 4-6a) with higher soil temperatures on DOY 167 (21.5°C; Figure 2c). This flux was 4 times higher (Table 4-3) than those when fertilization was advanced by 3 weeks on DOY 146 (~ 0.5 mg N m^{-2} h^{-1}; Figure 4-5a) with lower soil temperatures (14°C; Figure 4-2c). Temporal shifts in plant uptake due to changing the planting and fertilizer application dates was not important since rapid plant N uptake for all dates only occurred after the period of nitrification (high substrate availability for N_2O production). Average annual background (control) emissions (Table 4-3) for the seven scenarios was 105 mg N m^{-2} y^{-1} hence, the importance of accounting for emissions due to site land use history and snowmelt (average emission due to snowmelt was 39 mg N m^{-2} y^{-1}).

4.5 DISCUSSION

5.1 Sensitivity of N_2O emissions to changes in soil WFPS

Ecosys (Grant, 2001a,b) captured the sensitivity of N_2O emissions in response to changes in WFPS (threshold response) thereby allowing a better understand the episodic nature of these emissions. This "threshold" response in *ecosys* (Eq. [2.28]) occurs because the D_g of gases in the soil atmosphere is highly sensitive to changes in the soil's WFPS or θ_g (Millington and Quirk, 1960). The findings have indicated that modeled emissions in *ecosys* (Grant, 2001a,b) rose sharply with WFPS > 60% in a way that was consistent with the measured data (Figures 4-2, 4-3 and 4-4; R^2 of modeled versus measured data: 0.46; P < 0.001; MUE = 0.4) since such correlations are often low in the literature. The consistency of modeled and measured results **supports the hypothesis in *ecosys* (Grant, 2001a,b) outlined in the Introduction (section 4.1), that N_2O production increases sharply (threshold, non-linear response) at 90% > WFPS > 60%. This non-linear rise of N_2O emissions in the model can be explained by the D_g (Eq. [2.28]) of O_2 whereby at WFPS < 60%, the D_g (Eq. [2.28]) of O_2 is large enough to meet microbial demands. However, as WFPS increases above 60%, the D_g (Eq. [2.28]) of O_2 declines sharply and the unmet O_2 demand forces the need for alternative electron acceptors (Eqs. [2.10] – [2.18]) thus, higher N_2O production via nitrification (Eq. [2.10]) and denitrification (Eq. [2.18]) in the model** (same as chapter 2, except the hypothesis is now tested under field conditions). Correlations between modeled and measured (acetylene inhibition method) emissions obtained in other process – based modeling studies (e.g. Li, 2005) were similar using daily time-steps (R^2 = 0.45) models and also lower using both hourly (R^2 = 0.35) and daily (R^2 = 0.14) time-steps models, compared to

the results in this chapter. Other studies (e.g. Calanca et al., 2007) also showed the difficulties in simulating N_2O dynamics from soils. There was no unique function of N_2O emissions versus WFPS and/or temperature since emissions depended on a combination of favourable WFPS, temperature and N transformations after fertilization and also because of the complex "threshold" response of N_2O emissions. As a result, direct modeled and measured correlations of N_2O emissions versus WFPS and soil temperature were all small ($R^2 < 0.05$). Other process-based models (e.g. Li et al., 2005) showed low correlations (R^2 = 0 - 0.1) of daily N_2O emissions versus daily WFPS and soil temperature. The "threshold" response limits the extent to which simple correlations with WFPS and temperature can be used to predict N_2O emissions, hence the importance of processed-based model *ecosys* for simulating N_2O production.

Much of the unexplained variation in measured N_2O fluxes may be attributed to uncertainties in micrometeorological measurements (Laville et al., 1999; Phillips et a., 2007). Uncertainties may be 20 % due to changes in wind speed and direction which can modify the apparent N_2O source pattern (Laville et al., 1999) or due to uncertainties in calculations of transfer coefficients (25% during the day and 60% at night) (Phillips et a., 2007). Only a few earlier process – based modeling studies (e.g Grant and Pattey, 1999, Grant and Pattey, 2003; Grant et al., 2006) have used continuous N_2O micrometeorological measurements for model testing. Our results showed that *ecosys* captured the temporal variation of N_2O emissions except during soil cooling on DOY 145 – 147 (Figure 4-3e). The results showed that N_2O concentration gradients were large and they were measured under abnormal micrometeorological conditions (extremely low

friction velocities and sensible heat fluxes, thus low calculated eddy diffusivities) during this cooling period, during which larger N_2O fluxes were calculated than modeled.

This "threshold" response of N_2O emissions shows the importance of linking biological controls of N_2O emissions to physical controls in mathematical models as well as simulating N_2O emissions at an hourly time-step versus daily or monthly time-step models, in order to better capture the timing and magnitude of the entire emission events. Such temporal variability of N_2O emissions has been shown in previous studies (e.g., Grant et al, 1992; Grant and Pattey, 1999; Grant and Pattey 2003; Grant et al., 2006). During the main emission period (DOY 146-154; Figure 4-3e), the largest rainfalls resulted in the largest peak and longest emissions compared with emissions following smaller rainfalls. Grant and Pattey (2003) found a similar trend whereby larger rainfalls e.g. DOY 164-165 resulted in largest peak emissions and longest emissions events compared to emissions following smaller rainfalls e.g. DOY 151. These findings show the importance of sampling during the entire growing season to fully capture the temporal variability of N_2O emissions, thus improving the confidence in estimates for greenhouse gas inventories since calculation of EFs based on few data may tend to overestimate emissions.

5.2 Biases in seasonal N_2O emissions estimates

The episodic nature of these emissions requires that seasonal totals be derived from short-term (i.e., hourly) measured or modeled values rather than daily or weekly ones. Seasonal N_2O emissions for the period 8 May – 12 July were most of the time overestimated by an

average of 33% when estimates were based on one measurement per day (Table 4-2) compared to estimates based on continuous data set. This inaccuracy was due to the large diurnal variation of N_2O emissions compared to those of other greenhouse gases such as CO_2. Rochette et al. (1992) showed that diurnal variation of soil CO_2 emissions from a barley crop was only 17% in a nearby site to this experiment, while that of N_2O emissions varied from 25 to 51% (modeled) and 24 to 63% (measured). Findings from this chapter showed that estimates based on less frequent chamber measurements (Table 2) taken following rainfalls and during emission peaks as sometimes done in the field, were even more inaccurate (overestimated by an average of 95 and 146% for twice wk^{-1} and once wk^{-1} measurements). Similarly, Pattey et al. (2007) found that estimates from continuous tower measurements of N_2O emissions measured at snowmelt were lower (1.26 kg ha^{-1}) compared to measurements once d^{-1} at 11:00h (1.45 kg N ha^{-1}). Estimates were even larger (1.69 kg N ha^{-1}) when measurements were taken twice and once wk^{-1} (Pattey et al., 2007). A review by Bouwman et al. (2002) showed that high frequency measurements (> 1 d^{-1}) gave lower annual estimates e.g., 1.5 kg N ha^{-1} than low frequency measurements (< 1 wk^{-1}) e.g., 4.5 kg N ha^{-1}. It is therefore important to take sub-daily samples to fully capture the large sub-diurnal fluctuations of N_2O emissions, to improve the confidence in annual estimates for inventories. These results show the importance of mathematical models such as *ecosys* with short model time – steps. Models should have similar temporal resolution for accurate time-integrated estimates.

5.3 Sensitivity of N_2O emissions to changes in soil temperature

In addition to changes in WFPS, the temporal variability of N_2O emissions was attributed in *ecosys* to the changes of soil temperature. Results from this chapter showed that on DOY 167, modeled emissions were ~ 4 times higher at 21.5°C (Figure 4-6a) with higher soil temperatures (Figure 4-2c) when fertilization was delayed by 3 weeks (Table 4-3) than those on DOY 146 at 14°C (Figure 4-5a) with lower soil temperatures when fertilization was advanced by 3 weeks. Dobbie and Smith (2001) found similar results whereby emissions for an arable soil were larger (nearly 4 – fold) at soil temperature of 18°C compared to those at 12°C, with an apparent Q_{10} of 8.9. This large apparent Q_{10} value may be related to the complex "threshold" response involved in N_2O production since most microbial processes usually have much smaller Q_{10} of 2 – 3. *Ecosys* was also recently tested (Grant and Pattey, Submitted) against the measurements by Dobbie and Smith (2001) whereby the model simulated the large rises in N_2O emissions in their study, in response to the same temperature increments. Several studies (e.g., Grant, 1995; and Smith et al., 1998) have showed that N_2O emissions increase sharply at higher soil temperatures.

5.4 Sensitivity of N_2O emissions to changes in solutes (NH_4^+ and NO_3^-) during nitrification of fertilizer N due to changes in soil temperature

The temporal variability of N_2O emissions was also attributed in *ecosys* to the changes of in solutes (NH_4^+ and NO_3^-) during nitrification of fertilizer N. Most measured and modeled emissions coincided with a period of rapid nitrification in the model, indicated by declining NH_4^+ and rising NO_3^- (DOY 140 – 155) (Figure 4-3d). Emissions later

declined due to declining WFPS (Figure 4-2b) and available N substrates. This co-incidence suggests that emissions may be affected by the soil conditions under which nitrification of fertilizer occurs, as affected by timing of fertilizer application, even if the same fertilizer rate is used.

Low soil temperatures when fertilizer was applied on or before DOY 125 (original date), enabled limited nitrification to occur thus low N_2O emissions (Figure 4-4) and EFs (Table 4-3). In contrast, higher soil temperatures with later applications allowed greater nitrification thus higher emissions (Figure 4-5) and EFs (Table 4-3). Similar to other studies (Grant and Rochette, 1994; Grant, 1995), these results show that the WFPS threshold at which the transition among reduction reactions occurs decreases with higher temperatures. These results imply that fertilizer application dates not only should match crop uptake capacities but also should be applied at lower soil temperatures i.e., avoid late applications, to minimize loss of N through N_2O emissions. Also, it is important to consider fertilizer application dates in our N_2O inventories, since earlier or later applications can have a large impact on the EFs. Studies by Flechard et al. (2007) showed that EF for N_2O emissions in a moist soil (~ 60% WFPS) were higher (EF ~ 6%) at warm soil temperature of ~ 25°C compared to lower soil temperatures of ~ 10°C (EF ~ 2%). They also showed that high temperatures of ~ 25°C can cause large emissions (event-based EF ~ 5%) from comparatively dry soil (~ 30% WFPS), indicating that the soil warming effect outweighed the effect of low WFPS on N_2O emissions. Findings from this chapter show the importance of including climate impact on N_2O emissions, in process-based mathematical models, to fully represent the complex hypotheses involved

in N_2O emissions. In addition to the climate impact, *ecosys* represented other site-specific (land use, soil type, topography etc.) hypotheses involved in N_2O production. Results at different timing (Table 4-2) are specific to the timing and extent of soil warming at the Ottawa site in 2004. However, these results may explain some of the variability in EFs found in other experiments.

5.5 Future studies using ecosys

Future modeling work will enable *ecosys* to scale N_2O emissions from landscape (Metivier et al., In Prep.) to regional and national scales. Future modeling work will also enable *ecosys* to make predictions under different land uses and climate change scenarios. These predictions will then be used to make recommendations for sustainable land use management recommendations in order to enhance crop productivity and maintain environmental quality.

4.6 CONCLUSIONS

Ecosys (Grant, 2001a,b) captured the sensitivity of N_2O emissions in response to changes in WFPS (threshold response) thereby allowing a better understand the episodic nature of these emissions. Our findings have indicated that modeled emissions in *ecosys* (Grant, 2001a,b) rose sharply with WFPS > 60% in a way that was consistent with the measured data (Figures 4-2 and 4-3; R^2 of modeled versus measured data: 0.46; $P < 0.001$; MUE = 0.4) since such correlations are often low in the literature. The consistency of modeled and measured results **supports the hypothesis in *ecosys* (Grant, 2001a,b) outlined in the Introduction (section 4.1), that N_2O production increases sharply (threshold, non-linear response) at 90% > WFPS > 60%.** This "threshold" response limited the extent to which simple correlations with WFPS and temperature can be used to predict N_2O emissions, hence the importance of process - based model *ecosys* (Grant, 2001a,b), for simulating N_2O production.

Large diurnal variation was shown to cause biases in seasonal N_2O emissions if calculated from infrequent ($1day^{-1}$, 2 wk^{-1} and 1 wk^{-1}) measurements. It is therefore important to take sub-daily samples or have continuous datasets, to fully capture the large sub-diurnal fluctuations of N_2O emissions, in order to improve our confidence in annual estimates for inventories - Consequently, there is a need for an IPCC Tier III Methodology since this can provide more continuous data sets.

N_2O emissions and thus EFs, in *ecosys* was very sensitive to changes in T_s. Lower soil temperatures at all sites during DOY 144-147, caused lower modeled emissions, although

tower emissions were not lower. Results also showed that on DOY 167, modeled emissions were ~ 4 times higher at 21.5°C with higher soil temperatures for the 3 weeks later model scenario than those on DOY 146 at 14°C with lower soil temperatures for the 3 weeks earlier model scenario. Dobbie and Smith (2001) found similar results whereby emissions for an arable soil were larger (nearly 4 – fold) at soil temperature of 18°C compared to those at 12°C, with an apparent Q_{10} of 8.9. This large apparent Q_{10} value may be related to the complex "threshold" response involved in N_2O production since most microbial processes usually have much smaller Q_{10} of 2 – 3. *Ecosys* was also recently tested (Grant and Pattey, Submitted) against the measurements by Dobbie and Smith (2001) whereby the model simulated the large rises in N_2O emissions in their study, in response to same temperature increments. Several other studies (e.g., Grant, 1995; and Smith et al., 1998; Flechard et al., 2007) have showed that N_2O emissions are lower at lower soil temperatures. In contrast, some studies (Barnard et al., 2005; Bouwman et al., 2002) showed different responses of N_2O emissions to higher temperatures. Meta analysis (Bouwman et al., 2002) showed that soil warming had no effect on N_2O emissions in the field but had both positive and negative effects in the laboratory experiments. The review also emphasized the need for more soil warming studies (Bouwman et al., 2002). Such further studies may help resolve differences between measured and modeled emissions in this chapter.

The large temporal variability of N_2O in *ecosys* coincided with the temporal variability of solutes (NH_4^+ and NO_3) during nitrification of fertilizer N. Most measured and modeled emissions coincided with a period of rapid nitrification in *ecosys*, indicated by declining

NH_4^+ and rising NO_3^-. This large temporal variability of N_2O variation in the model was shown to rise strongly with temperature during nitrification of N fertilizer so that EFs were affected by timing of fertilizer application. EFs almost quadrupled when fertilizer applications were delayed (average: 1.67%), causing nitrification to occur in warmer soils (18°C) compared to earlier applications (average: 0.45%) when nitrification occurred in cooler soils (12°C). These results imply that fertilizer application dates not only should match crop uptake capacities but also should be applied at lower soil temperatures i.e., avoid late applications, to minimize loss of N through N_2O emissions. Maybe some of the large differences in N_2O emissions measured in experiments (Barnard et at., 2005) can be explained by differences in T_s due to different planting and fertilizer dates. Therefore, it may be necessary to incorporate the effect of T_s in current IPCC Tier II Methodology for Canada. However, there may be confounding effects of other factors e.g. WFPS, fertilizer use, soil residual and source (chapters 2 and 3) in the field, hence the need for process-based mathematical models such as *ecosys* that account for interacting site-specific factors affecting N_2O emissions. Finding from chapter 4 showed the importance of including climate impact on N_2O emissions in models, to fully represent the complex hypotheses involved in N_2O emissions. In addition to the climate impact, *ecosys* represented other site-specific (land use, soil type, topography etc.) hypotheses involved in N_2O production. Ours EFs can therefore contribute towards to the development of an IPCC Tier III Methodology.

4.7 REFERENCES

Barnard, R., Leadley, P.W., Hungate, B.A., 2005. Global change, nitrification, and denitrification: A review. Global Biogeochemical cycles 19, GB1007, doi:10.1029/2004GB002282.

Bateman, E.J., Baggs, E.M., 2005. Contributions of nitrification and denitrification to N_2O emissions from soils at different water-filled pore space. Biology & Fertility of Soils 41, 379-388.

Belser, L.W., Schmidt, E.L., 1980. Growth and oxidation kinetics of the three genera of ammonia oxidizers. FEMS Microbiology Letters 7, 213-216.

Blackmer, A.M., Robbins, S.G., Bremner, J.M., 1982. Diurnal variability in rate of emission of nitrous oxide from soils. Soil Science Society of America Journal 46, 937-942.

Bouwman, A.F., Boumans, L.J.M., Batjes, N.H., 2002. Emissions of N_2O and NO from fertilized fields: Summary of available measurement data. Global Biogeochemical cycles 16(4), 1058, doi:10.1029/2001GB001811.

Bouwman, A.F., 1996. Direct emission of nitrous oxide from agricultural soils. Nutrient Cycling in Agroecosystems 46, 53-70.

Brock, T.D., Madigan, M.T., 1991. Biology of Microorganisms, 6th ed., Prentice Hall, Englewood Cliffs, NJ.

Clay, D.E., Molina, J.A.E., Clapp, C.E., Linden, D.R., 1985. Nitrogen-tillage-residue management: II. Calibration of potential rate of nitrification by model simulation. Soil Science Society of America Journal 49, 322-325.

Davidson, E.A., 1991. Fluxes of nitrous oxide and nitric oxide from terrestrial ecosystems. In: Rogers, J.E., Whitman, W.B. (Eds.), Microbial Production and Consumption of Greenhouse Gases: Methane, Nitrogen Oxides and Halomethanes. American Society of Microbiology, Washington, D.C., pp. 219-235.

de Vries, D.A. 1963. Thermal properties of soils. In R. van wijk (Ed.). Physics of Plant Environment. North Holland Publishing, Amsterdam, The Netherlands, 210-235.

Dobbie, K.E., Smith, K.A., 2001. The effects of temperature, water-filled pore space and land use on N_2O emissions from an imperfectly drained gleysol. European Journal of Soil Science 52, 667-673.

Dobbie, K.E., Smith, K.A., 2003. Nitrous oxide emission factors for agricultural soils in Great Britain: the impact of soil water-filled pore space and other controlling variables. Global Change Biology 9, 204–218.

Flessa, H., Dörsch, P., Beese, F., 1995. Seasonal variation of N_2O and CH_4 fluxes in differently managed arable soils in southern Germany. Journal of Geophysical Research 100, 23115-23124.

Flechard, C.R., Ambus, P., Skiba, U., Rees, R.M., Hensen, A., van Amstel, A., van den Pol-van Dasselaar, A., Soussana, J.-F., Jones, M., Clifton-Brown, J., Raschi, A., Horvath, L., Neftel, A., Jocher, M., Ammann, C., Leifeld, J., Fuhrer, J., Calanca, P., Thalman, E., Pilegaard, K., Di Marco, C., Campbell, C., Nemitz, E., Hargreaves, K.J., Levy, P.E., Ball, B.C., Jones, S.K., van de Bulk, W.C.M., Groot, T., Blom, M., Domingues, R., Kasper, G., Allard, V., Ceschia, E., Cellier, P., Laville, P., Henault, C., Bizouard, F., Abdalla, M., Williams, M., Baronti, S., Berretti, F., Grosz, B., 2007. Effects of climate and management intensity on nitrous oxide emissions in grassland systems across Europe. Agriculture, Ecosystems and Environment 121, 135-152.

Focht, D.D., Verstraete, W., 1977. Biochemical ecology of nitrification and denitrification. Advances in Microbial Ecology 1, 135-214.

Grant, R.F., 1991. A technique for estimating denitrification rates at different soil temperatures, water contents, and nitrate concentrations. Soil Science 152, 41-52.

Grant, R.F., 1995. Mathematical modelling of nitrous oxide evolution during nitrification. Soil Biology & Biochemistry 27, 1117–1125.

Grant, R.F., 1997. Changes in soil organic matter under different tillage and rotation: mathematical modeling in *ECOSYS*. Soil Science Society of America Journal 61, 1159-1175.

Grant, R.F., 2001a. A Review of the Canadian Ecosystem Model - *ecosys*. In: Shaffer M. J., Ma, L., Hansen, S. (Ed), Modeling Carbon and Nitrogen Dynamics for Soil Management. CRC Press. Boca Raton, FL, pp. 173-263.

Grant, R.F., 2001b. Modeling Transformations of Soil Organic Carbon and Nitrogen at Differing Scales of Complexity. In: Shaffer M. J., Ma, L., Hansen, S. (Ed), Modeling Carbon and Nitrogen Dynamics for Soil Management. CRC Press. Boca Raton, FL, pp. 597-614.

Grant, R.F., 2004. Modeling topographic effects on net ecosystem productivity of boreal black spruce forests. Tree Physiology 24, 1-18.

Grant, R.F., Rochette, P., 1994. Soil Microbial respiration at Different Water Potentials and Temperatures: Theory and Mathematical Modeling. Soil Science Society of America Journal 58, 1681-1690.

Grant, R.F. Pattey, E., 1999. Mathematical modeling of nitrous oxide emissions from an agricultural field during spring thaw. Global Biogeochemical Cycles 13, 679-694.

Grant, R.F., Pattey, E., 2003. Modelling variability in N_2O emissions from fertilized agricultural fields. Soil Biology & Biochemistry 35, 225-243.

Grant, R.F., Pattey, E., 2007 (Submitted). Temperature sensitivity of N_2O emissions from fertilized agricultural soils: mathematical modelling in *ecosys*.

Grant, R.F., Nyborg, M., Laidlaw, J.W., 1992. Evolution of nitrous oxide from soil: II. Experimental results and model testing. Soil Science 156, 266-277.

Grant, R.F., Juma, N.J., McGill, W.B., 1993a. Simulation of carbon and nitrogen transformations in soils. I: mineralization. Soil Biology & Biochemistry 25, 1317-1329.

Grant, R.F., Juma, N.J., McGill, W.B., 1993b. Simulation of carbon and nitrogen transformation in soil: Microbial biomass and metabolic products. Soil Biology & Biochemistry 25, 1331-1338.

Grant, R.F., Nyborg, M., Laidlaw, J.W., 1993c. Evolution of nitrous oxide from soil: I. Model development. Soil Science 156, 259-265.

Grant, R.F., Izaurralde, R.C., Nyborg, M., Malhi, S.S., Solberg, E.D., Jans-Hammermeister, D., Stewart, B.A., 1998. Modeling tillage and surface residue effects on soil C storage under ambient versus elevated CO_2 and temperature in *ECOSYS*. In: Lal, R., Kimble, J.M., Follet, R.F. (Eds), Soil processes and carbon cycle. CRC Press Inc. Boca Raton, USA, pp. 527-547.

Grant, R.F., Amrani, M., Heaney, D.J., Wright, R., Zhang, M., 2004. Mathematical Modeling of Phosphorus Losses from Land Application of Hog and Cattle Manure. Journal of Environmental Quality 33, 210-231.

Grant, R.F., Pattey, E., Goddard, T.W., Kryzanowski, L.M., Puurveen, H., 2006. Modeling the effects of fertilizer application rate on nitrous oxide emissions. Soil Science Society of America Journal 70, 235-248.

Helgason, B.L., Janzen, H.H., Angers, D.A., Boehm, M., Bolinder, M., Desjardins, R.L., Dyer, J., Ellert, B.H., Gibb, D.J., Gregorich, E.G., Lemke, R., Massé, D., McGinn, S.M., McAllister, T.A., Newlands, N., Pattey, E., Rochette, P., Smith, W., VandenBygaart, A.J., Wang, H., 2005. GHGFarm: An assessment tool for estimating net greenhouse gas emissions fromCanadian farms. Agriculture & Agri-Food Canada, pp. 5-6.

Hénault, C., Devis, X., Page, S., Justes, E., Reau, R., Germon, J.C., 1998. Nitrous oxide emissions under different soil and land management conditions. Biology and Fertility of Soils 26, 199-207.

IPCC (Intergovernmental Panel on Climate Change), 2006. 2006 IPCC Guidelines for National Greenhouse Gas Inventories, Prepared by the National Greenhouse Gas Inventories Programme, Eggleston H.S., Buendia L., Miwa K., Ngara T. and Tanabe K. (Eds). Published: IGES, Japan.

Koike, I., Hattori, A., 1975. Growth yield of a denitrifying bacterium, *Pseudomonas denitrificans*, under aerobic and denitrifying conditions. Journal of General Microbiology 88, 1-10.

Laville, P., Jambert, C., Cellier, P., Delmas, R. 1999. Nitrous oxide fluxes from a fertilised maize crop using micrometeorological and chamber methods Agricultural & Forest Meteorology 96 (1999) 19 – 38.

Li, C., Frolking, S., Frolking, T.A., 1992. A model of nitrous oxide evolution from soil driven by rainfall events: 1. Model structure and sensitivity. Journal of Geophysical Research 97, 9759-9776.

Li., Y., Chen, D., Zhang, Y., Edis, R., Ding, H., 2005. Comparison of three modeling approaches for simulating denitrification and nitrous oxide emissions from loam-textured arable soils. Global Biogeochemical Cycles, 19, GB3002, doi:10.1029/2004GB002392.

Lim, B., Boileau, P., Bonduki, Y., van Amstel, A.R., Janssen, L.H.J.M., Olivier, J.G.J., Kroeze, C., 1999. Improving the quality of national greenhouse gas inventories. Environmental Science and Policy 2, 335-346.

Lu, Y., Huang, Y., Zou, J., Zheng, X., 2006. An inventory of N_2O emissions from agriculture in China using precipitation-rectified emission factor and background emission. Chemosphere 65, 1915-1924.

McGill, W.B., Hunt, H.W., Woodmansee, R.G., Reuss, J.O., 1981. Phoenix, a model of the dynamics of carbon and nitrogen in grassland soils. In F.E. Clark and T. Rosswall (Ed.) Terrestrial nitrogen cycles. Ecological Bulletin 33, 49-115.

Metivier, K.A, Grant, R.F. and Pattey, In. Prep. Modeling topographic effects on spatial variability of nitrous oxide emissions from fertilized agricultural fields.

Millington, R.J., 1959. Gas diffusion in porous media. Science. 130, 100-102.

Millington, R.J., Quirk, J.M., 1960. Transport in porous media. In: Van Beren, F.A. et al. (Eds.), 7th Trans. Int. Congr. Soil Sci. Vol. 1. Madison, WI. 14-24 Aug. Elsevier, Amsterdam, Science, pp. 97-06.

Molina, J.A.E., Clapp, C.E., Shaffer, M.J., Chichester, F.W., Larson, W.E., 1983. NCSOIL, a model of nitrogen and carbon transformations in soil: Description, calibration and behavior. Soil Science Society of America Journal 47, 85-91.

Morgan, R.P.C., Quinton, J.N., Smith, R.E., Govers, G., Poesen, J.W.A., Auerswald, K., Chisci, G., Torri, D., Styczen, M.E., Folly, A.J.V., 1998. The European Soil Erosion Model (EUROSEM): Documentation and user guide. Version 3.6. Silsoe College, Cranfield University, Silsoe, Bedford, UK.

Muller, C., 1999. Modelling soil-biosphere interactions. CABI Publishing, Wallingford, UK, pp. 52-53.

Myrold, D.D., 1998. Transformation of nitrogen. In: Sylvia, D.M., Fuhrmann, J.J., Hartel, P.G., Zuberer (Eds.). Principles and Applications of soil microbiology. Prentice Hall: Upper Saddle River, New Jersey, pp. 259-294.

Nyborg, M., Laidlaw, J.W., Solberg, E.D., Malhi, S.S., 1997. Denitrification and nitrous oxide emissions from a black Chernozemic soil during spring thaw in Alberta. Canadian Journal of Soil Science 77,153-160.

Olsen, K., Wellisch, M., Boileau, P., Blain, D., Ha, C., Henderson, L., Liang, C., McCarthy, J., McKibbon, S., 2003. Canada's Greenhouse Gas Inventory 1990-2001, pp. 1-4.

Pattey, E., Royds, W.G., Desjardins, R.L., Buckley, D.J., Rochette, P., 1996. Software description of a data acquisition and control system for measuring trace gas and energy fluxes by eddy-accumulation and correlation techniques. Computers and Electronics in Agriculture 15, 303-321.

Pattey, E., Edwards, G.C., Strachan, I.B., Desjardins, R.L., Kaharabata, S., Wagner-Riddle, C., 2006a. Towards standards for measuring greenhouse gas flux from agricultural fields using instrumented towers. Canadian Journal of Soil
from agricultural fields using instrumented towers. Canadian Journal of Soil Science 86, 373-400.

Pattey, E., Strachan, I.B., Desjardins, R.L., Edwards, G.C., Dow, D., MacPherson, J.I., 2006b. Application of a tunable diode laser to the measurement of CH_4 and N_2O fluxes from field to landscape scale using several micrometeorological techniques. Agriculture & Forest Meteorology 13, 222-236.

Pattey E., Edwards, G.C., Desjardins, R.L., Pennock, D., Smith W., Grant, B., MacPherson, J.I., 2007. Tools for quantifying N_2O emissions from Agroecosystems. Agriculture & Forest Meteorology 142(2-4), 103-119.

Pennock, D.J., van Kessel, C., Farrell, R.E., Sutherland, R.A., 1992. Landscape-scale variations in denitrification. Soil Science Society of America Journal 56, 770-776.

Pennock, D.J., Corre, M.D., 2001. Development and application of landform segmentation procedures. Soil & Tillage Research 58, 151-162.

Phillips, F.A, Leuning, R., Baigent, R., Kelly, K.B., Denmead, O.T. 2007. Nitrous oxide flux measurements from an intensively managed irrigated pasture using micrometeorological techniques. Agricultural & Forest Meteorology 143, 92–105.

Rao, P.S.C., Jessup, R.E., Reddy, K.R., 1984. Simulation of nitrogen dynamics in flooded soils. Soil Science 138, 54-62.

Rochette, P., Desjardins, R.L, Gregorich, E.G., Pattey, E., Lessard, R., 1992. Soil respiration in barley (Hordeum vulgare L.) and fallow fields. Canadian Journal of Soil Science 72, 591-603.

Rolston, D.E., Rao, P.S.C., Davidson, J.M., Jessup, R.E., 1984. Simulation of denitrification losses of nitrate fertilizer applied to uncropped, cropped and manure-amended field plots. Soil Science, 137, 270-279.

Ruser, R., Flessa, H., Russow, R., Schmidt, G., Buegger, F., Munch, J.C., 2006. Emission of N_2O, N_2 and CO_2 from soil fertilized with nitrate: effect of compaction, soil moisture and rewetting. Soil Biology & Biochemistry 38, 263–274.

Saxton, K.E. Rawls, W.J., 2006. Soil water characteristic estimates by texture and organic matter for hydrologic solutions. Soil Science Society of American Journal 70, 1569-1578.

Schmid, H.P., 2002. Footprint modeling for vegetation atmosphere exchange studies: a review and perspective. Agricultural and Forest Meteorology 113, 159-183.

Shields, J.A., Paul, E.A., Lowe, W.E., 1974. Factors influencing the stability of labelled microbial materials in soils. Soil Biology & Biochemistry 6, 31-37.

Smith, K.A., Thomson, P.E., Clayton, H., McTaggart, I.P., Conen, F., 1998. Effects of temperature, water content and nitrogen fertilisation on emissions of nitrous oxideby soils. Atmospheric Environment 32, 3301-3309.

Suzuki, I., Dular, U., Kwok, S.C., 1974. Ammonia or ammonium ion as substrate for oxidation by *Nitrosomonas europeae* cells and extracts. Journal of Bacteriology 120, 556-558.

Thornton, F.C., Bock, B.R., Tyler, D.D., 1996. Soil emissions of nitric oxide and nitrous oxide from injected anhydrous ammonium and urea. Journal of Environmental Quality 25, 1378-1384.

Wagner-Riddle, C., Thurtell, G.W., Kidd, G.E., Edwards, G.C., Simpson, I.J., 1996. Micrometeorological measurements of trace gas fluxes and natural ecosystems. Infrared Physics and Technology 37, 51-158.

Xu-Ri, Wang, M., Wang, Y., 2003. Using a modified DNDC model to estimate N_2O fluxes from semi-arid grassland in China. Soil Biology & Biochemistry 35, 615-620.

Yoshinari, T., Hynes, R., Knowles, R., 1977. Acetylene inhibition of nitrous oxide reduction and measurement of denitrification and nitrogen fixation in soil. Soil Biology & Biochemistry 9, 177–183.

CHAPTER 5.0: Using the *Ecosys* mathematical model to simulate topographic effects on spatial variability of nitrous oxide emissions from a fertilized agricultural soil (site: 1 < m^{-2}, fetch: ~ 5ha & field: ~ 42ha scales)

5.1 INTRODUCTION

Current Intergovernmental Panel of Climate Change (IPCC) Tier I methodology for quantifying N_2O emissions in greenhouse gas inventories, is based on a constant emission factor (EF) of 1% for all N inputs (Eggleston, 2006). An IPCC Tier II Methodology is now being used for Canada. It uses lower EFs (0.1 - 0.7%) in drier climates such as the Prairies and higher EFs (0.83 - 1.67%) for the more humid regions of Eastern Canada (Hegalson et al., 2005). However, the high spatial and temporal variability of N_2O emissions in response to changes in topography (e.g. Pennock and Corre, 2001; Pennock et al., 1992; Grant & Pattey, 2003), complicates the calculation of EFs. Coefficients of spatial variation in N_2O emissions can range from 120 to 230% (Flessa et al., 1995), when measured at spatial scales of several meters within field plots (e.g. Frolking et al., 1998: Henault et al., 1998). Temporal variability in N_2O fluxes is also large, with highly skewed frequency distributions and coefficients of variation > 150% at diurnal time scales (e.g. Flessa et al., 1995; Thornton et al. 1996). Because of the uncertainties associated with the current IPCC Tier I and II EFs (Olsen et al., 2003), more site-specific emission factors using mathematical models are needed for the development of an IPCC Tier III methodology.

N_2O emissions are highly variable spatially and temporally because of the strong physical (WFPS, oxygen (O_2), temperature), biological (soil organic matter, nitrifying and denitrifying bacteria populations) and chemical (ammonia (NH_3) and nitrate (NO_3^- concentrations) controls on N_2O production. N_2O emissions from soils are produced from

the microbiological processes nitrification and denitrification (e.g. Henault et al., 1998; Myrold, 1998). Nitrification typically is most rapid when O_2 is sufficient (water contents near field capacity, ≈ 60% WFPS), whereby NH_3 is oxidized to NO_2^- then to NO_3^- and O_2 is reduced to H_2O by nitrifying bacteria. However, under O_2-limiting conditions (e.g. after rainfall when WFPS > 60%), in a process called "nitrifier denitrification", ammonia oxidizers containing nitrite reductase may reduce NO_2^- as an alternative electron acceptor to produce NO and N_2O (Muller, 1999; Myrold, 1998). Denitrifiers can oxidize reduced C to CO_2 and reduce O_2 to H_2O under non-limiting O_2. When O_2 is insufficient (> 60% WFPS) to meet the demands of microbes, NO_3^- (e.g. from nitrification, fertilizer, residual N) becomes the alternative electron acceptor to O_2 and is reduced in a series of steps ($NO_3^- \rightarrow NO_2^- \rightarrow N_2O \rightarrow N_2$) via denitrification.

Transitions from one reduction reaction to another can be caused by small changes in soil WFPS ("threshold response"). This occurs because the diffusivity (D_g) of O_2 (and other gases) in the soil atmosphere varies according to a power function of the soil air-filled porosity (θ_g) (Millington, 1960), which in turn depends on WFPS. This variation is such that at certain WFPS, small declines in θ_g can cause large declines in D_g that may limit O_2 gaseous transfer to microsites causing a greater demand for alternative election acceptors. As a result, these small declines may cause a transition from the reduction of O_2 to that of NO_x by nitrifiers and denitrifiers, increasing N_2O production.

Transitions from one reduction reaction to another can also be caused by small changes in soil temperature. Higher temperatures can accelerate reduction of O_2 by

nitrifiers/denitrifiers thereby increasing the demand for O_2 electron acceptors at the microbial sites. As a result, microbial O_2 demand may exceed O_2 supply, resulting in the need for alternative electron acceptors (Grant and Rochette, 1994; Grant, 1995) and therefore transition to reduction of NO_2^- (nitrifiers) and NO_3^- (denitrifiers), accelerating production of N_2O. N_2O production may increase further with higher temperature because gaseous solubility of O_2 is reduced and hence aqueous O_2 ($[O_{2s}]$) maintained at microbial microsites declines. The solubility of N_2O also decreases therefore accelerating the release of previously accumulated aqueous N_2O in the soil profile. The WFPS threshold at which the transition among alternative reduction reactions occurs therefore decreases with higher temperatures (Grant and Rochette, 1994; Grant, 1995). The temperature effect on gaseous solubility and O_2 demand will cause this transition to be sharper at higher temperatures.

Studies by Grant and Pattey (2003) showed that both the temporal and spatial variability of N_2O emissions may be caused by topographically-driven flows of water and solutes (e.g. dissolved organic C (DOC), NH_3 and NO_3^-) through landscapes causing greater emissions in topographic positions in which water and solutes are gathered, than those from which they are shed. Pennock et al. (1992) demonstrated that soil moisture was the main factor affecting measured N_2O emissions and that higher soil moisture is often found at lower topographic positions of a landscape. Topography may also influence the spatial variation in soil chemical (pH, cation exchange capacity etc.) and physical properties (texture, bulk density etc.) (e.g. Rezaei and Gilkes, 2005; Osher and Buol, 1998). Penock and Frick (2001) shown that soil organic C was higher in depressions and

footslopes than in shoulder landform element complexes (topographic positions). Spatial variation in soil properties may subsequently affect microbiological processes nitrification/denitrification, thus N_2O emissions. A review by Bouwman et al. (2002) showed that organic soils used for crop production gave very high emissions compared to mineral soils. Emissions were generally larger in mineral soils with a fine soil texture, restricted drainage, and neutral to slightly acidic conditions (Bouwman et al., 2002).

The most common observation when sufficient N_2O flux measurements are made, is that most fluxes are low and only a few are high (Myrold, 1998). This results in a skewed frequency distribution that is most often described as lognormal; studies by Ball et al. (1997) showed such a pattern. This observation has been attributed to the formation of "hot spots" of activity where optimal conditions of anaerobiosis, adequate NO_3^- and available C coincide. Spatial variation in N_2O emissions can also be caused by that in soil temperature (Rover et al., 1999).

Because of the complex processes involved in N_2O emissions, there has been an increased use of mathematical models to account for site-specific effects on emission factors for national and regional inventories (e.g. Grant et al., 2006). If complex topographic effects on N_2O emissions are to be simulated, models must be able to simulate soil water and temperature as affected by surface and subsurface water movement within a topographically variable landscape (Grant, 2004). This requires the modeling of surface energy exchange and subsurface heat transfer, vertical (infiltration, drainage, root uptake and capillary rise) and lateral movement of water (driven by

differences in topographic position) and the effect of soil temperature and water on microbiological activity and gas exchange (Grant, 2004).

Ecosys (Grant, 2001a,b: website: www.ecosys.rr.ualberta.ca) is a processed - based three dimensional mathematical model which can capture the large spatial and temporal variability of N_2O emissions because it simulates the complex hypotheses of N_2O fluxes at the site scale (< 1 m^2) and also uses input data from DEMs to account for topographic effects at larger spatial (ha) scales, under site – specific past and current land use, climate and soil type. *Ecosys* ecosystem model explicitly represents oxidation-reduction reactions from which N_2O is generated, and gas transfer processes which control the transition between alternative reduction reactions. In this model, the key biological processes – mineralization, immobilization, nitrification, denitrification, root and mycorrhizal uptake controlling N_2O generation were coupled to the key physical processes – convection, diffusion, volatilization, dissolution - controlling the transport of gaseous reactants and products of these biological processes (Grant et al., 2006). Simulation of nitrificiation and denitrification in *ecosys* is sensitive to soil air-filled porosity (θ_g), which in turn depends on WFPS. Transitions from one reduction reaction to another can be caused by small changes in soil WFPS as well as temperature (non-linear response) (Grant and Rochette, 1994; Grant, 1995). However, in some current models (e.g. Lu et al., 2006), the response of N_2O emissions to changes in WFPS is linear.

Ecosys (Grant, 2001a,b) uses basic principles to simulate the vertical and lateral water redistribution within complex landscapes, and its effect on soil gas transfers (Grant and

Pattey, 2003; Grant, 2004) thus taking into account topographic effects on the spatial and temporal variability of N_2O emissions. Simulation of nitrificiation and denitrification in the model is also based on Michaelis-Menten kinetics whereas other models (e.g. Molina et al., 1983 and Clay et al., 1985) simulate denitrification based on first order kinetics with respect to soluble C or NO_3^- (e.g. Rolston et al., 1984 and Rao et al., 1984) as modified by dimensionless factors of temperature and WFPS. Some models impose constraints either on the magnitude of N_2O produced from nitrification (Li et al., 2005) or on the magnitude of N_2O emitted during snow cover (Li et al., 1992; Xu-Ri et al., 2003), even if environmental conditions favour higher emissions. However, in *ecosys*, there are no set constraints placed on N_2O production. *Ecosys* has been used to simulate temporal variability of N_2O emissions during winter and spring thaw (Grant, 1991; Grant et al., 1992; Grant et al., 1993c; Grant and Pattey, 1999) and spatial and temporal variability during early summer (Grant and Pattey, 2003; Grant et al., 2006).

In order to provide well constrained tests of N_2O emissions in *ecosys* at different spatial scales, accurate measuring techniques of N_2O are necessary. Most measurements of N_2O emissions are currently made with surface chambers over small areas (<1 m^2) (site scale). These measurements capture only small portions of spatial and temporal variability, and so are of limited value for long-term landscape estimates of N_2O emissions (Blackmer et al., 1982; Bouwman, 1996). Moreover, chambers tend to disturb the soil environment and require careful methodology (Hutchinson et al., 2000; Hutchinson and Livingston, 2001; Denmead, 1978; Rochette and McGinn, 2005) for minimizing inherent bias. The temporal variability of N_2O emissions may be better captured by micrometeorological

techniques (landscape-scale) in combination with tunable diode laser (TDL) technology (Campbell Scientific Inc., Logan, Utah) (Wagner-Riddle et al., 1996). However these techniques have low spatial resolution in the field and measure aggregated emissions from diverse topographic positions within a fetch area (Grant and Pattey, 2003). Earlier, *ecosys* was tested using either chamber data or micrometeorological data (Grant, 1991; Grant et al., 1992; Grant et al., 1993c; Grant, 1995; Grant and Pattey, 1999; Grant and Pattey, 2003; Grant et al., 2006) in different experiments. The ability of *ecosys* to simulate N_2O emissions simultaneously at both site and fetch scales with chamber and micrometeorological measurements respectively, will now be tested. Results should provide links between chamber and micrometeorological methods in order to establish a methodology to scale N_2O emissions from site to landscape.

Topographically-driven flows of water and solutes in *ecosys* are as a result of lateral water redistribution due to differences in gravitational water potential. This study aims to test **the hypotheses in *ecosys* that spatial variation in N_2O emissions can be explained in the model by (1) spatial and temporal variation in soil water-filled pore space (WFPS). The three-dimensional capability of the model allows the simulation of spatial and temporal variation of WFPS among topographic positions that shed or collect water according to topographically-driven water movement (surface Eq. [2.21]) and subsurface flow (Eqs. [21] and [24] and [A94 - A96] of Grant et al., 2004), even at a site with low topographic differences. Spatial variation in N_2O emissions can also be explained by (2) spatial variation in soil properties which may themselves be caused by topographically driven water movement.** The tested model

may then enable site-specific EFs to be developed for different land use systems on different topographies for use in an IPCC Tier III methodology.

5.2 MODEL DESCRIPTION

For full details of hypotheses of the model, refer to Grant, 2001a,b. For hypotheses specific to N_2O transformations in *ecosys*, refer to Grant and Pattey, 2003 and Grant et al., 2006. Refer to Chapter 2, Section 2.2 for equations beginning with "2."

5.3 MATERIALS & METHODS

5.3.1 Field Experiment

5.3.1.1 Site Management

The spatial variability of N_2O emissions was investigated during a field experiment from April 29th to July 31st, 2004 (same as chapter 4, section 4.3.1.1), on 30 ha of an Orthic Humic Gleysol soil located at the Canadian Food Inspection Agency Farm (0.2% slope) in Ottawa, Canada (45°18' N, 75°44'W). The annual precipitation for this area is 944 mm and annual average temperature is 6°C. Urea fertilizer was applied on May 4th at 112 kg N ha^{-1} to different topographic sections of the field (Figure 5-1) – lower (east; average elevation = 92.69 ± 21m) and higher (west; average elevation = 93.28 ± 36m) over a distance of 648m. Canola (*B. napus*) was planted at 7.2 kg ha^{-1} on May 7th, and harvested on September 1st and 2nd, 2004. Soil texture, organic C and N and inorganic N were measured through grid soil sampling (70m x 70m) across the entire field at 54 sample points (recorded using a geographic position system (GPS) (GeoXT, Trimble, Sunnyrate, California)) at depths 0 – 30cm and 30 – 60cm for each sample point.

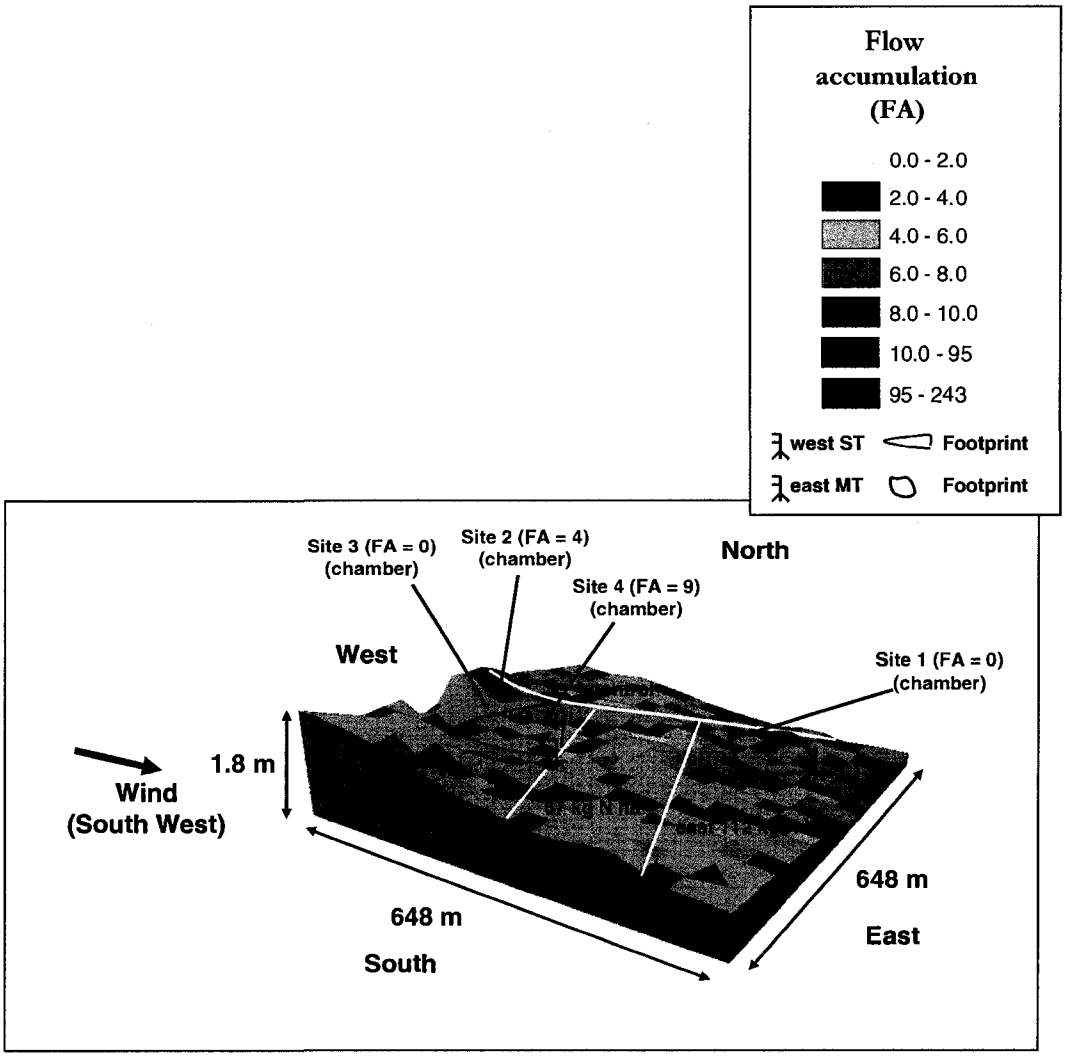

Figure 5-1: Flow accumulation map (excluding boundary grid cells) showing chamber (Site 1 (lower section) and (Sites 2,3,4) (higher section.), west ST (stationary tower) (higher fetch), MT (mobile tower) (lower fetch) and treatment locations for field site at the Greenbelt Research Farm, Ottawa 2004.

5.3.1.2 N_2O measurements

N_2O emissions for this study was examined at three different spatial scales – patch (m^2), tower fetch (ha) and field (42 ha).

5.3.1.2.1 N_2O measurements at patch (m^2) scale using surface chambers

Four sites (112 kg N ha^{-1} fertilized areas) within an east-west transect of the field, were chosen using a GPS (GeoXT, Trimble, Sunnyrate, California), to represent the general topographic features of the entire field, based on flow accumulation (FA) (Figure 6-1). Flow accumulation for a particular grid cell represents the number of grid cells that comprise its watershed. This number depends on the size of the grid cells into which the field is resolved. In this case FA was determined from 1296 m^2 grid cells selected for modeling (Section 5.3.2 below). The higher the flow accumulation number, the greater the flow of water into that particular grid cell. The FA values for each site within the 112 kg N ha^{-1} fertilized areas were:

(1) Site 1 - FA 0 (but adjacent to an area of high FA) (lower section of the field).
(2) Site 2 - FA 4 (higher section of the field).
(3) Site 3 - FA 0 (higher section of the field).
(4) Site 4 - FA 9 (higher section of the field).

Nitrous oxide flux from each of the four sites was measured using the static non-steady-state non flow-through chamber technique. At each site, four surface plexy collars (0.75 x 0.15m) were installed for N_2O sampling, by inserting them 5cm into the soil within a 2 x 3 m grid. The total chamber area was 0.11 m^2 and volume was 0.03 m^3. Chamber

sampling was done by placing a lid (0.10 x 0.75 x .015 m), with a rubber injection port and covered with aluminium foil to reflect sunlight, over each collar and then later withdrawing 24 ml samples from the headspace using a syringe after 0, 10, 20 and 30 minutes. Samples were then stored in pre-evacuated 12ml glass vials, pending analyses for N_2O using a gas chromatograph (GC) (3800 Custom, Varian Canada, Inc., Mississauga, Ontario). When measured N_2O concentrations were plotted versus time, emissions began to show non-linearity after the 20 min sample time. Fluxes were therefore calculated from a non-linear Hutchinson model (Hutchinson, 1981) with concentrations taken at times 0, 10 and 20 min.

5.3.1.2.2 N_2O measurements at fetch spatial scale using flux towers

N_2O emissions were measured at the fetch spatial scale using a stationary (ST) (west ST) tower located in the higher section of the field and using a mobile (MT) (east MT) tower located in the lower section of the field (Figure 5-1).

5.3.1.2.2.1 Stationary towers

N_2O fluxes from the higher fetch were calculated half hourly using the flux gradient technique (Pattey et al., 2006a). A closed-path tunable diode laser (TDL) (TGA-100, Campbell Scientific, Logan, Utah) was used to measure N_2O concentration differences from the west ST flux tower (Figure 5-1), at 10 Hz at two sampling heights separated by 1 m (Pattey et al., 2006b) (Results from this tower (continuous measurements) were also presented in chapter 4). Another stationary tower (east ST - not shown) was located in the lower fetch, which only captured a few N_2O measurements since the prevailing upwind

direction was south west of the field. Measurements from both lower and upper fetches of ST towers were used to derive seasonal totals. The eddy diffusivity coefficient used in the flux gradient technique was calculated from sensible heat and friction velocity (Pattey et al., 1996) measured using a 3-dimensional ultrasonic anemometer (Solent R3-HS,Gill Instruments Ltd, Lymington, Hampshire, UK).

5.3.1.2.2.2 Mobile tower

N_2O fluxes from the lower fetch were also calculated half hourly using the flux gradient technique (Pattey et al., 2006a) with the same eddy diffusivity coefficient as for the higher fetch (Section 3.1.2.2.1). N_2O concentration differences were measured using the east MT flux tower (close to Site 1) (Figure 5-1). The tower was moved according to wind direction at each sampling day, to sample the same fetch area. The tower consisted of a pole (3m) to support the upper and lower sampling tubes (1m inlet separation) connected to Teflon bags for air collection, an inlet 3-way valve, a pump (21V), a needle valve for controlling the flow, a timer and a battery. The 3m pole was raised as the crop grew, so that the lower inlet height was maintained at 2 m above the crop, giving the towers a fetch of 200 to 250 m. Prior to mobile tower sampling, Teflon sample bags (30L) were flushed with ambient air 3 times, then evacuated using a vacuum pump. Gas samples from the 2 sampling heights of the tower were then drawn into Teflon sample bags for 30 min at hourly intervals. The flow rate was set so that the Teflon sample bags were not completely full after the 30 min sampling period. Gas in the Teflon sample bags were analysed for N_2O using a TDL in a laboratory set for high resolution measurements. The structure of east MT (e.g. sampling heights) was identical to that of the west ST.

N_2O samples were taken from both mobile and stationary towers as well as from surface chambers simultaneously during several days. Surface chambers were sampled simultaneously with mobile towers on 14 days while MT was sampled on 21 days.

5.3.1.3 Soil moisture, temperature and supporting meteorological data

Dataloggers (CR500, Campbell Scientific Logan, Utah) were placed at chamber sites 1 and 2 (Figure 5-1) to continuously record soil volumetric water content (TDR CS615 water content reflectometer) and soil temperature (thermistors). For further description of datalogger and weather station set-up and precipitation, air temperature, soil water content and temperature results, refer to chapter 4.

5.3.2 Model Experiment

5.3.2.1 Model Inputs

The experimental field was represented in *ecosys* as a 20 x 20 matrix of 36m x 36m grid cells rendered in ArcGIS from a DEM of the field. Boundary conditions included surface run-off through the north, east, south and west boundaries where grid cell aspects permit, and subsurface drainage through the lower boundary of the landscape. Field topography was simulated from the slope and aspect of each grid cell, obtained in ArcGIS from the DEM. Bulk density, field capacity, wilting point and hydraulic conductivity were estimated using the Saxton (2006) pedo-transfer function calculator from measured soil properties at 54 sample points (section 5.3.1.1.). In order to determine the effect of topography alone on modeled N_2O emissions, soil properties were averaged into one soil

type, used for all 400 grid cells in the first model run (same as chapter 4, section 4.3.2.1) (Table 5-1).

Table 5-1: Properties of Orthic Humic Gleysol used in model runs

Depth (m)	Surface – 0.10	0.10 – 0.20	0.20 – 0.30	0.30- 0.60	0.60 – 0.90
*D_b, Mg m^{-3}	1.24 (1.16 – 1.4)	1.31 (1.23 - 1.47)	1.5	1.5	1.5
*θ_{FC}, m^3 m^{-3}	0.31 (0.29 – 0.34)	0.32 (0.13 – 0.23)	0.32	0.32	0.32
*θ_{WP}, m^3 m^{-3}	0.16 (0.15 – 0.17)	0.17 (0.14 – 0.24)	0.17	0.17	0.17
*Ks_{at}, mm h^{-1}	20 (11 – 33)	20 (11-33)	15	5	5
§Sand, g kg^{-1}	364 (123 – 519)	364 (123 – 519)	364 (123– 519)	491 (116 – 626)	491 (116 – 626)
§Silt, g kg^{-1}	431 (213 – 644)	431 (213 – 644)	431 (213 – 644)	331 (214 – 742)	331 (214 – 742)
§Clay, g kg^{-1}	205 (14 – 39)	205 (14 – 39)	205 (14 – 39)	178 (14 – 46)	178 (214 – 742)
γpH	7	7	7	7	7
γCEC, cmol kg^{-1}	16.8	16.8	16.8	17.5	17.5
§Org. C, g kg^{-1}	26 (4 – 31)	26 (4 – 31)	26 (4 – 31)	18 (2 – 23)	18 (2 – 23)
§Org. N, g Mg^{-1}	2210 (560 – 2500)	2210 (560 – 2500)	2210 (560 – 2500)	1430 (260 – 2280)	1430 (260 – 2280)

***Derived from Saxton (2006) pedo-transfer function calculator (data measured from grid soil sampling were used as input values). Abbreviations: D_b – bulk density, θ_{FC} – water content at -0.033 Mpa; θ_{WP} – water content at -1.5 Mpa; K_{sat} – saturated hydraulic conductivity.**

§Measured values from grid soil sampling.

γMeasured values from a few sampling points.

Numbers not in brackets indicate spatially – averaged soil properties used in the first model run and numbers within brackets indicate the full range of values used in 54 soil profile model run.

To determine the additional effect of variation in soil properties across the field on N_2O emissions, a second model run was also conducted. For this run, the 54 different soil profiles (Table 5-1 indicates range of values) derived from the grid soil sampling and Saxton (2006) pedo-transfer function calculator, were allocated to the 400 grid cells in the field based on proximity of each soil profile to each grid cell.

For both runs, a 3-year model spin-up was used to represent the agricultural history of the site in 2001 and 2002 (corn fertilized at 155 kg N ha^{-1}) and in 2003 (spring wheat fertilized at 78 kg N ha^{-1}) prior to the experiment in 2004. Management practices for 2004 were applied as in the field experiments (Section 5.3.1.1). All biological transformations were solved on an hourly time step (Eqs. [2.1-2.20]); water fluxes (Eqs. [2.21-2.26]) were calculated 25 times per time step and gas fluxes (Eqs. [2.27-2.28]) were calculated 500 times per time step, assuming constant surface boundary conditions during each hour. No adjustments of parameters were made to fit the model to the field site. All model parameters remained unchanged from earlier studies (e.g. Grant and Pattey, 2003; Grant et al., 2006).

5.3.2.1 Model Testing

Modeled results were examined at 3 spatial scales - Patch scale (m^2) for comparison with chambers, fetch scale (ha) for comparison with towers and field scale (42 ha).

5.3.2.1.1 Patch (m^2) scale

Measured soil moisture and temperature at Sites 1 and 2 were compared to modeled results from the grid cells in which these sites were located. Measured chamber N_2O fluxes at all 4 sites (Section 5.3.1.2.1) were compared to the modeled N_2O emissions from the grid cells in which these sites were located, using regression analysis. For each chamber site, the average and standard deviation of emissions from the 4 replicates were calculated for each measurement date.

5.3.2.1.2 Fetch (ha) scale

N_2O emissions from grid cells within the footprint of each tower (Figure 5-1) were averaged for comparison to flux tower measurements (Section 5.3.1.2.2.) according to a footprint model (Schmid, 2002). Measured emissions for the east and west 112 kg N ha^{-1} fertilizer treatments were separated according to the wind direction measured at the field site (Figure 5-1).The correlation between modeled and measured N_2O emissions was then evaluated using regression analysis.

5.3.2.1.3 Field (42 ha) scale

Boundary grid cells were removed from 20 x 20 grid output of modeled N_2O and WFPS, and remaining cells were plotted in ArcGIS in order to examine the spatial variability over the entire field for both model runs with and without soil variability.

5.4 RESULTS

5.4.1 Patch (m^2) scale spatial variability of soil water content, temperature and N_2O emissions (chamber) (assumed uniform soil)

5.4.1.1 Soil water content and temperature at patch (m^2) scale

A series of rainfall events in May e.g. DOY 145 and 153 (Figure 4-2a of chapter 4) led to increases in measured and modeled WFPS (Figure 4-2b of chapter 4). In *ecosys*, these events caused infiltration as well as topographically-driven surface flow (Eq. [21]) and subsurface flow (Eq. [24]; Eqs. [A94 - A96] of Grant et al., 2004) amongst the 400 interconnected grid cells. Measured results showed that Site 2 generally had higher WFPS than Site 1, however, modeled results showed little or no spatial variability. This probably occurred because only one soil file representative of field was used for the model run (Table 4-1) whereas some spatial variation was apparent in the field samples. However, the use of several soil files representing spatial variation in soil texture, field capacity etc., for the second model run also did not show as much spatial variation in WFPS (data not shown) as did the measured data.

There were little or no differences in measured and modeled soil temperature between Sites 1 and 2 (Figure 2c of chapter 4)

5.4.1.2 Spatial variability of N_2O emissions at patch (m^2) scale

5.4.1.2.1 N_2O emissions from single grid cells at different topographic positions

Physical and biological properties during N_2O emissions on DOY during DOY 145 - 153 are explained in detail in chapter 2. Following application on May 4th (DOY 125), urea was hydrolyzed in *ecosys* to produce [NH_{3s}]. The presence of large NH_{3s} in *ecosys* provided substrates for N_2O production via nitrification (Eq. [10]) and denitrification (Eq. [18]).

Rainfall events e.g. during DOY 145 - 153 (Figure 4-2a of chapter 4) led to increases in WFPS (Figure 4-2b of chapter 4), and declines in air-filled porosity θ_g, which caused declines in gas diffusivity D_g (Eq. [28]). These declines in turn reduced surface O_2 gas exchange and soil transport (Eq. [27]) lowering gaseous O_2 ([O_{2g}]) in the soil profile and slowing dissolution of O_{2g} to [O_{2s}] (Eq. [A30] in Grant et al., 2006; Figure 5-2a). Higher soil temperatures during soil warming on DOY 148 - 157 (Figure 4-2c of chapter 2) slowed dissolution of O_{2g} to [O_{2s}] (Eq. [A30] in Grant et al., 2006; Figure 5-2a) further and also led to an increase in microbial activity and therefore a higher demand for O_2 (Eqs. [2], [3a,b], [13] and [14a,b]), resulting in an overall decline in [O_{2s}]. Consequently, nitrifier demand for electron acceptors unmet by O_2 was transferred to NO_2^- ($R'_{NO2i,n}$ in Eq. [9]), which was then reduced to N_2O ($R_{NO2i,d}$ in Eq. [10] leading to rises in [N_2O_s] (Figure 5-2b). In the case of denitrifiers, lower [O_{2s}] (Eqs. [14a,b]) raised the demand for alternative electron acceptors (Eq. [13]) that was first transferred to NO_3^-, which was reduced to NO_2^- ($R_{NO3i,d}$ in Eq. [17]). Any remaining demand was transferred to NO_2^-, which was reduced to N_2O ($R_{NO2i,d}$ in Eq. [18]), and any remaining demand thereafter

was transferred to N_2O, which was reduced to N_2 ($R_{N2Oi,d}$ in Eq. [19]). These transitions among alternative reduction reactions caused high modeled [N_2O_s] to coincide with low modeled [O_{2s}] in the 0-10cm soil layer at each of the grid cells in which the chamber sites were located during rainfall events between DOY 138 – 156 (Figure 5-2). Because soil properties were assumed uniform in this model run, variation in gas concentration was attributed to differences in topography. Most modeled and measured emissions events from chambers (0.1 – 0.5 mg N_2O-N m^{-2} h^{-1}) occurred during this period (Figure 5-3), due to a combination of fertilizer application, rainfall and soil warming. Except for Site 2, the modeled emissions were able to capture the main measured emission events for this period in a way that was consistent with the measured data and similar RMSD and RMSE (Table 5-2).

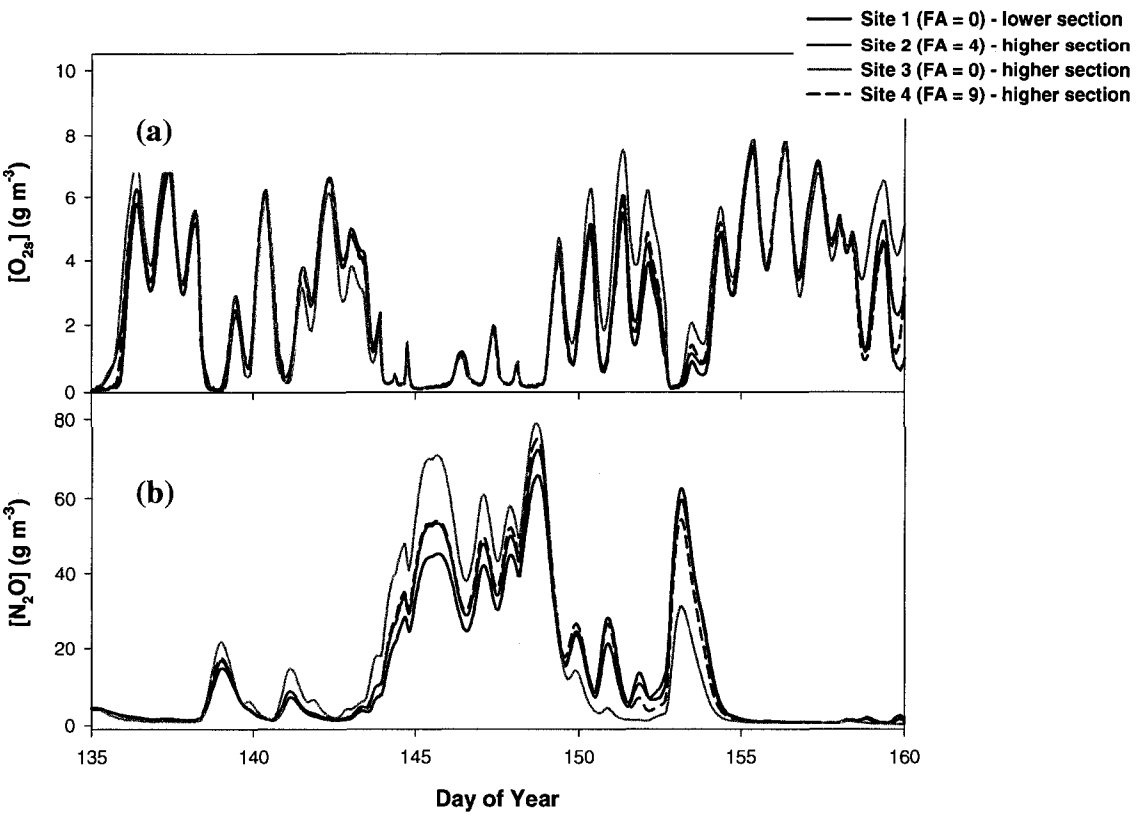

Figure 5-2 Modeled aqueous (a) O_2 ($[O_{2s}]$) and (b) N_2O ($[N_2O_s]$) concentrations in 0-10cm layer (Refer to Figure 1 for chamber sites location in field) from a uniform soil.

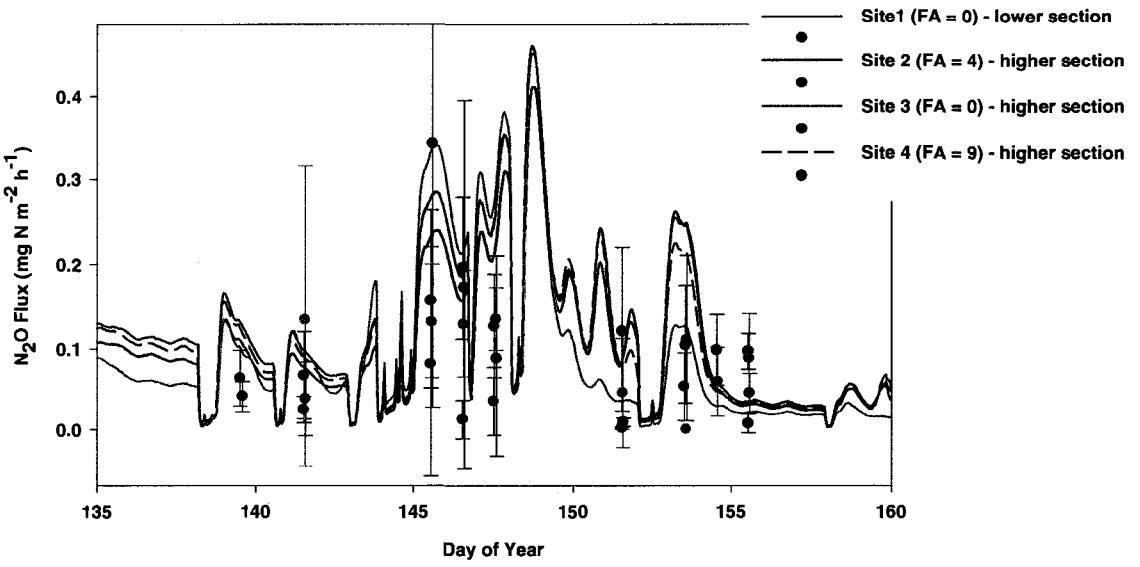

Figure 5-3: N_2O emissions from chambers modeled from a uniform soil (lines) and measured (symbols: mean (± standard deviation (n = 4)) at Ottawa during 2004 (Refer to Figure 5-1 for chamber sites location in field).

Table 5-2: Statistics for regression (measured vs. modeled data – log-transformed) and analysis of variance (ANOVA) of N_2O emissions measured from chambers, during emission events

(a) Regression	R^2 (measured vs. modeled data)	*P* (95% confidence level)	$^{\delta}n$	Modeled versus measured variation: Root mean square for difference (RMSD)
Site 1	0.74	0.01	8	0.31
Site 2	0.25	0.20	8	0.25
Site 3	0.54	0.06	7	0.17
Site 4	0.59	0.07	6	0.38
(b) ANOVA	Mean ($\mu g\ N_2O\text{-}N\ m^{-2}\ h^{-1}$)		$^{\S}n$	Root mean square for error (RMSE)
Site 1	54	0.28	21	0.43
Site 2	108	0.28	32	0.40
Site 3	102	0.28	27	0.42
Site 4	138	0.28	22	0.50

$^{\delta}$Is the number of measurement dates.

§Is the number of samples.

Even though there was rainfall later in the crop season e.g. on DOY 173 (Figure 4-2a of chapter 4), thus increase in WFPS (Figure 4-2b of chapter 4), emissions were low (no significant emissions were neither measured nor modeled after DOY 156). This was due to a decline in available NH_4^+ (Figure 4-2d) from plant uptake and consequent slowing of NH_3 oxidation ($X_{NH3i,n}$ in [4]), thus the rate of NO_2^- reduction ($R_{NO2i,n}$, in [10]) also declined, leading to a reduction in N_2O generation (Eqs. [19] and [10]). The reduction in N_2O emissions later in the season was also attributed to the decline in WFPS (Figure 4-2b of chapter 4) caused by rising evapotranspiration in response to canola growth (Eqs. [A.1], [A3], [A4], [18], [24], [25] and [A27] of Grant, 2001a).

5.4.1.2.2 Spatial variability of N_2O emissions from individual chambers in a 3 x 2m grid within a topographic position

Some of the inconsistencies between measured and modeled chamber emissions (Figure 5-3) may be due to high measured CVs amongst chamber replicates during emission events (28 to 195 %) over a 3 x 2m area. High CVs amongst chambers readings as well as infrequent chamber measurements, lowered the constraint in model testing. Due to the large CV amongst measured chamber replicates, there were no significant ($P > 0.05$) (Table 5-2) difference in hourly emissions amongst the different chamber sites.

5.4.1.2.3 Spatial variability of average N_2O emissions from replicated chambers at different topographic positions > 100m apart

Modeled [N_2O_s] (Figure 5-2b) and thus emissions (Figure 5-3) at Site 3 (FA = 0) were higher than those at the other Sites (FA > 0, except for Site 1) during the early stages of the N_2O emission event from DOY 146-148. However this site gave the lowest [N_2O_s] and thus emissions for the later part of the emission event (DOY 149.5 - 153). Upon soil warming and drainage from previous rainfall, lower FA for Site 3 caused θ_g to increase earlier so that gaseous pathways through the soil (Eq. [A30] –[A36] in Grant et. al., 2006) were restored earlier, raising [O_{2s}] earlier (Figure 2a) at this Site. Also, higher FA at Sites 2 and 4 caused lower θ_g during early stages of the emission event that suppressed N_2O volatilization, causing later but more sustained increases in N_2O later in the emission event. Consequently, ([N_2O_s]) (Figure 2b) and thus emissions (Figure 5-3) for Site 3 with lower FA peaked and declined earlier than did those at the other Sites with higher FA where progress through the emission event was slower (increased spatial variability).

Spatial variation (Table 5-3) can be seen at a seasonal time scale, although the magnitude may be smaller than that at an hourly time scale because much of the latter is caused by different rates of progress through similar emission events (Figure 5-3; section 5.4.1.2.3). Site 1 also gave the highest N_2O emissions even though FA was zero. This may be because it was adjacent to grid cells with high FA (FA = 91) and also because it was in the lower section of the field (Figure 5-1). Site 4 had the highest FA and gave the second highest modeled seasonal total N_2O emissions. However, there was a poor correlation with FA and measured seasonal total N_2O emissions (calculated from linear interpolation). These results show that N_2O emissions and thus EF may vary with small topographic differences (0.2% maximum slope) in a field, for the same fertilizer treatment, although the degree to which this variation can be corroborated by measurements is limited. Overall, measured variation (root mean square for error (RMSE)) was larger that the variation between modeled versus measured (root mean square for difference (RMSD)) results.

Table 5-3: Seasonal N_2O emissions for the period May 19th – July 9th (DOY 140 – 191) for each chamber site

Chamber site	Field section	Elevation (m)	Flow Accumulation (FA)	Modeled N_2O	Measured N_2O
				mg N m^{-2}	
Site 1	lower	92.67	0	61.4	41.8
Site 2	higher	93.27	4	55.0	74.3
Site 3	higher	93.34	0	51.0	72.1
Site 4	higher	93.02	9	58.8	60.9

5.4.2 Spatial variability of N_2O emissions at fetch (ha) (tower) seasonal time scale

The west ST (Figure 5-1) measured N_2O concentration differences from the higher fetch, when the upwind direction was south west of the field (Figure 5-1). In contrast, the east MT tower measured N_2O concentration differences from the lower fetch with any wind direction (tower position was changed to face into the prevailing wind direction with ~300m upwind fetch over the lower topographic section of the field). Modeled (Figure 5-4) emissions from the higher fetch were higher than those of the lower fetch during the early part of the emission event from DOY 146-149. However, during the later part of the emission event after DOY 151, the reverse trend was observed. This trend was attributed to the lower topographic positions located at the east fetch of the field. However, average FA was slightly larger at the higher (FA = 7.4±11.9) versus lower (FA = 5.5±11.2) fetch (Table 5-4). Measured results were similar to that of modeled whereby emissions were higher for the west ST than those of the east MT on DOY 147 and the opposite was seen on DOY 154 (at a smaller magnitude). However, because of lack of continuous measured data for the different topographic positions, it was difficult to fully compare the spatial variability of these emissions throughout the season. Modeled and measured N_2O emissions showed significant ($P < 0.05$) correlations (R^2: 0.38 (east MT) and 0.24 (west ST)). Modeled seasonal N_2O emissions were similar to that estimated from the lower and higher fetches (Table 5-4).

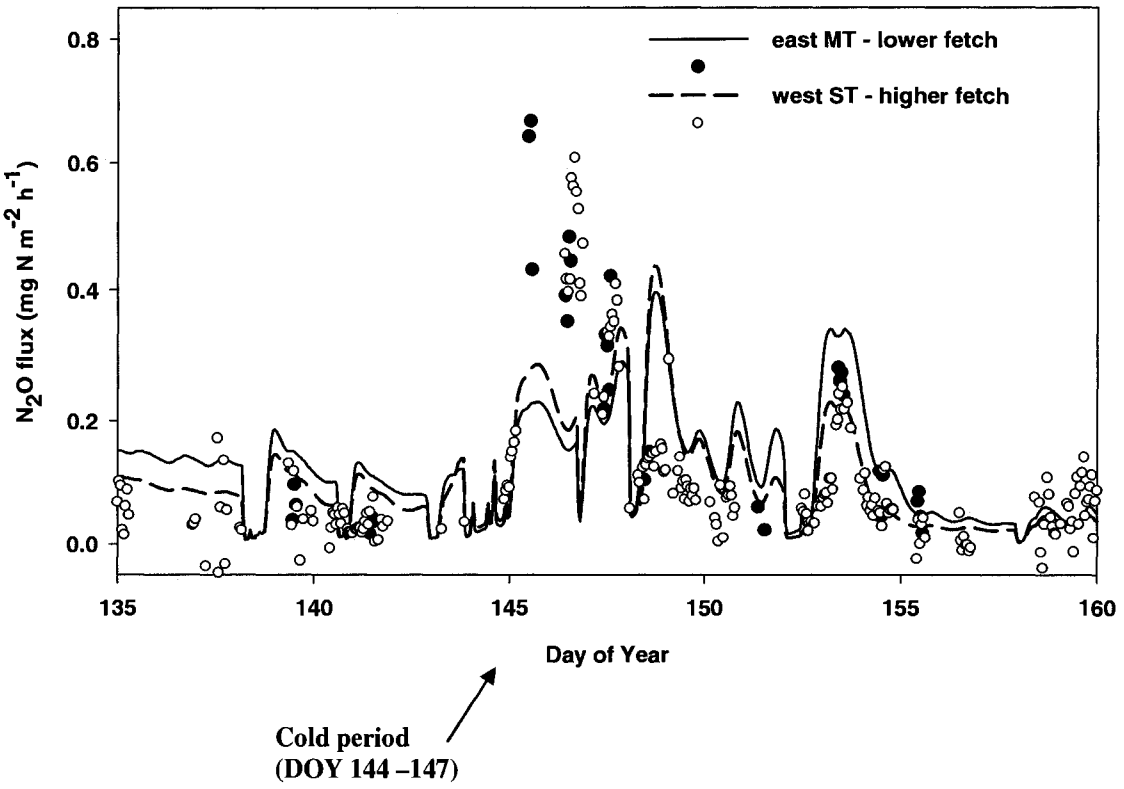

Figure 5-4: N_2O emissions from ST (stationary tower), mobile tower (MT), modeled from a uniform soil (lines) and measured (symbols) at Ottawa during 2004.

Table 5-4: Modeled seasonal N_2O emissions for the period May 9th – July 12th for stationary tower (ST) fetches. Modeled values = average ± standard deviation for all grid cells within the tower fetch (Figure 5-8).

Fertilizer Treatment (kg N ha^{-1})	112 (lower + higher)	112 (higher)	112 (lower)
Average Flow Accumulation (FA)	6.5 ± 11.5	7.4 ± 11.9	5.5 ± 11.2
Average elevation (m)	92.95± 0.24	92.73± 0.10	93.16 ± 0.12
Modeled (mg N m^{-2})	81.0 ± 12.5	80.6 ± 11.1	85.9 ± 13.6
Measured (mg N m^{-2})	87	*NA	*NA

***NA – Data not available**
(ST data Metivier et al., submitted).

5.4.3 Spatial variability of WFPS and N_2O emissions modeled at field scale (42 ha) for different time periods

5.4.3.1 Modeled spatial variability of WFPS at field scale (42 ha) over one day

Rainfall on DOY 153 (Figure 4-2a of chapter 4) caused WFPS to rise to 60 – 62% on DOY 154 (Figure 4-2b of chapter 4), during which an N_2O emission event was measured and modeled (Figures 5-3 and 5-4). WFPS (Figure 5-5) varied across the landscape because of surface (Eq. [21] and sub-surface (Eq. [24]) water flow, however, variation was small. This variation was caused by very small differences in topography, whereby grid cells both shed and received water at different areas of the field, as indicated by FA (Figure 5-1).

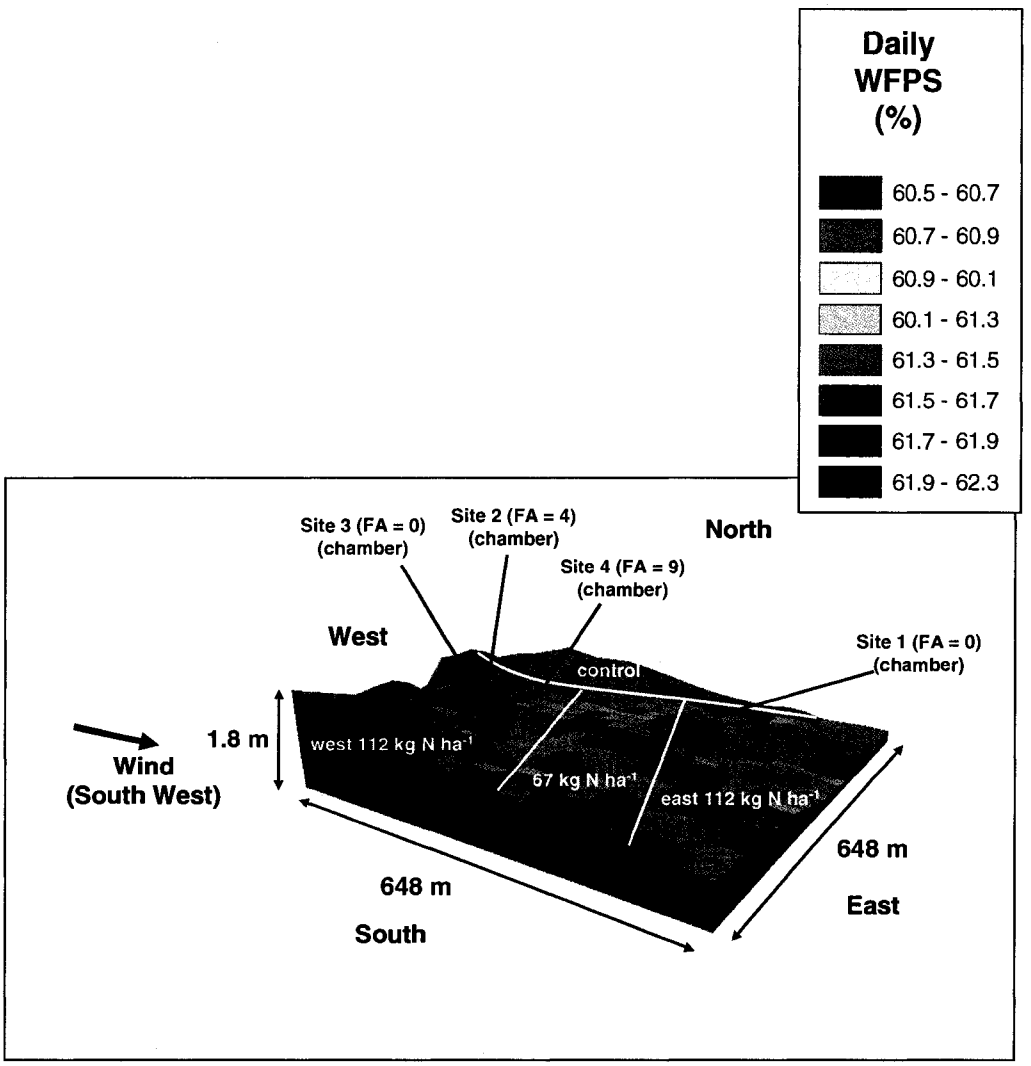

Figure 5-5: Modeled spatial variability of WFPS (0-10 cm) over field on DOY 154 from a uniform soil.

5.4.3.2 Modeled spatial variability of N_2O emissions at field scale (42 ha) over one day

Our findings have indicated that modeled spatial variation of N_2O emissions at the field scale (Figures 5-6, 5-7 and 5-8; Table 5-6) in *ecosys* (Grant 2001a,b) was due to small differences in topography (~1.8m over 600m), in a way that was consistent with the measured data (Table 5-2). Even with the small spatial variability of WFPS (CV = 0.45%) (Figure 5-5), there was large variation in N_2O emissions across the field (CV = 54%) (Figure 5-6) even with an assumed uniform soil due to spatial variation of FA (Figure 5-1; Table 5-3). For example Site 4 had higher FA and WFPS than Site 3 (Figures 5-1 and 5-5) therefore, Site 4 gave higher emissions than Site 3 (Figure 5-6; Table 5-3). Also, the lowest areas (north east of the field) had the highest WFPS and FA and thus gave the highest emissions.

Variation on DOY 154 (Figure 5-6; Table 5-5) was apparent throughout the emission period (Table 5-6). This variation was raised by introducing variation in soil properties (Table 5-6). This trend occurred due to the spatial variation in soil properties (model run with 54 soil profiles), which consequently raised that in N_2O emissions modeled. The CSV for both model runs varied throughout the season due to the temporal variability of N_2O at the site scale. Correlations of (1) FA versus soil properties (e.g. organic C and clay) and (2) soil properties versus N_2O emissions were all small ($R^2 < 0$). The correlation of FA versus N_2O emissions was also small ($R^2 = 0.1$), but significant ($P < 0.05$).

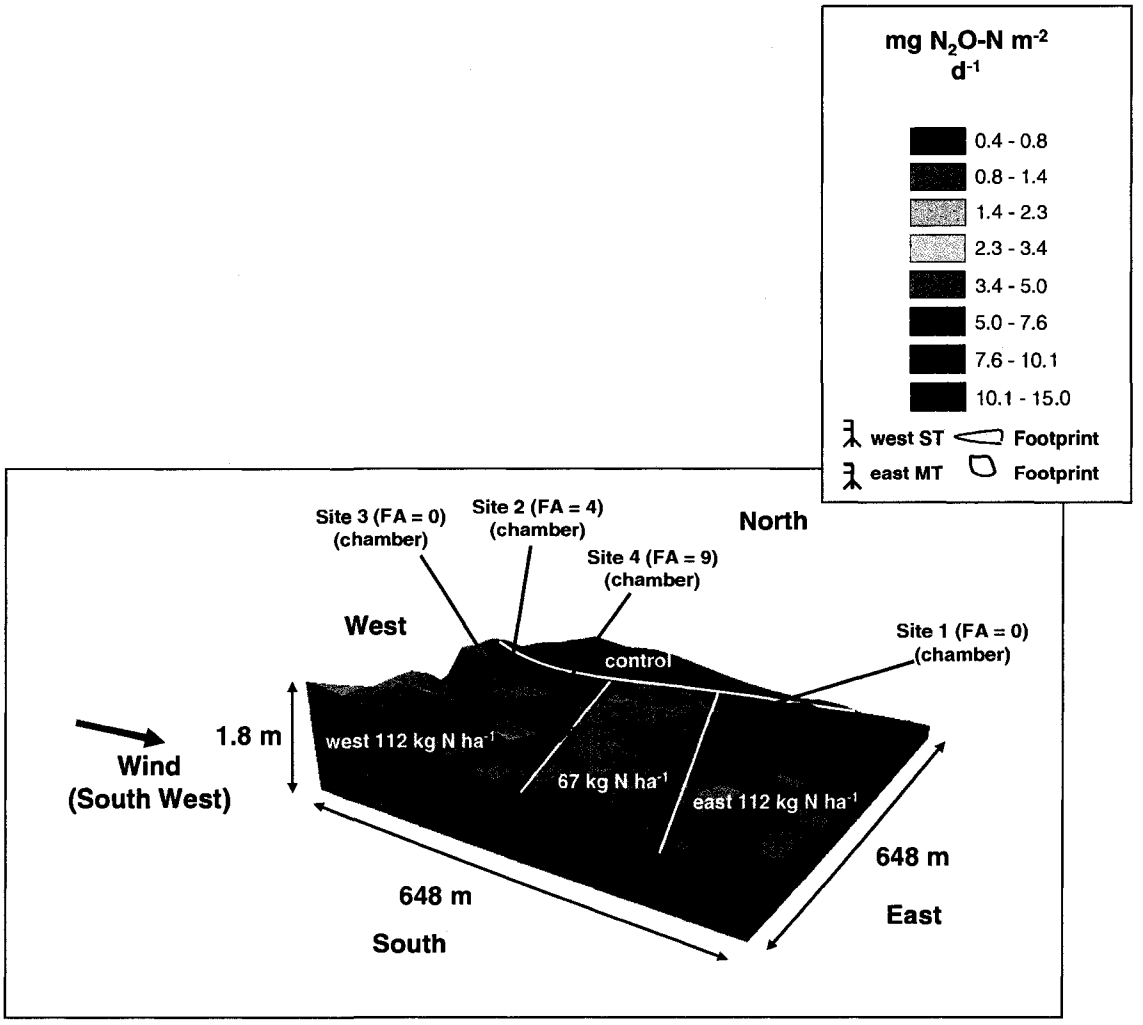

Figure 5-6: Modeled spatial variability of daily N_2O emissions over field during DOY 154 from an assumed uniform soil.

NB: Measured Total (west ST (stationary tower)): 4.53 mg N_2O-N m^{-2} d^{-1} (see Figure 5-4)

Table 5-5: Modeled and measured dailyN_2O emissions for DOY 154 for stationary towers (ST) fetches. Modeled values = average ± standard deviation for all grid cells within the tower fetch (Figure 5-6).

Fertilizer Treatment (kg N ha^{-1})	112 (lower + higher)	112 (higher)	112 (lower)
Modeled (mg N m^{-2} d^{-1})	5.6 ± 2.6	5.1 ± 2.4	6.2 ± 2.8
Measured (mg N m^{-2} d^{-1})	4.53	*NA	*NA

***NA – Data not available**

Table 5-6: Modeled coefficient of spatial variation (CSV) of grid cells within 112 kg Nha^{-1} treatment for May 26th – June 3rd (DOY 146 – 154) and annual N_2O totals.

Model run	CSV (%) for DOY 146 - 154									CSV (%) for annual N_2O totals
	146	147	148	149	150	151	152	153	154	
1 soil profile	18	16	14	11	17	38	57	65	54	25
54 soil profile	43	59	62	63	52	68	62	49	62	101

5.4.3.3 Modeled spatial variability of N_2O emissions at the field scale (42 ha) over an entire emission event

Spatial variability in N_2O emissions differed during different times of the day as a result of temporal variability in soil water content and temperature (Figure 5-7). For example, a CSV of 79% was modeled on DOY 153 at 5:00pm (Figure 5-7a) versus one of 50% on DOY 154 at 5:00am (Figure 5-7b). Changing variability in N_2O emissions may be attributed in part to that in WFPS, over the landscape (Figures 5-5) and temperature (DOY 154 - CSV = 0.53% (maximum temperature) and 0.14% (minimum temperature)). This diurnal variation was also apparent in N_2O emissions from the high (west ST) and low (east MT) fetches (Figure 5-4).

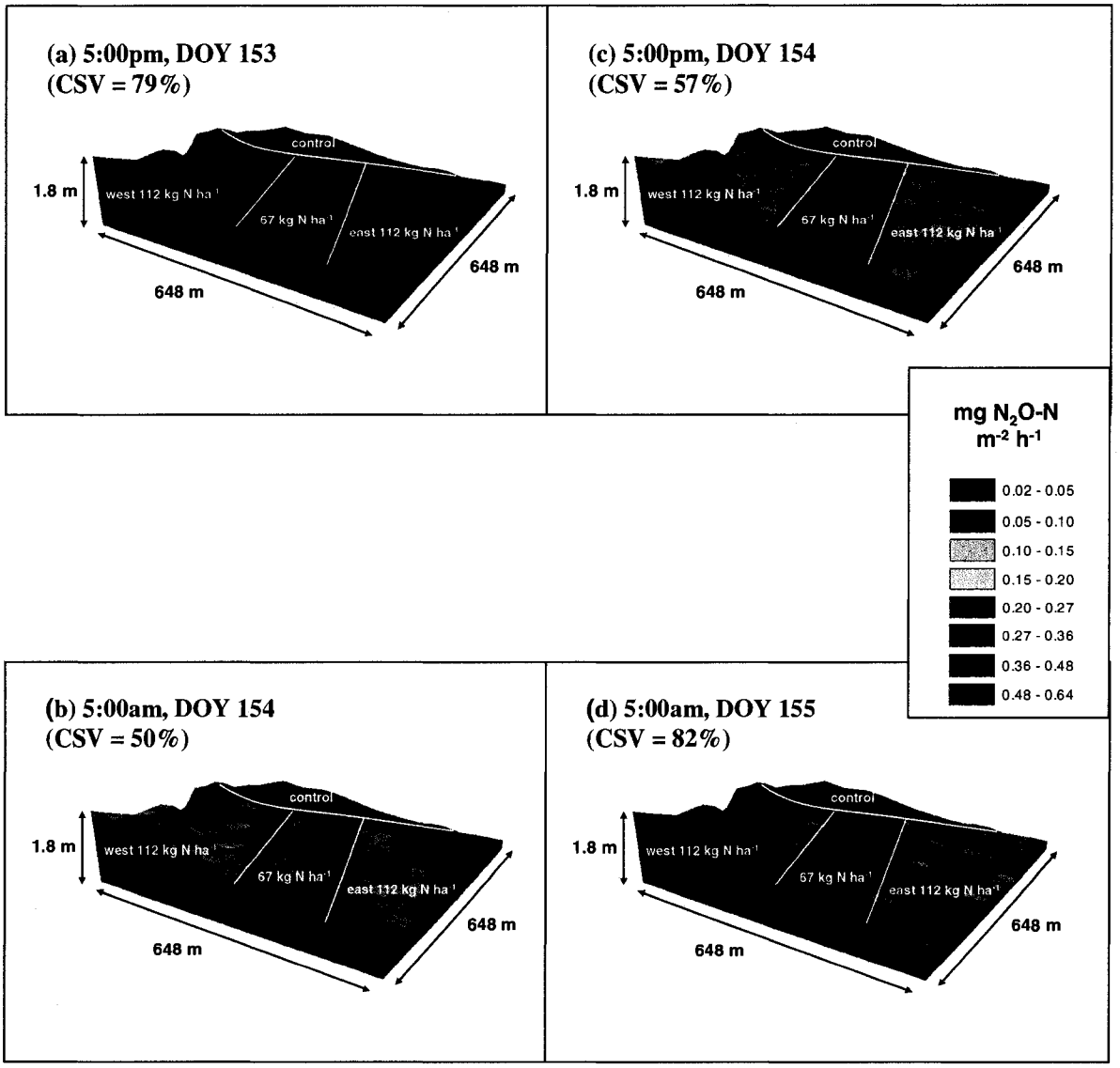

Figure 5-7: Modeled spatial and temporal variability of N_2O emissions during emission event on DOY 153 – 155 from an assumed uniform soil.

NB: These times were chosen in an attempt to cover minimum and maximum emissions during the emission event.

5.4.3.4 Modeled spatial variability of N_2O emissions at field scale (42 ha) over the season and year

The lowest topographic position of the field gave the highest seasonal total emissions and so were 'hot spots' for N_2O (indicated in Figure 5-8 by black arrow) since this area had high FA values (Figure 5-1). The EF (Table 5-7) was larger for the 112 kg N ha^{-1} lower fertilizer treatment compared to that of the 112 kg N ha^{-1} higher, because the lower section of the field had lower topography and thus higher range of FA values (Figure 5-1; Table 5-7) and therefore had more 'hot spots' for N_2O emissions (Figure 5-8). Overall, CSV of annual N_2O totals (Table 5-6) was higher for the second (101%) model run (variation attributed to both topography and soil properties) than that of the first (25%) model run (variation attributed to topography alone).

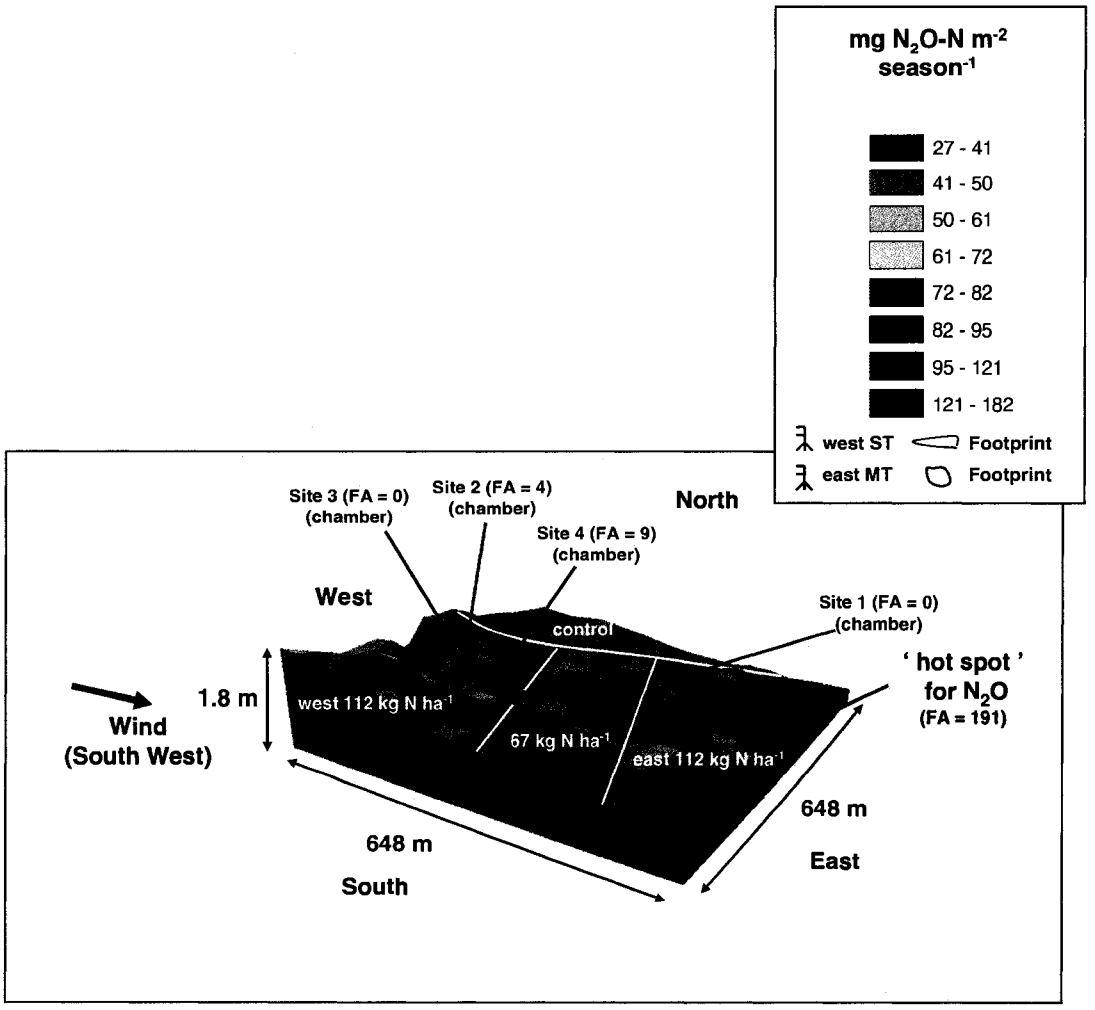

Figure 5-8: Modeled spatial variability of seasonal (DOY 128 – 194) totals of N_2O over field (Refer to Table 5-4 for modeled and measured fluxes for different treatments) from an assumed uniform soil.

NB: ST (stationary tower), MT (mobile tower)

Table 5-7: Modeled *annual emission factors at field scale

Fertilizer Treatment (kg N ha^{-1})	112 (higher)	112 (lower)
Average elevation (m)	92.69 ± 0.21	93.28 ± 0.36
Average Flow Accumulation (FA)	5 ± 11	24 ± 52
Modeled (mg N m^{-2})	0.1	0.3

***Annual emission factors calculated as ratio of increase in N_2O emissions attributed to increase in fertilizer application**

5.5 DISCUSSION

Generally, low EFs for 2004 for this study compared to those for Eastern Canada (0.83 - 1.67%) used in the IPCC Tier II Methodology (Hegalson et al., 2005), could be attributed to slightly overall lower average mean temperatures (March: 0°C, April: 5.5°C, May: 12.8°C and June: 17.1°C) compared to long-term normals for 1971 – 2000 (March: -2.5°C, April: 5.7°C, May: 13.4°C and June: 18.3°C) for the experimental area. In combination with early fertilization delayed soil warming caused fertilizer – induced nitrification to occur in comparatively cool soils. Earlier modeling studies showed that delayed fertilization by just one week caused an increase in N_2O emissions from 0.31% to 1.65% (chapter 4). Early fertilization may therefore reduce emissions since nitrification of fertilizer N can occur in cooler soils (chapter 4).

Results from this study showed that *ecosys* (Grant, 2001a,b) represented the spatial variation of N_2O emissions at the meter, fetch and field scales. High measured CSVs amongst chamber replicates over a 2 x 3m area (28 to 195 %) (Figure 5-3) indicate that spatial variation of N_2O emissions occurs at a meter spatial scale. This may be due to the heterogeneous nature of soil at very small spatial scales. Sextone et al. (1985) showed that anaerobic zones were detected in the centres of saturated soil aggregates whereas outside of the aggregate was fully aerated. Folorunso and Rolston (1984) reported that differences in measured N_2O fluxes may range from 282 to 379% at chamber locations only 1 to 2 m apart. Mathieu et al. (2006) showed that the CSV of measured N_2O emissions of 36 sampling points arranged in 3m x 3m grids was 71% (mean emissions was 645 g N ha^{-1} d^{-1} while a "hot spot" measured was 2525 g N ha^{-1} d^{-1}). Choudhary et al.

(2002) found CSV as high as 127% was measured amongst 12 chamber replicates (3 replicates per 17m x 3.6m plots). These results show that N_2O emissions associated with chamber measurement may vary amongst replicates located a few meters away. Some of the inconsistencies between measured and modeled chamber emissions may be due to high measured CSVs amongst chamber replicates. As a result, replicate variation (root mean square for error (RMSE)) was larger that the variation between modeled versus measured (root mean square for difference (RMSD)) results. Therefore the model hypothesis (Section 5.1) cannot be rejected. More research is needed to resolve unexplained chamber replicate spatial variation at the meter scale.

Our findings have indicated that modeled spatial variation of N_2O emissions at the field scale (Figures 5-6, 5-7 and 5-8; Table 5-6) in *ecosys* (Grant, 2001a,b) was due to small differences in topography (~1.8m over 600m), in a way that was consistent with the measured data (Table 5-2). The consistency of modeled and measured results **supports the hypothesis in *ecosys* (Grant, 2001a,b) outlined in the Introduction (section 5.1), that spatial variation in N_2O emissions, can be explained in the model by (1) spatial (Figure 5-5) and temporal variation (Figure 4-2b) in soil WFPS. The three-dimensional capability of the model allows the simulation of spatial and temporal variation of WFPS among topographic positions that shed or collect water (Figure 5-1) according to topographically-driven water movement (surface Eq. [2.21]) and subsurface flow (Eqs. [21] and [24] and [A94 - A96] of Grant et al., 2004), even at a site with low topographic differences. Spatial variation in N_2O emissions can also be explained by (2) spatial variation in soil properties (spatial variation in soil properties caused CSV of annual fluxes to increase from 25 % to 101%), which may**

themselves be caused by topographically driven water movement. High CSV of N_2O fluxes at a larger spatial scale (Figure 5-6), during emission events within the same fertilizer treatment (112 kg N ha^{-1}) was partly attributed in the model to spatial variation of WFPS (Figure 5-5), caused by different flow accumulation (FA) (Figure 5-1) within the field due to small differences in topography. Studies by Rover et. al. (1999) measured CSV > 150 %, due to a few areas of the field with extremely high N_2O emission rates or 'hot spots'. These results indicate that variations in both soil properties and in topography contributed towards the high CSV of N_2O emissions in the model. Also, soil properties themselves may be affected by topography. Flessa et al. (1995) showed that emissions were higher in a clay versus sandy soil (extensively managed field) and a loamy colluvial soil gave higher emissions than a silty soil (extensively managed field). Correlations of (1) FA versus soil properties (e.g. organic C and clay) and (2) soil properties versus N_2O emissions were all small ($R^2 < 0.1$) due to the complex biological, chemical and physical hypotheses involved N_2O generation. Such complex hypotheses limit the extent to which simple correlations can be used to predict N_2O emissions, hence the importance of processed-based model *ecosys*, for simulating N_2O production. More field measurements of soil properties e.g. field capacity, wilting point etc. may improve confidence in the values used as model inputs, thus simulations of N_2O emissions.

Modeled results within the two fertilized (112 kg N ha^{-1}) areas (Figure 5-1) generally showed that the lowest topographic positions of the field gave the highest seasonal N_2O emissions or were 'hot spots' for N_2O emissions since these areas had high FA (FA versus N_2O: $R^2 = 0.1$, $P < 0.05$) values. Consequently, annual EF modeled for the 112 kg

N ha^{-1} fertilizer application was larger in an area of the field with lower topography (0.3%) than that from higher (0.1%) (Table 5-7). This result extends earlier modeling studies (Grant and Pattey, 2003) that showed modeled emissions being highest at depressional topographic positions compared to the upper and mid positions, in a fairly flat field (0.5m maximum elevational differences). Similar to our results, Florinsky et al. (2004) showed that flow accumulation was largest at the lower topographic positions of a landscape, based on a digital elevation modeling in their study. They also found that soil moisture was increased from upper to lower topographic positions thus denitrification rate and amount of denitrification enzyme also followed a similar trend (Florinsky et al., 2004). However, they did not find any relationship between N_2O emissions and topographic position (Florinsky et al., 2004). Other studies (e.g. Ball et. al., 1997; Flessa et. al., 1995) have also shown that N_2O emissions can vary even in seemingly uniform landscapes. Pennock and Corre (2001) used landform segmentation procedures to classify landform elements into landform element complexes (LEC) from DEMs (Penock et al., 1987; Penock et al., 1994), and found that measured N_2O emissions were significantly higher at level depressions than at foot slopes, shoulder or midslopes LECs. Results from this chapter showed that some of this variation may be caused by differences in the progression of the emission events at different landscape positions (Figure 5-2) e.g. modeled emissions at Site 3 with lower FA were higher than those at the other sites with higher FA earlier in the emission event, and lower later in the emission event. Similar studies by Grant and Pattey (2003) showed that modeled emissions peaked and declined at the upper and mid positions earlier than at depressional positions, during an emission event. Spatial variation in annual N_2O emissions in the model was much less than that in

hourly emissions (Grant and Pattey, 2003). Other studies (Flessa et al., 1995) showed that spatial variation of hourly measured N_2O emissions was generally much larger (e.g. coefficient of variation (CV) = 233%) than that at an annual time scale (e.g. CV = 26%), for different research sites. This may explain results in this research whereby larger spatial variation of N_2O was found at hourly (Figure 5-3) versus seasonal time scales (Table 5-3). These results show that N_2O emissions may vary with small topographic differences (0.2% maximum slope) in a field, for the same fertilizer treatment. As a result, EF may vary depending on the sample location in the field. This shows the importance of using a three-dimensional model *ecosys*, with input from DEMs, in order to further understand the spatial and temporal variability of N_2O, and thus improve our future quantifications.

Other studies (Grant and Rochette, 1994; Grant, 1995) showed that the WFPS "threshold" at which the transition among alternative reduction reactions occurs decreases with higher temperatures. Similar results were found in chapter 4 whereby the large coefficients of diurnal temporal variation (CTV) (25 to 51% (modeled) and 24 to 63% (measured)) of N_2O emissions for our site was explained by "threshold" response of N_2O to changes in WFPS (> 0.6) and temperature. These physical controls of WFPS and temperature on N_2O in *ecosys* also explain the large spatial variation of N_2O across the field for different times of the day during the emission event (Figure 5-7). Therefore, calculation of N_2O EF based on once – daily measurements or longer may over- or under-estimate emissions, depending on the sample location, time of day or time course of the emission event when samples were taken. Similar to modeled results from this chapter

(Figure 5-7), Rover et. al. (1999) showed that measured emissions (measured) decreased from 9.00 to 13.00h and the spatial pattern over the field changed from the morning to the afternoon period. These results again show the importance of using mathematical model *ecosys*, at an hourly time-step, in order to fully capture the spatial and temporal variability of the entire emission event and thus make more accurate quantifications of N_2O emissions.

Ecosys can model the large spatial variation of N_2O emissions at different time scales – e.g. hourly, daily and annually etc. Generally, results showed that spatial variation of N_2O at hourly (Figure 5-3) and daily time-steps (Table 5-6) were larger than those at seasonal (Table 5-3) and annual (except for 54 soil profile run) time scales (Table 5-6). These findings suggest that spatial variation of N_2O emissions probably may not significantly affect the calculation of EFs. However, the field for this study was fairly flat and other fields (e.g. Li et al., 2005) with greater topographic differences may yield larger differences in emissions, within the same fertilizer treatment. Also, measuring spatial variation at a high resolution is important for first testing mathematical models, before they can be used in larger spatial scale studies.

Future modeling work will enable *ecosys* (Grant, 2001a,b) to scale N_2O emissions from landscape to regional and national scales, thus enabling N_2O inventories and projections to be made for Canada. Geo-referenced climate, activity data (Statistics Canada), soil data (Soil Landscapes Canada) and also access to Westgrid high-performance computing network and geographical information systems (GIS) computing facilities are available

for testing *ecosys* at provincial and national scales. More research is needed using both automated chambers (for better temporal resolution and higher number of sampling points for better spatial resolution) and micrometeorological towers simultaneously, under other land use management practices e.g. manure applications. These data can be further used to test *ecosys* simultaneously at chamber, tower and field scales to model both spatial and temporal variability of N_2O emissions for the development of more site-specific EFs, for the development of the IPCC Tier III methodology. This will also provide information for developing a methodology for scaling emissions from chamber to tower scales.

Ecosys (Grant, 2001a,b; website: www.ecosys.rr.ualberta.ca) has been used to predict the impact of climate change on short and long-term carbon and energy exchange in several agricultural (e.g. Grant et al., 1999; Grant et al., 2001a); forest (e.g. Grant et al., 2001b; Grant et al., 2005), artic (e.g. Grant et al., 2003) and grassland (e.g. Li et al., 2004) ecosystems. Recently, *ecosys* (Grant and Pattey, 2007 (Submitted)) was used to project climate impact on N_2O emissions. Future research will enable *ecosys* to make predictions under more land uses and climate change scenarios. These predictions can then be used to make recommendations for sustainable land use management recommendations in order to enhance crop productivity and maintain environmental quality. *Ecosys* has been used to simulate other greenhouse gases CH_4 (Grant, 1998) and CO_2 (e.g. Grant et al., 1999; Grant et al., 2001a,b; Grant et al., 2003; Grant et al., 2005) so that greenhouse gases inventories and projections for Canada can also be extended to these gases.

5.6 CONCLUSIONS

Results showed that *ecosys* (Grant, 2001a,b) represented the spatial variation of N_2O emissions at the meter, fetch and field scales. Our findings have indicated that modeled spatial variation of N_2O emissions at the field scale (Figures 5-6, 5-7 and 5-8; Table 5-6) in *ecosys* (Grant, 2001a,b) was due to small differences in topography (~1.8m over 600m), in a way that was consistent with the measured data (Table 5-2). The consistency of modeled and measured results **supports the hypothesis in *ecosys* (Grant, 2001a,b) outlined in the Introduction (section 5.1). Spatial variation in N_2O emissions can also be explained by spatial variation in soil properties (spatial variation in soil properties caused CSV of annual fluxes to increase from 25 % to 101%), which may themselves be caused by topographically driven water movement. High CSV of N_2O fluxes at a larger spatial scale (Figure 5-6), during emission events within the same fertilizer treatment (112 kg N ha^{-1}) was partly attributed in the model to spatial variation of WFPS (Figure 5-5), caused by different flow accumulation (FA) (Figure 5-1) within the field due to small differences in topography** High replicate variation of N_2O emissions was also found in the laboratory experiment in spite of soil mixing (chapter 2; section 7.1.2). Some of the inconsistencies between measured and modeled chamber emissions in our results may be due to high measured CVs amongst chamber replicates. As a result, replicate variation (root mean square for error (RMSE)) was larger that the variation between modeled versus measured (root mean square for difference (RMSD)) (Table 5-2) results therefore, the model hypothesis was not rejected. More research is needed to resolve unexplained chamber replicate spatial variation at the meter scale.

Generally, low EFs for 2004 could be attributed to slightly lower average mean temperatures compared to long-term normals for 1971 – 2000 for the experimental area, that delayed soil warming, causing reactions that generated N_2O to occur in comparatively cool soils. Modeled results within the two fertilized (112 kg N ha^{-1}) areas (Figure 5-1) generally showed that the lowest topographic positions of the field gave the highest seasonal N_2O emissions or were 'hot spots' for N_2O since these areas had high flow accumulation (FA) values. Consequently, EF modeled for the 112 kg N ha^{-1} fertilizer application was larger in an area of the field with lower topography compared to one with higher.. As a result, EF may vary depending on the sample location in the field. Results from chapter 5 showed that some of this variation may be caused by differences in the progression of the emission events at different landscape positions (Figure 5-3) as found by Grant and Pattey (2003). Large daily temporal variation in soil WFPS and temperature also led to large spatial variation of N_2O emissions across the field for different times of the day during the emission event (Figure 7). These results highlighted the importance of the use of 3-dimensional model *ecosys*, with input from DEMs, to fully capture the large spatial and temporal variability of N_2O emissions at different spatial scales even in seemingly flat landscapes, thus improve our future quantifications.

Ecosys can model the large spatial variation of N_2O emissions at different times scales – e.g. hourly, daily and annually etc.. Generally, our results showed that spatial variation of N_2O at hourly (Figure 5-3) and daily time-steps (e.g. 11 - 68%; Table 5-6) were large however, spatial variation of N_2O emissions at seasonal (Table 5-3) and annual (e.g. 25%; Table 5-6) (except for 54 soil profile run) time scales were smaller. These finding

suggests that spatial variation of N_2O emissions probably may not affect the calculation of EFs at an annual time scale as much as it does short-term emissions. However, our field was fairly flat (0.2% slope) and fields (e.g. Li et al., 2005) with greater topographic differences may yield larger differences in emissions within the same fertilizer treatment. Also, measuring spatial variation at a high resolution is important for first testing mathematical models, before they can be used larger spatial scale studies.

Results from *ecosys* for this chapter will be used in an attempt to develop a spatial integration scheme for N_2O emissions whereby emissions at the field scale can be simulated based on specific site information such as FA, topography, soil type etc. For example, N_2O produced for each FA classifications or range of values can be evaluated, and then FA can be further used as a tool for predicting emissions for other sites. The use of chamber measurements at the field scale will also be further evaluated e.g. what is the optimal investment of chamber measurements? Further analyses will be performed to determine the (a) frequency of chamber measurements (b) number of chamber sampling locations and (c) chamber method (s) integration scheme over time and space required for more accurate EFs at the field scale.

Future modeling work will enable *ecosys* (Grant, 2001a,b) to scale N_2O emissions from landscape to regional and national scales, thus enabling N_2O inventories and projections to be made for Canada. Geo-referenced climate, activity data (Statistics Canada), soil data (Soil Landscapes Canada) and also access to Westgrid high-performance computing network and geographical information systems (GIS) computing facilities are available

for testing *ecosys* at provincial and national scales. More research is needed using both automated chambers and micrometeorological towers simultaneously, under other land use management practices e.g. manure applications. These data can be further used to test *ecosys* simultaneously at chamber, tower and field scales to model both spatial and temporal variability of N_2O emissions for the development of more site-specific EFs, for the development of the IPCC Tier III methodology. This will also provide information for developing a methodology for scaling emissions from chamber to tower scales.

5.7 REFERENCES

Ball, B.C., Horgan, G.W., Clayton, H., Parker, J.P., 1997. Spatial variability of nitrous oxide fluxes and controlling soil topographic properties. Journal of Environmental Quality 26, 1399-1409.

Blackmer, A.M., Robbins, S.G., Bremner, J.M., 1982. Diurnal variability in rate of emission of nitrous oxide from soils. Soil Science Society of America Journal 46, 937-942.

Bouwman, A.F., Boumans, L.J.M., Batjes, N.H., 2002. Emissions of N_2O and NO from fertilized fields: Summary of available measurement data. Global Biogeochemical cycles 16(4), 1058, doi:10.1029/2001GB001811.

Bouwman, A.F., 1996. Direct emission of nitrous oxide from agricultural soils. Nutrient Cycling in Agroecosystems 46, 53-70.

Choudhary, M.A., Akramkhanov, A., Saggar, S., 2002. Nitrous oxide emissions from a New Zealand cropped soil: tillage effects, spatial and seasonal variability. Agriculture, Ecosystems and Environment 93, 33–43.

Clay, D.E., Molina, J.A.E., Clapp, C.E., Linden, D.R., 1985. Nitrogen-tillage-residue management: II. Calibration of potential rate of nitrification by model simulation. Soil Science Society of America Journal 49, 322-325.

Denmead, O.T., 1978. Chamber systems for measuring Nitrous oxide emission from soils in the field. Soil Science Society of America Journal 43, 89-95.

Eggleston, 2006. Intergovernmental Panel on Climate Change (IPCC), IPCC Guidelines for National Greenhouse Gas Inventories Volume 4; Agriculture, Forestry and other land use. Institute for Global Environmental Strategies, kanagawan Hayama, Japan.

Florinsky, I.V., McMahon, S., Burton, D.L., 2004. Topographic control of soil microbial activity: a case study of denitrifiers. Geoderma 119, 33–53.

Folorunso, O.A., Rolston, D.E., 1984. Spatial variability of field measured denitrification gas fluxes. Soil Science Society of America Journal 48, 1214-1219.

Frolking, S.E., et al., 1998. Comparison of N_2O emissions from soils at three temperate agricultural sites: simulations of year-round measurements by four models. Nutrient Cycling in Agroecosystems 52, 77–105.

Grant, R.F., 1991. A technique for estimating denitrification rates at different soil temperatures, water contents, and nitrate concentrations. Soil Science 152, 41-52.

Grant, R.F., 1995. Mathematical modelling of nitrous oxide evolution during nitrification. Soil Biology & Biochemistry 27, 1117–1125.

Grant, R.F., 1997. Changes in soil organic matter under different tillage and rotation: mathematical modeling in *ECOSYS*. Soil Science Society of America Journal 61, 1159-1175.

Grant, R.F., 1998. Simulation of methanogenesis in the mathematical model *ecosys*. Soil Biology & Biochemistry 30, 883-896.

Grant, R.F., 2001a. A Review of the Canadian Ecosystem Model - *ecosys*. In: Shaffer M. J., Ma, L., Hansen, S. (Ed), Modeling Carbon and Nitrogen Dynamics for Soil Management. CRC Press. Boca Raton, FL, pp. 173-263.

Grant, R.F., 2001b. Modeling Transformations of Soil Organic Carbon and Nitrogen at Differing Scales of Complexity. In: Shaffer M. J., Ma, L., Hansen, S. (Ed), Modeling Carbon and Nitrogen Dynamics for Soil Management. CRC Press. Boca Raton, FL, pp. 597-614.

Grant, R.F., 2004. Modeling topographic effects on net ecosystem productivity of boreal black spruce forests. Tree Physiology 24, 1-18.

Grant, R.F., Rochette, P., 1994. Soil Microbial respiration at Different Water Potentials and Temperatures: Theory and Mathematical Modeling. Soil Science Society of America Journal 58, 1681-1690.

Grant, R.F. and Pattey, E., 1999. Mathematical modeling of nitrous oxide emissions from an agricultural field during spring thaw. Global Biogeochemical Cycles 13, 679-694.

Grant, R.F., Pattey, E., 2003. Modelling variability in N_2O emissions from fertilized agricultural fields. Soil Biology & Biochemistry 35, 225-243.

Grant, R.F., and Pattey, E., Submitted 2007. Temperature sensitivity of N_2O emissions from fertilized agricultural soils: mathematical modelling in *ecosys*.

Grant, R.F., Nyborg, M., Laidlaw, J.W., 1992. Evolution of nitrous oxide from soil: II. Experimental results and model testing. Soil Science 156, 266-277.

Grant, R.F., Juma, N.J., McGill, W.B., 1993a. Simulation of carbon and nitrogen transformations in soils. I: mineralization. Soil Biology & Biochemistry 25, 1317-1329.

Grant, R.F., Juma, N.J., McGill, W.B., 1993b. Simulation of carbon and nitrogen transformation in soil: Microbial biomass and metabolic products. Soil Biology & Biochemistry 25, 1331-1338.

Grant, R.F., Nyborg, M., Laidlaw, J.W., 1993c. Evolution of nitrous oxide from soil: I. Model development. Soil Science 156, 259-265.

Grant, R.F., Izaurralde, R.C., Nyborg, M., Malhi, S.S., Solberg, E.D., Jans-Hammermeister, D., Stewart, B.A., 1998. Modeling tillage and surface residue effects on soil C storage under ambient versus elevated CO_2 and temperature in *ECOSYS*. In: Lal, R., Kimble, J.M., Follet, R.F. (Eds), Soil processes and carbon cycle. CRC Press Inc. Boca Raton, USA, pp. 527-547.

Grant, R.F., Wall, G.W., Kimball, B.A., Frumau, K.F.A., Pinter Jr., P.J., Hunsaker, D.J., Lamorte, R.L., 1999b. Crop water relations under different CO_2 and irrigation: testing of *ecosys* with the free air CO_2 enrichment (FACE) experiment. Agriculture & Forest Meteorology 95, 27–51.

Grant, R.F., Kimball, B.A., Brooks T.J., 2001a. Modeling interactions among carbon dioxide, nitrogen and climate on energy exchange of wheat in a Free Air carbon dioxide experiment. Agronomy Journal 93, 638-649.

Grant, R.F., Massheder, J.M, Hale, S.E., Moncrieff, J. B., Rayment, M, Scott, S.L., Berry, J.A., 2001b. Controls of carbon and energy exchanges by a black spruce – moss ecosystem: Testing the mathematical model *Ecosys* with data from the BOREAS experiment. Global Biogeochemical cycles 15, 129 – 147.

Grant, R.F., Oechel, W.C., Ping, C., Kwon, H., 2003. Carbon balance of coastal arctic tundra under changing climate. Global Change Biology 9, 16–36.

Grant, R.F., Amrani, M., Heaney, D.J., Wright, R., Zhang, M., 2004. Mathematical Modeling of Phosphorus Losses from Land Application of Hog and Cattle Manure. Journal of Environmental Quality 33, 210-231.

Grant , R.F., Arain, A., Arora, V., Barr, A., Black, T.A., Chen, J. Wang, S., Yuan, F., Zhang, Y., 2005. Intercomparison of techniques to model high temperature effects on CO_2 and energy exchange in temperate and boreal coniferous forests. Ecological Modelling 188, 217–252.

Grant, R.F., Pattey, E., Goddard, T.W., Kryzanowski, L.M., Puurveen, H., 2006. Modeling the effects of fertilizer application rate on nitrous oxide emissions. Soil Science Society of America Journal 70, 235-248.

Helgason, B.L., Janzen, H.H., Angers, D.A., Boehm, M., Bolinder, M., Desjardins, R.L., Dyer, J., Ellert, B.H., Gibb, D.J., Gregorich, E.G., Lemke, R., Massé, D., McGinn, S.M., McAllister, T.A., Newlands, N., Pattey, E., Rochette, P., Smith, W., VandenBygaart, A.J., Wang, H., 2005. GHGFarm: An assessment tool for estimating net greenhouse gas emissions fromCanadian farms. Agriculture & Agri-Food Canada, pp. 5-6.

Hénault, C., Devis, X., Page, S., Justes, E., Reau, R., Germon, J.C., 1998. Nitrous oxide emissions under different soil and land management conditions. Biology and Fertility of Soils 26, 199-207.

Hutchinson, G.L., Mosier, A.R., 1981. Improved soil cover method for field measurement of nitrous oxide fluxes. Soil Science Society of America Journal 45, 311-316.

Hutchinson, G.L., Livingston, G.P., Healy, R.W., Striegl, R.G., 2000. Chamber measurement of surface-atmosphere traces gas exchange: Numerical evaluation of dependence on soil, interfacial layer, and source/sink properties. Journal of Geophysical Research 105, 8865-8875.

Hutchinson, G.L., Livingston, G.P., 2001. Vents and seals in non-steady-chambers used for measuring gas exchange between soil and the atmosphere. European Journal of Soil Science 52, 675-682.

Li, T., Grant, R.F., Flanagan, L.B., 2004. Climate impact on net ecosystem productivity of a semi-arid natural grassland: modeling and measurement. Agricultural and Forest Meteorology 126, 99–116.

Mathieu, O., Lévéque, J., Hénault, C., Milloux, M-J., Bizouard, F., Andreux, F., 2006. Emissions and spatial variability of N_2O, N_2 and nitrous oxide mole fraction at the field scale, revealed with 15N isotopic techniques. Soil Biology & Biochemistry 38, 941–951

Millington, R.J., Quirk, J.M., 1960. Transport in porous media. In: Van Beren, F.A. et al. (Eds.), 7th Trans. Int. Congr. Soil Sci. Vol. 1. Madison, WI. 14-24 Aug. Elsevier, Amsterdam, Science, pp. 97-06.

Molina, J.A.E., Clapp, C.E., Shaffer, M.J., Chichester, F.W., Larson, W.E., 1983. NCSOIL, a model of nitrogen and carbon transformations in soil: Description, calibration and behavior. Soil Science Society of America Journal 47, 85-91.

Muller, C., 1999. Modelling soil-biosphere interactions. CABI Publishing, Wallingford, UK, pp. 52-53.

Myrold, D.D., 1998. Transformation of nitrogen. In: Sylvia, D.M., Fuhrmann, J.J., Hartel, P.G., Zuberer (Eds.). Principles and Applications of soil microbiology. Prentice Hall: Upper Saddle River, New Jersey, pp. 259-294.

Osher, L. J., Buol, S.W., 1998. Relationship of soil properties to parent material and landscape position in eastern Madre de Dios, Peru. Geoderma 83, 143–166.

Pattey, E., Edwards, G.C., Strachan, I.B., Desjardins, R.L., Kaharabata, S., Wagner-Riddle, C., 2006a. Towards standards for measuring greenhouse gas flux from agricultural fields using instrumented towers. Canadian Journal of Soil

from agricultural fields using instrumented towers. Canadian Journal of Soil Science 86, 373-400.

Pattey, E., Strachan, I.B., Desjardins, R.L., Edwards, G.C., Dow, D., MacPherson, J.I., 2006b. Application of a tunable diode laser to the measurement of CH_4 and N_2O fluxes from field to landscape scale using several micrometeorological techniques. Agriculture & Forest Meteorology 13, 222-236.

Pennock, D.J., Zebarth, B.J., de Jong, E., 1987. Landform classification and soil distribution in hummocky terrain, Saskatchewan, Canada. Geoderma 40, 297-315.

Pennock, D.J., van Kessel, C., Farrell, R.E., Sutherland, R.A., 1992. Landscape-scale variations in denitrification. Soil Science Society of America Journal 56, 770-776.

Pennock, D.J., Anderson, D.W., de Jong, E., 1994. Landscape-scale changes in indicators of soil quality due to cultivation in Saskatchewan, Canada. Geoderma 64, 1-19.

Pennock, D.J., Corre, M.D., 2001a. Development and application of landform segmentation procedures. Soil & Tillage Research 58, 151-162.

Pennock, D.J., Frick, A.H., 2001b. The role of field studies in landscape-scale applications of process models: an example of soil redistribution and soil organic carbon modeling using CENTURY. Soil & Tillage Research 58, 183-191.

Phillips, F.A, Leuning, R., Baigent, R., Kelly, K.B., Denmead, O.T. 2007. Nitrous oxide flux measurements from an intensively managed irrigated pasture using micrometeorological techniques. Agricultural & Forest Meteorology 143, 92–105.

Rao, P.S.C., Jessup, R.E., Reddy, K.R., 1984. Simulation of nitrogen dynamics in flooded soils. Soil Science 138, 54-62.

Rezaei, S.A. and Gilkes, R.J., 2005. The effects of landscape attributes and plant community on soil chemical properties in rangelands. Geoderma 125, 167–176.

Rochette, P., McGinn, S.M., 2005. Methods for measuring soil-surface gas fluxes. In: Handbook of Applied Techniques for Characterizing Processes in the Soil Environment. Alvarez-Benedí, J. and MuZoz-Carpena, R. (Eds.) CRC Press, in press.

Rolston, D.E., Rao, P.S.C., Davidson, J.M., Jessup, R.E., 1984. Simulation of denitrification losses of nitrate fertilizer applied to uncropped, cropped and manure-amended field plots. Soil Science, 137, 270-279.

Röver, M., Heinemeyer, O., Munch, J.C., Kaiser, E.-A., 1999. Spatial heterogeneity within the plough layer: high variability of N_2O emissions rates. Soil Biology & Biochemistry 31, 167-173.

Saxton, K.E. Rawls, W.J., 2006. Soil water characteristic estimates by texture and organic matter for hydrologic solutions. Soil Science Society of American Journal 70, 1569-1578.

Sextone, A.J., Revsech, N.P., Parkin, T.B. Tiedje, J.M., 1985. Direct measurement of oxygen profiles and denitrification rates in soil aggregates. Soil Science Society of American Journal 49, 645-651.

Schmid, H.P., 2002. Footprint modeling for vegetation atmosphere exchange studies: a review and perspective. Agricultural and Forest Meteorology 113, 159-183.

Uchida, Y., Clough, T.J., Kelliher, F.M., Sherlock, R.R., 2008. Effects of aggregate size, soil compaction, and bovine urine on N_2O emissions from a pasture soil. Soil Biology & Biochemistry 40, 924–931.

Wagner-Riddle, C., Thurtell, G.W., Kidd, G.E., Edwards, G.C., Simpson, I.J., 1996. Micrometeorological measurements of trace gas fluxes and natural ecosystems. Infrared Physics and Technology 37, 51-158.

Xu-Ri, Wang, M., Wang, Y., 2003. Using a modified DNDC model to estimate N_2O fluxes from semi-arid grassland in China. Soil Biology & Biochemistry 35, 615-620.

CHAPTER 6.0: Using the *Ecosys* to project the impact of climate change (increasing CO_2 and temperature) on future spatial and temporal variability of N_2O emissions from an agricultural soil

6.1 INTRODUCTION

Canada is committed to reduce its total greenhouse gases to 6% below 1990 levels over the period 2008 to 2012, under the Kyoto Protocol (Olsen et al., 2003). Current Intergovernmental Panel of Climate Change (IPCC) Tier I Methodology for quantifying N_2O emissions in greenhouse gas inventories, is based on a constant emission factor (EF) of 1% for all N inputs (Eggleston, 2006). However, uncertainties in estimates of N_2O emissions by IPCC guidelines may be 70% to 80% in arable soil at a national scale (Lim et al., 1999). This uncertainty may be attributed to large spatial and temporal variability of N_2O (e.g. Pennock and Corre, 2001; Pennock et al., 1992; Grant & Pattey, 2003). In addition to current uncertainties, a review by Barnard et al. (2005) found that global climate change impacts on N_2O emissions require more research. Addressing current uncertainties may improve our long – term predictions of climate changes impact on future N_2O emissions. Such projections are important since the sustainability of current land use management systems can be evaluated and then recommendations can be made for best management practices to mitigate future N_2O emissions from agricultural soils.

IPCC Tier II Methodology may improve current estimates because it is based on country-specific EF, derived from country-specific activity data (land use) (Eggleston, 2006). An IPCC Tier II Methodology is now being used for Canada which uses lower EFs (0.1 - 0.7%) in drier climates such as the Prairies and higher EFs (0.83 - 1.67%) for the more humid regions of Eastern Canada (Hegalson, 2005). IPCC Tier III Methodology involves

either the use of validated mathematical models or the use of measurement data in conjunction with activity data to simulate emissions (IPCC, 2006). Unlike Tier I and Tier II, Tier III addresses more of the large spatial and temporal variability of N_2O emissions and is capable of capturing longer-term legacy effects of land use and management (Eggleston, 2006) together with projected climate changes. In addition, mathematical models used in Tier III can improve N_2O estimates by contributing towards the continuity of measured data by estimating fluxes where measured data are missing. So far, Canada has not yet implemented the IPCC Tier III Methodology for N_2O inventories - This can be achieved by using *ecosys* (Grant, 2001a,b; website: www.ecosys.rr.ualberta.ca.), a detailed process – based mathematical model of terrestrial ecosystems.

Ecosys (Grant, 2001a,b) has been used to predict the impact of climate change on short and long-term carbon and energy exchange in several agricultural (e.g. Grant et al., 1999; Grant et al., 2001a); forest (e.g. Grant et al., 2001b; Grant et al., 2005), arctic (e.g. Grant et al., 2003) and grassland (e.g. Li et al., 2004) ecosystems. The model has also been used to predict long-term changes in soil C under different land use management systems (Grant et al., 2001c). Hypotheses for the complex biological, physical and chemical processes involved in N_2O production have already been incorporated into the model. Recently, *ecosys* (Grant and Pattey, 2007 (Submitted)) was used to project climate impact on N_2O emissions. *Ecosys* has also been used to model N_2O emissions at the site scale from laboratory experiments (Grant, 1991; Grant et al., 1992; Grant et al., 1993c; Grant, 1994; Grant, 1995) and agricultural field experiments using micrometeorological towers (Grant et al, 1992; Grant and Pattey, 1999; Grant and Pattey, 2003; Grant et al., 2006). In

earlier chapters (2 – 5), the ability of *ecosys* to simulate N_2O emissions at the laboratory, and plot (m^2), fetch and field (ha) spatial scales was tested, and derived more site - specific EFs, which can contribute towards the adoption of an IPCC Tier III methodology. The findings showed that in addition to other factors such as past (soil residual N) and present (fertilizer rate, source) land use, topography etc., climate (e.g. temperature and precipitation) had a substantial impact on N_2O emissions. Therefore, in addition to current estimates for N_2O inventories, it is also important to project the impact of climate change on N_2O emissions. For this chapter, *ecosys* (Grant, 2001a,b) will be used to do this. Such projections can be used as a tool in greenhouse gas inventories to reduce future emissions. If such applications are made in different countries, then ultimately global N_2O emissions can be reduced.

N_2O emissions are highly variable spatially and temporally because of the complex ecological controls on these emissions. It is therefore important to model N_2O emissions at appropriate time steps that capture this large variability. *Ecosys* can be tested at different temporal resolutions e.g. hourly, daily, monthly and yearly time-steps, which is necessary to capture the large temporal (Grant, 1991; Grant et al., 1992; Grant et al., 1993c; Grant and Pattey, 1999; Grant and Pattey, 2003; Grant et al., 2006) and spatial variability of N_2O emissions (Grant and Pattey, 2003; Grant et al., 2006). Other models simulate N_2O emissions at a daily (e.g. Gabrielle et al., 2006) or monthly (e.g. Roelandt et al., 2007) time-steps which does not allow testing at an hourly time-step, which is necessary to capture the large temporal (Grant, 1991; Grant et al., 1992; Grant et al., 1993c; Grant and Pattey, 1999; Grant and Pattey, 2003; Grant et al., 2006) and spatial

variability of N_2O emissions (Grant and Pattey, 2003; Grant et al., 2006). *Ecosys* (Grant 2001a,b) explicitly represents oxidation-reduction reactions from which N_2O is generated and gas transfer processes which control the transition between alternative electron acceptors used in these reactions. In this model, the key biological processes – mineralization, immobilization, nitrification, denitrification, root and mycorrhizal uptake controlling N_2O generation were coupled to the key physical processes – convection, diffusion, volatilization, dissolution - controlling the transport of gaseous reactants and products of these biological processes (Grant et al., 2006). In *ecosys*, N_2O is simulated based on the energetics of microbial oxidation-reduction reactions driven by alternative electron acceptors under aerobic vs. anaerobic conditions. Other processed-based models used in studies of N_2O emissions employ a semiempirical submodel for the production and reduction of N_2O in agricultural soils and do not use microbial respiration of organic C as a driver for denitrification (e.g. Gabrielle et al., 2006).

Simulation of nitrification and denitrification in *ecosys* is also based on Michaelis-Menten kinetics whereas other models (e.g., Molina et al., 1983 and Clay et al., 1985) simulate denitrification based on first order kinetics with respect to soluble C or NO_3^- (e.g., Rolston et al., 1984 and Rao et al., 1984) as modified by dimensionless factors of temperature and WFPS. Some models impose constraints either on the magnitude of N_2O produced from nitrification (Li et al., 2005) or on the magnitude of N_2O emitted during snow cover (Li et al., 1992; Xu-Ri et al., 2003), even if environmental conditions favour higher emissions. However, in *ecosys*, there are no set constraints placed on N_2O production.

Based on the literature, no projections of N_2O emissions were made using mathematical models that include the influence of topography on emissions. *Ecosys* (Grant, 2001a,b) is a three-dimensional model, which also uses input data from digital elevation models (DEMs) to account for topographic effects on the complex processes involved in N_2O generation. Such information can help us further understand both current and future spatial and temporal variability of N_2O emissions, thus improve our inventories. *Ecosys* includes hypotheses for surface energy exchange and subsurface heat transfer, vertical (infiltration, drainage, root uptake and capillary rise) and lateral (driven by differences in topographic position) water movement, and hypotheses for the effects of soil temperature and water content on autotrophic and heterotrophic activities (Grant, 2004; Grant et al., 1995a, Grant, 1995b; Grant, 1998; Grant, 1999; Grant, 2001a,b; Grant and Pattey, 2003). Previous studies by Grant and Pattey (2003) showed that modeled emissions were highest at depressional topographic positions compared to the upper and mid positions, in a fairly flat field (0.5m maximum elevational differences). Other field studies (e.g. Ball et. al., 1997; Flessa et. al., 1995) have also shown that N_2O emissions can vary even in seemingly uniform landscapes. Based on landform segmentation procedures to classify landform elements into landform element complexes (LEC) from digital elevation models (DEM) (Penock et al., 1987; Penock et al., 1994), Pennock and Corre (2001) found that measured N_2O emissions were significantly higher at level depressions than at foot slopes, shoulder or midslopes LECs. For this chapter, we will use *ecosys* (Grant 2001a,b) to also project impact of climate change on N_2O emissions from different topographic positions within a fairly flat field (0.2% slope).

6.1.1 Climate change impact on soil temperature, water content and C availability and the influence of these changes on N_2O emissions

Global carbon cycle models (IPCC, 2007) project an increase in atmospheric CO_2 concentration within the range of 735 – 1,088 ppm by 2100. Also, globally averaged surface temperature is projected to increase to 2.4 - 5.6°C by the end of the 21st century (IPCC, 2007). Precipitation is projected to increase by 2100 however, predictions of changing precipitation have been more uncertain than those of CO_2 and temperature (IPCC, 2007). These changes in CO_2, air temperature (T_a) and precipitation may affect N_2O emissions by changing soil (1) temperature (T_s) (2) water content, and (3) C availability. The combination of these climate changes and other site-specific conditions (land use changes, soil type, topography etc.) and the feedback mechanisms involved, will determine whether future N_2O emissions from Canadian agricultural soils will rise or fall.

6.1.1.1 Soil temperature

Higher soil temperatures have been shown to increase N_2O emissions in several studies (Grant, 1995; Smith et al. 1998; Dobbie and Smith, 2001; Flechard et al., 2007). In contrast, some studies covered in Barnard et al. (2005) showed different responses of N_2O emissions to higher temperatures. Rising temperatures may reduce plant C fixation and can reduce NEP (Coughenour and Chen, 1997) especially in dry conditions (Arneth et al., 1998), thus less organic C substrate may become available for N_2O production via denitrification. Because of the complexity of simulating increasing soil temperature due to climate change, ecosystem models should, therefore, include a fully coupled

simulation of heat and water exchanges between terrestrial surfaces and the atmosphere, and through the soil profile, by implementing a solution to the general heat flux equation (Grant et al., 2003).

6.1.1.2 Soil water content

Increasing WFPS as a result of projected rises in precipitation may affect the magnitude of N_2O emissions produced. N_2O emissions have been found to be highly sensitive to changes in soil WFPS (Dobbie and Smith, 2001; Dobbie and Smith, 2003; Bateman and Baggs, 2005; Rusier et al., 2006; chapter 2) and emissions are often described as having a non-linear or "threshold" response to WFPS. However, in some current models (e.g. Lu et al., 2006), the response to WFPS is linear. Rising temperatures due to climate change may lead to larger vapor pressure deficits thereby increasing evapotranspiration and thus reducing soil water content, especially in the tropics (Berthelot et al., 2002). Such changes may reduce overall N_2O production via nitrification/denitrification. In contrast, higher CO_2 levels may decrease transpiration therefore improve overall water use efficiency (WUE) (Nelson et al., 2004). Consequently, these changes may result in larger WFPS, which may increase N_2O production via nitrification and denitrification.

6.1.1.3 Carbon availability

Greater availability of organic C substrates due to projected rising CO_2 under climate change may lead to higher N_2O production via denitrification. Elevated CO_2 levels may increase gross primary productivity (GPP) (CO_2 fixation) and cause higher net ecosystem productivity (NEP) (Grant et al., 1999), thus more organic C substrates may become

available. However, greater CO_2 fixation may increase soil N uptake therefore lower N precursors (especially in N limited ecosystems) for N_2O generation e.g. NO_3^- concentrations, thus decrease N_2O emissions. A review by Barnard et al. (2005) found no significant effect of elevated CO_2 on N_2O emissions and that more research is necessary to better understand such responses.

The complex nature of the interaction between atmospheric CO_2 and stomatal resistance and its effects on CO_2 fixation, requires explicit simulation modeling of key processes governing transpiration and CO_2 fixation, which is important in climate change studies (e.g. Grant et al., 1999; Grant et al., 2001a,b; Grant et al., 2003; Grant et al., 2005). Earlier estimations of N_2O emissions have relied on simple multiplication factors for radiation use efficiency and stomatal resistance to simulate the effects of atmospheric CO_2 on crop growth and water use (e.g. Rosenzweig and Parry 1994; Hoogenboom et al., 1995). As a result, atmospheric CO_2 was not incorporated into evapotranspiration to simulate elevated atmospheric CO_2 effects on WUE. Other models (e.g. Kellomaki and Wang 1999, 2000) used site-specific parameterizations e.g. soil thermal properties, soil respiration and soil surface resistance to evaporation. Such limitations may restrict the extent to which models can predict climate change impacts on future SOC inputs and hence on N_2O emissions from diverse independent ecosystems.

6.1.1.2 Current and future N_2O emissions

Direct and indirect emissions from agricultural systems are now thought to contribute 6.2 Tg N_2O-N per year a total global source of 17.7 Tg N_2O-N per year (Kroeze et al., 1999).

Global N_2O concentrations are projected to rise to ~ 460ppb by 2100 (IPCC, 2001). Scott et al. (2002) projected a general increase in N_2O emissions from 1995 (365 ppm CO_2) to 2080 (+ 2.5°C, 560 ppm CO_2) for the United States crop production under present land use and suggested that emissions may be lowered if improved technology is used. Based on N_2O emissions in 2000, projections showed a decline in overall emissions for 2010 in Taiwan, due to a reduction in agricultural activities (Tsai and Chyan, 2006). Three projected scenarios for Belgium (Roelandt et al., 2007) showed no significant upward or downward trend while one scenario showed a strong decrease in N_2O emissions by 2050, due to lower projected cropland areas. However, reduced cropland areas may not reduce N_2O emissions since we may require more intensive agriculture (more N fertilization) to sustain food production, which may induce higher emissions. These few projections of N_2O emissions (Roelandt et al., 2007; Tsai and Chyan, 2006; Scott et al., 2002) were made using empirical models and are site-specific. However, empirical modeling may not fully represent the complex processes involved in N_2O production and the strong controls of on these processes under different conditions. We want to use a more process – based model, *ecosys* (Grant 2001a,b), and observe its performance in which all processes are represented e.g. changes in soil temperature, water content and C availability due to climate change and the influence of these changes on N_2O emissions. The complex hypotheses in the model can be simulated in diverse ecosystems with different site conditions e.g. different land use, climate, soil type, topography etc., and are not parameterized for specific site conditions.

6.1.2 Using *Ecosys* mathematical model to simulate climate change effects on soil temperature, water content and C availability and the influence of these changes on N_2O emissions

For this research, *ecosys* (Grant, 2001a,b) was used because in addition to modeling past and present N_2O emissions under site-specific conditions (past and current land use, soil type, topography etc.), the model can project future N_2O emissions by using weather data from climate change scenarios (e.g. air temperature, precipitation and CO_2).

6.1.2.1 Soil temperature

Soil temperatures in *ecosys* are controlled by canopy energy exchange calculated from an hourly two-stage convergence solution for the transfer of water and heat through a multi-layered multipopulation soil–root–canopy system (Grant et al., 2005). Rising air temperature in *ecosys* due to climate change will cause greater conductive (Eq. [A.5], [A.19], [A.26] of Grant, 2001a), convective and latent (Eq. [A.1] [A.3], [A.4], [A.18] of Grant, 2001a) energy exchanges from surface to subsurface (Eqs. [A.24] – [A.25], [A.27] of Grant, 2001a), thereby increasing soil temperature. Soil temperature can be modeled for diverse soil types since soil properties in the soil input file (texture, water content at field capacity and wilting point, horizontal and vertical saturated hydraulic conductivity etc.) can be changed depending on site-conditions. Surface and subsurface energy exchange are consequently affected by soil properties.

Rising T_s in *ecosys* drives autotrophic and heterotrophic microbial activity through an Arrhenius function that drives N fixation rates including nitrification and denitrification. Higher T_s in the model accelerates reduction of O_2 by nitrifiers and denitrifiers (N

mineralization rates also increase) thereby increasing the demand for O_2 electron acceptors at the microbial sites (Grant, 1991; Grant et al., 1992; Grant et al., 1993c; Grant, 1994; Grant; 1995a,b; Grant et al, 1992; Grant and Pattey, 1999; Grant and Pattey, 2003; Grant et al., 2006; Grant and Pattey, submitted 2007). As a result, microbial O_2 demand may exceed O_2 supply, resulting in the need for alternative electron acceptors (Grant and Rochette, 1994; Grant, 1995a,b) and therefore transition to reduction of NO_2^- (nitrifiers) and NO_3^- (denitrifiers), accelerating production of N_2O. N_2O production may increase further with higher temperature because modeled gaseous solubility declines and hence aqueous O_2 concentrations ($[O_{2s}]$) maintained at microbial microsites decline. The solubility of N_2O also decreases, therefore accelerating the release of previously accumulated aqueous N_2O in the soil profile. The water-filled pore space (WFPS) "threshold" at which the transition among alternative reduction reactions occurs therefore decreases with higher temperatures (Grant and Rochette, 1994; Grant, 1995a,b). The temperature effect on gaseous solubility and O_2 demand will cause this transition to be sharper at higher temperatures.

6.1.2.2 Soil water content

Ecosys will also capture the effect of changes in precipitation on N_2O emissions in the future. Changes in precipitations inputs into the model determine surface and subsurface flows of water. In *ecosys*, surface flow is calculated using a Manning equation while subsurface flow (e.g. Grant and Pattey 2003; Grant, 2004; Eqs. [2.21] and [24] and [A94 - A96] of Grant et al., 2004) is calculated using both Richards and Green-Ampt flow equations. This is important since surface and subsurface transport of water determine

soil WFPS, which is an important controller of N_2O production as well as emissions from the soil profile.

Ecosys simulates the "threshold" response of N_2O to changes in WFPS (Grant, 1991; Grant et al., 1992; Grant et al., 1993c; Grant, 1994; Grant; 1995; Grant and Pattey, 1999; Grant and Pattey, 2003; Grant et al., 2006; Grant and Pattey, submitted 2007). Transitions from one reduction reaction to another can be caused by small changes in soil WFPS. This occurs because the diffusivity (D_g) of O_2 (and other gases) in the soil atmosphere varies according to a power function of the soil air-filled porosity (θ_g) (Millington, 1960), which in turn depends on WFPS. This variation is such that at certain WFPS, small declines in θ_g can cause large declines in D_g that may limit O_2 gaseous transfer to microsites causing a greater demand for alternative electron acceptors. As a result, these small declines may cause a transition from the reduction of O_2 to that of NO_x by nitrifiers and denitrifiers, increasing N_2O production. Temporal variation in WFPS therefore strongly influences that in N_2O emissions. Studies by Grant (1991) have shown that transitions from one reduction reaction to another can be caused by very small changes in soil H_2O content.

Increased T_a in *ecosys* leads to increased saturated pressures (e_s) thus higher vapour pressure deficits and therefore increased evapotranspiration during closure of surface energy balances. Consequently, these changes may lead to lower WFPS and thereby lower N_2O production via nitrification/denitrification. In contrast, higher CO_2 levels may decrease transpiration by increasing stomatal resistance (stomatal closure) at higher

mesophyll CO_2 concentration (C_l (μmol mol^{-1}) for each leaf surface, thereby improving overall water use efficiency (WUE) (e.g. Grant et al., 1999; Grant et al., 2001a,b; Grant et al., 2003; Grant et al., 2005; Li et al., 2004). Grant et al. (2001a) showed that evapotranspiration was reduced by 9 % and 16% with fertilization of 35 and 7 g m^{-2} respectively in a wheat field, when treated with 548 versus 362 μmol mol^{-1} of CO_2. Consequently, these changes may result in wetter soils which may increase N_2O production via nitrification and denitrification.

6.1.2.3 Carbon availability

Rising CO_2 in *ecosys* will affect GPP and hence soil inputs through a biochemical model in which fixation of CO_2 in *ecosys* (Grant, 2001a,b) is calculated from coupled algorithms for carboxylation and diffusion (Grant, 2004), based on Michaelis-Menten function of an intercellular CO_2 concentration, itself driven by atmospheric CO_2 (Grant et al., 2001b). Therefore, leaf CO_2 fixation rates are directly affected by atmospheric CO_2, through the effects of atmospheric CO_2 on canopy CO_2 concentration and hence gaseous and aqueous mesophyll CO_2 concentration (e.g. Grant et al., 1999; Grant et al., 2001a,b; Grant et al., 2003; Grant et al., 2005). CO_2 fixation in *ecosys* is also affected by soil N uptake which may be raised by increased soil N transformations with higher T_a.

Greater CO_2 fixation (Eqs [20] – [29] of Grant, 2004) modeled in *ecosys* will result in more rapid litterfall (Eq. [29] - [37] of Grant, 2004), thus more microbial respiration (Eq. [8] and [9] of Grant, 2004) of organic matter, to produce substrates (dissolved organic carbon (DOC) for N_2O production via denitrification (Eqs. [2.16] – [2.18]). Also, more

rapid O_2 uptake increases the demand for alternative electron acceptors (Eqs. [2.10] – [2.18]). However, greater CO_2 fixation (Eqs [20] – [29] of Grant, 2004) in the model will also cause more rapid N uptake (e.g. R_{NH4} (g N m^{-3}) of Eqs. [39a,b] of Grant, 2004) reducing soil mineral N (especially in N deficient ecosystems), and decreasing N_2O production via nitrification (Eq. [2.10]) and denitrification (Eq. [2.10])

As described above, *ecosys* (Grant, 2001a,b) explicitly represents the hypotheses for how climate affects N_2O emissions and therefore can model past, current, and future emissions due to climate change from diverse ecosystems. *Ecosys* can also simulate microbial oxidation/reduction reactions under different soil amendments such as crop residue (Grant et al., 1993a), fertilizer (Grant et al., 1992; Grant, 1995; Grant et al., 2006) or manure, and under different soil management practices such as rotation and tillage (Grant, 1997; Grant et al., 1998; Grant et al., 1995; Grant and Rochette, 1994) or irrigation. For this research, **we propose to use *ecosys* (Grant, 2001a.b) mathematical model to predict the impact of climate change (increasing CO_2 and temperature) on future spatial and temporal variability of N_2O emissions from an agricultural soil.** Predictions of N_2O emissions at the field scale, will later enable *ecosys* (Grant, 2001a,b) to derive N_2O emissions at larger spatial scales for inventories (e.g. regional and national).

6.2 MODEL DESCRIPTION

6.2.1 Introduction

Ecosys (Grant, 2001a,b; website: www.ecosys.rr.ualberta.ca.) mathematical model can simulate the dynamics of C, N, P, heat and water of different ecosystems under a wide range of site-specific conditions (e.g. climate, land use, soil type, topography etc.). For full details of model hypotheses, refer to Grant, 2001a,b. For hypotheses specific to N_2O transformations in *ecosys*, refer to Chapter 2, Section 2.2 for equations beginning with "2." Hypotheses for ecosystem energy exchange and CO_2 fixation in *ecosys* are given explicitly in Grant, 2001a and Grant, 2004 - A brief description of the effects of climate change on N_2O emissions in the model is given below.

6.2.2 Using *Ecosys* mathematical model to simulate climate change impact on soil temperature, water content and C availability and the influence of these changes on N_2O emissions

As mentioned earlier, changes in CO_2, temperature and precipitation expected under climate change may subsequently affect N_2O emissions by changing soil temperature, water content and C availability.

6.2.2.1 Soil temperature

6.2.2.1.1 Ecosystem energy exchange (Grant, 2001a) - Effect of rising air temperatures on soil temperatures

Ecosys (Grant, 2001a) will capture the effect of rising air temperatures (T_a) on N_2O emissions since T_a inputs into the model influences soil temperature (T_s), which in turn controls emissions according to a "threshold response". First-order closure schemes are used to simulate hourly energy exchange between the atmosphere and each of several terrestrial surfaces in *ecosys* (Grant, 2001a,b) including the canopy of each species in the plant community (Eqs. [A.1]) - [A.15] of Grant, 2001a; also Grant et al., 1999; Grant and Baldocchi, 1992; Grant et al., 1993d; 1995a,c; 1999a) and snow, residue and soil surfaces (Eqs. [A.16]) - [A.23] of Grant, 2001a; also Grant et al., 1999; Grant et al., 1995b). In *ecosys,* soil temperature is modeled by coupling surface (Eqs. [A.3] – [A.5], [A.18] and [A.19] of Grant, 2001a) energy exchange to subsurface conductive, convective and latent heat transfers using a forward differencing scheme with heat capacities and thermal conductivities calculated from de Vries (1963) (Eqs.[A.24]) - [A.27] of Grant, 2001a).

Surface sensible heat fluxes (Grant, 2001a) are modeled in *ecosys* as:

(1) Canopy - Sensible heat from temperature differences between the plant canopy and the atmosphere (Eq. [A.5] of Grant, 2001a).

(2) Soil and residue surfaces - Sensible heat from temperature differences between the soil and residue surfaces and the atmosphere (Eq. [A.19] of Grant, 2001a).

Surface latent heat fluxes (Grant, 2001a) are modeled in *ecosys* as:

(1) Canopy – Latent heat (transpiration) from vapor pressure differences between mesophyll surfaces and the atmosphere (Eq. [A.3] of Grant, 2001a).

(2) Canopy – Latent heat (evaporation) from vapor pressure differences between wet canopy surfaces and the atmosphere (Eq. [A.4] of Grant, 2001a).

(3) Soil and residue surfaces – Latent heat (evaporation) from vapor pressure differences between soil and residue surfaces and the atmosphere (Eq. [A.18] of Grant, 2001a).

For climate change scenarios, rising T_a in *ecosys* (Grant, 2001a,b) causes:

(1) An increased influx of sensible heat into the canopy (Eq. [A.5] of Grant, 2001a) and soil (Eq. [A.19] and [A.26] of Grant, 2001a) thereby raising canopy temperatures (T_c) and T_s.

(2) Higher vapor pressure differences between (1) canopy mesophyll surfaces and the atmosphere (transpiration) (Eq. [A.1] and [A.3] of Grant, 2001a), (2) wet canopy surfaces and the atmosphere (evaporation) (Eqs.[A.1] and [A.4] of Grant, 2001a), (3) soil and residue surfaces and the atmosphere (evaporation) (Eqs.[A.18] of Grant, 2001a), and (4) latent heat loss due to subsurface heat and water transfer (Eqs. [A24] – [A25] and [A.27] of Grant, 2001a). Subsequently, this leads to higher latent heat fluxes from the canopy and soil.

6.2.2.1.2 Effect of rising soil temperatures on N_2O emissions

Rising T_s in *ecosys* accelerates microbial activity and therefore lead to a more rapid demand for O_2 (Eqs. [2.2], [2.3a,b], [2.13] and [2.14a,b]), through the Arrhenius function in Eqs. [2.1] & [2.12]. Aqueous O_2 concentrations at nitrifier microsites ($[O_{2mi,n}]$ in Eqs. [2.3a,b] and [2.7a,b]) consequently decline with respect to the Michaelis-Menten constant for O_2 uptake (K_{O2n} in Eqs. [2.3b] and [2.7b] [2.14]), therefore O_2 uptake by nitrifiers $R_{O2i,n}$ in Eqs. [2.3a] and [2.7a]) fails to meet O_2 demand (Eqs. [2.2] and [2.6]). This results in the need for alternative electron acceptors (Grant and Rochette, 1994; Grant, 1995) and therefore transition to reduction of NO_2^- (nitrifiers) (Eq. [2.10]) and NO_3^- (denitrifiers) (Eq. [2.11] – [2.18]) in *ecosys*, accelerating production of N_2O. N_2O production may increase further with higher temperature because gaseous solubility (Eq. [A30] in Grant et al., 2006) is lower and hence aqueous O_2 ($[O_{2s}]$) maintained at microbial microsites (Eqs. [2.3], [2.7] and [2.14]) declines with respect to K_m for uptake. The solubility of N_2O also decreases, therefore accelerating the release of previously accumulated aqueous N_2O in the soil profile (Eqs. [A30], [A33] and [A36] of Grant et al., 2006).

6.2.2.2 Soil water content

6.2.2.2.1 Transport of water (Grant and Pattey, 2003; Grant et al., 2004) - Effect of changes in precipitation, air temperature and CO_2 levels on soil WFPS

Ecosys (Grant, 2001a) will also capture the effect of changes in precipitation on N_2O emissions since precipitation inputs into the model influences soil WFPS, which in turn controls emissions according to a "threshold response". Rainfall events in *ecosys* lead to surface flow and subsurface flow (e.g. Grant and Pattey 2003; Grant, 2004; Eqs. [2.21] and [24] and [A94 - A96] of Grant et al., 2004) among interconnected grid cells in *ecosys*, each having defined slopes and aspects from which relative elevations were computed. Surface flow in the model is calculated as the product of runoff velocity v, depth of mobile surface water d, and width of flow paths L in west to east x and north to south y directions for each landscape position x,y (Eq. [2.21]). Runoff velocity (Eq. [2.22]) is calculated in x and y directions for each x,y from the hydraulic radius R (Eq. [2.23]), from slope s, and from Manning's roughness coefficient z_r calculated from microtopographic roughness and particle size according to Morgan et al. (1998). The depth of mobile surface water d in Eq. [2.23] is the positive difference between the surface water d_w + ice d_i and the maximum depth of surface water storage. Changes in the depth of surface water d_w arise from differences in surface flows among adjacent landscape positions.

Surface water accumulates in *ecosys* when precipitation is greater than infiltration, determined from water fluxes through soil profiles. These fluxes (Q_w in Eq. [2.24]) are calculated as the product of hydraulic conductance (K') and water potential (ψ)

differences in west to east x, north to south y and vertical z directions for each landscape position x, y, z. Water potentials are the sum of matric, osmotic and gravitational components. $K'_{(x,y,z)}$ is calculated from hydraulic conductivities of adjacent landscape positions (Eqs. [41a], [42a] and [43a] of Grant and Pattey, 2003). However, if ψ of one position exceeds the air entry potential (ψ_e), $K'_{(x,y,z)}$ is calculated from saturated hydraulic conductivities while $\delta\psi_{(x,y,z)}$ is calculated across the wetting front caused by saturated flow. Water movement between adjacent landscape positions thus alternates between Richards and Green-Ampt flow depending upon ψ vs. ψ_e in each position. Topographically-driven flows of water and solutes in *ecosys* (e.g. Grant and Pattey 2003; Grant, 2004) are, as a result of lateral water redistribution, due to differences in gravitational water potential. Surface and subsurface flows of water in the model subsequently determine WFPS in soils.

In *ecosys* (Grant, 2001a,b), rising T_a leads to greater loss of latent heat through higher vapor pressure differences (Eqs. [A.1], [A.3], [A.4] and [A.18] of Grant, 2001a). As a result, root water uptake (Eqs. [B1], [B2] and [B9] – [15] of Grant, 2001a) increase so that soil water potential (Eqs. [B.10] and [B15] of Grant, 2001a) and soil WFPS decline with rising T_a (especially in areas with low precipitation). Plants will respond by lowering the root (Eqs. [B.10] and [B15] of Grant, 2001a) and canopy water potential (ψ_{Ci}) (Eq. [A.3], [B1] and [B2] of Grant, 2001a) and raising stomatal resistance (Eqs [A.3] of Grant, 2001a; Eqs. [A.26] and [A.27] of Grant, 2004) by closing their stomates (Eqs. [B1], [B2] and [B9] – [15] of Grant, 2001a) to conserve water. These changes lead to lower canopy-root-soil water potential gradients (Grant, 2001a). Consequently,

transpiration (Eq. [A.3] of Grant, 2001a) and total root water uptake modeled will be lower but will only partially offset effects of increased latent heat on WFPS (Eqs. [B1], [B2] and [B9] – [15] of Grant, 2001a). These changes will also constrain CO_2 diffusion into leaves thus lowering CO_2 mesophyll concentration ($\boldsymbol{C'_I}$ (μmol mol^{-1}) and subsequently CO_2 fixation (Eqs [A.20] – [29] of Grant, 2004). If precipitation is large enough, CO_2 fixation (Eqs [A.20] – [29] of Grant, 2004) under can increase rising T_a since it is modified by an Arrhenius function (Eqs [A.22] of Grant, 2004) of leaf temperature.

Increased latent heat loss under rising T_a is partially offset by increased water use efficiency (WUE) under rising CO_2 levels for the climate change scenarios (Grant et al., 1999; Grant et al., 2001a). Higher CO_2 levels will decrease transpiration thus improving WUE in the model (e.g. Grant et al., 1999; Grant et al., 2001a,b; Grant et al., 2003; Grant et al., 2005; Li et al., 2004). This decrease is attributed to higher mesophyll CO_2 concentration (C_I (μmol mol^{-1}) within each leaf, causing higher leaf stomatal resistances (Eqs. [A.26] and [A.27] of Grant, 2004) (section 6.2.2.3.1 below). As a result, greater CO_2 fixation (Eqs [A.20] – [29] of Grant, 2004) can occur at lower soil WFPS and less latent heat (Eqs. [1] and [A.3] of Grant, 2001a) is lost with higher leaf resistances (Eqs. [A.26] and [A.27] of Grant, 2004), maintaining higher WFPS.

6.2.2.1.2 Effect of changes in soil water content on N_2O emissions

As mentioned earlier, precipitation, thus soil WFPS (Eq. [2.21]) and [2.24] and [A94 - A96] of Grant et al., 2004) can vary under climate change depending on the climate.

Ecosys simulates the "threshold response" of N_2O emissions to changes in WFPS whereby the D_g (Eq. [2.28]) of gases in the soil atmosphere is highly sensitive to changes in the soil's WFPS or θ_g (e.g., Grant, 1991; Grant et al., 1992; Grant et al., 1993c; Grant, 1994; Grant; 1995; Grant and Pattey, 1999; Grant and Pattey 2003; Grant et al., 2006; Grant and Pattey, submitted 2007). Scenarios in *ecosys* with higher precipitation levels lead to greater to surface flow (Eq. [2.21]) and subsurface flow (Eqs. [2.21] and [2.24] and [A94-A96] of Grant et al., 2004) thus, increases in WFPS (section 6.2.2.2.1). Larger WFPS cause declines in surface and subsurface gaseous diffusivity ($D_{g\gamma}$ in Eq. [2.28]), lowering gaseous O_2 ($[O_{2g}]$) in the soil profile and slowing dissolution of O_{2g} to O_{2s} (Eq. [A30] in Grant et al., 2006). Consequently (also due to other interacting factors e.g. temperature, N fertilizer etc.), nitrifier demand for electron acceptors unmet by O_2 is transferred to NO_2^- ($R'_{NO2i,n}$ in Eq. [2.9]), which is then reduced to N_2O ($R_{NO2i,d}$ in Eq. [2.10]) leading to rises in aqueous N_2O ($[N_2O_s]$). In the case of denitrifiers, lower $[O_{2s}]$ (Eqs. [2.14a,b]) raises the demand for alternative electron acceptors (Eq. [2.13]) that is first transferred to NO_3^-, which is reduced to NO_2^- ($R_{NO3i,d}$ in Eq. [2.17]). Any remaining demand is transferred to NO_2^-, which is reduced to N_2O ($R_{NO2i,d}$ in Eq. [2.18]), and any remaining demand thereafter was transferred to N_2O, which is reduced to N_2 ($R_{N2Oi,d}$ in Eq. [2.19]) (extremely wet conditions therefore can result in lower N_2O emissions).

In conditions with high future air temperatures and low precipitation, overall N_2O production ([Eqs. [2.10] and [2.18]) modeled can be lower due lower surface flow (Eq. [2.21]) and subsurface flow (Eqs. [2.21] and [2.24] and [A94-A96] of Grant et al., 2004) thus, lower WFPS (section 6.2.2.2.1) (section 6.2.2.2.1). Higher WUE under rising CO_2

can result in higher WFPS in *ecosys* (surface flow (Eq. [2.21]) and subsurface flow (Eqs. [21] and [24] and [A94 - A96] of Grant et al., 2004), which may increase N_2O production via nitrification (Eq. [2.10]) and denitrification (Eq. [2.18]).

6.2.2.3 Carbon availability

6.2.2.3.1 Gross primary productivity (CO_2 fixation) (Grant, 2004) - Effect of rising CO_2 levels and air temperatures on carbon availability

Fixation of CO_2 (Eqs. [20] – [29] of Grant, 2004) in *ecosys* (Grant 2001a,b) is calculated from coupled algorithms for carboxylation and diffusion (Grant, 2004). An initial carboyxlyation rate ($V'_{B,x,y,i,j,l,m,n,o}$) (Eq. [20] of Grant, 2004) is calculated as the lesser of CO_2 ($V_{C,x,y,i,j,l,m,n,o}$) and light-limited ($V_{J,x,y,i,j,k,l,m,n,o}$) reaction rates for each leaf surface defined by positions x and y, species i, branch j, node k, canopy layer l, azimuth m, inclination n and exposure (sunlit versus shaded) o, according to Farquhar et al. (1980) (Grant, 2004). $V_{C,x,y,i,j,l,m,n,o}$ (Eq. [21] of Grant, 2004) reaction rates is modified by a Michaelis-Menten function of a maximum reaction rate (V_{Cmax}) (μmol m^{-2} s^{-1}) (Grant 2001a; Grant, 2004). $V_{J,x,y,i,j,k,l,m,n,o}$ (Eq. [23] of Grant, 2004) is the product of electron transport rate (J (μmol^{-1} e^- m^{-2} s^{-1})) (Eq. [24] of Grant, 2004) and carboxylation efficiency (Y) μmol^{-1} CO_2 (μmol e^-)$^{-1}$) Eqs. [C.6] and [C.9] of Grant, 2004). Electron transport rate (Eq. [24] of Grant, 2004) is a rectangular hyperbolic function of a maximum rate (J_{max} in Eq. [25] of Grant, 2004) modified by an Arrhenius function for leaf temperature (f_J)) quantum efficiency (Q μmol e^- (μmol I)$^{-1}$) (Eq. [24] of Grant, 2004), absorbed irradiance (I μmol m^{-2} s^{-1}) (Eq. [19] of Grant, 2004; Grant et al., 2001c) and a shape coefficient (α) (Eq. [24] of Grant, 2004). An Arrhenius function of leaf temperature may be better suited

to capture the effects of temperature rises on CO_2 fluxes (Grant et al., 2005) as compared to models which do not use this function (e.g Liu et al., 1997; Chen et al., 1999).

CO_2 fixation (Eq. [20] of Grant, 2004) is then used to calculate an initial leaf stomatal resistance (r'_L (s m^{-1})) (Eq. [26] of Grant, 2004) required to maintain a fixed gradient between CO_2 concentration in the canopy boundary layer (C_B (μmol mol^{-1})) and that in the mesophyll ($\boldsymbol{C'_I}$ (μmol mol^{-1}) set from C_B). The r'_L (Eq. [26] of Grant, 2004) rises exponentially with declining canopy turgor (ψ_T (MPa) (Eq. [27] of Grant, 2004). Leaf resistance from Eq. [27] of Grant (2004) is used to calculate a mesophyll CO_2 concentration (C_I (μmol mol^{-1}) for each leaf surface at which gaseous diffusion ($\boldsymbol{V_G}$ (μmol mol^{-1} m^{-2} s^{-1}) (Eq. [29] of Grant, 2004) equals a final carboxylation rate (V_B) calculated from C_I (similar to initial carboyxlation rate V'_B was calculated from C'_I (Eqs. [20] – [22] of Grant, 2004), because V_B rises less with C_B then does C_B - C_I equilibrium between V_B and $\boldsymbol{V_G}$. Therefore, under increase C_B requires increased leaf resistance leading to decreased latent heat in section 6.2.2.1.1 Gross primary productivity (GPP) is the sum of all $V_{Bi,j,k,l,m,n,o}$ for each x,y (Grant, 2004).

Nutrient uptake in *ecosys* is calculated by solving for aqueous concentrations of NH_4^+, NO_3^- and $H_2PO_4^-$ at root and mycorrhizal surfaces at which convective + diffusive radial transport from the soil solution to the surfaces (Eqs. [39a] of Grant, 2004) equals active uptake (e.g. Eq. [39b] of Grant, 2004 for uptake of NH_4^+ (R_{NH4}; g N m^{-3} h^{-1})). The products of N and P uptake are added to root and mycorrhizal storage pools from which they are combined with storage C during plant growth (Eq. [18] of Grant, 2004). The

ratios of N and P to C in the storage pools determine those of N and P to C in new leaf growth, which in turn determines GPP (Eqs. [22] and [25] of Grant, 2004; Grant et al., 2001a). As a result, more rapid CO_2 fixation (Eq. [20] of Grant, 2004) under climate change in the model may lead to more rapid (e.g. Eq. [39b] of Grant, 2004 for uptake of NH_4^+ (R_{NH4}; g N m^{-3} h^{-1})) in order to maintain N and P to C ratios in storage pools and new leaf growth.

The carbohydrate product of GPP from Eq. [29] of Grant (2004) is added to C storage pools in each branch, some of which is transferred along concentration gradients to storage pools in each root layer (Grant, 2001a). If the C storage pool is depleted, actual respiration rate (R_a) (Eq. [31] of Grant, 2004) may become less than maintenance respiration rate (R_m) (Eq. [36] of Grant, 2004), in which case the difference is made up through respiration of remobilizable C in leaves or roots. Upon exhaustion of the remobilizable C in each root or leaf, the remaining C is lost from the branch or root axis as litterfall (Eqs. [29] – [37] of Grant, 2004) and added to residue at the soil surface or in the soil layer where it undergoes decomposition (heterotrophic respiration) (Eqs. [8] – [19] of Grant, 2004). As a result, more rapid CO_2 fixation (Eq. [20] of Grant, 2004) in the model under climate change may lead to more litterfall production (Eqs. [29] – [37] of Grant, 2004) thus, more rapid heterotrophic respiration (Eqs. [8] – [19] of Grant, 2004).

For climate change scenarios, rising CO_2 in *ecosys* increases gross primary productivity (GPP) (CO_2 fixation) (Eqs. [20] – [29] of Grant, 2004) as well as litterfall (Eqs. [29] – [37] of Grant, 2004). Grant et al. (2001a) showed that wheat phytomass was larger when

treated with 548 versus 362 μmol mol^{-1} of CO_2. However, since CO_2 fixation in *ecosys* is modified by a Michaelis-Menten function, fixation increases at a decreasing rate up to a maximum reaction rate (V_{cmax}) (μmol m^{-2} s^{-1}) (Eqs. [6.7] – [6.8]). N uptake (e.g. Eq. [39b] of Grant, 2004 for uptake of NH_4^+ (R_{NH4}; g N m^{-3} h^{-1}) in the model occurs because of the demand for N to combine with storage C during plant growth (Eq. [18] of Grant, 2004) and for new leaf growth, which in turn determines GPP (Eqs. [22] and [25] of Grant, 2004; Grant et al., 2001a).

CO_2 fixation (Eqs. [20] – [29] of Grant, 2004) can increase or decrease at high T_a in the model (Grant et al., 2001b; Grant et al., 2005) since the V_{cmax} (Eqs. [20] and [21]) of Grant, 2004) in the model is modified by an Arrhenius function (Eq. [6.8]) for leaf temperature with terms for low and high temperature inactivation. Subsequently, this will determine C availability for N_2O production via denitrification under rising T_a (Eqs. [2.11] - [2.18]).

6.2.2.3.2 Effect of higher carbon availability on N_2O emissions

Greater CO_2 fixation (Eqs. [20] – [29] of Grant, 2004) in *ecosys* will result in larger litterfall (Eq. [29] - [37] of Grant, 2004), thus more microbial respiration (Eq. [8] and [9] of Grant, 2004) of organic matter, to produce substrates (dissolved organic carbon (DOC) for N_2O production via denitrification (Eqs. [2.16] – [2.18]). Greater CO_2 fixation (Eqs. [20] – [29] of Grant, 2004) in the model can lead to larger N uptake (Eqs. [39a]; e.g. Eq. [39b] of Grant, 2004 for uptake of NH_4^+ (R_{NH4}; g N m^{-3} h^{-1})) thereby resulting in overall

low soil mineral N. NH_4^+ concentration ($[NH_4^+]$) (Eq. [2.1] – [2.4]) drives nitrification reaction rate and NO_3^- concentration ($[NO_3^-]$) (Eq. [2.16] - [2.17]) drives denitrification reaction rate through K_m terms. Consequently, low soil mineral N may lead to lower N_2O production via nitrification (Eq. [2.10]) and denitrification (Eq. [2.10]).

Projections of N_2O emissions are complex since future increase or decrease in emissions will be determined by a combination of these climate changes (CO_2, temperature and precipitation) and other site-specific conditions (land use changes, soil type, topography etc.). These predictions show the importance of using a process – based model such as *ecosys*.

6.3 METHODOLOGY

6.3. 1 Model Experiment

Ecosys (Grant, 2001a,b) mathematical model was used to predict future temporal and spatial variability of N_2O emissions for the Ottawa study site (chapters 4 - section 4.3.1, chapter 5 – section 5.3.1), under different climate change scenarios derived from Scott et al. (2002) (Table 6.1).

Table 6-1: Climate change scenarios used in *ecosys* used to predict future temporal and spatial variability of N_2O emissions for the Ottawa study site.

Model scenarios	Year	Temperature increase (^oC)	CO_2 concentration (ppm)
Current climate			
(1)	2004	0	370
Climate change			
(2)	2020	0.5	400
(3)	2050	1	480
(4)	2080	2.5	560

Note: Precipitation and relative humidity (RH) (2004) remained unchanged for climate change scenarios

We first examined N_2O emissions of all scenarios (Table 6-1) at the patch (grid cell) scale to examine temporal variability in climate change effects on N_2O emissions, then the 2050 scenario at the field scale to examine both temporal and spatial variability effects on emissions.

6.3.1.1 Future temporal variability of N_2O emissions (one grid cell simulations)

6.3.1.1.1 Current climate

The current scenario (Table 6-1) was the same as that of the Ottawa model experiment (chapters 4 - section 4.3.2, chapter 5 – section 5.3.2). Modeled soil temperature and water content simulated by *ecosys* (Grant, 2001a,b) for the current scenario, have already been tested against continuous soil temperature (thermistor) and WFPS (time domain reflectometry (TDR)) measurements (chapter 4, section 4.4.1). The model was also tested earlier against measured N_2O emissions from chamber (site scale) and micrometeorological (fetch scale) measurements. Soil chemical and physical properties of an Orthic Humic Gleysol (section 4.3.2, Table 4-1) located at the study site, were used for the simulation. A 4-year model run was used to represent the agricultural history of the site in 2001 and 2002 (corn fertilized at 155 kg N ha^{-1}) and in 2003 (spring wheat fertilized at 78 kg N ha^{-1}) prior to the experiment in 2004. For 2004 experimental year, urea fertilizer was applied on May 4th at 112 kg N ha^{-1} and canola (*B. napus*) was planted at 7.2 kg ha^{-1} on May 7th, and harvested on September 1st and 2nd, 2004. All biological transformations were solved on an hourly time step (Eqs. [2.1-2.20]); water fluxes (Eqs. [2.21-2.26]) were calculated 25 times per time step and gas fluxes (Eqs. [2.27-2.28]) were calculated 500 times per time step, assuming constant surface boundary conditions during each hour. No adjustments of parameters were made to fit the model to the field site. All model parameters remained unchanged from earlier studies (e.g. Grant and Pattey, 2003; Grant et al., 2006).

6.3.1.1.2 Climate change scenarios

The climate change scenarios were simulated in *ecosys* by:-

(1) Adding the climate change air temperature increment to all hourly temperatures of the current scenario.

(2) Using a multiplier for current CO_2 concentration to generate the climate change CO_2 concentration.

6.3.1.2 Future temporal and spatial variability of N_2O emissions (field – scale simulations, 400 grid cells, 42 ha)

To examine future temporal and spatial variability of N_2O emissions, the 2050 climate change run (Table 6 - 1) described in section 6.3.1.1.1 was repeated using *ecosys* (Grant, 2001a,b), at a field scale. The experimental field was represented in *ecosys* as a 20 x 20 matrix of 36m x 36m grid cells rendered in ArcGIS from a digital elevation model (DEM) of the field. Boundary conditions included surface run-off through the north, east, south and west boundaries and subsurface drainage through the lower boundary of the landscape. Field topography was simulated from the slope and aspect of each grid cell, obtained in ArcGIS from the DEM. Same as the Ottawa model experiment 4-year run (chapters 4 - section 4.3.2, chapter 5 – section 5.3.2), urea fertilizer was applied on May 4th at 112 kg N ha^{-1} to different topographic sections of the field, to compare with N_2O emissions in 2004.

6.4 RESULTS

6.4.1 Using *Ecosys* mathematical model to simulate climate change impact on soil temperature, water content and C availability and the influence of these changes on N_2O emissions (one grid cell)

N_2O emissions in *ecosys* (Grant, 2001a,b) were produced via nitrification (Eq. [2.10]) and denitrification (Eq. [2.18]) due to a combination of changes in soil temperature, soil water content, C availability and fertilizer application. Hourly modeled emissions derived from *ecosys* (Grant, 2001a,b) for the current climate scenario (2004) (Table 6-2) were tested earlier (chapters 5, section 5.4.1) against chamber measurements (grid cell scale) at 4 different sites within the same field, with 4 replicates per site. Results showed that *ecosys* captured the main emission events during the season, with modeled seasonal totals (DOY 140 - 191) of 57 mg N m^{-2} and measured ones of 62 mg N m^{-2}, averaged across the 4 sites (chapter 5, Table 3-3). Modeled emissions during DOY 146-147 (Figure 6-2d) were suppressed by low soil temperatures (Figure 6-1b) which led to a low EF in 2004 (Table 6-2).

6.4.1.1 Soil temperature

Modeled soil temperature simulated by *ecosys* (Grant, 2001a,b) for the current scenario (Table 6-1) was similar to that of continuous thermistor measurements (chapter 4, section 4.4.1). For the climate change scenarios, rising air temperatures (T_a) in *ecosys* (Grant, 2001a,b) led to greater conductive, convective and latent heat transfers at the soil surface (Eqs.[A.1] - [A.6] and [A.17] - [A.23] of Grant, 2001a; also Grant et al., 1999b; Grant and Baldocchi, 1992; Grant et al., 1993d; 1995a,c; 1999a; Grant et al., 1995b) and thereby greater heat transfers through the soil profile (Eqs. [A.24]) - [A.27] of Grant,

2001a). This led to higher modeled T_s for climate change scenarios compared to that of current climate (2004) (Figure 6-1b,f).

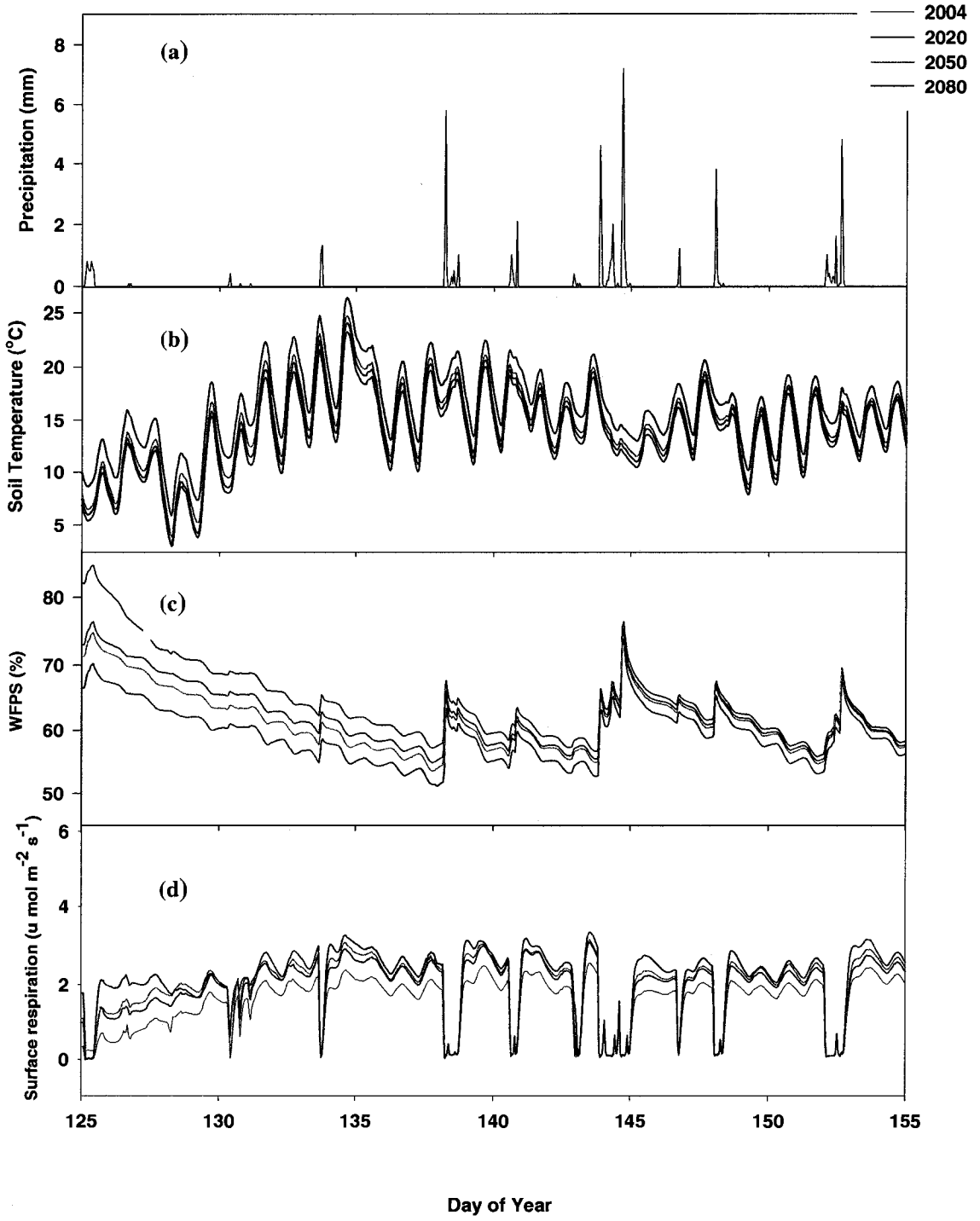

Figure 6-1: (a) Precipitation (b) modeled soil temperatures (10cm) (c) modeled soil water-filled space (WFPS) and (d) modeled soil CO_2 flux (surface respiration) at Ottawa canola field for different climate change scenarios (DOY 120 – 155).

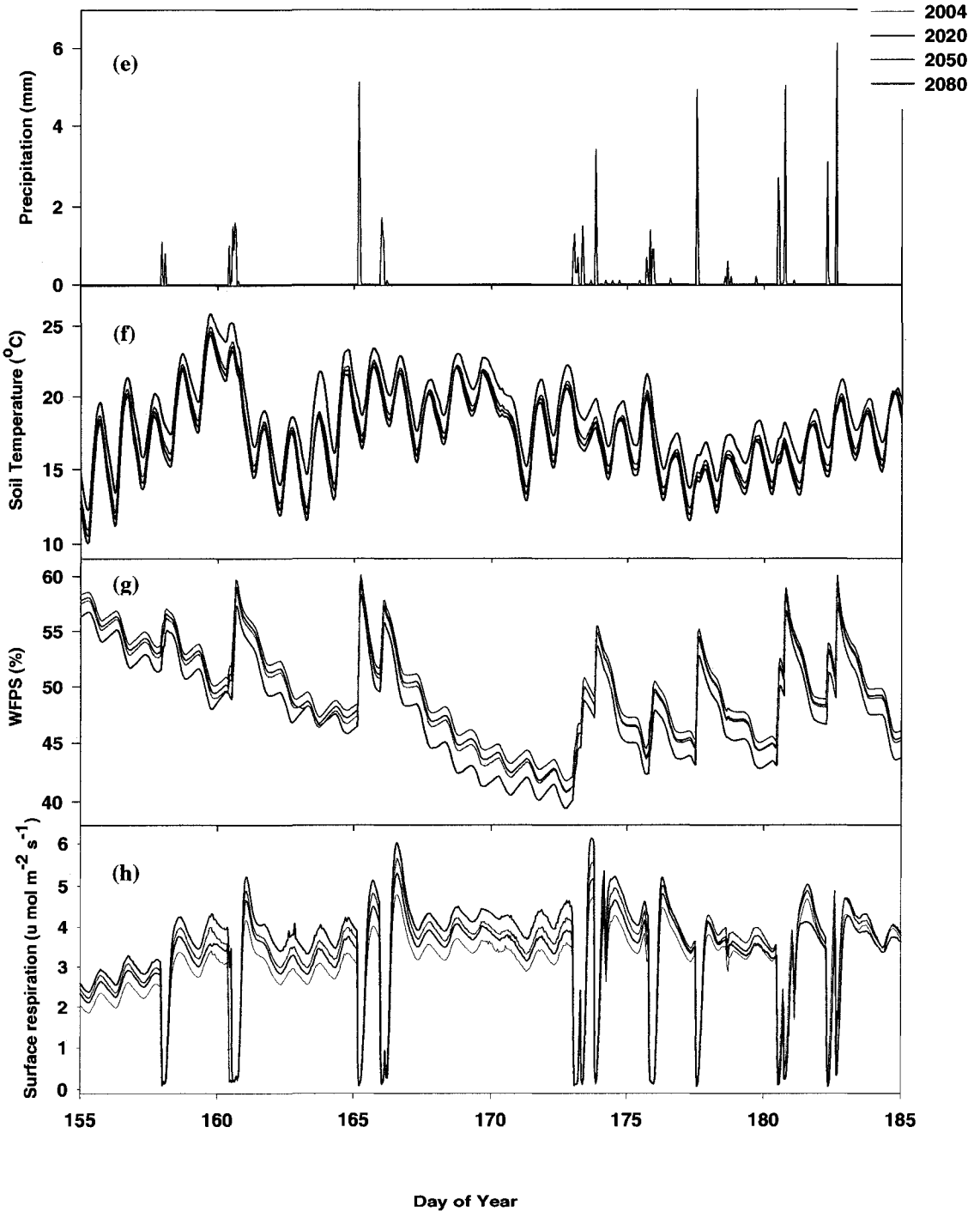

Figure 6-1 (cont'd): (e) Precipitation (f) modeled soil temperatures (10cm) (g) modeled soil water-filled space (WFPS) and (h) modeled soil CO_2 flux (surface respiration) at Ottawa canola field for different climate change scenarios (DOY 155 – 185).

Table 6-2: Modeled annual fertilizer emission factors (EFs) (including snowmelt) derived from *ecosys* simulations under current and climate change scenarios (one grid cell)

Model scenarios	Year	Temp-erature (°C) increase	CO_2 concen-tration (ppm)	N_2O emissions (112 kg N ha^{-1})	N_2O emissions (control)	Annual EFs (%)
				(mg N m^{-2} yr^{-1})		
Current						
(1)	2004		370	123	89	0.31
Climate change						
(2)	2020	0.5	400	152	85	0.59
(3)	2050	1	480	162	84	0.70
(4)	2080	2.5	560	98	61	0.32

***Annual EFs -Calculated as N_2O emissions attributed to fertilizer application minus those of the control, divided by the total N fertilizer applied.**

Higher temperatures for the 2050 climate change scenario led to larger N_2O emissions (Figure 6-2d) and EFs (Table 6-2) compared to those of 2004 and 2020 scenarios. This trend occurred because soil warming in *ecosys* led to a greater reduction in the aqueous solubility of O_2 (Eq. [A30] in Grant et al., 2006), thus slowing the dissolution of O_{2g} to O_{2s} (Eq. [A30] in Grant et al., 2006) therefore lowering $[O_{2s}]$ that sustained O_2 uptake by microbial populations (Eqs. [2.3], [2.7] and [2.14]). Higher soil temperatures also led to an increase in microbial activity and therefore a higher demand for O_2 (Eqs. [2.2], [2.3a,b], [2.13] and [2.14a,b], through the Arrhenius function in Eqs. [2.1] & [2.12] as evidenced by higher CO_2 emissions (Figure 6-1d,h). Aqueous O_2 concentrations at nitrifier microsites ($[O_{2mi,n}]$ in Eqs. [2.3a,b] and [2.7a,b]) declined with respect to the Michaelis-Menten constant for O_2 uptake (K_{O2n} in Eqs. [2.3b] and [2.7b] [2.14]),

therefore O_2 uptake by nitrifiers $R_{O2i,n}$ in Eqs. [2.3a] and [2.7a]) failed to meet O_2 demand (Eqs. [2.2] and [2.6]). Subsequently, alternative electron acceptors were used to produce N_2O (Figure 6-2d) in *ecosys* via nitrification (Eq. [2.10]) and denitrification (Eq. [2.18]).

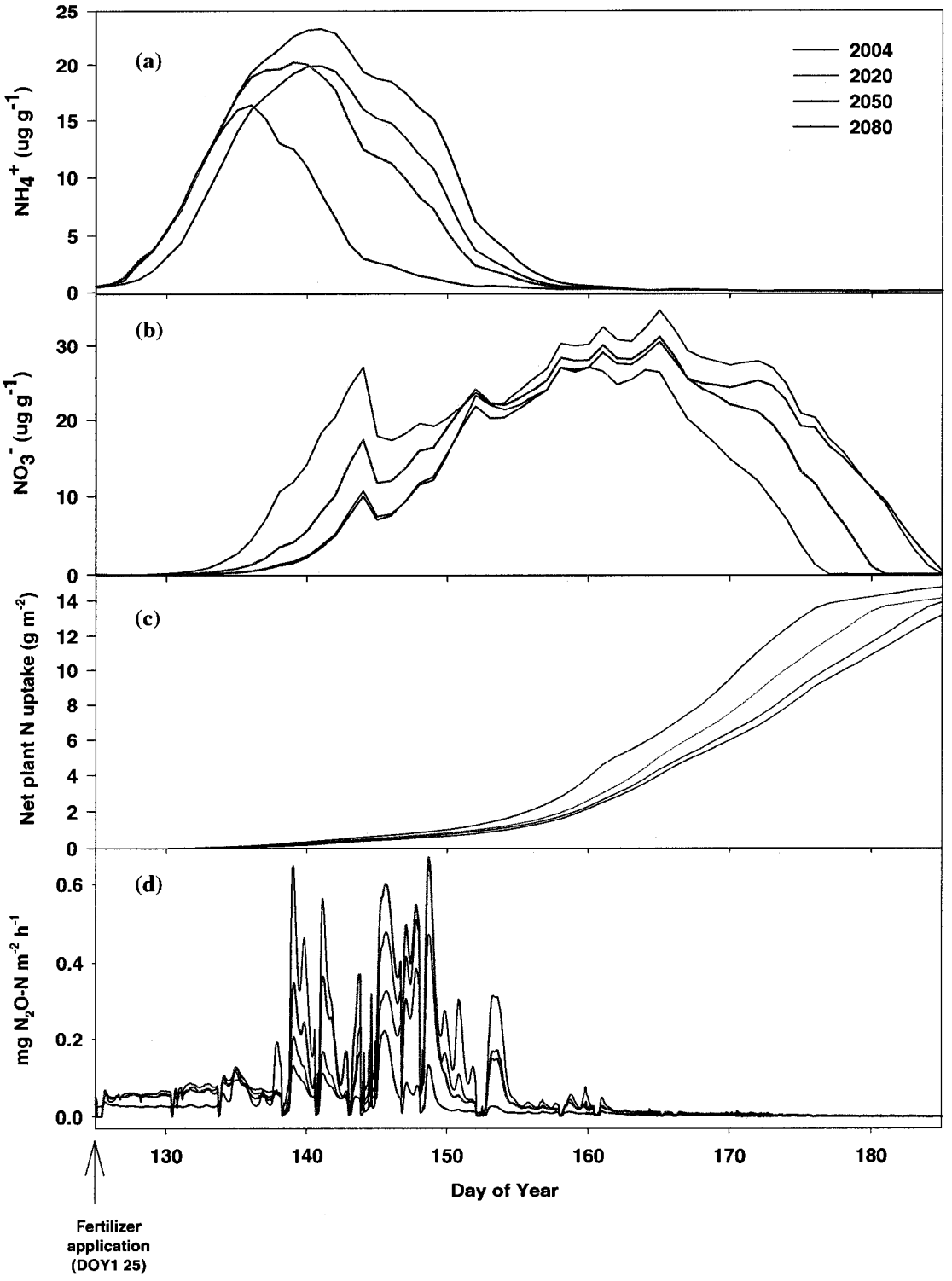

Figure 6-2: Modeled (a) Soil NH_4^+ (b) and NO_3^- (10cm) (c) net plant N uptake and (d) N_2O emissions at Ottawa canola field, for different climate change scenarios.

The seasonal pattern of N_2O emissions (Figure 6-1d) from the climate change scenarios were different from that of the current climate due to higher temperatures (Figure 6-1b,f). Higher air temperatures (Figure 6-1) for the climate change scenarios (Table 6-1) also resulted in earlier and more rapid modeled net plant uptake (e.g. R_{NH4} (g N m^{-3}) of Eqs. [39a,b] of Grant, 2004; Figure 6-2,c) because of more rapid active uptake of NH_4^+ and NO_3^- at root and mycorrhizal surfaces (Eq. [39b] of Grant, 2004), through an Arrhenius function of soil temperature (f_{tr}) as in Eqs. 30 of Grant, 2004. Also, net plant N uptake was earlier for the climate change scenarios due to earlier soil warming compared to that of the current climate.

6.4.1.2 Soil water content

Modeled temporal variability of WFPS was similar to measured results (time domain reflectometry (TDR) readings) however, the spatial variability of modeled WFPS was less than that of measured results. The highest modeled T_s (Figure 6-1b,f) for the 2080 scenario resulted in the earliest onset of snowmelt (Eqs. [A.27 of Grant, 2001a) thus the highest surface (Eq. [2.21]) and subsurface flow (Eqs. [21] and [24] and [A94 - A96] of Grant et al., 2004). Consequently, these changes resulted in the largest WFPS for the 2080 scenario during the snowmelt period (~DOY 60 - 104, data not shown) versus those of the other climate change scenarios. However, the 2080 scenario had the lowest WFPS (Figure 6-1c,g) during spring/summer periods, due to greater loss of latent heat. In *ecosys*, latent heat loss was accelerated through higher vapor pressure differences between (1) canopy mesophyll surfaces and the atmosphere (transpiration) (Eqs. [A.1] and [A.3] of Grant, 2001a) (2) wet canopy surfaces and the atmosphere (evaporation) (Eqs. [A.1] and [A.4] of Grant, 2001a) (3) soil and residue surfaces and the atmosphere (evaporation) (Eq. [A.18] of Grant, 2001a) and (4) latent heat loss due to subsurface heat and water transfer (Eqs. [A24] – [A25] and [A.27] of Grant, 2001a). However, increased latent heat loss was partially offset by reduced transpiration due to greater leaf stomatal resistance (Eq. [A.3] of Grant, 2001a; Eqs. [26] and [27] of Grant, 2004) as a result of higher CO_2 levels for the climate change scenarios.

Urea was hydrolyzed in *ecosys* (Grant, 2001a,b) to produce [NH_{3s}] (NH_{3s} and NH_4^+ are in dynamic equilibrium) during DOY 125 - 140 following application on May 4th (DOY 125), for all model scenarios (Figure 6-2a). Nitrification during DOY 136 -158 caused a

rapid decline in NH_4^+ and increase in NO_3^- (Figure 6-2a,b), which coincided with the largest emission events (Figure 6-2d) for the season. These changes were attributed in the model to rapid oxidation of NH_{3s} and reduction of O_2 by nitrifiers to produce NO_2^- (Eqs. [2.1] – [2.4]). This drove the oxidation of NO_2^- and reduction of O_2 by nitrifiers to produce NO_3^- (Eqs. [2.5] – [2.8]); (Figure 6-2b). This oxidation occurred because of overall declining WFPS (Figure 6-1c,g) for all scenarios whereby the diffusivity (D_{gy} in Eq. [28]) of O_2 into the soil at ≈ 60% WFPS, thus gaseous O_2 ($[O_{2g}]$) in the soil profile and dissolution of O_{2g} to O_{2s} (Eq. [A30] in Grant et al., 2006), were rapid enough to meet the demands of nitrifiers. This provided NO_2^- for N_2O production via nitrification (Eq. [2.10]) and NO_3^- for N_2O production via denitrification (Eq. [2.18]). Peak modeled emissions events occurred earliest (DOY 139 - 147) for the 2080 scenario compared to those of 2004, 2020 and 2050 scenarios (DOY 146 - 154) (Figure 6-2d). This trend was attributed in *ecosys* to earlier nitrification (Eqs. [2.1] – [2.8]; DOY 136 -150) in 2080 versus other scenarios (DOY 140 – 158) as a result of earlier decline in soil WFPS and earlier rise in T_s (Figure 6-1c). Therefore, substrates were available earlier for N_2O production via nitrification (Eq. [2.10]) and denitrification (Eq. [2.18]). Decline in NO_3^- co-incided with plant N uptake (Eqs. [19], [30] – [33], [39a,b] – [42] of Grant, 2004; Figure 6-2,c) for all model scenarios.

N_2O emissions (Figure 6-2d) generally followed rainfall (Figure 6-1a) and increase in WFPS (Figure 6-1c) during nitrification (Figure 6-2a,b) (seen as decline in NH_4^+ and increase in NO_3^-). Generally, rainfall events e.g. during DOY 139 - 154 (Figure 6-1a) led to increases in WFPS (Figure 6-1c), which caused declines in surface and subsurface

gaseous diffusivity ($D_{g\gamma}$ in Eq. [2.28]), lowering gaseous O_2 ($[O_{2g}]$) in the soil profile and slowing dissolution of O_{2g} to O_{2s} (Eq. [A30] in Grant et al., 2006). Aqueous O_2 concentrations at nitrifier microsites ($[O_{2mi,n}]$ in Eqs. [2.3a,b] and [2.7a,b]) declined with respect to the Michaelis-Menten constant for O_2 uptake (K_{O2n} in Eqs. [2.3b] and [2.7b] [2.14]), therefore O_2 uptake by nitrifiers $R_{O2i,n}$ in Eqs. [2.3a] and [2.7a]) failed to meet O_2 demand (Eqs. [2.2] and [2.6]). Subsequently, alternative electron acceptors were used to produce N_2O in *ecosys* via nitrification (Eq. [2.10]) and denitrification (Eq. [2.18]).

Emissions (Figure 6-2d) and EFs (Table 6-2) were generally lowest for the 2080 scenario compared to the other climate change scenarios because WFPS (Figure 6-1c,g) was generally lowest for the spring and summer periods. Consequently, this led to larger surface and subsurface gaseous diffusivity ($D_{g\gamma}$ in Eq. [2.28]) of ($[O_{2g}]$), thus greater dissolution of O_{2g} to O_{2s} (Eq. [A30] in Grant et al., 2006). As a result, more O_2 was available for (1) oxidation of NO_2^- (Eqs. [2.5]- [2.8]) and (2) oxidation of DOC by heterotrophs (Eqs. [2.12]- [2.15]), thus less N_2O was produced via nitrification (Eq. [2.10]) and denitrification (Eq. [2.18]).

For all scenarios, emissions modeled in the field e.g. on DOY 154 (Figure 6-2d) were delayed for several hours following rainfall e.g. on DOY 153 (Figure 6-1d). Re-establishment of gaseous pathways during drainage led to subsequent emissions. Even though there was rainfall later in the crop season e.g. on DOY 165 (Figure 6-1f), and thus increase in WFPS (Figure 6-1g), little or no emissions were modeled after DOY 160 for any climate change scenario (Figure 6-2d). This was due to a decline in available NH_4^+

(Figure 6-2a) and consequent slowing of nitrification. NH_3 oxidation ($X_{NH3i,n}$ in Eq.[2.4]) was slowed by declining [NH_{3s}], thus the rate of NO_2^- reduction ($R_{NO2i,n}$, in Eq. [2.10]) also declined, leading to a reduction in N_2O generation (Eqs. [10] and [18]). The reduction in N_2O emissions later in the season was also attributed to the decline in WFPS (Figure 6-1g) caused by rising evapotranspiration.

6.4.1.3 Carbon availability

Higher atmospheric CO_2 levels for climate change scenarios (Table 6-1) led to more rapid CO_2 fixation (Eqs. [20] – [29] of Grant, 2004) which resulted in greater litterfall (Eqs. [29] - [37] of Grant, 2004). Modeled litterfall increased from 281 g C m^{-2} y^{-1} in 2004 to 487 g C m^{-2} y^{-1} in 2080. Greater litterfall (Eqs. [29] - [37] of Grant, 2004) led to more microbial respiration (Eq. [8] and [9] of Grant, 2004; Figure 6-1d,h) of organic matter and greater O_2 demand, to produce substrates (dissolved organic carbon (DOC) for N_2O production via denitrification (Eqs. [2.16] – [2.18]). Annual total soil respiration in *ecosys* increased from 497 g C m^{-2} y^{-1} in 2004 to 685 g C m^{-2} y^{-1} in 2080 (e.g. Figure 6-1d,h). Consequently, EFs (Table 6-2) were higher for the 2020 and 2050 climate change scenarios than for the current climate. In contrast, emissions were lower in 2020 and 2050 as well as from 2080 climate change scenarios without N (control runs) (Table 6-2) than those of 2004 because of more rapid CO_2 fixation (Eqs. [20] – [29] of Grant, 2004) in the *ecosys* due to higher CO_2 levels, thus more rapid N uptake (Eqs. [39a]; e.g. Eq. [39b] of Grant, 2004 for uptake of NH_4^+ (R_{NH4}; g N m^{-3} h^{-1}) which resulted in lower soil mineral N. Lower soil mineral in addition to the N limited environment in control runs, led lower

N_2O production via nitrification (Eq. [2.10]) and denitrification (Eq. [2.10]).

Emission factor was lower for 2080 because the effect of soil drying (Eqs. [A.1], [A.3], [A.4], [A.18], [A.24] – [A.25] and [A.27] of Grant, 2001a) (Figure 6-1c,g) on N_2O production (Eqs. [2.16] – [2.18]) outweighed the effect of greater litterfall (Eq. [29] and [37] of Grant, 2004) and microbial respiration (Figure 6-1d,h) caused by higher CO_2 levels and increase in T_s from higher T_a. However, the cumulative effect of litterfall on soil respiration may become apparent over several years, so that results should in future research be evaluated over longer time periods. Also, more rapid CO_2 fixation (Eqs. [20] – [29] of Grant, 2004) in the model for the 2080 scenario led to more rapid N uptake (Eqs. [39a]; e.g. Eq. [39b] of Grant, 2004 for uptake of NH_4^+ (R_{NH4}; g N m^{-3} h^{-1}); Figure 6-2c) later in the growing season, thereby resulting in overall lower soil mineral (Figure 6-2a,b) compared to the other scenarios. Consequently, N_2O production via nitrification (Eq. [2.10]) and denitrification (Eq. [2.10]) modeled for 2080, was lower after DOY 143 (Figure 6-2d).

6.4.2 Future spatial variability of N_2O (field – scale, 400 grid cells, 42 ha)

Hourly modeled emissions derived from *ecosys* (Grant, 2001a,b) for the current climate scenario (2004) (Table 6-3) were also tested earlier against continuous half - hourly micrometeorological tower measurements at a larger fetch scale (chapter 4 5.4.1; chapter 5, sections 5.4.1). Results showed that *ecosys* captured the main emission events during

the season, with modeled seasonal totals (DOY 128 - 194) of 81 mg N m^{-2} and measured of 87 mg N m^{-2} (chapter 4, Table 4-2).

A series of rainfall events in May 2004 e.g. DOY 139 - 154 (Figure 6-1d) led to increases in measured and modeled WFPS (Figure 6-1c). In *ecosys* (Grant 2001a,b), these events caused infiltration as well as topographically-driven surface flow (Eq. [2.21]) and subsurface flow (Eqs. [2.24] and [A94 - A96] of Grant et al., 2004) among the 400 interconnected grid cells in *ecosys* (Grant, 2001a,b) each having defined slopes and aspects from which relative elevations were computed. Topographically-driven flows of water and solutes in *ecosys* were as a result of lateral water redistribution due to differences in gravitational water potential. Consequently, WFPS (e.g. Figure 5-5, chapter 5) varied across the landscape, however, variation was small. This variation was caused by very small differences in topography, whereby grid cells both shed and received water at different areas of the field, as indicated by flow accumulation (FA) (Figure 5-1, chapter 5).

Similar to the current climate (Figure 6-3a; chapter 5), we found that redistribution in WFPS across the landscape resulted in spatial variation in N_2O emissions within the same treatment for 2050 (Figure 6-3b). The lowest topographic positions of the field gave the highest annual total emissions or were 'hot spots' for N_2O emissions (indicated in Figure 6-3a,b by pink arrow) since these areas had high FA values (Figure 5-1, chapter 5) and (e.g. Figure 5-5, chapter 5).

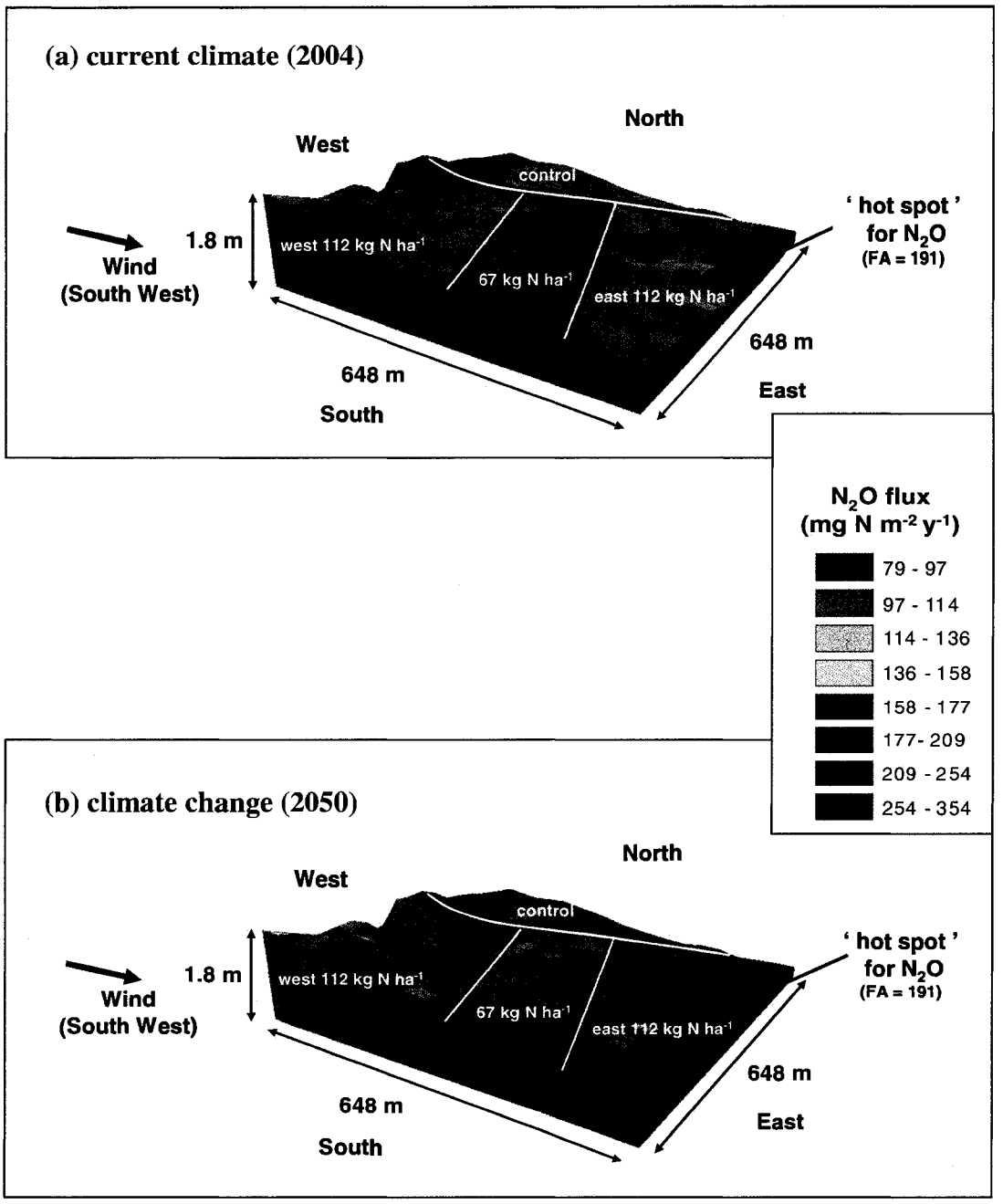

Figure 6-3: Modeled spatial variability of cumulative annual N_2O emissions for (a) current climate (2004) and (b) climate change scenario (2050), at Ottawa canola field.

The EF (Table 6-3) was larger for the 112 kg N ha^{-1} east fertilizer treatment compared to that of the 112 kg N ha^{-1} west, because the east section of the field had lower topography and thus higher range of FA values (Figure 5-1, chapter 5) and therefore had more 'hot spots' for N_2O (Figure 6-3). Overall, CSV of annual N_2O totals within the 112 kg N ha^{-1} was similar (18%) in 2050 to that of the current climate (25%) in 2004 (chapter 5). Also similar to the finding under current climate in 2004, these projected results for 2050 show that N_2O emissions thus EF may vary with small topographic differences (0.2% maximum slope) in a field, for the same fertilizer treatment.

Table 6-3: Modeled annual fertilizer emission factors (EFs) (including snowmelt) derived from *ecosys* simulations under current and climate change scenarios (400 grid cells = 42ha)

Model scenarios	Year	Temp-erature (°C) increase	CO_2 concen-tration (ppm)	N_2O emissions (112 kg N ha^{-1})		N_2O emissions (control)	Annual EFs (%)	
				(mg N m^{-2} yr^{-1})				
				§up-per	γlow-er		up-per	low-er
Current	2004		370	130	157	120	0.1	0.3
Climate change	2050	1	480	164	189	102	0.6	0.8

***Annual emission factors -Calculated as N_2O emissions attributed to fertilizer application minus those of the control, divided by the total N fertilizer applied.**

§represents west area of field (higher topography).

γ represents east area of field (lower topography).

EFs were 0.5% larger for the 2050 climate change scenario (Table 6-3) versus that of the current climate. This finding was due to combination of higher temperatures and CO_2

levels (discussed in section 6.4.1) for the 2050 scenario but partially offset by lower soil water content (Table 6-1; Figure 6b,f). However, emissions from the 2050 control run (Table 6-3) were the lower than 2004 because the higher CO_2 concentrations combined with the N limitation (discussed in section 6.4.1.3).

6.5 DISCUSSION

6.5.1 Using *Ecosys* mathematical model to simulate climate change impact on soil temperature, water content and C availability and the influence of these changes on N_2O emissions (one grid cell)

Earlier testing against measured data for the Ottawa experimental site (chapters 4 and 5) showed that *ecosys* (Grant, 2001a,b) represented the site-specific (past and present land use, climate, soil type, topography etc.) complex physical, chemical and biological hypotheses involved in N_2O production. Results from this chapter showed that ***ecosys* (Grant, 2001a,b) also predicted climate change impacts on future spatial and temporal variability of N_2O emissions for this site.** These findings allowed us to better understand how increasing CO_2 and temperature in the future may affect these complex N_2O hypotheses thus, the climate change feedback mechanisms involved in its generation. Results from this study showed that EFs may more than double by 2050; This is important since such results imply that we may need to re-estimate N_2O emissions from fertilization in future inventories.

Ecosys represented future temporal variability of N_2O emissions thereby providing further insights into the episodic ("threshold") nature of these emissions. Such temporal variability of N_2O throughout the season have been shown in previous studies (e.g. Grant et al, 1992; Grant and Pattey, 1999; Grant and Pattey, 2003; Grant et al., 2006) and also for the current climate scenario (chapters 4 and 5). This episodic nature of N_2O emissions shows the importance of linking biological controls of N_2O emissions to physical controls in mathematical models, hence the importance of processed - based model *ecosys* (Grant, 2001a,b), for simulating both current and future N_2O emissions. Current (e.g. Freibauer,

2003; Lu et al., 2006) and future (e.g. Roelandt et al., 2007) simulations of N_2O emissions based on empirical modeling, may not fully represent the large temporal variability of N_2O emissions.

The large temporal variability of current and future modeled results also showed the importance of simulating N_2O emissions at an hourly time-step versus daily or monthly time-step models, in order to better capture the timing and magnitude of the entire emission events. Due to the large temporal variability of N_2O emissions, calculation of EFs based on infrequent data (e.g. once – daily measurements or longer) may over- or under-estimate emissions depending on the time of day, time course of the emission event or time during the season when samples are taken. Consequently, our findings show the importance of hourly sampling during the entire growing season to fully capture the temporal variability of N_2O emissions, thus improving our confidence in estimates for greenhouse gas inventories.

6.5.1.1 Soil temperature

Generally, low EFs for 2004 (Tables 6-2; 6-3) for our study compared to those for Eastern Canada (0.83 - 1.67%) used in the IPCC Tier II Methodology (Hegalson et al., 2005), could be attributed to slightly overall lower average mean temperatures (March: 0°C, April: 5.5°C, May: 12.8°C and June: 17.1°C) compared to long-term normals for 1971 – 2000 (March: -2.5°C, April: 5.7°C, May: 13.4°C and June: 18.3°C) for our experimental area. In combination with early fertilization (4 May), delayed soil warming

in 2004 caused fertilizer – induced nitrification to occur in comparatively cool soils. Earlier modeling studies showed that if fertilization were delayed by just one week N_2O emissions would increase from 0.31% to 1.65% of fertilizer N (Metivier et al., 2007 (Submitted)). Early fertilization may therefore reduce emissions since nitrification of fertilizer N can occur in cooler soils (Metivier et al., 2007 (Submitted)).

Higher air temperatures (Figure 6-1) for the 2020 and 2050 climate change scenarios (Table 6-1) resulted in higher annual N_2O emissions (Table 6-2) than that for the current climate. Previous studies (e.g. Grant, 1995; and Smith et al., 1998; Grant & Pattey, 2007 (Submitted); Flechard et al., 2007) have shown that N_2O emissions are higher with higher soil temperatures. Our results showed that EF in 2004 (Table 2) was ~ 2.2 times larger in 2050 due to a 1°C temperature rise. Dobbie and Smith (2001) found similar results whereby emissions for an arable soil were nearly 16 – fold larger at soil temperature of 12°C compared to those at 5°C, with an apparent Q_{10} ~ 50, (corresponding to ~ 2.3 – fold increase in emissions for each 1°C temperature rise). Studies by Flechard et al. (2007) showed that a soil temperature increase from ~ 8 to 10°C can cause event-based EF to increase from ~ 0.25 to ~1%. The apparently large Q_{10} values from these studies may be related to physical controls governing the complex "threshold" response involved in N_2O production since most microbial processes have much smaller Q_{10} of 2 – 3. In *ecosys* the large response of N_2O emissions to T_s were simulated using biologically reasonable Q_{10} of ~ 2 in the Arrhenius functions controlling microbial reactions (Eqs. [2.1], [2.5] and [12]).

Peak modeled emissions events started and finished earliest (DOY 139 - 147) for the 2080 scenario (Table 6-1) compared to those of 2004, 2020 and 2050 scenarios (DOY 146 - 154) (Figure 6-2c) due to the earliest onset of snowmelt (Eqs. [A.27] of Grant, 2001a) and soil warming (Figure 6-1b,f). Our results suggest that emissions may be affected by the soil conditions under which nitrification of fertilizer occurs, as affected by temporal variability of temperature and WFPS, even if the same fertilizer rate was used. These results further support the use of *ecosys* mathematical model to fully capture the large temporal variability of N_2O emissions.

6.5.1.2 Soil water content

In contrast to 2020 and 2050, 2080 scenario gave the lowest annual N_2O emissions and EF was similar to that of the current climate (2004, no temperature increments). This trend occurred because nitrification (Eqs. [2.1] – [2.8]; Figure 6-2a,b) finished earlier and also the overall WFPS (Figure 6-1c,g) was lowest for the spring/summer months, compared to the other projections. There are few studies in the literature that examined the effect of soil warming on N_2O emissions. A study by Kamp et al. (1998) showed similar results to ours whereby total N_2O emissions were similar for the control (8 kg N_2O-N ha^{-1}) and heated plots (7.6 kg N_2O-N ha^{-1} – temperature increase of 3°C). Results from their (Kamp et al., 1998) study showed that soil moisture was lower for the heated plots. They also showed that N_2O emissions occurred earlier due to a 3°C increase in soil temperature (Kamp et al., 1998). A study by Peterjohn et al. (1994) showed that there were no significant differences in N_2O emissions between heated plots (temperature

increase of 5°C) and control plots probably due to the absence of soil NO_3^- and net nitrification.

6.5.1.3 Carbon availability

Higher CO_2 levels for the 2020 and 2050 climate change scenarios (Table 6-1) also contributed to higher EFs (Table 6-2) because of greater CO_2 fixation (Eqs. [20] – [29] of Grant, 2004). Grant et al. (1999) showed that under 550 μmol mol^{-1} CO_2 and low versus high irrigation, crop water relations in *ecosys* allowed the model to simulate a measured increase of 20 versus 10% in seasonal wheat biomass, and a measured decrease of 2 versus 5% in seasonal evapotranspiration (higher water use efficiency). Other studies (Ineson et al., 1998; Kettunen et al., 2005; 2006; 2007a,b) have also shown an increase in measured biomass production due to elevated CO_2. When conditions for denitrification were favorable (high N concentrations and high soil moisture), elevated CO_2 enhanced N_2O emissions (Kettunen et al., 2005; 2007a; 2007b (P = 0.085); (Kettunen et al., 2005 (P = 0.05)) due to greater C substrates produced by roots. Ineson et al. (1998) showed that elevated CO_2 resulted in a 27% increase in N_2O production as a result of root-derived available C. Bergstom et al. (1994) found that simultaneous additions of C and NH_4^+ enhanced N_2O emissions more than additions of NH_4^+ alone. In contrast, emissions from the 2080 fertilized and control run modeled (Table 6-2) were the lowest because these scenarios had the highest CO_2 concentrations thus greatest CO_2 fixation (Eqs [20] – [29] of Grant, 2004) therefore, more rapid N uptake. More rapid N uptake (g. R_{NH4} (g N m^{-3}) of Eqs. [39a,b] of Grant, 2004; Figure 6-2c) reduced soil mineral N thus decreasing overall N_2O production via nitrification (Eq. [2.10]) and denitrification (Eq. [2.10]). A

review (Barnard et al., 2005) showed that elevated CO_2 did not significantly alter N_2O fluxes measured in the field or laboratory in herbaceous or forest ecosystems and also emphasized the need for more climate change studies to provide further insights.

Our results also suggest that climate change may therefore require adjustments of fertilizer application and planting dates so that (1) fertilizer availability match crop uptake capacities i.e. take up NH_4^+, reduce nitrification (2) fertilization applications are conducted at lower soil temperatures to minimize loss of N through N_2O emissions (3) crops are planted earlier to maximize length of growing season. Our results are specific to all site conditions for the canola field at Ottawa (climate scenarios assumed constant land use), and emissions may therefore be different compared to those of other studies. However, in a sensitivity study of model results when fertilizer application and planting date were shifted a few days earlier in 2004 and harvesting date was advanced by 8 days in *ecosys* for the 2050 model scenario (Table 6-2), EF decreased from 0.7 to 0.6%. This reduction was attributed in the model to a combination of (1) nitrification of fertilizer N occurring in cooler soil (Chapter 4) and (2) extended growing season resulting greater N uptake (Eq. [A22] of Grant et al., 2006). Our findings show the importance of the use of processed - based mathematical model *ecosys* (Grant, 2001a,b), to fully represent the complex hypotheses involved in the prediction of N_2O emissions. Based on the available literature, no projections of climate change together with land use impact of N_2O emissions have been made for Canada. Our results can contribute to large scale studies where land use is considered. Other factors (e.g. N_2O emissions from manure

management, industries and the energy sector etc.) will also determine whether future emissions will increase or decrease.

6.5.2 Future spatial variability of N_2O (field – scale, 400 grid cells, 42 ha)

Ecosys represented future spatial variation of N_2O emissions at the field scale. Modeled results generally showed that for the same fertilizer treatment, the lowest topographic positions of the field gave the highest seasonal N_2O emissions (Figure 6-3) thus higher annual EF (Table 6-3) or were 'hot spots' for N_2O emissions. Generally, 'hot spots' became "hotter" with climate change (2004 versus 2050 annual total emissions: $R^2 = 0.9$; $P < 0.05$). Our results shows the importance of using a three-dimensional mathematical model *ecosys* (Grant, 2001a,b), with input from DEMs, in order to further understand the spatial and temporal variability of N_2O emissions thus improve our future estimates.

6.5.3 Future Prospects

Future modeling work will enable *ecosys* (Grant, 2001a,b) to scale N_2O emissions from landscape to regional and national scales, thus enabling N_2O inventories and projections to be made for Canada. Geo-referenced climate, activity data (Statistics Canada) and soil data are available in Canada for testing *ecosys* at provincial scale and national level (also access to Westgrid high-performance computing network and geographical information systems (GIS)) computing facilities at the University of Alberta). More research is needed using both chamber (e.g. automated for better temporal resolution and higher

number of sampling points for better spatial resolution) and micrometeorological simultaneously, under other land use management practices e.g. manure applications. This data can be further used to test *ecosys* simultaneously at chamber, tower and field scales to model both spatial and temporal variability of N_2O emissions for the development of more site-specific EFs, for the development of the IPCC Tier III methodology. This will also provide information for developing a methodology for scaling emissions from chamber to tower scales. Such future research will enable *ecosys* to make predictions under different land uses and climate change scenarios. These predictions can then be used to make recommendations for sustainable land use management recommendations in order to enhance crop productivity and maintain environmental quality. *Ecosys* has been used to simulate other greenhouse gases CH_4 (Grant, 1998) and CO_2 (e.g. Grant et al., 1999; Grant et al., 2001a,b; Grant et al., 2003; Grant et al., 2005) so that greenhouse gases inventories and projections for Canada can also be extended to these gases.

6.6 CONCLUSIONS

Results from chapter 6 showed that ***ecosys* (Grant, 2001a,b) predicted climate change impacts on future spatial and temporal variability of N_2O emissions for the Ottawa site** (chapters 4 and 5). These findings allowed a better understanding of how increasing CO_2 and temperature in the future may affect behaviour arising from the complex N_2O hypotheses thus, the climate change feedback mechanisms involved in N_2O generation. Results from this study showed that EFs may more than double by 2050 due to rising CO_2 and temperature levels but would decline with lower WFPS by 2080; This is important since such results imply that we may need to re-estimate N_2O emissions from fertilization in future inventories.

Ecosys represented future temporal variability of N_2O emissions thereby providing further insights into the episodic ("threshold") nature of these emissions. This episodic nature of N_2O emissions shows the importance of linking biological controls of N_2O emissions to physical controls in mathematical models, hence the importance of a processed - based model *ecosys* (Grant, 2001a,b), for simulating both current and future N_2O emissions. Higher air temperatures (Figure 6-1) for the 2020 and 2050 climate change scenarios (Table 6-1) resulted in higher annual N_2O emissions (Table 6-2) than that for the current climate. These results suggest that emissions may be affected by the soil conditions under which nitrification of fertilizer occurs, as affected by temporal variability of temperature and WFPS, even if the same fertilizer rate was used. In contrast to 2020 and 2050, 2080 scenario gave the lowest annual N_2O emissions (Figure 6-2d) and EF (Table 6-2) was similar to that of the current climate (2004, no temperature

increments). This trend occurred because nitrification (Eqs. [2.1] – [2.8]; Figure 6-2a,b) finished earlier and also the overall WFPS (Figure 6-1c,g) was lowest for the spring/summer months, compared to the other projections. Lowest WFPS (Figure 6-1c,g) during spring/summer periods for the 2080 scenario was due to greater modeled loss of latent heat. These results further support the use of *ecosys* mathematical model to fully capture the large temporal variability of N_2O due to changes in both temperature and WFPS.

Higher atmospheric CO_2 levels for climate change scenarios (Table 6-1) led to more rapid CO_2 fixation (Eqs. [6.6] – [6.9]; Eqs. [24] – [29] of Grant, 2004) which resulted in greater litterfall (Eqs. [29] and [37] of Grant, 2004). Greater litterfall (Eqs. [29] and [37] of Grant, 2004) led to more microbial respiration (Eq. [8] and [9] of Grant, 2004) of organic matter and greater O_2 demand, to produce substrates (greater dissolved organic carbon (DOC) for N_2O production via denitrification (Eqs. [2.16] – [2.18]), thus higher EFs for 2020 and 2050 (Table 6-2). In contrast, emissions from the 2080 fertilized and control run modeled (Table 6-2) were the lowest because these scenarios had the highest CO_2 concentrations thus greatest CO_2 fixation (Eqs [20] – [29] of Grant, 2004) therefore, more rapid N uptake. More rapid N uptake (g. R_{NH4} (g N m^{-3}) of Eqs. [39a,b] of Grant, 2004; Figure 6-2c) reduced soil mineral N thus decreasing overall N_2O production via nitrification (Eq. [2.10]) and denitrification (Eq. [2.10]). These findings may explain why variable results have been reported in the literature since the effect of rising CO_2 levels on N_2O emissions will be depend on the soil mineral N or N limitation. A review by Barnard et al. (2005) showed no significant effect of elevated CO_2 on N_2O emissions but

emphasized the need for more climate change studies to provide further insights. However, reduced NO_3^- has been used to explain decreased denitrifying enzyme activity at elevated CO_2 in several studies (Tscherko, et al., 2001; Barnard et al., 2004a). Findings from chapter 6 suggest that N_2O inventories should account for CO_2 effects on N_2O emissions especially since CO_2 levels may change in the future. As mentioned in chapter 3, soil residual N should be part of inventories since this will also determine how elevated CO_2 levels will affect N_2O emissions in the future. These results again shows the importance of using process-based models such as *ecosys* (Grant, 2001a,b) in order to fully represent the complex hypotheses involved in the prediction of effects of climate change (e.g. air temperature, precipitation and CO_2) on N_2O emissions, thus improve future estimates.

Ecosys also projected future spatial variation of N_2O at the field scale. Overall, CSV of annual N_2O emission totals within the 112 kg N ha^{-1} fertilized area for 2050 was similar to that of the current climate in 2004. Projected 2050 results showed that EF modeled for the 112 kg N ha^{-1} fertilizer application was larger than that of 2004 but for both years, emissions were higher in the lower compared to the upper topographic areas. These results shows the importance of using three-dimensional mathematical model *ecosys* (Grant, 2001a,b), with input from DEMs, in order to fully represent the complex hypotheses involved in the prediction of N_2O emissions, thus improve our future estimates. Based on the literature, there were no projection studies of N_2O emissions using processed – based models that include the influence of topography.

Both current and future projections of N_2O EFs are important since the sustainability of current land use management systems can be evaluated under future climates. Recommendations can then be made for best management practices to mitigate future N_2O emissions from agricultural soils. Canada has to reduce its total greenhouse emissions by 2012 under the Kyoto Protocol (Olsen et al., 2003) therefore, the best management practices can be determined to help meet the national reduction targets by this year and future years. This can be achieved by using a processed – based mathematical model *ecosys* (Grant, 2001a,b), since emissions can be determined from diverse scenarios of different land use, climate, soil type, topography etc. Future greenhouse gas projections can therefore be used as a tool in inventories to reduce emissions. If such applications for an IPCC Tier III Methodology are made in different countries, then ultimately global N_2O emissions can be reduced.

Ecosys (Grant, 2001a,b; website: www.ecosys.rr.ualberta.ca) has been used to predict the impact of climate change on short and long-term carbon and energy exchange in several agricultural (e.g. Grant et al., 1999; Grant et al., 2001a); forest (e.g. Grant et al., 2001b; Grant et al., 2005), artic (e.g. Grant et al., 2003) and grassland (e.g. Li et al., 2004) ecosystems. Recently, *ecosys* (Grant and Pattey, 2007 (Submitted)) was used to project climate impact on N_2O emissions. Future research will enable *ecosys* to make predictions under more land uses and climate change scenarios. These predictions can then be used to make recommendations for sustainable land use management recommendations in order to enhance crop productivity and maintain environmental quality. *Ecosys* has been used to simulate other greenhouse gases CH_4 (Grant, 1998) and CO_2 (e.g. Grant et al., 1999; Grant et al., 2001a,b; Grant et al., 2003; Grant et al., 2005) so that greenhouse gases

inventories and projections for Canada can also be extended to these gases.

6.7 REFERENCES

Ball, B.C., Horgan, G.W., Clayton, H., Parker, J.P., 1997. Spatial variability of nitrous oxide fluxes and controlling soil topographic properties. Journal of Environmental Quality 26, 1399-1409.

Barnard, R., L. Barthes, X. Le Roux, H. Harmens, A. Raschi, J. F. Soussana, B. Winkler, Leadley, P.W., 2004. Atmospheric CO_2 elevation has CO_2 little effect on nitrifying and denitrifying enzyme activity in four European grasslands. Global Change Biology 10, 488– 497.

Barnard, R., Leadley, P.W., Hungate, B.A., 2005. Global change, nitrification, and denitrification: A review. Global Biogeochemical cycles 19, GB1007, doi:10.1029/2004GB002282.

Bateman, E.J., Baggs, E.M., 2005. Contributions of nitrification and denitrification to N_2O emissions from soils at different water-filled pore space. Biology & Fertility of Soils 41, 379-388.

Berthelot, M. Friedlingstein, P., Ciais, P., Monfray, P., Dufresne, J.L., Le Treut, H., Fairhead, L., 2002. Global response of the terrestrial biosphere to CO_2 and climate change using a coupled climate-carbon cycle model. Global Biogeochemical cycles 16, NO. 4, 1084, doi:10.1029/2001GB001827.

Chen, J.M., Liu, J., Cihlar, J., Goulden, M.L., 1999. Daily canopy photosynthesis model through temporal and spatial scaling for remote sensing applications. Ecological Modelling 124, 99–119.

Clay, D.E., Molina, J.A.E., Clapp, C.E., Linden, D.R., 1985. Nitrogen-tillage-residue management: II. Calibration of potential rate of nitrification by model simulation. Soil Science Society of America Journal 49, 322-325.

Davidson, E.A., 1991. Fluxes of nitrous oxide and nitric oxide from terrestrial ecosystems. In: Rogers, J.E., Whitman, W.B. (Eds.), Microbial Production and Consumption of Greenhouse Gases: Methane, Nitrogen Oxides and Halomethanes. American Society of Microbiology, Washington, D.C., pp. 219-235.

de Vries, D.A. 1963. Thermal properties of soils. In R. van wijk (Ed.). Physics of Plant Environment. North Holland Publishing, Amsterdam, The Netherlands, 210-235.

Dobbie, K.E., Smith, K.A., 2001. The effects of temperature, water-filled pore space and land use on N_2O emissions from an imperfectly drained gleysol. European Journal of Soil Science 52, 667-673.

Dobbie, K.E., Smith, K.A., 2003. Nitrous oxide emission factors for agricultural soils in Great Britain: the impact of soil water-filled pore space and other controlling variables. Global Change Biology 9, 204–218.

Eggleston 2006. Intergovernmental Panel on Climate Change (IPCC), IPCC Guidelines for National Greenhouse Gas Inventories Volume 4; Agriculture, Forestry and other land use. Institute for Gloabal Environmental Strategies, kanagawan Hayama, Japan.

Farquhar, G.D., von Caemmerer, S., Berry, J.A., 1980. A biochemical model of photosynthetic CO_2 assimilation in leaves of C_3 species. Planta 149, 78 – 90.

Flessa, H., Dörsch, P., Beese, F., 1995. Seasonal variation of N_2O and CH_4 fluxes in differently managed arable soils in southern Germany. Journal of Geophysical Research 100, 23115-23124.

Flechard, C.R., Ambus, P., Skiba, U., Rees, R.M., Hensen, A., van Amstel, A., van den Pol-van Dasselaar, A., Soussana, J.-F., Jones, M., Clifton-Brown, J., Raschi, A., Horvath, L., Neftel, A., Jocher, M., Ammann, C., Leifeld, J., Fuhrer, J., Calanca, P., Thalman, E., Pilegaard, K., Di Marco, C., Campbell, C., Nemitz, E., Hargreaves, K.J., Levy, P.E., Ball, B.C., Jones, S.K., van de Bulk, W.C.M., Groot, T., Blom, M., Domingues, R., Kasper, G., Allard, V., Ceschia, E., Cellier, P., Laville, P., Henault, C., Bizouard, F., Abdalla, M., Williams, M., Baronti, S., Berretti, F., Grosz, B., 2007. Effects of climate and management intensity on nitrous oxide emissions in grassland systems across Europe. Agriculture, Ecosystems and Environment 121, 135-152.

Focht, D.D., Verstraete, W., 1977. Biochemical ecology of nitrification and denitrification. Advances in Microbial Ecology 1, 135-214.

Freibauer, A., 2003. Regionalised inventory of biogenic greenhouse gas emissions from European agriculture. European Journal of Agronomy 19, 135-160.

Gabrielle, B., Laville, P., Duval, O., Nicoullaud, B., Germon, J.C., Henault, C., 2006. Process-based modeling of nitrous oxide emissions from wheat cropped soils at the subregional level. Global Biochemical Cycles 20, 1-11.

Grant, R.F., 1991. A technique for estimating denitrification rates at different soil temperatures, water contents, and nitrate concentrations. Soil Science 152, 41-52.

Grant, R.F., 1994c. Simulation of ecological controls on nitrification. Soil Biology & Biochemistry 26, 305–315.

Grant, R.F., 1995a. Dynamics of energy, water, carbon and nitrogen in agricultural ecosystems: simulation and experimental validation. Ecological Modelling 81, 169–181.

Grant, R.F., 1995b. Mathematical modelling of nitrous oxide evolution during nitrification. Soil Biology & Biochemistry 27, 1117–1125.

Grant, R.F., 1997. Changes in soil organic matter under different tillage and rotation: mathematical modeling in *ECOSYS*. Soil Science Society of America Journal 61, 1159-1175.

Grant, R.F., 1998. Simulation of methanogenesis in the mathematical model *ecosys*. Soil Biology & Biochemistry 30, 883-896.

Grant, R.F., 1999. Simulation of methanotrophy in the mathematical model *ecosys*. Soil Biology & Biochemistry 31, 287–297.

Grant, R.F., 2001a. A Review of the Canadian Ecosystem Model - *ecosys*. In: Shaffer M. J., Ma, L., Hansen, S. (Ed), Modeling Carbon and Nitrogen Dynamics for Soil Management. CRC Press. Boca Raton, FL, pp. 173-263.

Grant, R.F., 2001b. Modeling Transformations of Soil Organic Carbon and Nitrogen at Differing Scales of Complexity. In: Shaffer M. J., Ma, L., Hansen, S. (Ed), Modeling Carbon and Nitrogen Dynamics for Soil Management. CRC Press. Boca Raton, FL, pp. 597-614.

Grant, R.F., 2004. Modeling topographic effects on net ecosystem productivity of boreal black spruce forests. Tree Physiology 24, 1-18.

Grant, R.F., Baldocchi, D.D., 1992. Energy transfer over crop canopies: simulation and experimental verification. Agriculture & Forest Meteorology 61, 129–149.

Grant, R.F., Rochette, P., 1994. Soil Microbial respiration at Different Water Potentials and Temperatures: Theory and Mathematical Modeling. Soil Science Society of America Journal 58, 1681-1690.

Grant, R.F. Pattey, E., 1999. Mathematical modeling of nitrous oxide emissions from an agricultural field during spring thaw. Global Biogeochemical Cycles 13, 679-694.

Grant, R.F., Pattey, E., 2003. Modelling variability in N_2O emissions from fertilized agricultural fields. Soil Biology & Biochemistry 35, 225-243.

Grant, R.F., Pattey, E., 2007 (Submitted). Temperature sensitivity of N_2O emissions from fertilized agricultural soils: mathematical modelling in *ecosys*.

Grant, R.F., Nyborg, M., Laidlaw, J.W., 1992. Evolution of nitrous oxide from soil: II. Experimental results and model testing. Soil Science 156, 266-277.

Grant, R.F., Juma, N.J., McGill, W.B., 1993a. Simulation of carbon and nitrogen transformations in soils. I: mineralization. Soil Biology & Biochemistry 25, 1317-1329.

Grant, R.F., Juma, N.J., McGill, W.B., 1993b. Simulation of carbon and nitrogen transformation in soil: Microbial biomass and metabolic products. Soil Biology & Biochemistry 25, 1331-1338.

Grant, R.F., Nyborg, M., Laidlaw, J.W., 1993c. Evolution of nitrous oxide from soil: I. Model development. Soil Science 156, 259-265.

Grant, R.F., Rochette, P., Desjardins, R.L., 1993d. Energy exchange and water use efficiency of field crops: validation of a simulation model. Agronomy Journal 85, 916–928.

Grant, R.F., Garcia, R.L., Pinter Jr, P.J., Hunsaker, D., Wall, G.W., Kimball, B.A., LaMorte, R.L., 1995a. Interaction between atmospheric CO_2 concentration and water deficit on gas exchange and crop growth: Testing of *ecosys* with data from the free air CO_2 enrichment (FACE) experiment. Global Change Biology 1, 443 - 454.

Grant, R.F., Izaurralde, R.C., Chanasyk, D.S., 1995b. Soil temperature under different soil managements: testing a simulation model. Agriculture & Forest Meteorology 73, 89-113.

Grant, R.F., Kimball, B.A., Pinter, P.J.J., Wall, G.W., Garcia, R.L., La Morte, R.L., Hunsaker, D.J., 1995c. Carbon dioxide effects on crop energy balance: testing *ecosys* with a the free air CO_2 enrichment (FACE) experiment. Agronomy Journal 87, 446–457.

Grant, R.F., Izaurralde, R.C., Nyborg, M., Malhi, S.S., Solberg, E.D., Jans-Hammermeister, D., Stewart, B.A., 1998. Modeling tillage and surface residue effects on soil C storage under ambient versus elevated CO_2 and temperature in *ECOSYS*. In: Lal, R., Kimble, J.M., Follet, R.F. (Eds), Soil processes and carbon cycle. CRC Press Inc. Boca Raton, USA, pp. 527-547.

Grant, R.F., Black, T.A., den Hatog, G., Berry, J.A., Gower, S.T., Heumann, H.H., Blamken, P.D., Yang, P.C., Russell, C., 1999a. Diurnal and annual exchanges of mass and energy between an aspen-hazelnut forest and the atmosphere: testing the mathematical model *ecosys* with data from the BOREAS experiment. Journal of Geophysical Research 104, 699-717.

Grant, R.F., Wall, G.W., Kimball, B.A., Frumau, K.F.A., Pinter Jr., P.J., Hunsaker, D.J., Lamorte, R.L., 1999b. Crop water relations under different CO_2 and irrigation: testing of *ecosys* with the free air CO_2 enrichment (FACE) experiment. Agriculture & Forest Meteorology 95, 27–51.

Grant, R.F., Kimball, B.A., Brooks T.J., 2001a. Modeling interactions among carbon dioxide, nitrogen and climate on energy exchange of wheat in a Free Air carbon dioxide experiment. Agronomy Journal 93:638-649.

Grant, R.F., Massheder, J.M, Hale, S.E., Moncrieff, J. B., Rayment, M, Scott, S.L., Berry, J.A., 2001b. Controls of carbon and energy exchanges by a black spruce – moss ecosystem: Testing the mathematical model *Ecosys* with data from the BOREAS experiment. Global Biogeochemical cycles 15, 129 – 147.

Grant, R.F., Juma, N.G., Robertson, J.A., Izaurralde R.C., McGill, W.B., 2001c. Long – term changes in soil C under different fertilizer, manure and rotation: Testing the mathematical model *Ecosys* with data from the Breton plots. Soil Science Society of American Journal 65, 204-214.

Grant, R.F., Oechel, W.C., Ping, C., Kwon, H., 2003. Carbon balance of coastal arctic tundra under changing climate. Global Change Biology 9, 16–36.

Grant, R.F., Amrani, M., Heaney, D.J., Wright, R., Zhang, M., 2004. Mathematical Modeling of Phosphorus Losses from Land Application of Hog and Cattle Manure. Journal of Environmental Quality 33, 210-231.

Grant , R.F., Arain, A., Arora, V., Barr, A., Black, T.A., Chen, J. Wang, S., Yuan, F., Zhang, Y., 2005. Intercomparison of techniques to model high temperature effects on CO_2 and energy exchange in temperate and boreal coniferous forests. Ecological Modelling 188, 217–252.

Grant, R.F., Pattey, E., Goddard, T.W., Kryzanowski, L.M., Puurveen, H., 2006. Modeling the effects of fertilizer application rate on nitrous oxide emissions. Soil Science Society of America Journal 70, 235-248.

Helgason, B.L., Janzen, H.H., Angers, D.A., Boehm, M., Bolinder, M., Desjardins, R.L., Dyer, J., Ellert, B.H., Gibb, D.J., Gregorich, E.G., Lemke, R., Massé, D., McGinn, S.M., McAllister, T.A., Newlands, N., Pattey, E., Rochette, P., Smith, W., VandenBygaart, A.J., Wang, H., 2005. GHGFarm: An assessment tool for estimating net greenhouse gas emissions fromCanadian farms. Agriculture & Agri-Food Canada, pp. 5-6.

Hénault, C., Devis, X., Page, S., Justes, E., Reau, R., Germon, J.C., 1998. Nitrous oxide emissions under different soil and land management conditions. Biology and Fertility of Soils 26, 199-207.

Ineson, P., Coward, P.A., Hartwig, U.A., 1998. Soil gas fluxes of N_2O, CH_4 and CO_2 beneath *Lolium perenne* under elevated CO_2: The Swiss free air carbon dioxide enrichment experiment. Plant and Soil 198, 89–95.

Intergovernmental Panel on Climate Change (IPCC), 2001. IPCC 3rd Assessment Report. http://www.ipcc.ch/ipccreports/assessments-reports.htm

IPCC (Intergovernmental Panel on Climate Change), 2006. 2006 IPCC Guidelines for National Greenhouse Gas Inventories, Prepared by the National Greenhouse Gas

Inventories Programme, Eggleston H.S., Buendia L., Miwa K., Ngara T. and Tanabe K. (Eds). Published: IGES, Japan.
Intergovernmental Panel on Climate Change (IPCC), 2007. IPCC 4th Assessment Report. http://www.ipcc.ch/ipccreports/ar4-wg2.htm

Kamp, T., Steindl, H., Hantschel, R.E., Beese, F., Munch, J-C., 1998. Nitrous oxide emissions from a fallow and wheat field as affected by increased soil temperatures. Biology and Fertility of Soils 27, 307–314.

Kettunena, R., Saarnio, S., Martikainen, P., Silvola, J., 2005. Elevated CO_2 concentration and nitrogen fertilisation effects on N_2O and CH_4 fluxes and biomass production of *Phleum pratense* on farmed peat soil. Soil Biology & Biochemistry 37, 739–750.

Kettunen, R., Saarnio, S., Martikainen, P.J., Silvola, J., 2006. Increase of N_2O fluxes in agricultural peat and sandy soil under elevated CO_2 concentration: concomitant changes in soil moisture, groundwater table and biomass production of *Phleum pratense* Nutrient Cycling in Agroecosystems 74, 175–189.

Kettunen, R., Saarnio, S., Martikainen, P.J., Silvola, J., 2007a. Can a mixed stand of N_2-fixing and non-fixing plants restrict N_2O emissions with increasing CO_2 concentration? Soil Biology & Biochemistry 39, 2538–2546.

Kettunen, R., Saarnio, S., Silvola, J., 2007b. N_2O fluxes and CO_2 exchange at different N doses under elevated CO_2 concentration in boreal agricultural mineral soil under *Phleum pratens.* Nutrient Cycling in Agroecosystems 78, 197–209.

Kellomaki, S.,Wang, K.-Y., 1999. Short-term environmental controls of heat and water vapour fluxes above a boreal coniferous forest: model computations compared with measurements by eddy correlation. Ecological Modelling 124, 145–173.

Kellomaki, S., Wang, K.-Y., 2000. Short-term environmental controls on carbon dioxide flux in a boreal coniferous forest: model computation compared with measurements by eddy covariance. Ecological Modelling 128, 63–88.

Koike, I., Hattori, A., 1975. Growth yield of a denitrifying bacterium, *Pseudomonas denitrificans*, under aerobic and denitrifying conditions. Journal of General Microbiology 88, 1-10.

Kroeze, C., Mosier, A., Bouman, L., 1999. Closing the global N_2O budget: a retrospective analysis. Global Biogeochemical cycles 13, 1-8.

Laville, P., Jambert, C., Cellier, P., Delmas, R. 1999. Nitrous oxide fluxes from a fertilised maize crop using micrometeorological and chamber methods Agricultural & Forest Meteorology 96 (1999) 19 – 38.

Li, C., Frolking, S., Frolking, T.A., 1992. A model of nitrous oxide evolution from soil driven by rainfall events: 1. Model structure and sensitivity. Journal of Geophysical Research 97, 9759-9776.

Li., Y., Chen, D., Zhang, Y., Edis, R., Ding, H., 2005. Comparison of three modeling approaches for simulating denitrification and nitrous oxide emissions from loam-textured arable soils. Global Biogeochemical Cycles, 19, GB3002, doi:10.1029/2004GB002392.

Li, T., Grant, R.F., Flanagan, L.B., 2004. Climate impact on net ecosystem productivity of a semi-arid natural grassland: modeling and measurement. Agricultural and Forest Meteorology 126, 99–116.

Lim, B., Boileau, P., Bonduki, Y., van Amstel, A.R., Janssen, L.H.J.M., Olivier, J.G.J., Kroeze, C., 1999. Improving the quality of national greenhouse gas inventories. Environmental Science and Policy 2, 335-346.

Liu, J., Chen, J.M., Cihlar, J., Park,W., 1997.Aprocess-based boreal ecosystems productivity Simulator using remote sensing inputs. Remote sensing of Environment 62, 158–175.

Lu, Y., Huang, Y., Zou, J., Zheng, X., 2006. An inventory of N_2O emissions from agriculture in China using precipitation-rectified emission factor and background emission. Chemosphere 65, 1915-1924.

McGill, W.B., Hunt, H.W., Woodmansee, R.G., Reuss, J.O., 1981. Phoenix, a model of the dynamics of carbon and nitrogen in grassland soils. In F.E. Clark and T. Rosswall (Ed.) Terrestrial nitrogen cycles. Ecological Bulletin 33, 49-115.

Metivier, K.A, Grant, R.F. and Pattey, In. Prep. Modeling topographic effects on spatial variability of nitrous oxide emissions from fertilized agricultural fields.

Millington, R.J., 1959. Gas diffusion in porous media. Science. 130, 100-102.

Millington, R.J., Quirk, J.M., 1960. Transport in porous media. In: Van Beren, F.A. et al. (Eds.), 7th Trans. Int. Congr. Soil Sci. Vol. 1. Madison, WI. 14-24 Aug. Elsevier, Amsterdam, Science, pp. 97-06.

Molina, J.A.E., Clapp, C.E., Shaffer, M.J., Chichester, F.W., Larson, W.E., 1983. NCSOIL, a model of nitrogen and carbon transformations in soil: Description, calibration and behavior. Soil Science Society of America Journal 47, 85-91.

Morgan, R.P.C., Quinton, J.N., Smith, R.E., Govers, G., Poesen, J.W.A., Auerswald, K., Chisci, G., Torri, D., Styczen, M.E., Folly, A.J.V., 1998. The European Soil Erosion Model (EUROSEM): Documentation and user guide. Version 3.6. Silsoe College, Cranfield University, Silsoe, Bedford, UK.

Muller, C., 1999. Modelling soil-biosphere interactions. CABI Publishing, Wallingford, UK, pp. 52-53.

Myrold, D.D., 1998. Transformation of nitrogen. In: Sylvia, D.M., Fuhrmann, J.J., Hartel, P.G., Zuberer (Eds.). Principles and Applications of soil microbiology. Prentice Hall: Upper Saddle River, New Jersey, pp. 259-294.

Nelson, J.A., Morgan, J.A., LeCain, D.R., Mosier, A.R., Milchunas, D.G., Parton, B.A., 2004. Elevated CO_2 increases soil moisture and enhances plant water relations in a long-term field study in semi-arid shortgrass steppe of Colorado. Plant and Soil 259, 169–179.

Nyborg, M., Laidlaw, J.W., Solberg, E.D., Malhi, S.S., 1997. Denitrification and nitrous oxide emissions from a black Chernozemic soil during spring thaw in Alberta. Canadian Journal of Soil Science 77,153-160.

Olsen, K., Wellisch, M., Boileau, P., Blain, D., Ha, C., Henderson, L., Liang, C., McCarthy, J., McKibbon, S., 2003. Canada's Greenhouse Gas Inventory 1990-2001, pp. 1-4.

Pattey, E., Royds, W.G., Desjardins, R.L., Buckley, D.J., Rochette, P., 1996. Software description of a data acquisition and control system for measuring trace gas and energy fluxes by eddy-accumulation and correlation techniques. Computers and Electronics in Agriculture 15, 303-321.

Pattey, E., Edwards, G.C., Strachan, I.B., Desjardins, R.L., Kaharabata, S., Wagner-Riddle, C., 2006a. Towards standards for measuring greenhouse gas flux from agricultural fields using instrumented towers. Canadian Journal of Soil
from agricultural fields using instrumented towers. Canadian Journal of Soil Science 86, 373-400.

Pattey, E., Strachan, I.B., Desjardins, R.L., Edwards, G.C., Dow, D., MacPherson, J.I., 2006b. Application of a tunable diode laser to the measurement of CH_4 and N_2O fluxes from field to landscape scale using several micrometeorological techniques. Agriculture & Forest Meteorology 13, 222-236.

Pattey E., Edwards, G.C., Desjardins, R.L., Pennock, D., Smith W., Grant, B., MacPherson, J.I., 2007. Tools for quantifying N_2O emissions from Agroecosystems. Agriculture & Forest Meteorology 142(2-4), 103-119.

Pennock, D.J., Zebarth, B.J., de Jong, E., 1987. Landform classification and soil distribution in hummocky terrain, Saskatchewan, Canada. Geoderma 40, 297-315.

Pennock, D.J., van Kessel, C., Farrell, R.E., Sutherland, R.A., 1992. Landscape-scale variations in denitrification. Soil Science Society of America Journal 56, 770-776.

Pennock, D.J., Anderson, D.W., de Jong, E., 1994. Landscape-scale changes in indicators of soil quality due to cultivation in Saskatchewan, Canada. Geoderma 64, 1-19.

Pennock, D.J., Corre, M.D., 2001. Development and application of landform segmentation procedures. Soil & Tillage Research 58, 151-162.

Peterjohn, W.T, Melillo, J.M., Steudler, P.A., Newkirk, K.M., 1994. Responses of trace gas fluxes and N availability to experimentally elevated soil temperatures. Ecological Applications 4, 617 – 625.

Phillips, F.A, Leuning, R., Baigent, R., Kelly, K.B., Denmead, O.T. 2007. Nitrous oxide flux measurements from an intensively managed irrigated pasture using micrometeorological techniques. Agricultural & Forest Meteorology 143, 92–105.

Rao, P.S.C., Jessup, R.E., Reddy, K.R., 1984. Simulation of nitrogen dynamics in flooded soils. Soil Science 138, 54-62.

Rochette, P., Desjardins, R.L, Gregorich, E.G., Pattey, E., Lessard, R., 1992. Soil respiration in barley (Hordeum vulgare L.) and fallow fields. Canadian Journal of Soil Science 72, 591-603.

Roelandt, C., Dendoncker, N., Rounsevell, M., Perrin, D. and Van Wesemael, B. 2007. Projecting future N_2O emissions from agricultural soils in Belgium. Global Change Biology 13, 18-27.

Rolston, D.E., Rao, P.S.C., Davidson, J.M., Jessup, R.E., 1984. Simulation of denitrification losses of nitrate fertilizer applied to uncropped, cropped and manure-amended field plots. Soil Science, 137, 270-279.

Ruser, R., Flessa, H., Russow, R., Schmidt, G., Buegger, F., Munch, J.C., 2006. Emission of N_2O, N_2 and CO_2 from soil fertilized with nitrate: effect of compaction, soil moisture and rewetting. Soil Biology & Biochemistry 38, 263–274.

Saxton, K.E. Rawls, W.J., 2006. Soil water characteristic estimates by texture and organic matter for hydrologic solutions. Soil Science Society of American Journal 70, 1569-1578.

Schmid, H.P., 2002. Footprint modeling for vegetation atmosphere exchange studies: a review and perspective. Agricultural and Forest Meteorology 113, 159-183.

Scott, M.J., Sands, R.D., Rosenberg, N.J., Izaurralde, R.C., 2002. Future N_2O from US agriculture: projecting effects of changing land use, agricultural technology, and climate on N_2O emissions Global Environmental Change 12, 105–115.

Shields, J.A., Paul, E.A., Lowe, W.E., 1974. Factors influencing the stability of labelled microbial materials in soils. Soil Biology & Biochemistry 6, 31-37.

Smith, K.A., Thomson, P.E., Clayton, H., McTaggart, I.P., Conen, F., 1998. Effects of temperature, water content and nitrogen fertilisation on emissions of nitrous oxideby soils. Atmospheric Environment 32, 3301-3309.

Suzuki, I., Dular, U., Kwok, S.C., 1974. Ammonia or ammonium ion as substrate for oxidation by *Nitrosomonas europeae* cells and extracts. Journal of Bacteriology 120, 556-558.

Thornton, F.C., Bock, B.R., Tyler, D.D., 1996. Soil emissions of nitric oxide and nitrous oxide from injected anhydrous ammonium and urea. Journal of Environmental Quality 25, 1378-1384.

Tsai, W-T., Chyan, J-M., 2006. Estimation and projection of nitrous oxide (N_2O) emissions from anthropogenic sources in Taiwan. Chemosphere 63, 22-30.

Tscherko, D., Kandeler, E., Jones, T.H., 2001. Effect of temperature on below-ground N-dynamics in a weedy model ecosystem at ambient and elevated atmospheric CO_2 levels, Soil Biology & Biochemistry 33, 491– 501.

Wagner-Riddle, C., Thurtell, G.W., Kidd, G.E., Edwards, G.C., Simpson, I.J., 1996. Micrometeorological measurements of trace gas fluxes and natural ecosystems. Infrared Physics and Technology 37, 51-158.

Xu-Ri, Wang, M., Wang, Y., 2003. Using a modified DNDC model to estimate N_2O fluxes from semi-arid grassland in China. Soil Biology & Biochemistry 35, 615-620.

Yoshinari, T., Hynes, R., Knowles, R., 1977. Acetylene inhibition of nitrous oxide reduction and measurement of denitrification and nitrogen fixation in soil. Soil Biology & Biochemistry 9, 177–183.

CHAPTER 7.0: Summary, recommendations and research prospects

7.1 Summary

7.1.1 CHAPTER 1.0: General Introduction

Current Intergovernmental Panel of Climate Change (IPCC) Tier I methodology for quantifying N_2O emissions in greenhouse gas inventories, is based on a constant emission factor (EF) of 1% for all N inputs (IPCC, 2006). However, uncertainties in estimates of N_2O emissions by IPCC guidelines may be 70% to 80% in arable soil at a national scale (Lim et al., 1999). This uncertainty may be attributed to large spatial and temporal variability of N_2O (e.g. Pennock et al., 1992; Pennock and Corre, 2001; Grant and Pattey, 2003), which complicates the calculation of EFs. An IPCC Tier II Methodology is now being used for Canada. It uses lower EFs (0.1 - 0.7%) in drier climates such as the Prairies and higher EFs (0.83 - 1.67%) for the more humid regions of Eastern Canada (Hegalson, 2005).

IPCC Tier III Methodology involves either the use of validated mathematical models or the use of measurement data (e.g. N_2O fluxes) in conjunction with activity data (e.g. fertilizer use) to simulate emissions (IPCC, 2006). Unlike Tier I and II, Tier III addresses more of the large spatial and temporal variability of N_2O and is capable of capturing longer-term legacy effects of land use and management (IPCC, 2006) together with projected climate change effects. Global CO_2, surface temperature and precipitation levels are projected to increase by 2100 (IPCC, 2007). Mathematical models can also improve N_2O inventories by contributing towards the continuity of measured data by modeling fluxes where measured data are missing. Because of the uncertainties

associated with using the current IPCC Tier I and Tier II Methodologies (Eggleston, 2006), mathematical models such as *ecosys* (Grant, 2001a,b: website: www.ecosys.rr.ualberta.ca) can contribute towards the development of more accurate site - specific EFs needed for the adoption of an IPCC Tier III Methodology. Addressing current uncertainties may improve our long – term predictions of climate change impacts on future N_2O emissions. Such projections are important since the sustainability of current land use management systems can be evaluated and then recommendations can be made for best management practices, to mitigate future N_2O emissions from agricultural soils.

N_2O emissions are highly variable spatially and temporally because of the strong physical (water-filled pore space (WFPS), oxygen (O_2), temperature), biological (soil organic matter, nitrifying and denitrifying bacteria populations) and chemical (ammonia (NH_3) and nitrate (NO_3^-) concentrations) controls on N_2O production. Such controls are influenced by site – specific factors e.g. land use, climate, soil type and topography. *Ecosys* (Grant, 2001a,b) processed – based mathematical model was used for this research because it can capture the large spatial and temporal variability of N_2O emissions and it can simulate the complex feedback mechanisms involved in climate change. This is attributed to the model's capability to simulate the complex biological, physical and chemical hypotheses of N_2O fluxes at the site scale ($< 1\ m^2$) and also uses input data from DEMs to account for topographic effects at larger spatial (ha) scales, under site – specific past and current land use, climate, soil type, topography etc.. *Ecosys* has been used to model N_2O emissions at site scale from laboratory experiments (Grant,

1991; Grant et al., 1992; Grant et al., 1993c; Grant, 1994; Grant, 1995) and agricultural field experiments using micrometeorological towers (Grant et al, 1992; Grant and Pattey, 1999; Grant and Pattey, 2003; Grant et al., 2006). Recently, *ecosys* (Grant and Pattey, 2007 (Submitted)) was used to project climate impact on N_2O emissions. In order to provide well-constrained tests for *ecosys*, a combination of micrometeorological techniques and surface chamber measurements from laboratory samples and fertilized fields was used to provide measured N_2O emissions at spatial scales from the m^2 through ha to field and at temporal scales from the hour through the day to the season.

7.1.2 CHAPTER 2.0: Modeling temporal variability of N_2O emissions from fertilized a agricultural soil using the Ecosys mathematical model (site scale: 1 < m^{-2})

Ecosys (Grant, 2001a,b) simulates the large **temporal** variability or "threshold" response of N_2O emissions to changes in WFPS. In *ecosys*, the key biological processes – mineralization, immobilization, nitrification, denitrification, root and mycorrhizal uptake controlling N_2O generation are coupled to the key physical processes – convection, diffusion, volatilization, dissolution - controlling the transport of gaseous reactants and products of these biological processes (Grant et al., 2006). Transitions from one reduction reaction (nitrification/denitrification) to another in *ecosys* can be caused by small changes in soil WFPS ("threshold" response). This occurs because the diffusivity (D_g) of O_2 (and other gases) in the soil atmosphere varies according to a power function of the soil air-filled porosity (θ_g) (Millington, 1960), which in turn depends on WFPS. This variation is such that at certain WFPS, small declines in θ_g can cause large declines in D_g that may limit O_2 gaseous transfer to microsites causing a greater demand for alternative electron

acceptors. As a result, these small declines may cause a transition from the reduction of O_2 to that of NO_x by nitrifiers and denitrifiers, increasing N_2O production.

Based on earlier results from preliminary laboratory experiments (e.g. suitable sampling time for linear accumulation of N_2O emissions), a fully replicated laboratory experiment was designed whereby chambers (Hutchinson and Mosier, 1981) were used to monitor N_2O emissions, prior to gas chromatography (GC) analysis. Results from the replicated laboratory experiment were used to test *ecosys* (Grant, 2001a,b) at the site scale (< 1 m^2) to better understand the "threshold" response of N_2O (temporal variability) emissions under transient aerobic and anaerobic conditions caused by changes in WFPS (chapter 2).

Ecosys modeled the sensitivity of N_2O emissions in response to changes in WFPS ("threshold" response) thereby allowing us to better understand the episodic nature of these emissions. This "threshold" response in *ecosys* (Eq. [2.28]) occurred because the D_g of gases in the soil atmosphere was highly sensitive to changes in the soil's WFPS or θ_g. Findings showed that small changes in WFPS led to large changes in N_2O emissions under certain WFPS in this laboratory experiment. Modeled emissions rose non-linearly (Figure 2-7; R^2 of cumulative N_2O emissions versus WFPS = 0.99) with WFPS from values of 60% through 75% to 90% in a way that was consistent with the measured data (Figure 2-6: close to 0 mg N_2O-N m^{-2} h^{-1} at 60% to ~ 4.6 N_2O-N m^{-2} h^{-1} at 90%; Table 2-2: R^2: 0.26 (75%) and 0.67 (90%) WFPS, $P < 0.001$ and similar RMSD and RMSE). The consistency of modeled and measured results **supports the hypothesis in *ecosys* (Grant, 2001a,b) outlined in the Introduction (section 2.1), that N_2O production increases**

sharply (threshold, non-linear response) at 90% > WFPS > 60%. This non-linear rise of N_2O emissions in the model can be explained by the D_g (Eq. [2.28]) of O_2 whereby at WFPS < 60%, the D_g (Eq. [2.28]) of O_2 is large enough to meet microbial demands. However, as WFPS increases above 60%, the D_g (Eq. [2.28]) of O_2 declines sharply and the unmet O_2 demand forces the need for alternative electron acceptors (Eqs. [2.10] – [2.18]) thus, higher N_2O production via nitrification (Eq. [2.10]) and denitrification (Eq. [2.18]) in the model. Such temporal variability of N_2O emissions has been shown in previous studies (Grant, 1991; Grant et al., 1992; Grant et al., 1993c; Grant, 1994; Grant, 1995; Grant and Pattey, 1999; Grant and Pattey, 2003; Grant et al., 2006). Measured data from other studies (e.g. Dobbie and Smith, 2001; Bateman and Baggs 2005; Rusier et al., 2006) showed a similar large temporal variability of N_2O emissions. Findings from chapter 2 showed the importance of using mathematical model *ecosys* (Grant, 2001a,b), that linked biological controls of N_2O emissions to physical controls, thereby enabling the "threshold" response to be simulated. However, in some current models (e.g. Lu et al., 2006), the response of N_2O emissions to WFPS is assumed linear.

Inaccurate EFs may limit our ability to track our progress in meeting the reduction targets for the Kyoto protocol (Olsen et al., 2003). Results from the laboratory experiment showed that frequent sampling may be necessary in order to fully capture the episodic nature of N_2O emissions and thus, help improve the accuracy of EFs for inventories. However, continuous measurements of N_2O fluxes may be difficult sometimes. Mathematical models such as *ecosys* (Grant, 2001a,b) can provide continuous data sets

for calculations of more accurate EFs needed for the development of an IPCC Tier III Methodology. In addition, results from this experiment demonstrated the importance of short model time steps required to represent rapid changes in N_2O emissions. In addition to simulating N_2O emissions at smaller temporal resolutions (e.g. daily, monthly, annually etc.), *ecosys* (Grant, 2001a,b) simulated N_2O emissions at an hourly time-step which was necessary to better capture the timing and magnitude of the entire emission events versus daily (e.g. Gabrielle et al., 2006) or monthly time-step models. There was also large replicate variation even though the soil was well mixed. These findings suggest that microspatial variation in the soil leads to variation in N_2O emissions and that there may be even larger spatial variation of N_2O emissions in the field. Consequently, there is a need for greater understanding of this spatial variation and its effects on N_2O EFs in the field.

7.1.3 CHAPTER 3.0: Modeling the sensitivity of N_2O emissions from agricultural soils to changes in past and current land use management practices and inter-annual variation in precipitation using the Ecosys mathematical model (site scale: m^{-2})

Ecosys (Grant, 2001a,b) was further tested at the site scale (m^2), but now to simulate the sensitivity of N_2O emissions to changes in past and current fertilizer use (chapter 3). The Michaelis-Menten kinetics used in *ecosys* enables the model to simulate the sensitivity of nitrificiation and denitrification thus of, N_2O emissions to different past (soil residual N/ initial N concentration) and current fertilizer N application (non-linear response). However, other models (e.g. Molina et al., 1983 and Clay et al., 1985) simulate denitrification based on first order kinetics with respect to soluble C or NO_3^- (e.g. Rolston

et al., 1984 and Rao et al., 1984) as modified by dimensionless factors of temperature and WFPS. The model was also used to examine the effect of inter-annual variation of precipitation (Table 3-4: 2003 being the wettest year while 2002 was a drought year) on N_2O emissions (chapter 3).

Modeled results from *ecosys* were compared to N_2O fluxes measured with surface chambers and ancillary data (soil temperature, WFPS and mineral NH_4^+ and NO_3^-), from field-plot experiments in Edmonton. N_2O emission response to fertilizer N addition in *ecosys* varied depending on soil residual N levels. Because N_2O production is driven by soil residual N (controls availability of alternative electron acceptors e.g. NH_4^+, NO_3^-), then rises in N_2O emissions will depend on rises in soil residual N. **It is hypothesized in *ecosys* (Grant, 2001a,b) that these rises occur in stages (non – linear response) (Figure 2-1) upon fertilizer N addition and can be explained by the immobilization capacity of the ecosystem (Grant et al., 2006).** Modeled results from *ecosys* (Grant, 2001a,b) showed that N_2O emissions and EFs for the lower fertilizer rate (90 kg N m^{-2} y^{-1}) for the Long-term fertilized site (Figure 3-1 – 3-3; Table 3-6, 3-7) and all rates for the Short-term fertilized site (Figure 3-4; Table 3-6, 3-7) were low and this was generally consistent with the measured data (Table 3-10), due to the presence of low soil residual N and comparatively high C:N ratios (Tables 3-5; 3-8). The general consistency of modeled and measured results **supports the Stage 1 (non – linear) response hypothesis in *ecosys* (Grant, 2001a,b) outlined in the Introduction (section 3.1), whereby low soil residual N due to low rates of past fertilizer application, leads largely to immobilization (crop and soil uptake capacity) (N limited) (Grant et al., 2006) (Figure 2-1; B') of all or**

most of current fertilizer N added (Figure 2-1; AB). Consequently, low soil residual N remains thus low N_2O production via nitrification (Eq. [2.10]) and denitrification (Eq. [2.18]) in the model (Figure 2-1; AB').

In contrast to the Stage 1 response, modeled results from *ecosys* (Grant, 2001a,b) showed that N_2O emissions and EFs for the higher fertilizer rate (180 kg N m^{-2} y^{-1}) for the Long-term fertilized site (Figure 3-1 – 3-3; Table 3-6, 3-7) were higher and this was generally consistent with the measured data (Table 3-10) with a few significant correlations in some cases (e.g., R^2 of modeled versus measured data: 0.77 (2001, spring 180 kg N ha^{-1}), $P < 0.001$), due to the presence of higher soil residual N and comparatively low C:N ratios (Tables 3-5; 3-8). The general consistency of modeled and measured results in these cases **supports the Stage 2 (non – linear) response hypothesis in *ecosys* (Grant, 2001a,b) outlined in the Introduction (section 3.1), whereby higher soil residual N due to larger rates of past fertilizer application, leads to less immobilization (Figure 2-1; C') of the current fertilizer N added (Figure 2-1; BC') compared to that of the Stage 1 response, due to the addition of N greater than the immobilization capacity of the ecosystem (Grant et al., 2006). Consequently, higher soil residual N remains thus higher N_2O production via nitrification (Eq. [2.10]) and denitrification (Eq. [2.18]) in the model (Figure 2-1; BC') (intermediate N_2O emissions).**

Emissions were high in *ecosys* (Grant, 2001a,b) for the replicated experiment (chapter 2) even without fertilizer N addition in a way that was consistent with the measured data (Figure 2-6; Table 2-2: R^2 of modeled versus measured data: 0.26 (75%) and 0.67 (90%)

WFPS, $P < 0.001$), due to the presence of very high soil residual N (Table 2-1). After the addition of the fertilizer treatment in the model, little N_2O emissions were simulated and this was also consistent with the measured data especially for the 90% WFPS and first cycle (Figure 2-8; R^2 of modeled versus measured data: 0.57 (90% + 75 kg N) and 0.33 (90% + 150 kg N) WFPS, $P < 0.001$). The consistency of modeled and measured results **supports the Stage 3 (non – linear) response hypothesis in *ecosys* (Grant, 2001a,b) outlined in the Introduction (section 2.1), whereby very high soil residual N due to very large rates of past fertilizer application large rates of past fertilizer application (and also there was a lack of recent residue input, therefore greater net mineralization), leads to high N_2O emissions and little of the current fertilizer N added (Figure 2-1; DE) is immobilized (Figure 2-1; E'). Consequently, very high soil residual N remains but little further increase in N_2O production occurs because of an N excess in the ecosystem, which lead to the maximum rate for N_2O production via nitrification (Eq. [2.10]) and denitrification (Eq. [2.18]) in the model (Figure 2-1; DE').** These conditions are represented in the model as v-max (maximum reaction rate) for nitrification/denitrification (Eqs. [2.1] - [2.0]) according to the Michaelis-Menten kinetics (Eqs. [2.1], [2.3b], [2.5], [2.7b], [2.10], [2.12], [2.14b] and [2.17] - [2.19]. This was found in the laboratory soil only therefore, the same results may not be in the field.

Findings from this chapter showed that an increase in fertilizer rate does not necessarily cause a proportional increase (non - linear) in N_2O emissions, due to complex site-specific conditions such as soil residual mineral N levels. Emissions can therefore be under or over estimated if inventories are based on a single EF irrespective of fertilizer

land use history, as done in the IPCC Tier 1 Methodology. Modeled site-specific EFs derived from this study were within the range 0 – 3% (although 18 g N m^{-2} y^{-1} is outside the range of normal practice here), which is larger than those (0.1 - 0.7% for the Prairies) used in the IPCC Tier II Methodology for Canada (Hegalson, 2005). Their study did not account for the influence of fertilizer history but did consider emissions from areas under fallow (Hegalson, 2005). A review by Barnard et al. (2005) suggests that the response of N_2O flux to N addition was highly variable, and that there was no clear correlation with the amount of N added. May be the lack of correlation could have been attributed to fertilizer application to soils with variable soil residual N levels. In some cases, the studies (Barnard et al., 2005) showed that application of ~ 425 kg N ha^{-1} gave little or no difference in emissions between control and fertilized plots. The review suggests that N saturation of some ecosystems could be an explanation for the variable response of N_2O emissions to N addition (Barnard et al., 2005) however, no soil residual N measurements were presented for these studies. Future studies involving the response of N_2O emissions to N addition should therefore be accompanied by frequent soil residual N measurements. Findings from our study emphasizes the importance of incorporating the non-linear rise of N_2O emissions due to different soil residual N levels in inventories – This can be achieved by using a process-based three-dimensional mathematical model *ecosys* (Grant, 2001a,b), in an IPCC Tier III Methodology.

N_2O emission response to fertilizer N addition in *ecosys* also varied with fertilizer source. Modeled results from *ecosys* (Grant, 2001a,b) showed that N_2O emissions and EFs were higher for the hog manure (Figure 3-6; Tables 3-6, 3-7) compared to urea fertilizer

(Figure 3-1; Tables 3-6, 3-7) for similar N application rates (e.g. Modeled EFs (2003): 0.5% (90 kg N ha^{-1} (urea)) versus 3% (87 kg N ha^{-1} (hog manure)), with a few significant correlations in some cases (e.g., R^2 of modeled versus measured data:0.48 (2003, 87 kg N ha^{-1}), $P < 0.001$), due to the presence of both mineral N and organic C sources in hog manure (Table 3-3). The consistency of modeled and measured results in these cases **supports the Stage 2 (non – linear) response hypothesis in *ecosys* (Grant, 2001a,b) outlined in the Introduction (section 3.1). A consequence of this hypothesis is that: An organic source (hog manure) will give higher N_2O emissions than those of inorganic source (urea). The model explanation for this trend is that readily available N and organic C in hog manure (less C limitation) increases the demand for alternative electron acceptors (Eqs. [2.10] – [2.18]) compared to that of urea fertilizer (C limited), leading to higher N_2O emissions since N and organic C promote microbiological activity of nitrification (Eq. [2.10]) and denitrification (Eq. [2.18]) in the model. Organic C from hog manure may increase heterotrophic respiration (Eq. [8] and [9] of Grant, 2004) in the model, thereby leading to O_2 limitations and, thus, increased demand for alternative electron acceptors (Eqs. [2.10] – [2.18]) compared to that of urea fertilizer.** These finding again show the importance of the use of site-specific EFs as is done in *ecosys* since a similar fertilizer rate can give different emissions depending on whether the source is organic or inorganic.

N_2O emissions in *ecosys* also varied with inter-annual variation in precipitation. Modeled results from *ecosys* (Grant, 2001a,b) showed that N_2O emissions and EFs were highest in 2003 (Figures 3-1-3-3; Tables 3-6, 3-7) compared to the other years, with general

consistency (Table 3-10; e.g. Higher modeled and measured EFs for spring urea applications in 2003 versus 2002 (drought year in Alberta, Canada)), due to highest precipitation in 2003. Other studies (e.g. Flechard et al. 2007; Lu et al., 2006) found a similar trend. Higher rainfall (e.g. Figure 3-3a versus 3-2a) in *ecosys* can be used to explain larger surface flow (Eq. [2.21]) and subsurface flow (Eqs. [21] and [24] and [A94 - A96] of Grant et al., 2004) which resulted in further increases in WFPS > 60% (e.g. Figure 3-3b versus Figure 3-2b). The general consistency of modeled and measured results **supports the hypothesis in *ecosys* (Grant, 2001a,b) outlined in the Introduction (section 3.1), that N_2O production increases sharply (threshold, non-linear response) at 90% > WFPS > 60%. This non-linear rise of N_2O emissions in the model can be explained by the D_g (Eq. [2.28]) of O_2 whereby at WFPS < 60%, the D_g (Eq. [2.28]) of O_2 is large enough to meet microbial demands. However, as WFPS increases above 60%, the D_g (Eq. [2.28]) of O_2 declines sharply and the unmet O_2 demand forces the need for alternative electron acceptors (Eqs. [2.10] – [2.18]) thus, higher N_2O production via nitrification (Eq. [2.10]) and denitrification (Eq. [2.18]) in the model.** Consequently, in order to have better quantification of N_2O emissions, the inter-annual variation of precipitation should be taken into account in inventories. Flechard et al (2007) also proposed an empirical model which showed that EFs were higher with higher soil WFPS and temperature. However, at some sites the total precipitation was lower than others but emissions were higher due to the soil WFPS remaining higher throughout the year than most sites. These results showed the importance of modeling WFPS distribution based on intra-annual variation of precipitation, and its effects on N_2O emissions. Such complex relationships again

highlights the importance of a process-based mathematical model *ecosys* (Grant, 2001a,b), that accounts for inter and intra-annual variations of precipitation and its effects on N_2O emissions, in addition to many other site-specific factors. Using an IPCC Tier III Methodology thus may help improve the accuracy of N_2O inventories thereby allowing Canada to better track its reduction targets.

Although there were a few significant correlations between modeled and measured N_2O emissions for this chapter, there were also many small and insignificant correlations (chapter 3, section 3.4). These low correlations may be attributed the large spatial variation in the chamber readings as well as the infrequent chamber readings which limited the model testing experiment thus, reduced the certainty of the findings. Studies by Grant and Pattey, (2003) showed that both the temporal and spatial variability of N_2O emissions may be caused by topographically-driven flows of water and solutes (e.g. DOC, NH_3 and NO_3^-) through landscapes causing greater emissions in topographic positions in which water and solutes are gathered, than at positions from which they are shed. Consequently, *ecosys* was further tested using measured data from both micrometeorological (high temporal resolution) and chamber techniques (chapters 4 and 5), to investigate the effect of topography and also soil properties on N_2O emissions.

7.1.4 CHAPTER 4.0 Using the Ecosys mathematical model to simulate temporal variability of nitrous oxide emissions from a fertilized agricultural soil (field scale: ~ 5ha)

Ecosys (Grant, 2001a,b) simulates the large **temporal** variability or "threshold" response of N_2O emissions to changes in soil temperature (T_s). Transitions from one reduction reaction to another in *ecosys* can be caused by small changes in soil temperature. Higher temperatures can accelerate reduction of O_2 by nitrifiers/denitrifiers thereby increasing the demand for O_2 electron acceptors at the microbial sites. As a result, microbial O_2 demand may exceed O_2 supply, resulting in the need for alternative electron acceptors (Grant and Rochette, 1994; Grant, 1995) and therefore transition to reduction of NO_2^- (nitrifiers) and NO_3^- (denitrifiers), accelerating production of N_2O. N_2O production may increase further with higher temperature because gaseous solubility is reduced and hence aqueous O_2 concentrations ($[O_{2s}]$) maintained at microbial microsites decline. The solubility of N_2O also decreases, therefore accelerating the release of previously accumulated aqueous N_2O in the soil profile. The temperature effect on gaseous solubility and O_2 demand will cause this transition to be sharper and its WFPS threshold value to be lower at higher temperatures. Solute (NH_4^+ and NO_3) concentrations in *ecosys* during nitrification of fertilizer N can also contribute towards this large temporal variability of N_2O emissions.

Following the experiments in Edmonton (chapter 3), *ecosys* (Grant, 2001a,b) was used to simulate N_2O emissions using at different spatial scales – meter (m^2), fetch (~5 ha) and field (~ 42ha), using a 20 x 20 matrix of 36m x 36m grid cells rendered in ArcGIS from a DEM to represent topography of a fertilized agricultural field in Ottawa (chapters 4 and

5). Modeled results were compared to measured data from micrometeorological towers, equipped with a tunable diode laser (TDL) and using flux-gradient technique, to assess temporal N_2O variability (Pattey et al., 2006a,b) (chapter 4). Grid cell simulations were also performed using original, earlier and later planting and fertilizer dates, to show the influence of changing precipitation and temperature patterns on N_2O emissions and EFs. Fertilizer application, precipitation and temperature were main the factors responsible for N_2O emissions. *Ecosys* (Grant, 2001a,b) captured the sensitivity of N_2O emissions in response to changes in WFPS (threshold response) (temporal variation) thereby allowing a better understand the episodic nature of these emissions. The findings have indicated that modeled emissions in *ecosys* (Grant, 2001a,b) rose sharply with WFPS > 60% in a way that was consistent with the measured data (Figures 4-2, 4-3 and 4-4; R^2 of modeled versus measured data: 0.46; $P < 0.001$; MUE = 0.4) since such correlations are often low in the literature. The consistency of modeled and measured results **supports the hypothesis in *ecosys* (Grant, 2001a,b) outlined in the Introduction (section 4.1), that N_2O production increases sharply (threshold, non-linear response) at 90% > WFPS > 60%**(same hypothesis as in chapter 2 except now tested in the field). This "threshold" response limited the extent to which simple correlations with WFPS and temperature can be used to predict N_2O emissions, hence the importance of process - based model *ecosys* (Grant, 2001a,b), for simulating N_2O production.

The episodic nature of these emissions requires that seasonal totals be derived from short-term (i.e., hourly) measured or modeled values rather than from isolated daily or weekly measurements as is done now. Seasonal N_2O emissions for the period 7 May – 12 July

were most of the time overestimated when estimates were based on one measurement per day compared to estimates based on continuous data set (per half-hour) (Table 4-2). Estimates based on less frequent chamber measurements (2 wk^{-1} and 1 wk^{-1}) were even more inaccurate (Table 4-2). Other studies (Pattey et al., 2007; Bouwman et al., 2002) showed similar results. This inaccuracy was due to the large diurnal variation of N_2O emissions compared to those of other greenhouse gases such as CO_2. Rochette et al. (1992) showed that diurnal variation of soil CO_2 emissions from a barley crop was only 17% in a nearby site to ours, while that of N_2O was higher in this study, ranging from 25 to 51% (modeled) and 24 to 63% (measured), during emission events (0 to 0.8 mg N_2O-N m^2 h^{-1}) (Figure 4-2e). It is therefore important to take sub-daily samples or have continuous datasets, to fully capture the large sub-diurnal fluctuations of N_2O emissions, in order to improve our confidence in annual estimates for inventories - Consequently, there is a need for an IPCC Tier III Methodology since this can provide more continuous data sets.

N_2O emissions and thus EFs, in *ecosys* was very sensitive to changes in T_s. Lower soil temperatures at all sites during DOY 144-147 (Figure 4-3c), caused lower modeled emissions (Figure 4-3e), although tower emissions were not lower. Higher soil temperatures in *ecosys* in the field during soil warming on DOY 148-157 (chapter 4; Figure 4-2c), reduced the aqueous solubility of O_2 (Eq. [A30] in Grant et al., 2006), thus slowing the dissolution of O_{2g} to O_{2s} (Eq. [A30] in Grant et al., 2006), therefore lowering $[O_{2s}]$ lowering $[O_{2s}]$ that sustained O_2 uptake by microbial populations (Eqs. [2.3a,b], [2.7a,b] and [2.14a,b]). Higher soil temperatures also led to an increase in microbial

activity and therefore a higher demand for O_2 (Eqs. [2.2], [2.3a,b], [2.13] and [2.14a,b], through the Arrhenius function in Eqs. [2.1] and [2.12]. Aqueous O_2 concentrations at nitrifier microsites ($[O_{2mi,n}]$ in Eqs. [2.3a,b] and [2.7a,b]) declined with respect to the Michaelis-Menten constant for O_2 uptake (K_{O2n} in Eqs. [3b] and [7b]), therefore O_2 uptake by nitrifiers ($R_{O2i,n}$ in Eqs. [2.3a] and [2.7a]) failed to meet O_2 demand (Eqs. [2.2] and [2.6]). Subsequently, alternative electron acceptors were used to produce N_2O in *ecosys* (Eqs. [2.10] and [2.18]). Results from chapter 4 also showed that on DOY 167, modeled emissions were ~ 4 times higher at 21.5°C (Figure 4-5a) with higher soil temperatures (Figure 4-2c) for the 3 weeks later model scenario (Table 4-3) than those on DOY 146 at 14°C (Figure 4-4a) with lower soil temperatures for the 3 weeks earlier model scenario. Dobbie and Smith (2001) found similar results whereby emissions for an arable soil were larger (nearly 4 – fold) at soil temperature of 18°C compared to those at 12°C, with an apparent Q_{10} of 8.9. This large apparent Q_{10} value may be related to the complex "threshold" response involved in N_2O production since most microbial processes usually have much smaller Q_{10} of 2 – 3. *Ecosys* was also recently tested (Grant and Pattey, 2007 (Submitted)) against the measurements by Dobbie and Smith (2001) whereby the model simulated the large rises in N_2O emissions in their study, in response to same temperature increments. Several other studies (e.g., Grant, 1995; and Smith et al., 1998; Flechard et al., 2007) have showed that N_2O emissions are lower at lower soil temperatures. In contrast, some studies covered in Barnard et al. (2005) showed different responses of N_2O emissions to higher temperatures.

The large temporal variability of N_2O in *ecosys* coincided with the temporal variability of solutes (NH_4^+ and NO_3) during nitrification of fertilizer N. Most measured and modeled emissions coincided with a period of rapid nitrification in *ecosys*, indicated by declining NH_4^+ and rising NO_3^- (DOY 140 – 155) (Figure 4-3d). Even though there was rainfall later in the crop season e.g. on DOY 173 (Figure 4-2a), thus increase in WFPS (Figure 4-2b), emissions were low (no significant emissions were measured and modeled after DOY 156). This was due to a decline in available NH_4^+ (Figure 4-2d) from plant uptake and consequent slowing of NH_3 oxidation ($X_{NH3i,n}$ in Eq.[2.4]), thus the rate of NO_2^- reduction ($R_{NO2i,n}$, in [10]) also declined, leading to a reduction in N_2O generation (Eqs. [2.10] and [2.18]). The reduction in N_2O emissions later in the season was also attributed to the decline in WFPS (Figure 4-2b) caused by more rapid evapotranspiration. EFs almost quadrupled for the same fertilizer rate when fertilizer applications were delayed (average EF: 1.67%), causing nitrification to occur in warmer soils (18°C) compared to earlier applications (average EF: 0.45%) when nitrification occurred in cooler soils (12°C). These results imply that fertilizer application dates not only should match crop uptake capacities but also should be applied at lower soil temperatures i.e., avoid late applications, to minimize loss of N through N_2O emissions. Maybe some of the large differences in N_2O emissions measured in experiments (Barnard et at., 2005) can be explained by differences in T_s due to different planting and fertilizer dates. Therefore, it may be necessary to incorporate the effect of T_s in current IPCC Tier II Methodology for Canada. However, there may be confounding effects of other factors e.g. WFPS, fertilizer use, soil residual and source (Sections 7.12 and 7.13) in the field, hence the need for process-based mathematical models such as *ecosys* that account for interacting site-

specific factors affecting N_2O emissions. Finding from chapter 4 showed the importance of including climate impact on N_2O emissions in models, to fully represent the complex hypotheses involved in N_2O emissions. In addition to the climate impact, *ecosys* represented other site-specific (land use, soil type, topography etc.) hypotheses involved in N_2O production. Ours EFs can therefore contribute towards to the development of an IPCC Tier III Methodology. A study by Flechard et al (2007) showed that although there was high variability, EFs generally increased with increasing temperature (0 - 25°C) between WFPS of 65 and 85%. The study (Flechard et al., 2007) also found that EFs of up to 6.5% are predicted for a soil temperature of 25°C and WFPS between 70 and 80%. However, such warm and wet conditions rarely occur simultaneously in European grasslands (Flechard et al., 2007). As a result, these high EFs may be more applicable for Tropical countries. Meta analysis (Bouwman et al., 2002) showed that soil warming had no effect on N_2O emissions in the field but had both positive and negative effects in the laboratory experiments. The review also emphasized the need for more soil warming studies (Bouwman et al., 2002).

7.1.5 CHAPTER 5.0: Using the Ecosys mathematical model to simulate topographic effects on spatial variability of nitrous oxide emissions from a fertilized agricultural soil (site: 1 < m^{-2}, fetch: ~ 5ha & field: ~ 42ha scales)

Ecosys (Grant, 2001a,b) can model the large **spatial variability** of N_2O because it is a three-dimensional model, which also uses input data from digital elevation models (DEMs) to account for topographic effects on the complex processes involved in N_2O generation. Such information can help us further understand both spatial and temporal variability of N_2O emissions, thus improve N_2O inventories. *Ecosys* includes hypotheses

for surface energy exchange and subsurface heat transfer, vertical (infiltration, drainage, root uptake and capillary rise) and lateral (driven by differences in topographic position) water redistribution, and hypotheses for the effects of soil temperature and water content on autotrophic and heterotrophic activities (includes soil gas transfers) (Grant, 2004; Grant et al., 1995a, Grant, 1995b; Grant, 1998; Grant, 1999; Grant, 2001a,b; Grant and Pattey, 2003). Current (e.g. Freibauer, 2003; Lu et al., 2006) and future (e.g. Roelandt et al., 2007) simulations of N_2O emissions based on empirical modeling, may not fully represent the large spatial and temporal variability of N_2O.

Modeled results from the Ottawa site (chapter 4) were also compared to fluxes measured with surface chambers placed at different topographic positions to measure spatial variability of N_2O emissions at the meter scale, and with stationary and mobile micrometeorological flux towers to assess spatial N_2O variability at the fetch scale (chapter 5). Results showed that *ecosys* (Grant, 2001a,b) represented the spatial variation of N_2O at the meter, fetch and field scales. Our findings have indicated that modeled spatial variation of N_2O emissions at the field scale (Figures 5-6, 5-7 and 5-8; Table 5-6) in *ecosys* (Grant, 2001a,b) was due to small differences in topography (~1.8m over 600m), in a way that was consistent with the measured data (Table 5-2). The consistency of modeled and measured results **supports the hypothesis in *ecosys* (Grant, 2001a,b) outlined in the Introduction (section 5.1), that spatial variation in N_2O emissions, can be explained in the model by (1) spatial (Figure 5-5) and temporal variation (Figure 4-2b) in soil WFPS. The three-dimensional capability of the model allows the simulation of spatial and temporal variation of WFPS among topographic**

positions that shed or collect water (Figure 5-1) according to topographically-driven water movement (surface Eq. [2.21]) and subsurface flow (Eqs. [21] and [24] and [A94 - A96] of Grant et al., 2004), even at a site with low topographic differences. Spatial variation in N_2O emissions can also be explained by (2) spatial variation in soil properties (spatial variation in soil properties caused CSV of annual fluxes to increase from 25 % to 101%), which may themselves be caused by topographically driven water movement. Topographically-driven flows (surface flow (Eq. [21]) and subsurface flow (Eq. [24]; Eqs. [A94 - A96] of Grant et al., 2004) of water and solutes in *ecosys* are as a result of lateral water redistribution due to differences in gravitational water potential. Coefficients of spatial variation (CSVs) amongst 4 chamber replicates (2m x 3 m grid) during emission events were 28 to 195 %, indicating that spatial variation of N_2O occurred at a very small spatial scale. High replicate variation of N_2O emissions was also found in the laboratory experiment in spite of soil mixing (chapter 2; section 7.1.2). Other studies showed that spatial variation in N_2O emissions can even occur at the aggregate level (Uchida et al., 2008; Sextone et al., 1985) and at chamber locations only 1 to 2 m apart (Folorunso and Rolston, 1984). Some of the inconsistencies between measured and modeled chamber emissions in our results may be due to high measured CVs amongst chamber replicates. As a result, replicate variation (root mean square for error (RMSE)) was larger that the variation between modeled versus measured (root mean square for difference (RMSD)) (Table 5-2) results therefore, the model hypothesis was not rejected.

Modeled results within the two fertilized (112 kg N ha^{-1}) areas (Figure 5-1) generally showed that the lowest topographic positions of the field gave the highest seasonal N_2O emissions or were 'hot spots' for N_2O emissions since these areas had high flow accumulation (FA) values (FA versus N_2O: $R^2 = 0.1$, $P < 0.05$). Consequently, EF modeled for the 112 kg N ha^{-1} fertilizer application was larger in an area of the field with lower topography (0.3%) compared to one with higher (0.1%). As a result, EF may vary depending on the sample location in the field. Other studies (e.g. Flessa et. al., 1995; Ball et. al., 1997; Pennock and Corre, 2001) found similar results. Results from chapter 5 showed that some of this variation may be caused by differences in the progression of the emission events at different landscape positions (Figure 5-3) as found by Grant and Pattey (2003). Large daily temporal variation in soil WFPS and temperature also led to large spatial variation of N_2O emissions across the field for different times of the day during the emission event (Figure 7).

Generally, low EFs (Tables 6-2; 6-3) for 2004 could be attributed to slightly lower average mean temperatures (May: 12.8°C and June: 17.1°C) compared to long-term normals for 1971 – 2000 (May: 13.4°C and June: 18.3°C) for the experimental area, that delayed soil warming, causing reactions that generated N_2O to occur in comparatively cool soils. When spatial variation in soil properties were represented in a second model run, CSV of annual fluxes (field scale) increased from 25 % to 101%. These results highlighted the importance of the use of three-dimensional mathematical model *ecosys*, with input from DEMs, to fully capture large spatial and temporal variability of N_2O emissions at different spatial scales even in seemingly flat landscapes, thus improve our

future estimates.

Ecosys can model the large spatial variation of N_2O emissions at different times scales – e.g. hourly, daily and annually etc.. Generally, our results showed that spatial variation of N_2O at hourly (Figure 5-3) and daily time-steps (e.g. 11 - 68%; Table 5-6) were large however, spatial variation of N_2O at seasonal (Table 5-3) and annual (e.g. 25%; Table 5-6) (except for 54 soil profile run) time scales were smaller. These finding suggests that spatial variation of N_2O probably may not affect the calculation of EFs at an annual time scale as much as it does short-term emissions. However, our field was fairly flat (0.2% slope) and fields (e.g. Li et al., 2005) with greater topographic differences may yield larger differences in emissions within the same fertilizer treatment. Also, measuring spatial variation at a high resolution is important for first testing mathematical models, before they can be used larger spatial scale studies.

Results from *ecosys* for this chapter will be used in an attempt to develop a spatial integration scheme for N_2O emissions whereby emissions at the field scale can be simulated based on specific site information such as FA, topography, soil type etc. For example, N_2O produced for each FA classifications or range of values can be evaluated, and then FA can be further used as a tool for predicting emissions for other sites. The use of chamber measurements at the field scale will also be further evaluated e.g. what is the optimal investment of chamber measurements? Further analyses will be performed to determine the (a) frequency of chamber measurements (b) number of chamber sampling

locations and (c) chamber method (s) integration scheme over time and space required for more accurate EFs at the field scale.

7.1.6 CHAPTER 6.0: Using Ecosys to project the impact of climate change (increasing CO_2 and temperature) on future spatial and temporal variability of N_2O emissions from an agricultural soil

For this research, *ecosys* (Grant, 2001a,b) processed – based mathematical model was used because in addition to modeling past and present N_2O emissions under site-specific conditions (past and current land use, soil type, topography etc.), the model can also simulate the complex feedback mechanisms involved in climate change by using weather data from climate change scenarios (e.g. air temperature, precipitation and CO_2). *Ecosys* (Grant, 2001a,b) has been used to predict the impact of climate change on short and long-term carbon and energy exchange in several agricultural (e.g. Grant et al., 1999b; Grant et al., 2001a); forest (e.g. Grant et al., 1999a; Grant et al., 2001b; Grant et al., 2005), arctic (e.g. Grant et al., 2003) and grassland (e.g. Li et al., 2004) ecosystems. The model has also been used to predict long-term changes in soil C under different land use management systems (Grant et al., 2001c). Recently, *ecosys* (Grant and Pattey, 2007 (Submitted)) was used to project climate impact on N_2O emissions. Earlier testing against measured data from this research (chapters 2 - 5) showed that *ecosys* (Grant, 2001a,b) represented the site-specific (past and present fertilizer use, climate, soil type, topography etc.) complex physical, chemical and biological hypotheses involved in N_2O production. *Ecosys* therefore captured the large spatial and temporal variability of N_2O emissions.

The sensitivity of N_2O emissions to changes in T_s in *ecosys* (Grant, 2001a,b) was simulated in earlier studies (Grant, 1991; Grant et al., 1992; Grant et al., 1993c; Grant, 1994; Grant; 1995; Grant and Pattey, 1999; Grant and Pattey, 2003; Grant et al., 2006; Grant and Pattey, 2007 (Submitted)), which is important for climate change modeling. Soil temperatures in *ecosys* are controlled by canopy energy exchange calculated from an hourly two-stage convergence solution for the transfer of water and heat through a multi-layered multipopulation soil–root–canopy system (Grant et al., 2005). Rising air temperature in *ecosys* due to climate change will cause greater conductive (Eq. [A.5], [A.19] and [A.26] of Grant, 2001a), convective and latent (Eq. [A.1] [A.3], [A.4] and [A.18] of Grant, 2001a) energy exchanges from surface to subsurface (Eqs. [A24] – [A25] and [A.27] of Grant, 2001a), thereby increasing soil temperature. Soil temperature can be modeled for diverse soil types since soil properties in the soil file input (texture, water content at field capacity and wilting point, horizontal and vertical saturated hydraulic conductivity etc.) can be changed depending on site-conditions. Surface and subsurface energy exchange are consequently affected by soil properties.

Ecosys will also capture the effect of future changes in precipitation on N_2O emissions. The sensitivity of N_2O to changes in precipitation in *ecosys* (Grant, 2001a,b) was simulated in earlier studies (Grant, 1991; Grant et al., 1992; Grant et al., 1993c; Grant, 1994; Grant; 1995; Grant and Pattey, 1999; Grant and Pattey, 2003; Grant et al., 2006; Grant and Pattey, 2007 (Submitted)), which is important for climate change modeling. Changes in precipitations inputs into the model determine surface and subsurface flows of water. In *ecosys*, surface flow is calculated using a Manning equation while subsurface

flow (e.g. Grant and Pattey 2003; Grant, 2004; Eqs. [2.21] and [24] and [A94 - A96] of Grant et al., 2004) is calculated using both Richards and Green-Ampt flow equations. This is important since surface and subsurface transport of water determine soil WFPS, which is an important controller of N_2O production as well as emissions from the soil profile. Increased T_a in *ecosys* leads to increased saturated pressures (e_s) at evaporating surfaces thus higher vapour pressure deficits and therefore increased evapotranspiration. Consequently, these changes may lead to lower WFPS and thereby lower N_2O production via nitrification/denitrification. In contrast, higher CO_2 levels during climate change may decrease transpiration by increasing stomatal resistance (stomatal closure) at higher mesophyll CO_2 concentration (C_l (μmol mol^{-1}) for each leaf surface, thereby improving overall water use efficiency (WUE) (e.g. Grant et al., 1999a,b; Grant et al., 2001a,b; Grant et al., 2003; Grant et al., 2005; Li et al., 2004). Grant et al. (2001a) showed that evapotranspiration was reduced by 9 % and 16% with fertilization of 35 and 7 g m^{-2} respectively in a wheat field, when treated with 548 versus 362 μmol mol^{-1} of CO_2. Consequently, these changes may result in wetter soils which may increase N_2O production via nitrification and denitrification.

Rising CO_2 in *ecosys* will increase GPP and hence soil C inputs by which N transformation reactions that generate N_2O are driven through a biochemical model in which leaf CO_2 fixation rates are directly affected by atmospheric CO_2, through the effects of atmospheric CO_2 on canopy CO_2 concentration and hence gaseous and aqueous mesophyll CO_2 concentration (e.g. Grant et al., 1999a,b; Grant et al., 2001a,b; Grant et al., 2003; Grant et al., 2005). Fixation of CO_2 in *ecosys* (Grant, 2001a,b) is calculated

from coupled algorithms for carboxylation and diffusion (Grant, 2004), based on Michaelis-Menten function of a maximum reaction rate (Grant et al., 2001b). CO_2 fixation in *ecosys* is also affected by soil N uptake which may be raised by soil N transformations hastened by higher T_a. Greater CO_2 fixation (Eqs [20] – [29] of Grant, 2004) modeled in *ecosys* will result in faster litterfall (Eq. [29] - [37] of Grant, 2004), thus more microbial respiration (Eq. [8] and [9] of Grant, 2004) of organic matter, to produce substrates (dissolved organic carbon (DOC) for N_2O production via denitrification (Eqs. [2.16] – [2.18]). However, more rapid CO_2 fixation (Eqs [20] – [29] of Grant, 2004) in the model may also lead to more rapid N uptake g. R_{NH4} (g N m^{-3}) of Eqs. [39a,b] of Grant, 2004) thus lowering soil mineral N (especially in N deficient ecosystems) and decreasing N_2O production via nitrification (Eq. [2.10]) and denitrification (Eq. [2.10]).

Results from chapter 6 showed that ***ecosys* (Grant, 2001a,b) predicted climate change impacts on future spatial and temporal variability of N_2O emissions for the Ottawa site** (chapters 4 and 5). These findings allowed a better understanding of how increasing CO_2 and temperature in the future may affect behaviour arising from the complex N_2O hypotheses thus, the climate change feedback mechanisms involved in N_2O generation. Results from this study showed that EFs may more than double by 2050 due to rising CO_2 and temperature levels but would decline with lower WFPS by 2080; This is important since such results imply that we may need to re-estimate N_2O emissions from fertilization in future inventories. For this chapter, it was assumed that there will be no changes in future precipitation.

Ecosys represented future temporal variability of N_2O emissions thereby providing further insights into the episodic ("threshold") nature of these emissions. This episodic nature of N_2O emissions shows the importance of linking biological controls of N_2O emissions to physical controls in mathematical models, hence the importance of processed - based models such as *ecosys*, (Grant, 2001a,b) for simulating both current and future N_2O emissions. Higher air temperatures (Figure 6-1) for the 2020 and 2050 climate change scenarios (Table 6-1) resulted in higher annual N_2O emissions (Table 6-2) than that for the current climate. Previous studies (e.g. Grant, 1995; and Smith et al., 1998; Grant & Pattey, 2007 (Submitted); Flechard et al., 2007) have shown that N_2O emissions are rise rapidly with soil temperatures. Peak modeled emissions events started and finished earliest (DOY 139 - 147) for the 2080 scenario (Table 6-1) compared to those of 2004, 2020 and 2050 scenarios (DOY 146 - 154) (Figure 6-2c) due to the earliest onset of snowmelt (Eqs. [A.27] of Grant, 2001a) due to earlier soil warming (Figure 6-1b,f). These results suggest that emissions may be affected by the soil conditions under which nitrification of fertilizer occurs, as affected by temporal variability of temperature and WFPS, even if the same fertilizer rate was used.

In contrast to 2020 and 2050, 2080 scenario gave the lowest annual N_2O emissions (Figure 6-2d) and EF (Table 6-2) was similar to that of the current climate (2004, no temperature increments). This trend occurred because nitrification (Eqs. [2.1] – [2.8]; Figure 6-2a,b) finished earlier and also the overall WFPS (Figure 6-1c,g) was lowest for the spring/summer months, compared to the other projections. Lowest WFPS (Figure 6-1c,g) during spring/summer periods for the 2080 scenario was due to greater loss of latent

heat. In *ecosys*, latent heat loss was accelerated through higher vapor pressure differences between (1) canopy mesophyll surfaces and the atmosphere (transpiration) (Eqs. [A.1] and [A.3] of Grant, 2001a) (2) wet canopy surfaces and the atmosphere (evaporation) (Eqs. [A.1] and [A.4] of Grant, 2001a) (3) soil and residue surfaces and the atmosphere (evaporation) (Eq. [A.18] of Grant, 2001a) and (4) latent heat loss due to subsurface heat and water transfer (Eqs. [A24] – [A25] and [A.27] of Grant, 2001a). However, increased latent heat loss was partially offset by reduced transpiration due to greater leaf stomatal resistance (Eq. [A.3] of Grant, 2001a; Eqs. [26] and [27] of Grant, 2004) as a result of higher CO_2 levels for the climate change scenarios. Lowest WFPS in 2080 led to larger surface and subsurface gaseous diffusivity ($D_{g\gamma}$ in Eq. [2.28]) of ($[O_{2g}]$), thus greater dissolution of O_{2g} to O_{2s} (Eq. [A30] in Grant et al., 2006). As a result, more O_2 was available for (1) oxidation of NO_2^- (Eqs. [2.5]- [2.8]) and (2) oxidation of DOC by heterotrophs (Eqs. [2.12]- [2.15]), thus less N_2O was produced via nitrification (Eq. [2.10]) and denitrification (Eq. [2.18]). A study by Kamp et al. (1998) showed similar results whereby total N_2O emissions were similar for the control and heated plots and soil moisture was lower for the heated plots. These results further support the use of mathematical model *ecosys* to fully capture the large temporal variability of N_2O emissions due to changes in both temperature and WFPS.

Higher atmospheric CO_2 levels for climate change scenarios (Table 6-1) led to more rapid CO_2 fixation (Eqs. [6.6] – [6.9]; Eqs. [24] – [29] of Grant, 2004) which resulted in greater litterfall (Eqs. [29] and [37] of Grant, 2004). Greater litterfall (Eqs. [29] and [37] of Grant, 2004) led to more microbial respiration (Eq. [8] and [9] of Grant, 2004) of

organic matter and greater O_2 demand, to produce substrates (greater dissolved organic carbon (DOC) for N_2O production via denitrification (Eqs. [2.16] – [2.18]), thus higher EFs for 2020 and 2050 (Table 6-2). Studies (e.g. Grant et al., 1999a,b; Grant et al., 2001a,b; Grant et al., 2003; Grant et al., 2005; Li et al., 2004) showed that elevated CO_2 increases biomass production and decreases evapotranspiration (higher water use efficiency). Earlier studies have shown that higher CO_2 levels may have contrasting effects on N_2O emissions. Several studies (Ineson et al., 1998; Kettunen et al., 2005; 2006; 2007a,b) showed that when conditions for denitrification were favorable (high N concentrations and high soil moisture), elevated CO_2 enhanced N_2O emissions due to greater C substrates produced by roots. In contrast, emissions from the 2080 fertilized and control run modeled (Table 6-2) were the lowest because these scenarios had the highest CO_2 concentrations thus greatest CO_2 fixation (Eqs [20] – [29] of Grant, 2004) therefore, more rapid N uptake. More rapid N uptake (g. R_{NH4} (g N m^{-3}) of Eqs. [39a,b] of Grant, 2004; Figure 6-2c) reduced soil mineral N thus decreasing overall N_2O production via nitrification (Eq. [2.10]) and denitrification (Eq. [2.10]). These findings may explain why variable results have been reported in the literature since the effect of rising CO_2 levels on N_2O emissions will be depend on the soil mineral N or N limitation.

A review by Barnard et al. (2005) showed no significant effect of elevated CO_2 on N_2O emissions but emphasized the need for more climate change studies to provide further insights. However, reduced NO_3^- has been used to explain decreased denitrifying enzyme activity at elevated CO_2 in several studies (Tscherko, et al., 2001; Barnard et al., 2004a). Findings from chapter 6 suggest that N_2O inventories should account for CO_2 effects on

N_2O emissions especially since CO_2 levels may change in the future. As mentioned in earlier (Section 7.1.3), soil residual N should be part of inventories since this will also determine how elevated CO_2 levels will affect N_2O emissions in the future. These results again shows the importance of using process-based model *ecosys* (Grant, 2001a,b), in order to fully represent the complex hypotheses involved in the prediction of effects of climate change (e.g. air temperature, precipitation and CO_2) on N_2O emissions, thus improve future quantifications.

Ecosys also projected future spatial variation of N_2O emissions at the field scale. Overall, CSV of annual N_2O totals within the 112 kg N ha^{-1} fertilized area for 2050 was similar (18%) to that of the current climate (25%) in 2004 (chapter 5, section 5.3.4). Projected 2050 results showed that EF modeled for the 112 kg N ha^{-1} fertilizer application was larger (0.8% - east section, lower topography area and 0.6% - west section, higher topography area) than that of 2004 (0.3 and 0.1% respectively (chapter 5, Table 5-7)). These results shows the importance of using three-dimensional models such as *ecosys* (Grant, 2001a,b) with input from DEMs, in order to fully represent the complex hypotheses involved in the prediction of N_2O emissions, thus improve our future estimates. Based on the literature, there were no projection studies of N_2O emissions using processed – based models that include the influence of topography.

Both current and future projections of N_2O EFs are important since the sustainability of current land use management systems can be evaluated under future climates. Recommendations can then be made for best management practices (e.g. earlier planting

and later harvesting dates for the 2050 model scenario (Table 6-2) caused EF to decrease from 0.7 to 0.6%) to mitigate future N_2O emissions from agricultural soils. Canada has to reduce its total greenhouse emissions by 2012 under the Kyoto Protocol (Olsen et al., 2003) therefore, the best management practices can be determined to help meet the national reduction targets by this year and future years. This can be achieved by using a processed – based mathematical model *ecosys* (Grant, 2001a,b), since emissions can be determined from diverse scenarios of different land use, climate, soil type, topography etc. Future greenhouse gas projections can therefore be used as a tool in inventories to reduce emissions. If such applications for an IPCC Tier III Methodology are made in different countries, then ultimately global N_2O emissions can be reduced.

7.2 Recommendations and research prospects

Future modeling work will enable *ecosys* (Grant, 2001a,b; website: www.ecosys.rr.ualberta.ca) to scale N_2O emissions from landscape to regional and national scales, thus enabling N_2O inventories and projections to be made for Canada. Geo-referenced climate, activity data (Statistics Canada) and soil data are available in Canada for testing *ecosys* at provincial scale and national level (also access to Westgrid high-performance computing network and geographical information systems (GIS)) computing facilities at the University of Alberta).

More research is needed to resolve unexplained chamber replicate spatial variation at the meter scale. More field measurements of soil properties e.g. field capacity, wilting point etc. may also improve confidence in the values used as model inputs, thus estimates of

N_2O emissions. More research is needed using both chamber (e.g. automated for better temporal resolution and higher number of sampling points for better spatial resolution) and micrometeorological methods simultaneously, under other land use management practices e.g. manure applications. This data can be further used to test *ecosys* simultaneously at chamber, tower and field scales to model both spatial and temporal variability of N_2O emissions for the development of more site-specific EFs, for the development of the IPCC Tier III methodology. This will also provide information for developing a methodology for scaling emissions from chamber to tower scales.

Ecosys (Grant, 2001a,b) has been used to predict the impact of climate change on short- and long-term carbon and energy exchange in several agricultural (e.g. Grant et al., 1999a,b; Grant et al., 2001a); forest (e.g. Grant et al., 2001b; Grant et al., 2005), artic (e.g. Grant et al., 2003) and grassland (e.g. Li et al., 2004) ecosystems. Recently, *ecosys* (Grant and Pattey, 2007 (Submitted)) was used to project climate impact on N_2O emissions. Future research will enable *ecosys* to make predictions under different land uses and climate change scenarios. These predictions can then be used to make recommendations for sustainable land use management recommendations in order to enhance crop productivity and maintain environmental quality. *Ecosys* has been used to simulate other greenhouse gases CH_4 (Grant, 1998) and CO_2 (e.g. Grant et al., 1999a,b; Grant et al., 2001a,b; Grant et al., 2003; Grant et al., 2005) so that greenhouse gases inventories and projections for Canada can also be extended to these gases.

7.3 REFERENCES

Ball, B.C., Horgan, G.W., Clayton, H., Parker, J.P., 1997. Spatial variability of nitrous oxide fluxes and controlling soil topographic properties. Journal of Environmental Quality 26, 1399-1409.

Barnard, R., Leadley, P.W., Hungate, B.A., 2005. Global change, nitrification, and denitrification: A review. Global Biogeochemical cycles 19, GB1007, doi:10.1029/2004GB002282.

Bateman, E.J., Baggs, E.M., 2005. Contributions of nitrification and denitrification to N_2O emissions from soils at different water-filled pore space. Biology & Fertility of Soils 41, 379-388.

Belser, L.W., Schmidt, E.L., 1980. Growth and oxidation kinetics of the three genera of ammonia oxidizers. FEMS Microbiology Letters 7, 213-216.

Blackmer, A.M., Robbins, S.G., Bremner, J.M., 1982. Diurnal variability in rate of emission of nitrous oxide from soils. Soil Science Society of America Journal 46, 937-942.

Bouwman, A.F., Boumans, L.J.M., Batjes, N.H., 2002. Emissions of N_2O and NO from fertilized fields: Summary of available measurement data. Global Biogeochemical cycles 16(4), 1058, doi:10.1029/2001GB001811.

Bouwman, A.F., 1996. Direct emission of nitrous oxide from agricultural soils. Nutrient Cycling in Agroecosystems 46, 53-70.

Brock, T.D., Madigan, M.T., 1991. Biology of Microorganisms, 6th ed., Prentice Hall, Englewood Cliffs, NJ.

Clay, D.E., Molina, J.A.E., Clapp, C.E., Linden, D.R., 1985. Nitrogen-tillage-residue management: II. Calibration of potential rate of nitrification by model simulation. Soil Science Society of America Journal 49, 322-325.

Davidson, E.A., 1991. Fluxes of nitrous oxide and nitric oxide from terrestrial ecosystems. In: Rogers, J.E., Whitman, W.B. (Eds.), Microbial Production and Consumption of Greenhouse Gases: Methane, Nitrogen Oxides and Halomethanes. American Society of Microbiology, Washington, D.C., pp. 219-235.

de Vries, D.A. 1963. Thermal properties of soils. In R. van wijk (Ed.). Physics of Plant Environment. North Holland Publishing, Amsterdam, The Netherlands, 210-235.

Dobbie, K.E., Smith, K.A., 2001. The effects of temperature, water-filled pore space and land use on N_2O emissions from an imperfectly drained gleysol. European Journal of Soil Science 52, 667-673.

Dobbie, K.E., Smith, K.A., 2003. Nitrous oxide emission factors for agricultural soils in Great Britain: the impact of soil water-filled pore space and other controlling variables. Global Change Biology 9, 204–218.

Eggleston, 2006. Intergovernmental Panel on Climate Change (IPCC), IPCC Guidelines for National Greenhouse Gas Inventories Volume 4; Agriculture, Forestry and other land use. Institute for Global Environmental Strategies, kanagawan Hayama, Japan.

Flessa, H., Dörsch, P., Beese, F., 1995. Seasonal variation of N_2O and CH_4 fluxes in differently managed arable soils in southern Germany. Journal of Geophysical Research 100, 23115-23124.

Flechard, C.R., Ambus, P., Skiba, U., Rees, R.M., Hensen, A., van Amstel, A., van den Pol-van Dasselaar, A., Soussana, J.-F., Jones, M., Clifton-Brown, J., Raschi, A., Horvath, L., Neftel, A., Jocher, M., Ammann, C., Leifeld, J., Fuhrer, J., Calanca, P., Thalman, E., Pilegaard, K., Di Marco, C., Campbell, C., Nemitz, E., Hargreaves, K.J., Levy, P.E., Ball, B.C., Jones, S.K., van de Bulk, W.C.M., Groot, T., Blom, M., Domingues, R., Kasper, G., Allard, V., Ceschia, E., Cellier, P., Laville, P., Henault, C., Bizouard, F., Abdalla, M., Williams, M., Baronti, S., Berretti, F., Grosz, B., 2007. Effects of climate and management intensity on nitrous oxide emissions in grassland systems across Europe. Agriculture, Ecosystems and Environment 121, 135-152.

Focht, D.D., Verstraete, W., 1977. Biochemical ecology of nitrification and denitrification. Advances in Microbial Ecology 1, 135-214.

Folorunso, O.A., Rolston, D.E., 1984. Spatial variability of field measured denitrification fluxes. Soil Science Society of America Journal 48, 1214-1219.

Freibauer, A., 2003. Regionalised inventory of biogenic greenhouse gas emissions from European agriculture. European Journal of Agronomy 19, 135-160.

Gabrielle, B., Laville, P., Duval, O., Nicoullaud, B., Germon, J.C., Henault, C., 2006. Process-based modeling of nitrous oxide emissions from wheat cropped soils at the subregional level. Global Biochemical Cycles 20, 1-11.

Grant, R.F., 1991. A technique for estimating denitrification rates at different soil temperatures, water contents, and nitrate concentrations. Soil Science 152, 41-52.

Grant, R.F., 1994. Simulation of ecological controls on nitrification. Soil Biology & Biochemistry 26, 305–315.

Grant, R.F., 1995a. Dynamics of energy, water, carbon and nitrogen in agricultural ecosystems: simulation and experimental validation. Ecological Modelling 81, 169–181.

Grant, R.F., 1995b. Mathematical modelling of nitrous oxide evolution during nitrification. Soil Biology & Biochemistry 27, 1117–1125.

Grant, R.F., 1997. Changes in soil organic matter under different tillage and rotation: mathematical modeling in *ECOSYS*. Soil Science Society of America Journal 61, 1159-1175.

Grant, R.F., 1998. Simulation of methanogenesis in the mathematical model *ecosys*. Soil Biology & Biochemistry 30, 883-896.

Grant, R.F., 1999. Simulation of methanotrophy in the mathematical model *ecosys*. Soil Biology & Biochemistry 31, 287–297.

Grant, R.F., 2001a. A Review of the Canadian Ecosystem Model - *ecosys*. In: Shaffer M. J., Ma, L., Hansen, S. (Ed), Modeling Carbon and Nitrogen Dynamics for Soil Management. CRC Press. Boca Raton, FL, pp. 173-263.

Grant, R.F., 2001b. Modeling Transformations of Soil Organic Carbon and Nitrogen at Differing Scales of Complexity. In: Shaffer M. J., Ma, L., Hansen, S. (Ed), Modeling Carbon and Nitrogen Dynamics for Soil Management. CRC Press. Boca Raton, FL, pp. 597-614.

Grant, R.F., 2004. Modeling topographic effects on net ecosystem productivity of boreal black spruce forests. Tree Physiology 24, 1-18.

Grant, R.F., Rochette, P., 1994. Soil Microbial respiration at Different Water Potentials and Temperatures: Theory and Mathematical Modeling. Soil Science Society of America Journal 58, 1681-1690.

Grant, R.F. Pattey, E., 1999. Mathematical modeling of nitrous oxide emissions from an agricultural field during spring thaw. Global Biogeochemical Cycles 13, 679-694.

Grant, R.F., Pattey, E., 2003. Modelling variability in N_2O emissions from fertilized agricultural fields. Soil Biology & Biochemistry 35, 225-243.

Grant, R.F., Pattey, E., 2007 (Submitted). Temperature sensitivity of N_2O emissions from fertilized agricultural soils: mathematical modelling in *ecosys*.

Grant, R.F., Nyborg, M., Laidlaw, J.W., 1992. Evolution of nitrous oxide from soil: II. Experimental results and model testing. Soil Science 156, 266-277.

Grant, R.F., Juma, N.J., McGill, W.B., 1993a. Simulation of carbon and nitrogen transformations in soils. I: mineralization. Soil Biology & Biochemistry 25, 1317-1329.

Grant, R.F., Juma, N.J., McGill, W.B., 1993b. Simulation of carbon and nitrogen transformation in soil: Microbial biomass and metabolic products. Soil Biology & Biochemistry 25, 1331-1338.

Grant, R.F., Nyborg, M., Laidlaw, J.W., 1993c. Evolution of nitrous oxide from soil: I. Model development. Soil Science 156, 259-265.

Grant, R.F., Garcia, R.L., Pinter Jr, P.J., Hunsaker, D., Wall, G.W., Kimball, B.A., LaMorte, R.L., 1995a. Interaction between atmospheric CO_2 concentration and water deficit on gas exchange and crop growth: Testing of *ecosys* with data from the free air CO_2 enrichment (FACE) experiment. Global Change Biology 1, 443 - 454.

Grant, R.F., Izaurralde, R.C., Chanasyk, D.S., 1995b. Soil temperature under different soil managements: testing a simulation model. Agriculture & Forest Meteorology 73, 89-113.

Grant, R.F., Kimball, B.A., Pinter, P.J.J., Wall, G.W., Garcia, R.L., La Morte, R.L., Hunsaker, D.J., 1995c. Carbon dioxide effects on crop energy balance: testing ecosys with a the free air CO_2 enrichment (FACE) experiment. Agronomy Journal 87, 446–457.

Grant, R.F., Izaurralde, R.C., Nyborg, M., Malhi, S.S., Solberg, E.D., Jans-Hammermeister, D., Stewart, B.A., 1998. Modeling tillage and surface residue effects on soil C storage under ambient versus elevated CO_2 and temperature in *ECOSYS*. In: Lal, R., Kimble, J.M., Follet, R.F. (Eds), Soil processes and carbon cycle. CRC Press Inc. Boca Raton, USA, pp. 527-547.

Grant, R.F., Black, T.A., den Hatog, G., Berry, J.A., Gower, S.T., Heumann, H.H., Blamken, P.D., Yang, P.C., Russell, C., 1999a. Diurnal and annual exchanges of mass and energy between an aspen-hazelnut forest and the atmosphere: testing the mathematical model *ecosys* with data from the BOREAS experiment. Journal of Geophysical Research 104, 699-717.

Grant, R.F., Wall, G.W., Kimball, B.A., Frumau, K.F.A., Pinter Jr., P.J., Hunsaker, D.J., Lamorte, R.L., 1999b. Crop water relations under different CO_2 and irrigation: testing of *ecosys* with the free air CO_2 enrichment (FACE) experiment. Agriculture & Forest Meteorology 95, 27–51.

Grant, R.F., Kimball, B.A., Brooks T.J., 2001a. Modeling interactions among carbon dioxide, nitrogen and climate on energy exchange of wheat in a Free Air carbon dioxide experiment. Agronomy Journal 93:638-649.

Grant, R.F., Massheder, J.M, Hale, S.E., Moncrieff, J. B., Rayment, M, Scott, S.L., Berry, J.A., 2001b. Controls of carbon and energy exchanges by a black spruce – moss ecosystem: Testing the mathematical model *Ecosys* with data from the BOREAS experiment. Global Biogeochemical cycles 15, 129 – 147.

Grant, R.F., Juma, N.G., Robertson, J.A., Izaurralde R.C., McGill, W.B., 2001c. Long – term changes in soil C under different fertilizer, manure and rotation: Testing the mathematical model *Ecosys* with data from the Breton plots. Soil Science Society of American Journal 65, 204-214.

Grant, R.F., Oechel, W.C., Ping, C., Kwon, H., 2003. Carbon balance of coastal arctic tundra under changing climate. Global Change Biology 9, 16–36.

Grant, R.F., Amrani, M., Heaney, D.J., Wright, R., Zhang, M., 2004. Mathematical Modeling of Phosphorus Losses from Land Application of Hog and Cattle Manure. Journal of Environmental Quality 33, 210-231.

Grant , R.F., Arain, A., Arora, V., Barr, A., Black, T.A., Chen, J. Wang, S., Yuan, F., Zhang, Y., 2005. Intercomparison of techniques to model high temperature effects on CO_2 and energy exchange in temperate and boreal coniferous forests. Ecological Modelling 188, 217–252.

Grant, R.F., Pattey, E., Goddard, T.W., Kryzanowski, L.M., Puurveen, H., 2006. Modeling the effects of fertilizer application rate on nitrous oxide emissions. Soil Science Society of America Journal 70, 235-248.

Helgason, B.L., Janzen, H.H., Angers, D.A., Boehm, M., Bolinder, M., Desjardins, R.L., Dyer, J., Ellert, B.H., Gibb, D.J., Gregorich, E.G., Lemke, R., Massé, D., McGinn, S.M., McAllister, T.A., Newlands, N., Pattey, E., Rochette, P., Smith, W., VandenBygaart, A.J., Wang, H., 2005. GHGFarm: An assessment tool for estimating net greenhouse gas emissions fromCanadian farms. Agriculture & Agri-Food Canada, pp. 5-6.

Hénault, C., Devis, X., Page, S., Justes, E., Reau, R., Germon, J.C., 1998. Nitrous oxide emissions under different soil and land management conditions. Biology and Fertility of Soils 26, 199-207.

Hutchinson, G.L., Mosier, A.R., 1981. Improved soil cover method for field measurement of nitrous oxide fluxes. Soil Science Society of America Journal 45, 311-316.

Ineson, P., Coward, P.A., Hartwig, U.A., 1998. Soil gas fluxes of N_2O, CH_4 and CO_2 beneath *Lolium perenne* under elevated CO_2: The Swiss free air carbon dioxide enrichment experiment. Plant and Soil 198, 89–95.

Intergovernmental Panel on Climate Change (IPCC), 2007. IPCC 4th Assessment Report. http://www.ipcc.ch/ipccreports/ar4-wg2.htm

IPCC (Intergovernmental Panel on Climate Change), 2006. 2006 IPCC Guidelines for National Greenhouse Gas Inventories, Prepared by the National Greenhouse Gas Inventories Programme, Eggleston H.S., Buendia L., Miwa K., Ngara T. and Tanabe K. (Eds). Published: IGES, Japan.

Kamp, T., Steindl, H., Hantschel, R.E., Beese, F., Munch, J-C., 1998. Nitrous oxide emissions from a fallow and wheat field as affected by increased soil temperatures. Biology and Fertility of Soils 27, 307–314.

Kettunena, R., Saarnio, S., Martikainen, P., Silvola, J., 2005. Elevated CO_2 concentration and nitrogen fertilisation effects on N_2O and CH_4 fluxes and biomass production of *Phleum pratense* on farmed peat soil. Soil Biology & Biochemistry 37, 739–750.

Kettunen, R., Saarnio, S., Martikainen, P.J., Silvola, J., 2006. Increase of N_2O fluxes in agricultural peat and sandy soil under elevated CO_2 concentration: concomitant changes in soil moisture, groundwater table and biomass production of *Phleum pratense* Nutrient Cycling in Agroecosystems 74, 175–189.

Kettunen, R., Saarnio, S., Martikainen, P.J., Silvola, J., 2007a. Can a mixed stand of N_2-fixing and non-fixing plants restrict N_2O emissions with increasing CO_2 concentration? Soil Biology & Biochemistry 39, 2538–2546.

Kettunen, R., Saarnio, S., Silvola, J., 2007b. N_2O fluxes and CO_2 exchange at different N doses under elevated CO_2 concentration in boreal agricultural mineral soil under *Phleum pratens.* Nutrient Cycling in Agroecosystems 78, 197–209.

Koike, I., Hattori, A., 1975. Growth yield of a denitrifying bacterium, *Pseudomonas denitrificans*, under aerobic and denitrifying conditions. Journal of General Microbiology 88, 1-10.

Laville, P., Jambert, C., Cellier, P., Delmas, R. 1999. Nitrous oxide fluxes from a fertilised maize crop using micrometeorological and chamber methods Agricultural & Forest Meteorology 96 (1999) 19 – 38.

Li, C., Frolking, S., Frolking, T.A., 1992. A model of nitrous oxide evolution from soil driven by rainfall events: 1. Model structure and sensitivity. Journal of Geophysical Research 97, 9759-9776.

Li, T., Grant, R.F., Flanagan, L.B., 2004. Climate impact on net ecosystem productivity of a semi-arid natural grassland: modeling and measurement. Agricultural and Forest Meteorology 126, 99–116.

Li., Y., Chen, D., Zhang, Y., Edis, R., Ding, H., 2005. Comparison of three modeling approaches for simulating denitrification and nitrous oxide emissions from loam-textured arable soils. Global Biogeochemical Cycles, 19, GB3002, doi:10.1029/2004GB002392.

Lu, Y., Huang, Y., Zou, J., Zheng, X., 2006. An inventory of N_2O emissions from agriculture in China using precipitation-rectified emission factor and background emission. Chemosphere 65, 1915-1924.

Lim, B., Boileau, P., Bonduki, Y., van Amstel, A.R., Janssen, L.H.J.M., Olivier, J.G.J., Kroeze, C., 1999. Improving the quality of national greenhouse gas inventories. Environmental Science and Policy 2, 335-346.

McGill, W.B., Hunt, H.W., Woodmansee, R.G., Reuss, J.O., 1981. Phoenix, a model of the dynamics of carbon and nitrogen in grassland soils. In F.E. Clark and T. Rosswall (Ed.) Terrestrial nitrogen cycles. Ecological Bulletin 33, 49-115.

Metivier, K.A, Grant, R.F. and Pattey, In. Prep. Modeling topographic effects on spatial variability of nitrous oxide emissions from fertilized agricultural fields.

Millington, R.J., 1959. Gas diffusion in porous media. Science. 130, 100-102.

Millington, R.J., Quirk, J.M., 1960. Transport in porous media. In: Van Beren, F.A. et al. (Eds.), 7th Trans. Int. Congr. Soil Sci. Vol. 1. Madison, WI. 14-24 Aug. Elsevier, Amsterdam, Science, pp. 97-06.

Molina, J.A.E., Clapp, C.E., Shaffer, M.J., Chichester, F.W., Larson, W.E., 1983. NCSOIL, a model of nitrogen and carbon transformations in soil: Description, calibration and behavior. Soil Science Society of America Journal 47, 85-91.

Morgan, R.P.C., Quinton, J.N., Smith, R.E., Govers, G., Poesen, J.W.A., Auerswald, K., Chisci, G., Torri, D., Styczen, M.E., Folly, A.J.V., 1998. The European Soil Erosion Model (EUROSEM): Documentation and user guide. Version 3.6. Silsoe College, Cranfield University, Silsoe, Bedford, UK.

Muller, C., 1999. Modelling soil-biosphere interactions. CABI Publishing, Wallingford, UK, pp. 52-53.

Myrold, D.D., 1998. Transformation of nitrogen. In: Sylvia, D.M., Fuhrmann, J.J., Hartel, P.G., Zuberer (Eds.). Principles and Applications of soil microbiology. Prentice Hall: Upper Saddle River, New Jersey, pp. 259-294.

Nyborg, M., Laidlaw, J.W., Solberg, E.D., Malhi, S.S., 1997. Denitrification and nitrous oxide emissions from a black Chernozemic soil during spring thaw in Alberta. Canadian Journal of Soil Science 77,153-160.

Olsen, K., Wellisch, M., Boileau, P., Blain, D., Ha, C., Henderson, L., Liang, C., McCarthy, J., McKibbon, S., 2003. Canada's Greenhouse Gas Inventory 1990-2001, pp. 1-4.

Pattey, E., Royds, W.G., Desjardins, R.L., Buckley, D.J., Rochette, P., 1996. Software description of a data acquisition and control system for measuring trace gas and energy fluxes by eddy-accumulation and correlation techniques. Computers and Electronics in Agriculture 15, 303-321.

Pattey, E., Edwards, G.C., Strachan, I.B., Desjardins, R.L., Kaharabata, S., Wagner-Riddle, C., 2006a. Towards standards for measuring greenhouse gas flux from agricultural fields using instrumented towers. Canadian Journal of Soil from agricultural fields using instrumented towers. Canadian Journal of Soil Science 86, 373-400.

Pattey, E., Strachan, I.B., Desjardins, R.L., Edwards, G.C., Dow, D., MacPherson, J.I., 2006b. Application of a tunable diode laser to the measurement of CH_4 and N_2O fluxes from field to landscape scale using several micrometeorological techniques. Agriculture & Forest Meteorology 13, 222-236.

Pattey E., Edwards, G.C., Desjardins, R.L., Pennock, D., Smith W., Grant, B., MacPherson, J.I., 2007. Tools for quantifying N_2O emissions from Agroecosystems. Agriculture & Forest Meteorology 142(2-4), 103-119.

Pennock, D.J., van Kessel, C., Farrell, R.E., Sutherland, R.A., 1992. Landscape-scale variations in denitrification. Soil Science Society of America Journal 56, 770-776.

Pennock, D.J., Corre, M.D., 2001. Development and application of landform segmentation procedures. Soil & Tillage Research 58, 151-162.

Phillips, F.A, Leuning, R., Baigent, R., Kelly, K.B., Denmead, O.T. 2007. Nitrous oxide flux measurements from an intensively managed irrigated pasture using micrometeorological techniques. Agricultural & Forest Meteorology 143, 92–105.

Rao, P.S.C., Jessup, R.E., Reddy, K.R., 1984. Simulation of nitrogen dynamics in flooded soils. Soil Science 138, 54-62.

Rochette, P., Desjardins, R.L, Gregorich, E.G., Pattey, E., Lessard, R., 1992. Soil respiration in barley (Hordeum vulgare L.) and fallow fields. Canadian Journal of Soil Science 72, 591-603.

Roelandt, C., Dendoncker, N., Rounsevell, M., Perrin, D. and Van Wesemael, B. 2007. Projecting future N_2O emissions from agricultural soils in Belgium. Global Change Biology 13, 18-27.

Rolston, D.E., Rao, P.S.C., Davidson, J.M., Jessup, R.E., 1984. Simulation of denitrification losses of nitrate fertilizer applied to uncropped, cropped and manure-amended field plots. Soil Science, 137, 270-279.

Ruser, R., Flessa, H., Russow, R., Schmidt, G., Buegger, F., Munch, J.C., 2006. Emission of N_2O, N_2 and CO_2 from soil fertilized with nitrate: effect of compaction, soil moisture and rewetting. Soil Biology & Biochemistry 38, 263–274.

Saxton, K.E. Rawls, W.J., 2006. Soil water characteristic estimates by texture and organic matter for hydrologic solutions. Soil Science Society of American Journal 70, 1569-1578.

Sextone, A.J., Revsech, N.P., Parkin, T.B. Tiedje, J.M., 1985. Direct measurement of oxygen profiles and denitrification rates in soil aggregates. Soil Science Society of American Journal 49, 645-651.

Schmid, H.P., 2002. Footprint modeling for vegetation atmosphere exchange studies: a review and perspective. Agricultural and Forest Meteorology 113, 159-183.

Shields, J.A., Paul, E.A., Lowe, W.E., 1974. Factors influencing the stability of labelled microbial materials in soils. Soil Biology & Biochemistry 6, 31-37.

Smith, K.A., Thomson, P.E., Clayton, H., McTaggart, I.P., Conen, F., 1998. Effects of temperature, water content and nitrogen fertilisation on emissions of nitrous oxideby soils. Atmospheric Environment 32, 3301-3309.

Suzuki, I., Dular, U., Kwok, S.C., 1974. Ammonia or ammonium ion as substrate for oxidation by *Nitrosomonas europeae* cells and extracts. Journal of Bacteriology 120, 556-558.

Thornton, F.C., Bock, B.R., Tyler, D.D., 1996. Soil emissions of nitric oxide and nitrous oxide from injected anhydrous ammonium and urea. Journal of Environmental Quality 25, 1378-1384.

Tscherko, D., Kandeler, E., Jones, T.H., 2001. Effect of temperature on below-ground N-dynamics in a weedy model ecosystem at ambient and elevated atmospheric CO_2 levels, Soil Biology & Biochemistry 33, 491– 501.

Uchida, Y., Clough, T.J., Kelliher, F.M., Sherlock, R.R., 2008. Effects of aggregate size, soil compaction, and bovine urine on N_2O emissions from a pasture soil. Soil Biology & Biochemistry 40, 924–931.

Wagner-Riddle, C., Thurtell, G.W., Kidd, G.E., Edwards, G.C., Simpson, I.J., 1996. Micrometeorological measurements of trace gas fluxes and natural ecosystems. Infrared Phys. Technol 37, 51-158.

Xu-Ri, Wang, M., Wang, Y., 2003. Using a modified DNDC model to estimate N_2O fluxes from semi-arid grassland in China. Soil Biology & Biochemistry 35, 615-620.

Yoshinari, T., Hynes, R., Knowles, R., 1977. Acetylene inhibition of nitrous oxide reduction and measurement of denitrification and nitrogen fixation in soil. Soil Biology & Biochemistry 9, 177–183.